SHEAR TRANSFER BETWEEN PRECAST PRESTRESSED BRIDGE BEAMS AND IN-SITU CONCRETE CROSSHEAD IN CONTINUOUS STRUCTURES

By

KAMAL MIRTALAIE, B.Sc , M.Sc

A Thesis Submitted in Fulfilment of the Requirement for the Degree of Doctor of Philosophy

Department of Civil Engineering
The University of Leeds
LEEDS LS2 9JT

April 1988

ACKNOWLEDGEMENTS

I would like to express my sincere gratitude to Professor A.R. Cusens, Head of Civil Engineering Department at Leeds University for the opportunity to work on this project. I would like to thank Mr. A.E. Gamble for his constructive critisism, encouragement and helpful supervision throughout the course of this work.

I would like to express my gratitude to the Isfahan University of Technology (Iran) for their provision of the scholarship.

I also extend my thanks to the technical staff of the Department for their assistance in the preparation of specimens, testing and photography.

The author also wishes to thank the Northamptonshire County Council Bridge Department for their assistance with design details for Barnes Meadow Interchange.

K. Mirtalaie

Leeds

April 1988

ABSTRACT

A detailed investigation was made to study the shear transfer between precast prestressed beams and in-situ concrete in a relatively new method of construction of continuous bridge decks where the ends of precast beams are connected to an integral in-situ crosshead away from the supports.

Two series of tests were carried out. In the first series 1/3 scale models of the M.o.T, C&CA M-8 sections were used, and these were modified in the second series to study the effect of the beam's top flanges within the connection. One of the most important mechanisms of shear transfer proved to be the top flanges of the precast beam.

For the precast beams with top flanges (first series), and with a 300mm beam embedment length, it was discovered that:

a) The shear force is transferred from a small length at the end of the beam.

b) The in-situ concrete nibs (concrete surrounding the web) can take this shear force without stirrups.

c) There is no need either to project all the bars from the precast into the in-situ concrete or to prestress the connection transversly as a means of improving shear transfer.

d) It was possible to transfer the whole shear force at the connection with a reduced embedment length of 100mm with nib stirrups.

For the precast beam without top flanges, the transfer of the shear force at the connection required other improving details. In this respect transverse prestressing and web shear connectors were utilized effectively. The effect of projecting bars was also examined.

In the general behaviour of composite continuous beams subjected to shear a detailed comparison was made between different Code predictions for the web cracking shear and web crushing strength. A mathematical model is also proposed to predict the stirrup stress according to shear span, effective depth and stirrup ratio when failure is controlled by web crushing. Stirrup stress measurement in the vicinity of continuous support made it possible to predict the enhanced shear strength and a design method is proposed for the continuous beams. A comparion is also made between different Code predictions in this respect.

To obtain more information about the strength of web shear connectors used in the secod series, a separate dowel shear specimen was designed. Different interface conditions including bond, dowel bar size and strength and the effect of shrinkage were examined. A design method is proposed together with a comparison with different Code predictions.

TABLE OF CONTENTS

Chapter Three

Design and Preparation of Test Beams and Experimental Measurements

Chapter Four

General Behaviour of Composite Beams Subjected to Shear

PRINCIPAL NOTATION

A_s	Total Cross-Sectional Area of the Flexural Reinforcement
A_{sv}	Cross-Sectional Area of a Single Stirrup
a	Shear Span
b	Breadth of the Beam
d	Effective Depth of the Section
E_c	Concrete Modulus of Elasticity
f_y	Yield Stress of Flexural Reinforcement
f_{yv}	Yield Stress of Shear Reinforcement
f_{cu}	Compressive Strength of Concrete Cube
f'_c	Compressive Strength of Concrete Cylinder
f_t	Concrete Tensile Strength
f_{cp}	Average Prestress (Prestress at the Centroid)
M_o	Decompression Moment at Transfer
M_{sdu}	Maximum Moment in the Shear Region under Consideration
r	Stirrup Ratio ($r=A_{sv}/bS_v$)
S_v	Stirrup Spacings
V_{co}	Web Cracking Shear
V_u	Ultimate Shear Resistance of the Section
V_c	Shear Carried by Concrete
V_s	Shear Carried by Stirrups
V_p	Vertical Component of the Prestressing Force
V_1	Shear Force Transferred by the Top Flanges at the Connection
V_2	Shear Force Transferred by the Bond between Web and the Nibs
V_3	Shear Force Transferred by the Top Slab
z	Lever Arm ($z=jd$)
α	Stirrup Angle with Horizontal
β	Angle of Inclination of the Line joining the Loading Point and the Support
θ	Angle of Inclination of the Shear Cracks
ϕ	Strength Reduction Factor in ACI Code
ρ	Flexural Reinforcement Ratio ($\rho=As/bd$)
ν	Poisson's Ratio

ε_x	Horizontal Normal Strain
ε_y	Vertical Normal Strain
σ_x	Horizontal Normal Stress
σ_y	Vertical Normal Stress
γ_{xy}	Shear Strain
τ_{RD}	Basic Concrete Shear Strength in the CEB Code

LIST OF TABLES

LIST OF PLATES

CHAPTER ONE

INTRODUCTION

1.1 Continuous Precast Prestressed Bridges

Continuity of bridge superstructure over supports has been well recognised as a more efficient and cost effective solution than the simply supported spans alternative, where substructure conditions facilitate.

1.1.1. Advantages

A continuous multi-span bridge may be superior to a series of simple spans in several respects:

a) With the establishment of continuity moments and deflections at midspan sections are less, permitting reductions in sectional dimensions, positive moment reinforcement and prestressing levels. This significant saving in span material cost is, however, partially offset by continuity material costs, although an overall reduction in material should result.

b) The loadcarrying capacity of simply supported beams is governed by the capacity of a single section. In a continuous beam, however, formation of plastic hinges and redistribution of moments will increase the overall capacity of the structure.

c) In continuous bridge construction, joints between adjacent spans at the support are eliminated. This is desirable for the following reasons : (i) It provides an improved riding surface, (ii) It prevents the penetration of water and de-icing salts into piers and deck ends thus increasing durability, and (iii) It eliminates the initial and subsequent maintenance cost of joints .

1.1.2 Disadvantages

There are equally some disadvantages with continuous structures. The most important ones are being :

a) Secondary stresses due to creep, shrinkage, temperature changes and differential support settlement can be significant for continuous structures unless they are controlled and allowed for in the design.

b) Reversal of moments could be significant when live loads are much heavier than dead load and partial load

ing on the spans are considered.

c) Difficulty in achieving continuity for precast elements. For in-situ construction continuity is easily obtained but in the case of precast elements it may require additional construction stages.

1.2 Continuity Connections for Precast Elements

Various methods have been developed to achieve continuity in the connection between precast beams.

1.2.1 Cap Cables

In this method precast beams are connected by 'cap cables' as in Fig.1.1 and post-tensioned after erection of beams. The cap cables establish continuity across the support, but large friction loss is associated with this method due to the sharp curvature of the tendons. It is also difficult to thread tendons through the duct unless the profile is made into a circular curve and if bars are used they must be prebent to a definite curvature. This method has been used in France.

1.2.2 Post-tensioned Cables in Deck Slab

This solution is in fact a modification of the cap cable method. Short lengths of cables are positioned in the deck slab between the longitudinal precast beams and post-tensioned after the construction of in-situ deck as in fig. 1.2. This method was suggested by Leonhardt.

1.2.3 Post-tensioned Bolts

Precast elements are post-tensioned together with short bolts either diagonally or horizontally as in fig.1.3a and 1.3b. The main disadvantage of this method is its uneven surface over the\ support specially in type b. Several bridges, gantries and harbour structures have been constructed in the Netherlands using this method.

1.2.4 Transverse Prestressing

In this method instead of longitudinal tightening as described in previous methods, the beams' end are stressed transversly to use the frictional effect as a mean of longitudinal continuity (see Figs.1.4a and 1.4b). In 1954 Christiani & Nielsen of London built a prestressed concrete bridge at Northam, which has been a crossing point for the river between Southampton and Portsmouth through recorded history. The bridge is made up of longitudinal precast prestressed 'T' beams assembled side by side. For a distance from the end of the beam the 'T' head is left out and the rectangular area thus formed above the pier is filled in with a precast junction slab.

After assembly on the piers cables are threaded through transverse

sleeves cast into the beam's and junction slabs and the cables are stressed to form the required continuity over the support.

This method has also been used by overlapping the longitudinal elements over the support, casting an in-situ concrete diaphragm and finally transversly post-tensioning as in Fig.1.4b.

1.2.5 Precast Prestressed Rods

In composite construction precast prestressed (pretensioned) concrete rods are placed over the support and then an in-situ concrete deck slab is cast as in Fig.1.5. The use of these rods gives some of the advantages of prestressing whilst avoiding a post-tensioning operation on site. The concrete rods are prestressed and when they are bonded to surrounding concrete it results in a stiffer performance, cracking is delayed and cracks are closed on removal of loads within the service load.

1.2.6 Conventional Bar Reinforcement (Live Load Continuity)

This is the most common and simplest method of achieving continuity in bridge construction. Precast beams are positioned simply on the piers leaving small gaps between the beams' end (Fig.1.6 stage I). Steel reinforcement is placed over the support and finally an in-situ concrete is cast over the whole deck and between the units(see Fig.1.6 stage II). The complete system is thus continuous for live loads only and for long spans where dead load is significant in comparison with live loads, the full benefit of continuity can not be obtained.

1.2.7 Unconventional Full Continuous System

Recently the use of precast beams in superstructures where they are supported away from the substructure has enabled larger spans to be developed without excessive increase in the lengths of precast units, whilst it gives full continuity for some dead and all live loads, together with a number of other advantages.

Few bridges have been constructed in the U.K. using this new method (three examples being M11 Woodford Interchange, Barnes Meadow Interchange, Northampton and York Ring Road, North Yorkshire, built in 1970, 1983 and 1986 respectively) and at present there is little evidence of this method being widely used in other countries.

The method of construction is as follows:

I) Precast elements are temporarily supported on scaffolding on each side of previously constructed piers or columns at a distance of more than the support thickness (see Fig.1.7 stages I,II).

II) Continuity steel is fixed over the support into each span (see Fig.1.7 stages I,II).

III) An in-situ concrete crosshead is cast together with the deck slab (see Fig.1.7 stages III,IV).

IV) Temporarily scaffolding is removed after concrete has reached the required strength (Fig.1.7 stages III,IV).

There are a number of useful advantages with this new system:

a) Achieving full continuity for some dead and all live loads.

b) To use smaller precast beam lengths than the pier distances for the reason of overall standardization, Transportation restrictions, etc.

c) Where piers are located radially, the deck plan curvature requires longer spanning elements on the outside than inside of the curve. This could

be easily overcome by slight variation of the width of in-situ crosshead.

d) In the case of individual columns in the substructure, the use of conventional method previously described implies the need for a rather deep transverse beam over the columns which reduces the available headroom under the bridge. By employing this new system a constant construction depth can be obtained along the bridge.

1.3 Scope of proposed Research

The main problem associated with the above mentioned new method of continuous bridge construction was previously considered to be the transfer of shear force from the precast beams to the in-situ crosshead.

This proposed study is to investigate the whole nature of shear transfer in this region where precast beams and in-situ concrete crosshead meet and to compare different conditions and parameters affecting the structural efficiency.

These parameters can be listed as follows:

a) The effect of shear reinforcement in the nibs(in-situ concrete between the beams in the embedded part) upon the shear transfer capacity of the connection.

b) The effect of precast beam sectional geometry on the shear capacity of the joint.

c) To observe the effect of bending moment magnitude upon the shear transfer capacity.

d) To examine the overlapping length effect on the shear capacity of the connection.

e) To observe the effect of transverse prestressing upon the longitudinal shear strength of the joint.

f) The effect of shear connectors between the web and in-situ nibs on the shear transfer behaviour.

g) The contribution of projecting bars from the precast beam's end as dowels to shear transfer capacity.

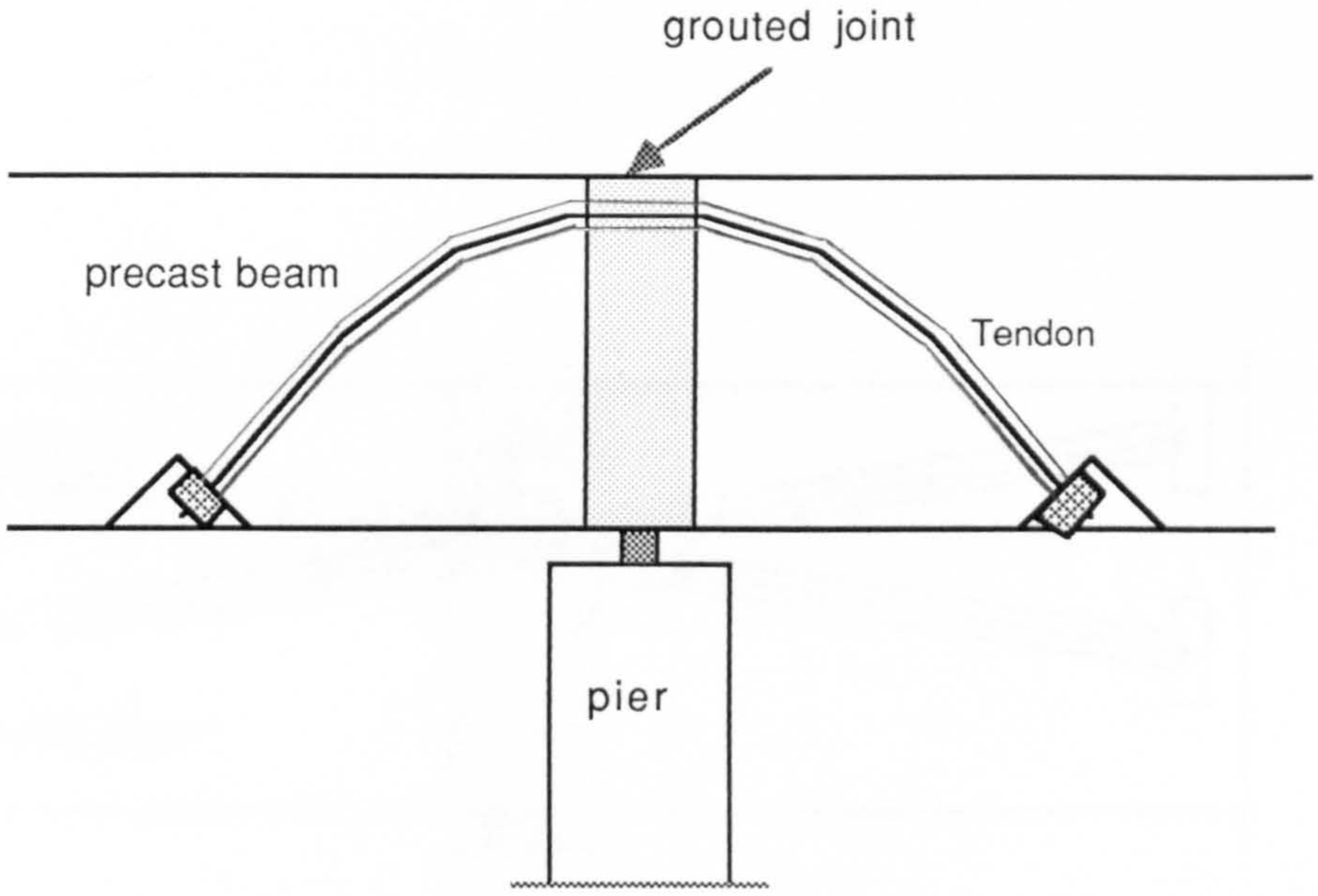

FIG. 1.1 Cap Cables

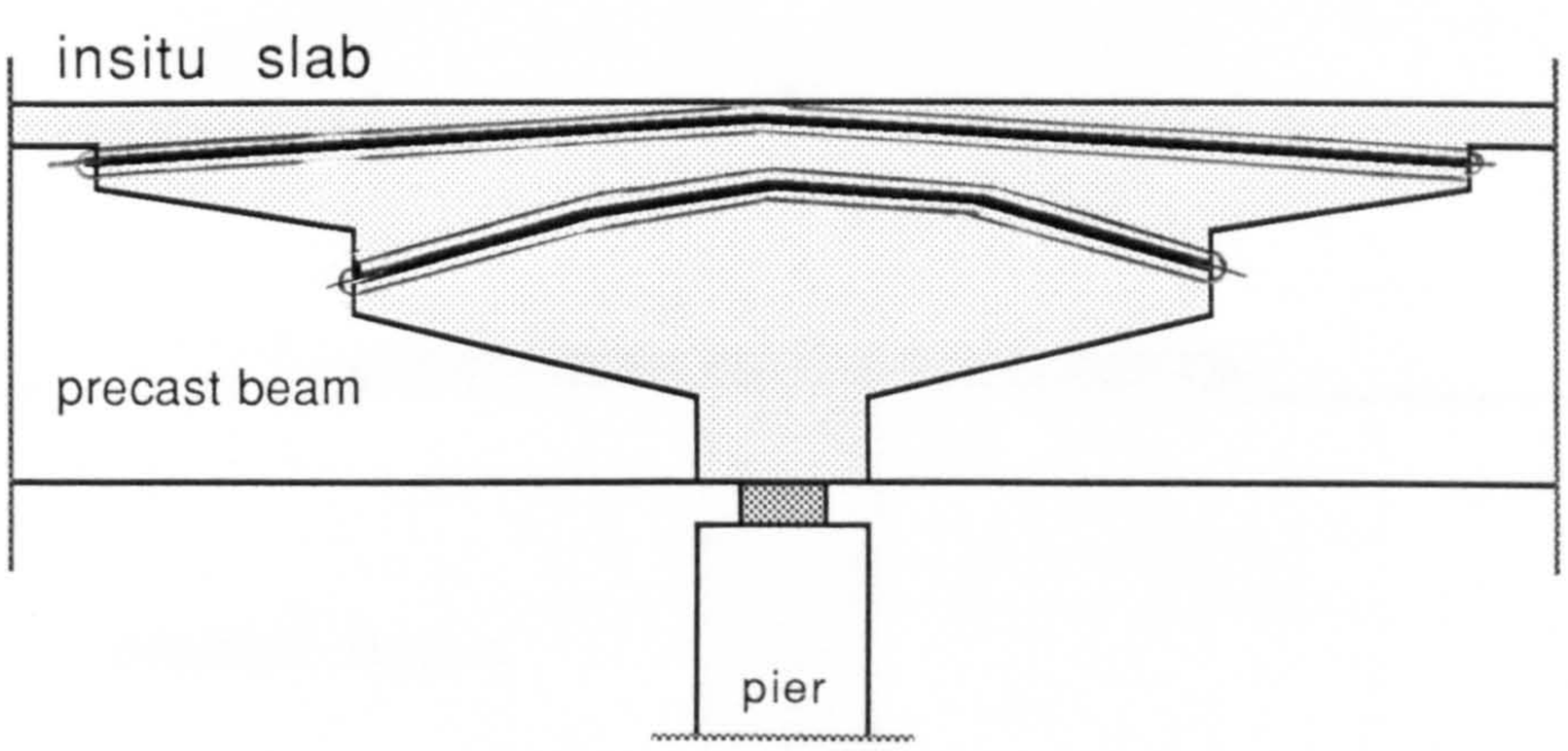

FIG. 1.2 Deck Slab Post-tensioning

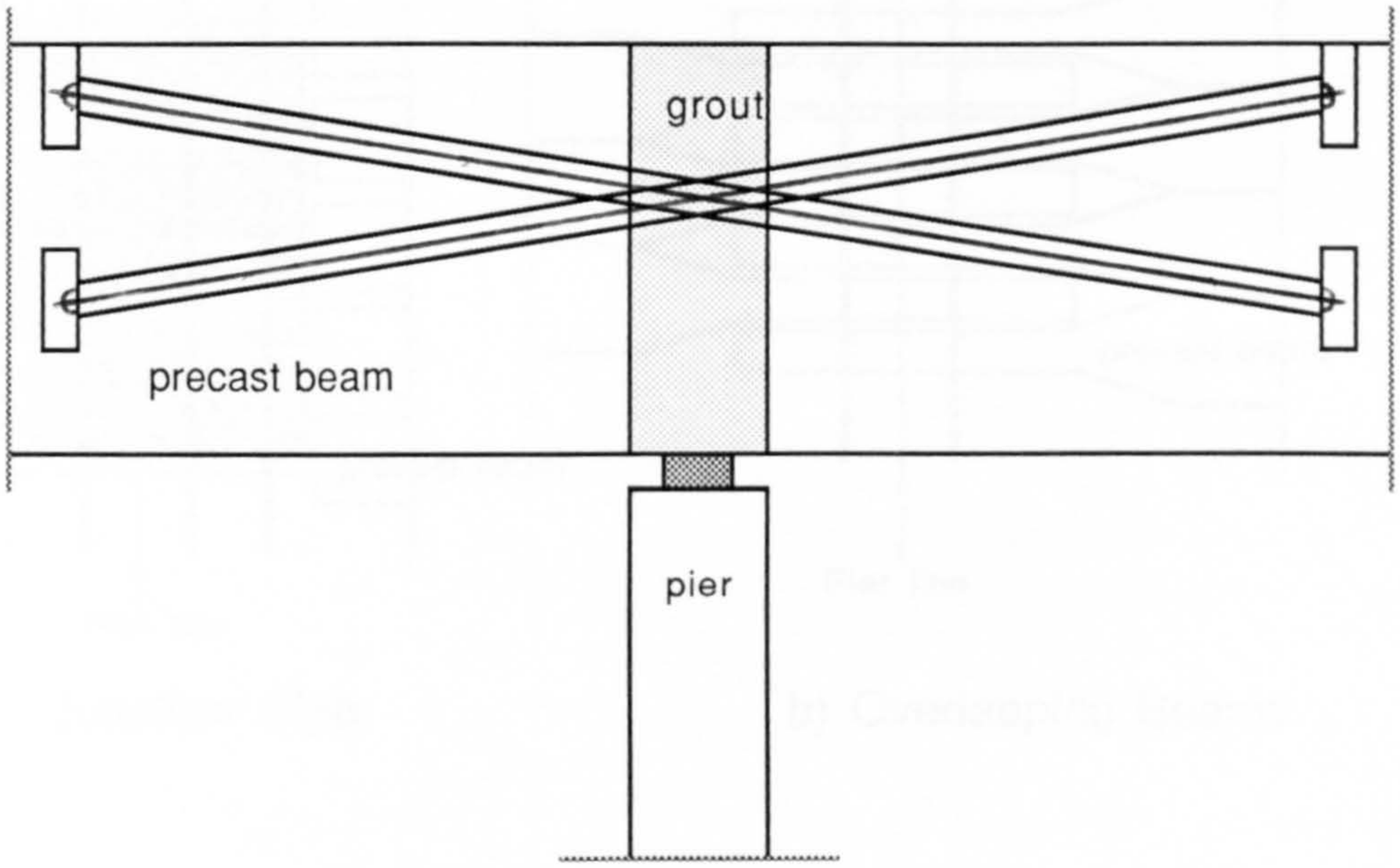

(a)

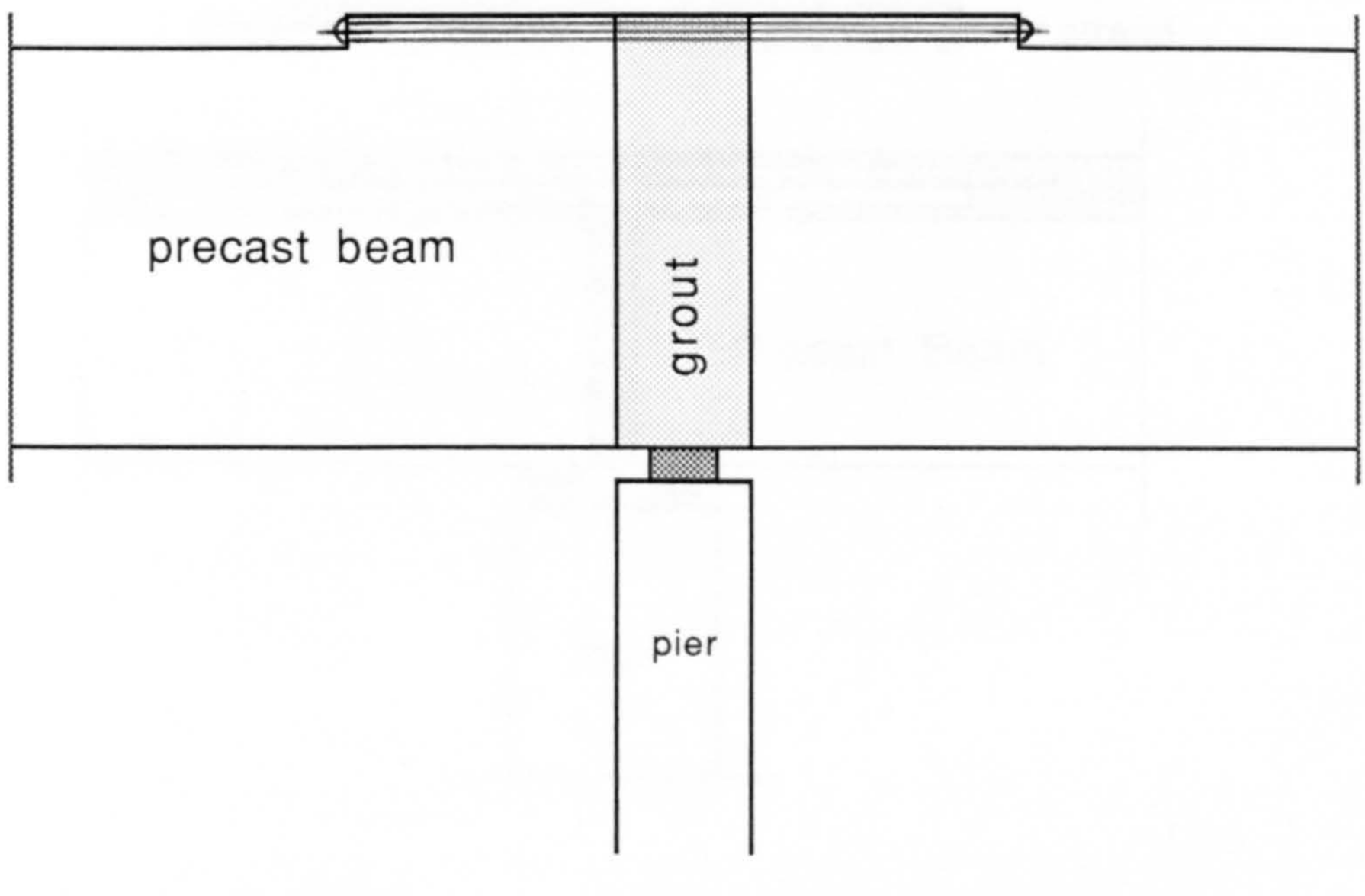

(b)

FIG. 1.3 Bolt Post-tensioning

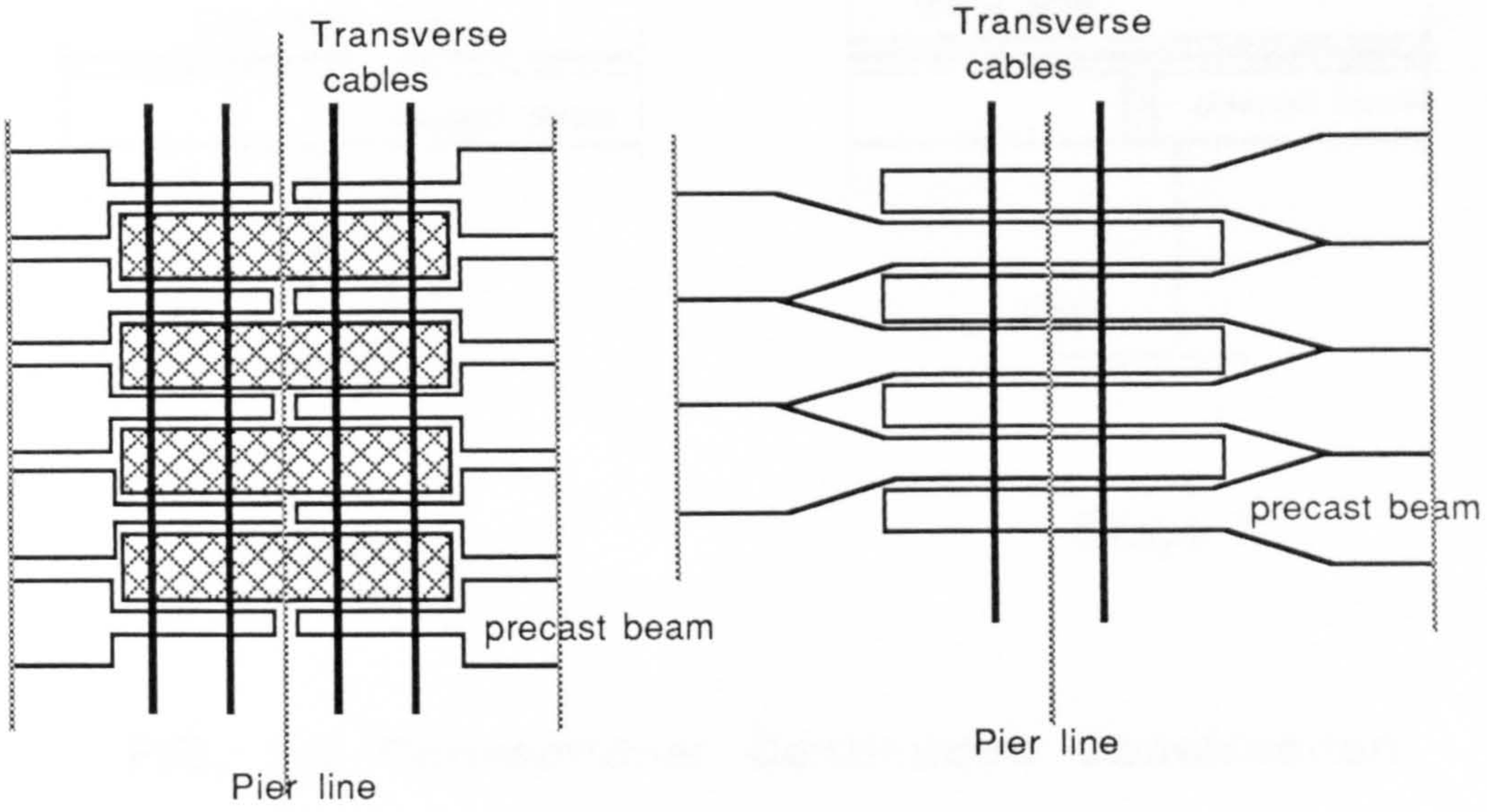

a) Junction Slab

b) Overlapping Beams

FIG. 1.4 Transverse Prestressing

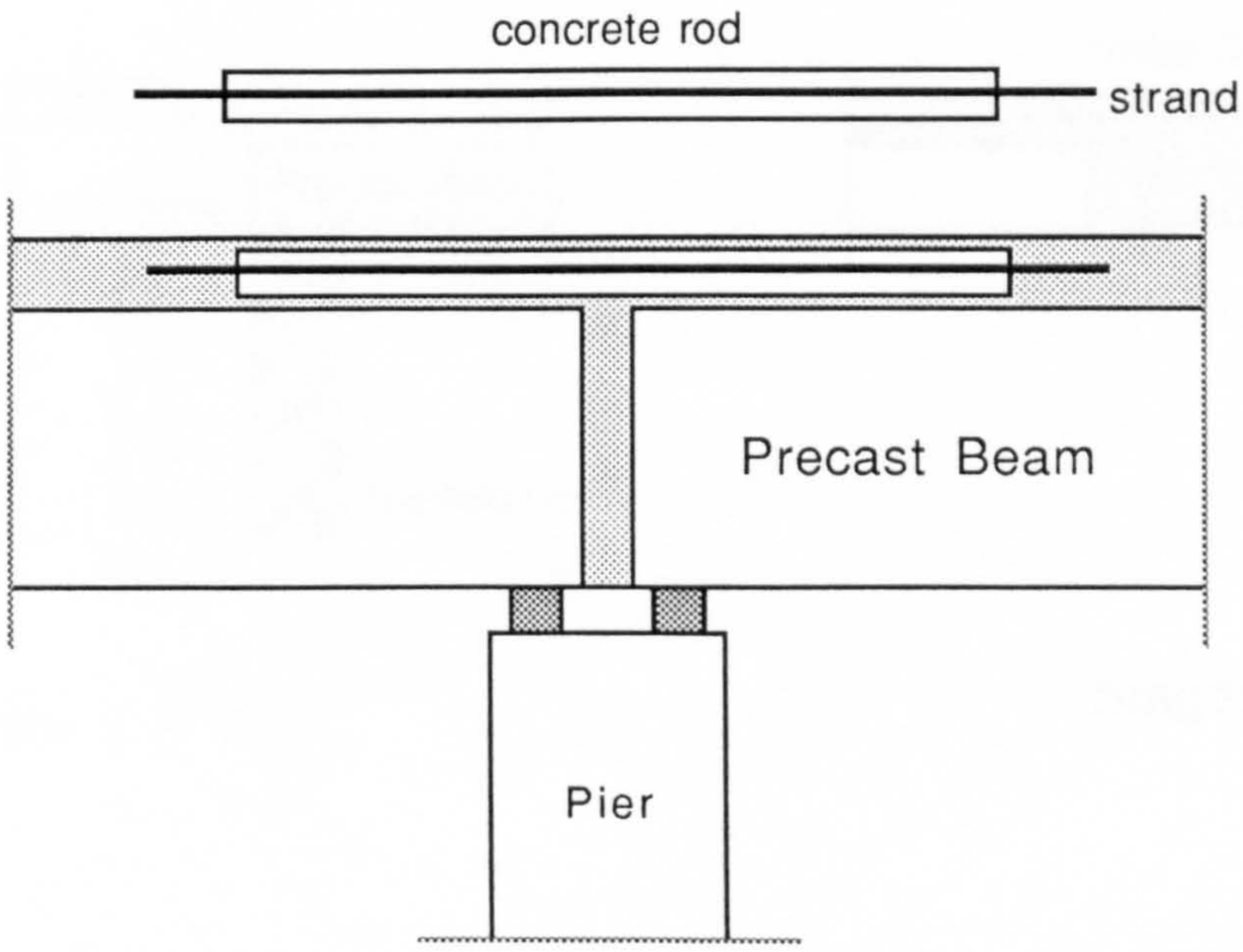

FIG. 1.5 Precast Prestressed Rods

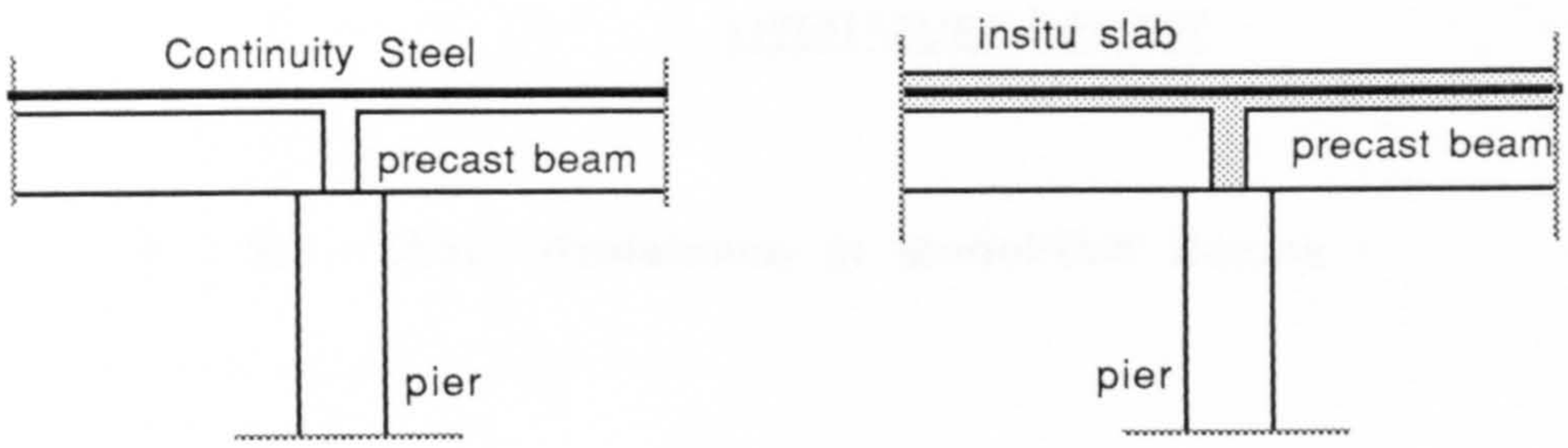

Stage I

Stage II

FIG. 1.6 Conventional Continuous Construction

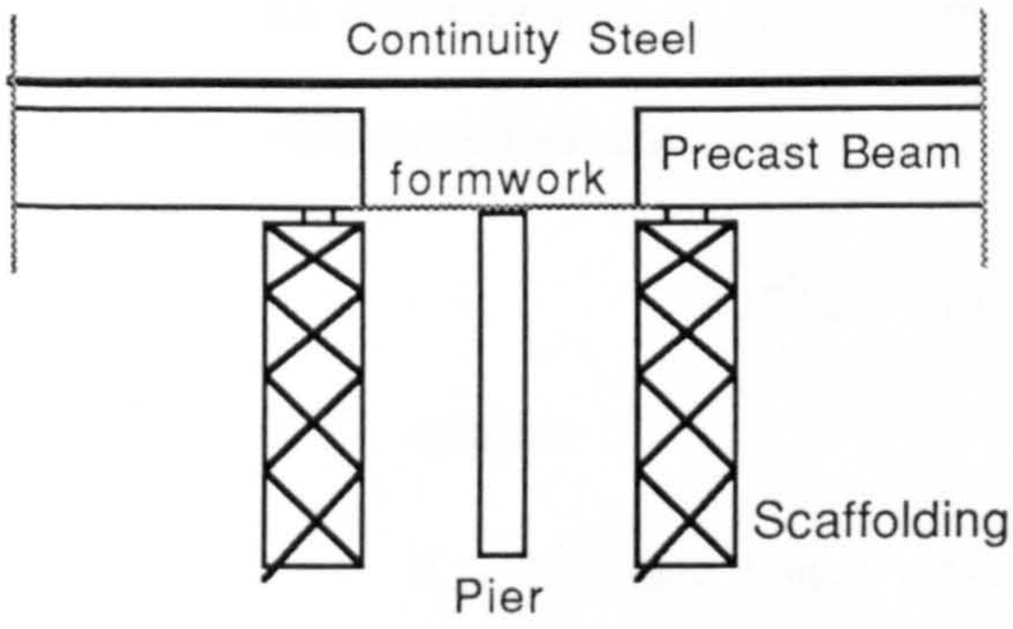

Stages I & II

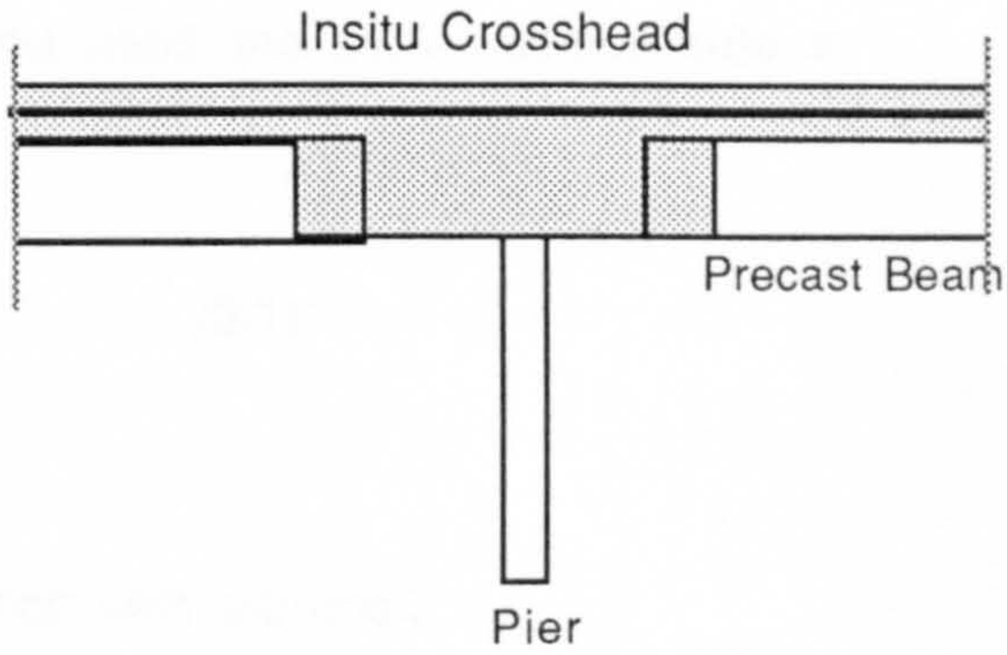

Stages III & IV

FIG. 1.7 New Type of Continuous Structures

CHAPTER TWO

LITERATURE REVIEW

2.1 Shear Resistance in Monolithic Beams

Extensive experimental works particularly in recent years have been undertaken to identify several aspects of shear transfer mechanisms. A useful historical review was produced by Bresler and McGregor[21] and by Hognestad.[22]

The background of the ACI code[23,81] widely used since 1963, was reported by ACI-ASCE Committee 326[24] in 1962. A similar report on the state of the art by ACI-ASCE Joint Committee 426 was published[25] in 1973.

In the U.K. in 1969 The Shear Study Group published a report[26] for the design of reinforced concrete for shear which formed the basis of the current code of practice BS8110: "Structural use of Concrete" [27] .

ACI-ASCE Committee 326 suggested that the reinforcement can develop its yield stress at the ultimate shear and used the superposition rule to introduce this equation:

$$v_u=v_c+krf_{yv} \qquad (2.1)$$

where:

v_u= Ultimate shear stress in the section with stirrups.,

v_c= Ultimate shear stress in the section without stirrups.,

$k=\sin\alpha(\sin\alpha+\cos\alpha)$, Stirrups' effectiveness.,

$r=A_{sv}/(b\ S_v\ \sin\alpha)$

α=Stirrups' angle of inclination with horizontal.,

f_{yv}= Stirrups' yield strength.,

b ,S_v= Width of section and stirrups' spacings respectively.,

2.2 Shear Transfer in Cracked Section

When a section subjected to shear force cracks, the mechanism of shear transfer changes to a complicated statically indeterminate internal structure which necessitates experimental verification to recognize and evaluate different modes of shear transfer.

A large amount of research work has been carried out by the investigators and finally it was stated that the most important mechanisms of shear transfer in reinforced concrete are the following[25] (see Fig.2.1a).

I) Compression zone of concrete beam.

II) Cracked surfaces(Interface shear)

III) Dowel action of longitudinal reinforcement.

IV) Arch action.

V) Stirrups (in beams with stirrups)

At the beginning it was thought that the compressive zone of the beam provided the most significant contribution to shear transfer. This was due to the belief that the cracked portion of the beam could not carry vertical loads. This concept was later challenged by other researchers who concluded that the concrete between cracks (so called cantilevers or teeth) would fail at very low loads if there was no interface interaction [29,30] and the importance of interface shear strength (described by some as aggregate interlock, surface roughness, interface friction, etc.) came into account.

2.2.1 Shear Transfer by Concrete Compressive Zone

Acharyar and Kemp[31] estimated that at failure the concrete compressive zone can carry up to 40% of the total shear force in a beam without shear reinforcement.

Taylor[32,33] developed a method to determine the shear stresses in the

compressive zone by measuring the longitudinal strains and using the mathematical relationship between normal and shear stress. He found that this part of the beam transfers 20% to 40% of the shear force in a beam without shear reinforcement.

2.2.2 Interface Shear (Aggregate Interlock)

Interface shear is a more recently recognized viable mechanism. Taylor[34] observed that it is a function of the cracked surface roughness, and in high strength concrete where there is a relatively smooth fracture surface as a result of aggregate cracking, the shear transfer by aggregate interlock was reduced. Paulay and Loeber[35] observed that the largest single factor affecting shear displacement is crack width. They also concluded that the size and shape of aggregate does not effect the ultimate shear.

Taylor[36] also observed that longitudinal steel percentage, concrete strength, shear span to effective depth ratio, beam size(depth) and aggregate type have a significant effect on the aggregate interlock shear transfer and this mechanism generally carries 33% to 50% of the shear force in a beam without shear reinforcement.

In recent investigations Bazant and Gambarova[51] and also Sandro, Gambarova and Karakoc[52] formulated constitutive stress-displacement relationships for aggregate interlock with a so called 'rough crack' method. They concluded that diagonal cracks in thin-webbed sections give substantial contribution to the ultimate shear, which is larger in sections having inclined shear cracks rather than flexural-shear cracks.

2.2.3 Dowel Shear Transfer

Dowel shear force is the transverse component of the force in the

longitudinal reinforcement. It is a combination of shear stress in the reinforcement and the behaviour of reinforcement in the concrete as a beam on an elastic foundation as described by Jones[37]. To evaluate the magnitude and factors affecting the dowel force, a number of investigators including Krefeld and Thurston[39], Fenwick[40] ,Lorentsen[41], and Taylor[38] developed experimental methods to illustrate dowel action. They concluded that the dowel strength is dependent on a number of variables such as concrete strength, cover to the bars, stirrups' spacing, main reinforcement size and layout. It was concluded from their investigations that this mechanism is less dominant in beams although it is more important in some other structures such as connections between precast elements. The shear force carried by dowel action was suggested by Taylor to be 15% to 25% .

2.2.4 Shear Transfer by Arch Action

Arch action is the beam's resistance to shear by inclined compression. It has been investigated by a number of researchers including Neville[42], Kani[43,44] and Fenwick[30] that after inclined cracking and internal redistribution of forces, the shear transfer mechanism will be transformed to a tied arch system in which a rather high compressive force is transferred to the support which has to be taken by the main reinforcement bond, thus imposing a heavy demand on the anchorage, as described by Park and Paulay[45]. Evidence of arch action can be seen from the tensile cracks on the top of the beam near the supports, as in Fig.2.1b. This mechanism is not only outside the outermost cracks but also it occurs between all cracks acting with stirrups close to the base of cracks as supports to the arches[44]. Fenwick and Paulay[30] observed that arch action can only occur at the expense of slip (i.e complete loss of bond transfer) and Mlingwa[60] pointed out that beams with unbonded prestressing tendons would invariably have a higher resistance to

shear and a lower strength in flexure due to arch action than the corresponding prestressed beams with bonded tendons.

2.3 Modes of Shear Failure

Investigations by Fenwick[30], Taylor[32], Kani[43] and Regan[53] have shown that the cause of diagonal failure is linked with the stress condition in the region of "Concrete Cantilevers" which form between flexural cracks.

Warner[46] observed that the shear failure mode depends on a number of variables including the geometry of the section (slenderness), loading arrangement and amount of shear reinforcement. It is also suggested[47] that in prestressed beams the prestressing level could influence the mode of shear failure. Fenwick[30] and Kani[54] found experimentally that the shear failure mode depends on shear span to effective depth ratio.

In recent years Kotsovos[55] and Kotsovos et al[56] suggested a new concept of shear failure mechanism in which diagonal failure is very closely related to the shape of the path along which the compressive force is transferred to the support rather than the stress conditions existing in the region of 'concrete cantilevers'.

They also showed that in 'T' beams with a shear span to effective depth ratio greater than 2.5, the shear span is provided by the flange and not as was widely considered, by the web. The most acceptable modes of shear failure have been suggested to be:

i) Diagonal tension

ii) Shear compression

iii) Web crushing

2.3.1 Diagonal Tension

This shear failure mode occurs in relatively thick-webbed sections with high a/d ratio (a/d>3.0) and low stirrup percentage, as described by Sethunarayanan[47], Mathey[48] and Evans[49]. Failure occurs shortly after the application of diagonal cracking load and the subsequent arch action is not capable of taking the cracking load. When stirrups exist in the section they yield immediately after the load has caused cracks to develope rapidly into the compressive zone, whereupon the failure is sudden[47,48,49,50]

2.3.2 Shear Compression

This is a common mode of shear failure for thick-webbed and rectangular sections[57] with a moderate shear span to effective depth ratio (2.5<a/d<4.0) and with low or medium levels of prestressing in prestressed beams. After the failure of the beam action, the propagation of an inclined crack reduces the compressive zone excessively. A point is reached when the available area of concrete in the vicinity of the applied load becomes too small to resist the compression force, and the concrete crushes. This is usually a failure of arch action[45,57,58].

Leonhardt[59] observed that the position of failure is where the value of M/V.d attains its maximum, causing crushing of the concrete due to a combination of compressive and shear stresses.

2.3.3 Web Crushing

This mode of shear failure is produced by the high diagonal compressive stress resulting from shear stresss. It can be seen simply from the truss analogy hypothesis that the inclined members of truss (concrete struts) are

under axial compression[15] or a combined bending and axial load[7].

Web crushing could be described as gradual rather than catastrophic and is more likely to occur in thin-webbed sections (d /b >5.0) having a rather low shear span to effective depth ratio (1.5<a/d<3.0) and with relatively stiff top and bottom flanges[7,15,16,17] .

The upper limit for shear capacity of a section can be assumed to be its web crushing strength and it cannot be increased even by increasing the stirrup percentage[18]. This limit is defined as a maximum nominal shear stress in codes. Web crushing is very variable and current codes give its lower limit[18] .

2.4 Shear Resistance in Composite Beams

As explained in chapter one, composite concrete structures are those consisting of precast beams and a top concrete slab with suitable horizontal connections to ensure composite action. This type of construction has the advantage of speed and simplicity in practice producing a monolithic system after hardening of the top slab.

In spite of considerable research work on shear resistance of monolithic concrete sections, there is a relatively small amount relating to shear of composite beams.

2.4.1 Conventional Continuous Composite Beams

Conventional continuous bridges are made up of precast units, as described previously, which are continuous for live loads only. An extensive experimental work was undertaken in Portland Cement Association (PCA) concerning this type of structure[7,8,9,10,11].

Mattock and Kaar[8] investigated the behaviour of this type of structure

subjected to shear, and details of their tests and results are as follows:

The test program was designed to observe the influence of the following two variables on shear strength:

a) Amount of stirrups (varying from 0.38% to 1.14%)

b) Position of external loads (shear span effect),

The test beams consisted of a 33' precast prestressed 1/2 scale model connected to a 9' length beam, having the same cross-section, with a top slab.

Supports and loading arrangements were as shown in Fig.2.2 to simulate the condition at a support section of a continuous beam. The shear span (measured from the first load) to effective depth ratio was between 1.0 and 4.5. Strain measurements showed that the stirrup strain was very small before the formation of diagonal cracks but it increased suddenly afterwards. Similar conclusions were reached by Bennett[12,13, with stirrups in the region of diagonal cracking yielding almost immediately after cracking.

Most of the beams failed in a web shear crushing mode. The crushing zone was located in the lower part of the web where the compressive stresses were high, and flexural cracks due to the negative support bending moments were too steeply inclined to lead to a shear failure.

The initial inclined crack widths were found to be between 0.08mm and 0.1mm. As far as ductility is concerned, from the deflection measurements, it was shown that the ductility increases with an increase in the shear reinforcement.

The inclined cracking load and ultimate shearing strength were also shown to be higher in beams with a smaller shear span to effective depth ratio .

Mattock and Kaar interpreted shear strength in terms of the observed mode of failure of their test beams. In order to explain this mode they hypothesized that the inclined cracks divide the shear span into a series of strut members which fail under the action of combined axial load and bending.

For the web crushing mode of failure a free diagram and equilibrium condition for a single strut can be drawn as in Fig.2.3. This strut can fail at its lower end as a result of the combined axial force C in the strut and the bending produced by the shearing force acting at the upper end of the strut.

When the amount of shear reinforcement increases the shear force in the strut decreases and strut can fail in direct compression. Any further increase in the reinforcement can not increase the web crushing strength of the section.

The direction of inclined cracks was thus felt to be controlled by the loading position and depth of the beam

It was also concluded that the contribution of stirrups to the shearing strength continued to decrease with an increase in the shear span to effective depth ratio.

This is in disagreement with McGregor's[14]results in simply supported beams,where an increase in the shear span to effective depth ratio beyond 3.5 did not affect the effectiveness of the web reinforcement. To explain this discrepancy Mattock and Kaar[8] suggested that the diagonal cracks developed from flexural cracks were usually restricted to that part of the shear span near the loading point and did not extended over the whole length of the shear span in the case in which the cracks were caused by excessive principal tensile stresses in the web. Hence the reduced shear strength was the result of excessive cracking over the entire length of the shear span associated with shear in the uncracked section.

For shear strength analysis the strength is divided into two parts: a) the shear required to cause inclined cracking and b) the increase in strength beyond inclined cracking resulting from the stirrups.

For a given concrete strength it was suggested that the effect of stirrups to the shear strength can be expressed as:

$$(V_u-V_c)/bdSin\beta=6.24(r\ f_{yv})-0.44(rf_y)^2/\sqrt{f'_c} \quad \text{(PSI)}.....(2.2)$$

A rather conservative linear equation was proposed:

$$A_{sv}=S_v(V_u-V_c)/3.5\ d\ f_{yv}\ Sin\beta \quad .....(2.3)$$

Where:

β is the angle of inclination of the line drawn between the loading point and support.

According to their suggestions, a rather ductile failure could exist if the shear failure load is at least 80% of the load required to cause a flexural failure. It was also suggested that in a continuous composite beam such as their test beam, the first interior support could be investigated for the shear.

Bennett[12,13] carried out two series of shear tests on different types of fullsized composite bridge beams to study the adequacy of the current British code, CP110, and M.o.Tmethods in an initial series, and examined the efficiency of different types of stirrups in a second series. It was found that both design methods were very conservative.

Clarke and Evans[61] investigated the adequacy of the CP110 and BS5400 methods for shear design of composite beams. Tests on two sizes of composite beams consisting of a precast post-tensioned section and a cast-in-place top flange have shown that both methods (CP110 and BS5400) for shear design of monolithic prestressed beams can be used for composite sections giving an adequate safety margin.

Tay[62] in an experimental study on full-sized 'M5' precast prestressed composite beams compared different methods of shear design in current codes of practice for both static and repeated loadings.

It was found that CP110 and D.Tp (Department of Transport) design methods for ultimate shear resistance were conservative for beams with a high level of prestressing but they slightly overestimated shear strength of beams with low levels of prestressing.

He concluded that the D.Tp method of superposition gives the best prediction of ultimate web shear and CEB-FIP method is the most conservative of all methods.

2.4.2 Unconventional (New) Continuous Composite Structure

The method of construction for this type of bridge structures was explained in chapter one (section 1.2.7) where it was mentioned that there have been very few bridges constructed using this method. The only published research works on this type of structure are those of Sturrock[3] and Pritchard[4,5], in which a test program was conducted by the Cement and Concrete Association to examine the soundness of the previously designed M11 Woodford Interchange prior to its construction.

The test beams were not true models of the prototype but they were similar in many respects (see Fig. 2.4a).

It is worth noting that in the initial design of the bridge the designer had proposed constructing a tapered end block at the end of the beam (Fig. 2.4b) although this was never utilised for reasons of economy. However, the Author (present investigation)observed that by leaving this end block out the original beam section is in fact stronger in the shear transfer region of the embedded length. This is discussed in greater detail later in the thesis.

The shear capacity of the joint was not determined since the flexural strength of either precast or insitu concrete were the controlling factors. Since no tests were carried out in which a tapered end block was included, it was decided to omit this feature from the prototype design, for economical reasons, provided sufficient lateral restraint (transverse prestress) was utilized to ensure composite action.

Sturrock's[3] tests were carried out in two phases. Phase1 consisted of tests on five single 1/5 scale precast prestressed beams of an inverted 'T' beam

section connected to a rectangular insitu beam which is then cast simultaneously with the top flange of the precast beam to form a composite section.

The loading was arranged so that first a positive bending moment was produced in the connection by applying a span load , then a cantilever load was applied to increase the shear force in the connection which has some cracks from the first loading stage. This was to simulate the effect of support settlements. The major variable in this phase was the magnitude of bending moment at the connection. Four specimens were tested to failure in shear at the joint to support region although in the fourth one the concrete nibs showed a tendency to splay outwards in the overlapping part and it failed at a lower load.

The fifth specimen was tested to improve the bearing between insitu and precast beam by transverse clamping of the joint with an average applied compressive stress of about 0.3 N/mm^2 in the overlapping part. The effect of this modification was that it could carry slightly more shear force but the mode of failure was different. It failed in a "shear compression" mode under the span point load and the increased shear capacity permitted full hinging over the support to occur with considerable rotation at the support.

Phase 2 considered the behaviour of the actual bridge subjected to a combination of longitudinal and transverse bending and shear stresses. The test specimen consisted of three longitudinal elements similar to those in phase 1 connected to an insitu crosshead together with the top slab.

Transverse prestressing was applied by 28mm Macalloy stressing bars, and the loading arrangement produced a transverse bending moment over the support with an eight points spreader beam. The beam failed in a shear compression mode similar to the fifth specimen in the first phase.

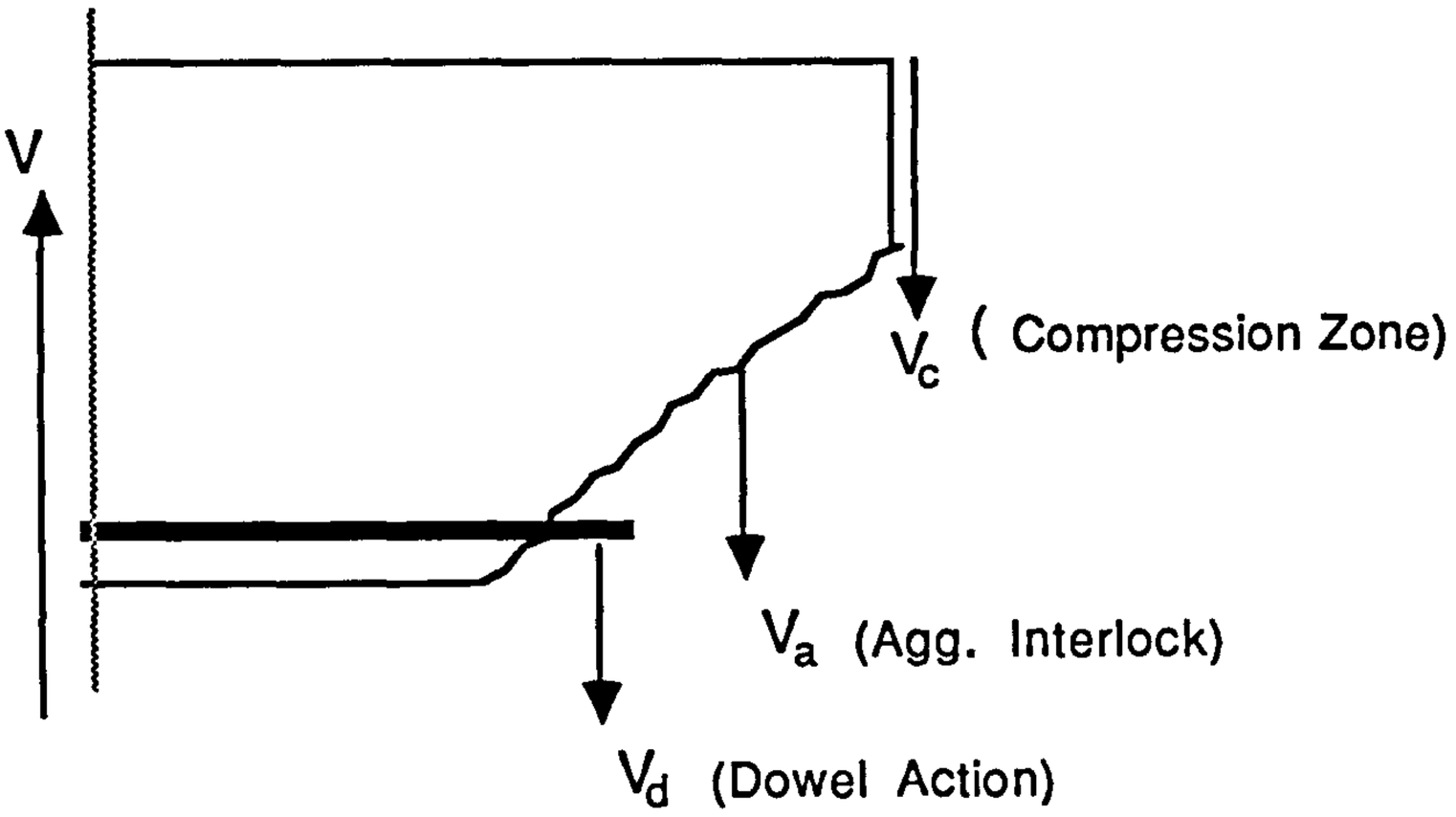

FIG. 2.1a Shear Transfer at a Cracked Section

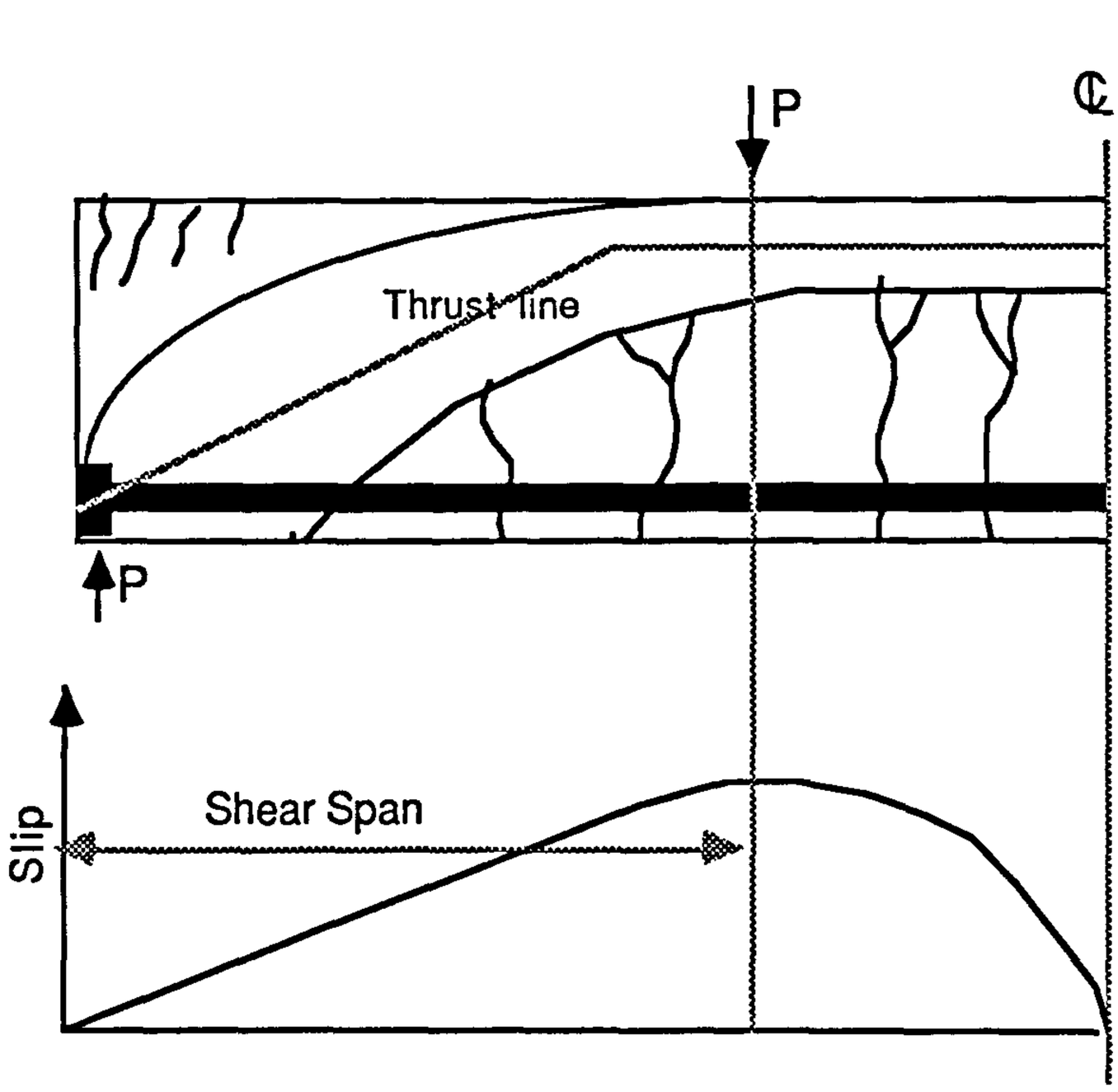

FIG. 2.1b Arch Action and Slip in the Reinforcement

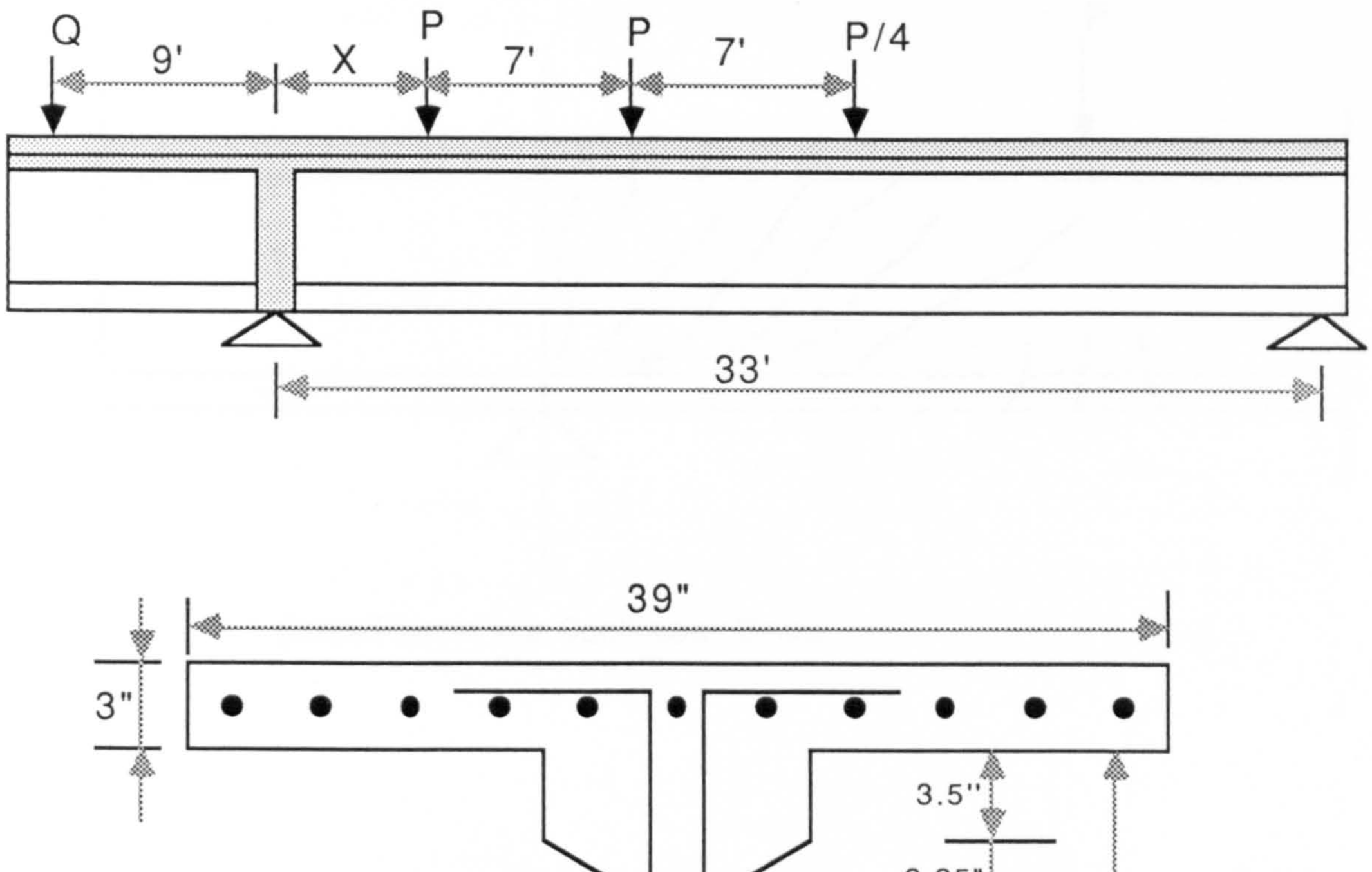

FIG. 2.2 Mattock and Kaar Test Beam[8]

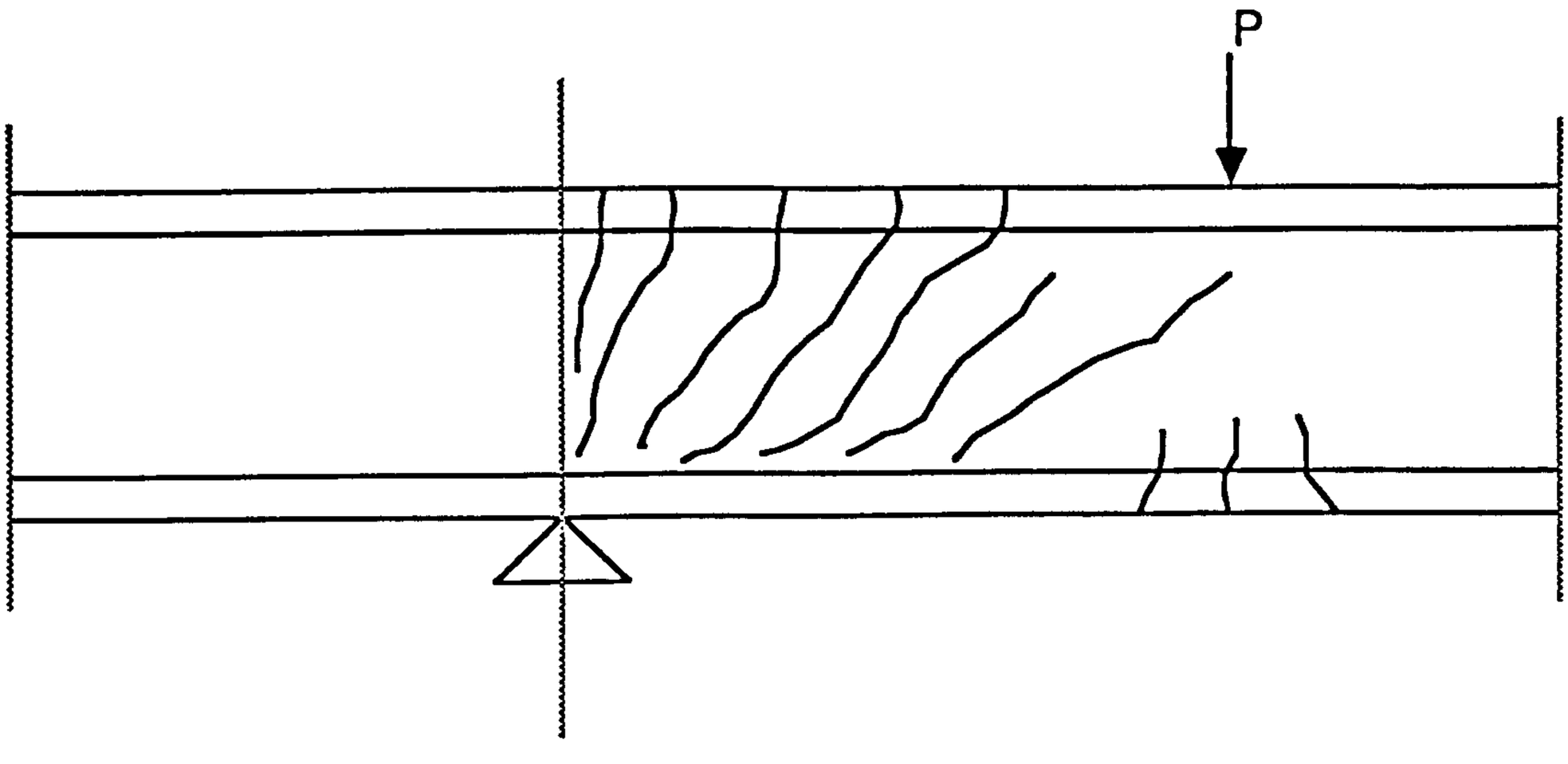

Crack Pattern in a Continuous Beam

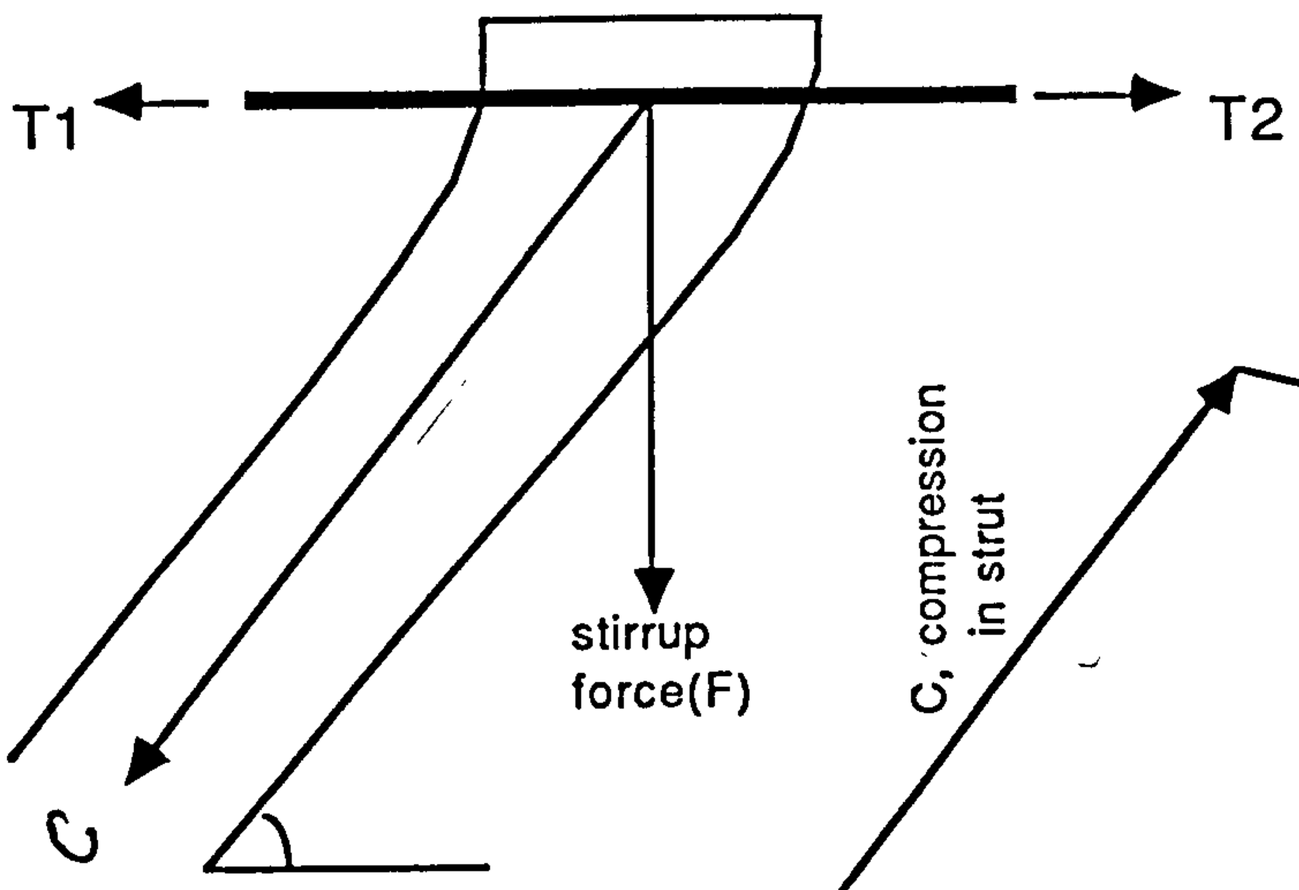

Forces acting on a
single strut

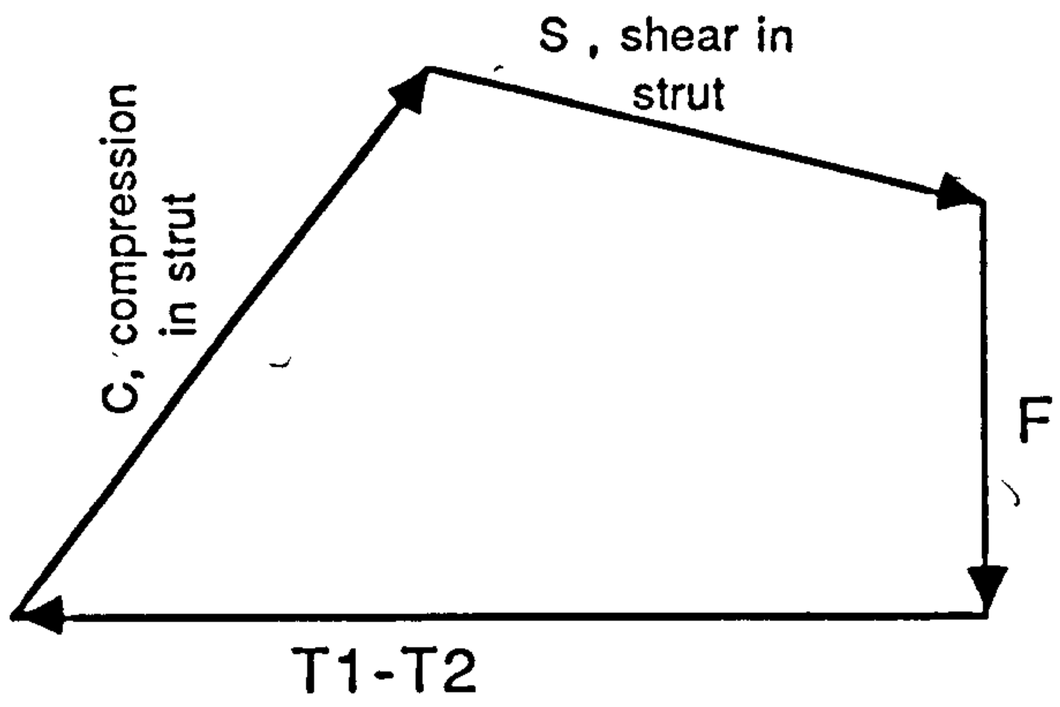

Polygon of forces acting at
top of compression strut

FIG. 2.3 Mechanism of Diagonal Compression Failure[8]

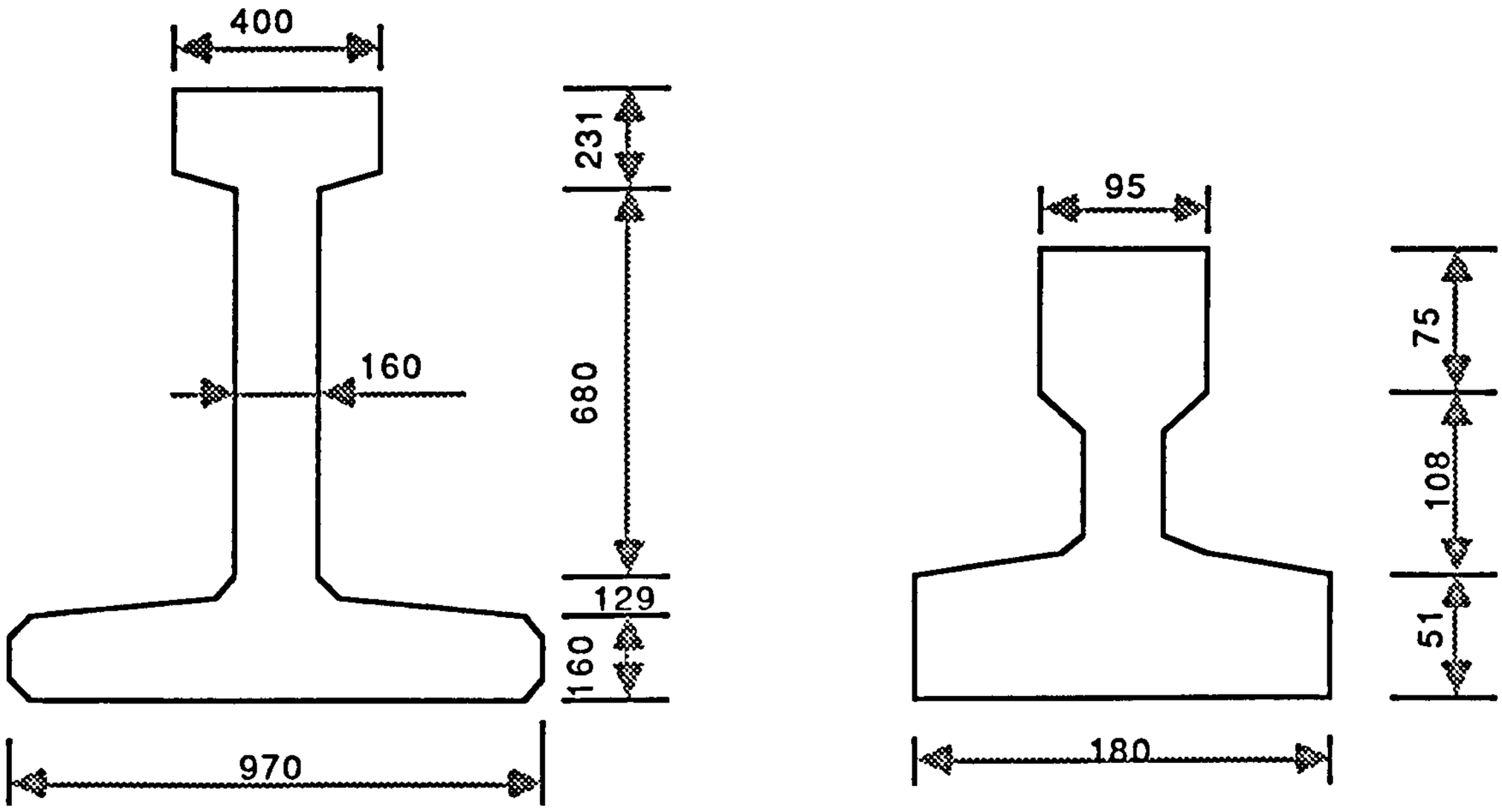

(I) (II)

FIG. 2.4a I) Prototype M-8 and II) Model for Testing
(Refs. 3,4,5)

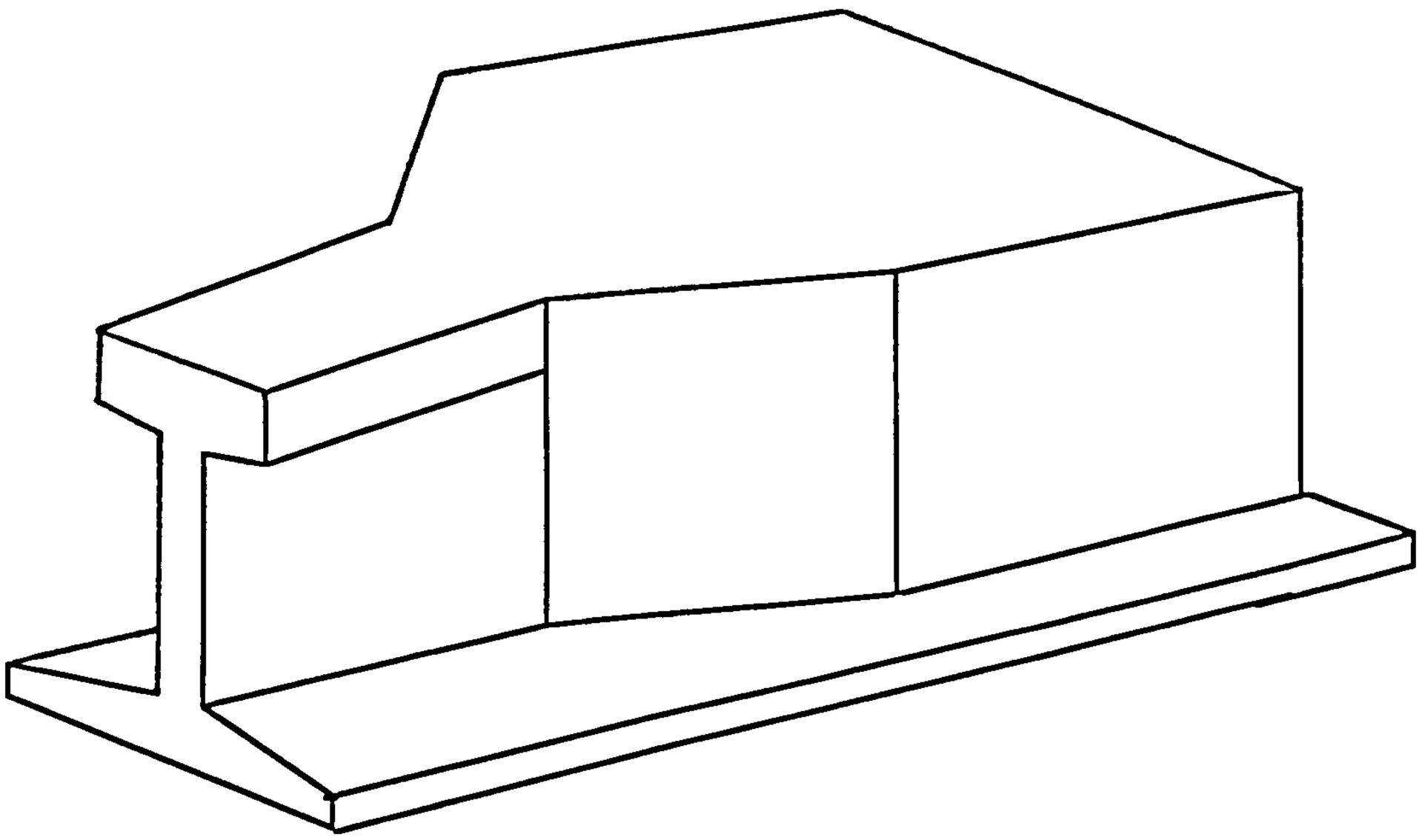

FIG. 2.4b Initially Proposed Tapered End Block[3]

CHAPTER THREE

DESIGN AND FABRICATION OF TEST BEAMS AND EXPERIMENTAL MEASUREMENTS

3.1 Test Program

The test program was designed to observe the behaviour of the connection between a precast-pretensioned M-beam and an insitu concrete crosshead support when subject to shearing forces. Different construction details at the joint were also examined to determine the efficiency and practicality of including physical connections between precast and insitu concretes.

3.2 Test Beam

3.2.1 Prototype Beam

M-beams are standard beam sections which are widely used in medium span bridges throughout the U.K. Although initially developed to be installed at one metre centres they have since been used at centres up to nearly twice this figure in standard beam and slab bridge decks, and the range of sections[63] from 720mm to1360mm (M2 to M10) enables single spans of up to almost 30 metres to be achieved.

When consideration was given to utilising design data from an existing bridge, the scheme chosen namely Barnes Meadow Interchange, Northampton had incorporated M8 beams, and it was for this reason that the research project adopted this particular size for the model.

3.2.2 Model Beam

The model M8 beam has a cross-sectional scale factor of 1/3 to give a height of 400mm (see also Figs. 3.1a and 3.1b). As far as the longitudinal scale

factor is concerned, it is not of great importance to have the same scale factor provided that deflection is not a subject of major importance. The maximum span for an M8 section is about 27 metres and the longitudinal scale factor of 1/9 adopted here gave a 3.0 metres span.

3.3 Manufacture of Pretensioned Beam

3.3.1 Reinforcement Cage

The reinforcement cage was fabricated in the laboratory and placed in the model prior to the pretensioning operation (see Fig. 3.6 for size and number bars).

Transverse horizontal web holes for those beams with either transverse post-tensioning or web shear connectors were formed by placing 10mm plain bars covered with polythene at the required locations in the web in the end overlapping zone. These bars were thus effectively restrained from any movement during casting and vibration, and were later withdrawn soon after demoulding. Link reinforcement was made as a one piece web and flange type (see Fig. 3.2a).

3.3.2 Prestressing Strands

Bridon 8mm low relaxation 7-wire (Supa-7L-R) prestressing strands with an actual steel cross-section of 38.0mm^2 and a minimum breaking load of 70kN were used. Test specimens of prestressing strands and high yield bars were load tested in an Instron machine and typical stress-strain curves for strands and high yield bars are shown in Figs. 3.3a to 3.3d.

3.3.3 Pretensioning Operation

Having decided to use pretensioned prestressed beams it was necessary to

have the strands stressed inside the mould prior to the concreting. The prestressing bed used comprised a set of heavy steel channels, which are capable of transmitting the total prestressing force, against which the prestressing strands were anchored in transverse end steel plates. (see Fig. 3.4) .

The whole end plate with the strands was pulled with two 200kN jacks placed between the steel bed and a short beam holding the end plate via two thick bolts (see Fig. 3.4). Before final stressing , strands were stressed individually to 5kN each with a CCL jack to take up any slack and then all the strands were stressed together as described above, to 70% of their breaking load.

3.3.4 Deflected Strands

Since the beam is to be used in a continuous structure it was decided to deflect some of the strands to have the required strength in the negative bending moment zone. Sets of rollers were mounted in the steel side moulds and contact surfaces between the rollers and side moulds and also between rollers and strands were lubricated to minimize the frictional losses.

3.3.5 Concrete Mix for Precast Beam

Aggregate: The Maximum size of coarse aggregate was 10mm to give approximately the same scale factor as the test beams and fine aggregate grading was according to zone three of BS882.

Cement: Ordinary portland cement with no additives was used all the beams.

Mix proportion:

Aggregate cement ratio: 4.8

Water cement ratio: 0.5

Percentage fine Agg. : 34.5%

Because of the relatively small dimensions of beam (e.g. 56mm web thickness) and the high amount of shear reinforcement in the connection zone, there was a potential congestion problem for concreting. Consequently a very workable concrete having a slump of 80mm to 120mm was used. Compacting was assisted by two mounted vibrators on the top of the moulds along the beam length.The concrete strength for the precast beams was between 62 to 72 N/mm^2.

3.3.6 Release of Prestressing Force

Usually 7 days after casting the beam, compressive and tensile strengths of concrete were obtained from control specimens and the prestressing force was released subject to sufficient concrete strength having been achieved.

3.3.7 Curing

Normally beams were cured in the curing room in 100% humidity for about 3 to 7 days and then transported to the main laboratory to be prepared for the insitu concrete casting.

3.4 Manufacture of In-situ Crosshead and its Connection to Precast Beam

3.4.1 Formwork

The insitu concrete comprised a full depth rectangular section which overlapped the M-beam by 300mm (or 100mm in some later tests) and continued along the top of the M-beam with a depth of 60mm as a composite top flange. The M-beam was placed on a smooth bed, two deep side channels were

employed to form the sides of the rectangular section and also to hold two angle sections forming the top flange of the M-beam (see Fig. 3.5).

3.4.2 Reinforcement

A reinforcement cage for the solid box and top flange was fabricated and placed into the mould and over the top flange of the M-beam. Longitudinal deformed bars at the top of the solid box were extended along the top flange to take the negative bending stress produced in the support section and at the joint (see Plate 3.2).

Link reinforcement in the nibs (in-situ concrete overlapping the M-beam) was installed as in Fig. 3.2a.

In two tests all of the longitudinal bars and strands from the precast beam were extended into the in-situ section but in the rest only a nominal amount (3 No. T8 bars) at the bottom of M-beam extend into the in-situ concrete. This allowed for possible positive bending moment at the joint during the lifting. It is worth mentioning here that in practice this reinforcement is required for possible positive bending moment as a result of shrinkage and support settlement. Each test beam had specific connection details to represent different ways of achieving shear transfer and Figs. 3.6a,b,... show details of the M-beams , in-situ concrete and connections. These details will also be discussed in the 'experimental results' section later in the thesis.

3.4.3 Concrete Mix and Curing of the Insitu Concrete

The cement and aggregates used for the M-beam were also adopted for the insitu concrete in the beam. The mix proportions were as follows :

Aggregate cement ratio : 6.35

Water cement ratio : 0.6

Percentage fine Agg. : 35.6%

The compressive strength of the insitu concrete at the time of testing varied between 50 to 55N/mm^2.

As there was no congestion problem for this part the allowable slump was between 30mm to 50mm.

Generally the formwork was stripped after ten days and the beam was cured in the laboratory under hessien and polythene sheeting before testing.

3.5 Horizontal Shear Connectors

The contact surface between the precast and insitu concrete should be capable of resisting horizontal shear forces produced by the vertical shear force. The connection was designed according to BS8110[27] which uses a different method from the previous code CP110[64] which was very conservative. The CP110 service method is based on the bond failure between precast and insitu concrete so the contribution of steel connectors are not additive. It is also debatable whether horizontal shear is a serviceability problem.

BS8110 considers this as an ultimate limit state problem and a less conservative method taking into account the effect of steel strength is recommended. In the design of the test beams it was necessary to provide extra shear connectors, in addition to the stirrups particularly in the region of high shear (between span load and continuous support).

The contact surface skin and laitence were removed by the use of a needle gun prior to casting the insitu concrete.

3.6 Experimental Measurement

3.6.1 Deflection

Mechanical dial gauges with an accuracy of 0.01mm/Div. were used to

measure the deflections. These were mounted at the top of the bottom flange at midspan and cantilever, making it possible to measure the deflections up to failure without damaging the gauges.

3.6.2 Stirrup Strain Measurement

The following methods were considered for the measurement of strain in the stirrups:

a) The use of electrical strain gauges

b) Mechanical method

In the first method strains are measured by mounting electrical resistance strain gauges on the reinforcement and using a data logger. In the second method strain can be measured by means of two DEMEC discs located on steel studs which are soldered to the leg of the stirrup and project to the surface of beam through sleeves comprising greased PVC tubes, to prevent them adhering to the concrete. It has been reported[62] that there are problems associated with this method involving movement of the studs during the casting and also breaking of the connection between studs and stirrup when inclined cracks widen, which results in the effective loss of the gauge. In addition to this mechanical measurement of stirrup strain is practically more difficult and less accurate than the electrical method.

In view of these problems, it was decided to adopt the electrical method . Surface preparation prior to installation of gauges was carried out in the following way:

a) Removing the deformed bar ribs, over a length of 35mm of the stirrup's leg.

b) Cleaning the smooth surface with the application of acetone, an acid solution (conditioner) and finally an alkali solution (neutralizer).

T6 stirrups were used together with 5mm strain gauge (TML-PL5) with a

nominal resistance of 120.0 Ohms and a gauge factor of 2.0. The adhesive used was a P-2 two parts epoxy resin type . As this is not a fast curing adhesive it was necessary to cure the joint for about ten hours under a uniform pressure applied with a spring clamp while covering the gauge with a piece of silicon rubber.

Since the gauged stirrups are eventually totally inside the concrete, they must be covered carefully to resist against mechanical shocks and water penetration. Coating agents used are as follows :

1) M-coat 'D' for the electrical insulation.

2) M-coat 'G' or Bostik which are two parts materials and become like rubber after curing. This coating is to absorb the mechanical shocks during the fixing and concreting.

3) An oil paint to prevent water penetration

4) Bituminous paint coating for extra waterproofing.

'PTFE' wires were soldered to the gauge prior to coating. These are waterproof wires with a high tensile strength to prevent breaking during the casting.

3.6.3 Surface Strain Measurement

Surface strains were measured either mechanically by the use of DEMEC gauges or electrically by TML-PL60 gauges. In the former case metal DEMEC discs were glued to the surface of the concrete. For electrical strain gauges the surface was cleaned and covered with fast setting Araldite epoxy resin, curing for about 10 hrs. and finally rubbed with a fine sand paper. The surface was cleaned and the gauge fixed with Cyanoacrylate super glue adhesive.

3.6.4 Interface Strain Measurement

In the overlapping zone it was decided to measure the surface strain of the

precast web embedded in the concrete as well as the external surface strain at the same level on the insitu nib, for comparison. For this purpose PL60 electrical gauges were fixed to the surface of the precast beam in the region which would be embedded in the insitu concrete (see plate 3.1). The coating was as described in 3.6.2, to prevent damage and water penetration.

3.6.5 Arrangement of the Gauges

The mechanical or electrical gauges fixed on the surface were either longitudinal (individual) or rosette (set of three). The former determine the strain distribution vertically while the latter may be used to determine the principal strains. A rosette consists of at least three gauges in different directions at one point (normally horizontal,vertical and inclined directions).

For electrical PL60 rosette formation, the gauges were fixed so that their central marks passed through one point rather than fixing them separately. This was to get a more accurate result.

3.6.6 Vertical Separation Between Precast and Insitu Beam

When the connection is under a shearing force, the precast beam and insitu concrete have a tendency to separate from each other. The best place to measure this separation was along the overlapping zone between the bottom flange of the precast beam and lower part of the insitu nib as in Fig.3.7. The DEMEC gauge used had a length of 2" with an accuracy of 24 micro strain per division.

3.7 Detection and Measurement of Crack Widths

A hand lamp and a magnifying glass were used to detect the first cracks. The cracking load was noted and all inclined and flexural cracks were marked up to

failure. For the measurement of the inclined crack width a hand microscope with an accuracy of 0.02mm per division was used.

3.8 Measurement of the Prestressing Force during Manufactur of the Beam

For each strand a cylindrical load cell was placed between the end plate and the anchor barrel to measure individual forces in the strands. (A further check was made by the jack pressure dial gauge which gives the total force). The load cells were designed to withstand the maximum prestressing force (70% of the breaking load) within their elastic capacity. Four PL5 electrical resistance strain gauges were fixed (horizontally and vertically) and connected to form an electrical Wheatstone bridge (see Fig.3.8). The same type of load cell was also at a later stage used to measure the post-tensioning force in the beam with transverse prestressing.

3.9 Data Logging System

An Intercole Compulog datalogging system was used to read the strain gauges and load cells. The Compulog has a maximum capacity of 99 channels and a reading speed of 33 channels per second. The system can accept either a quarter bridge or a full bridge connection and for these tests Plessy 23-Pin plugs were used for quarter bridge connections (10 channels per plug). In addition two dummy gauges were fixed on a 100mm by 100mm cube, one of which comprised a PL5 gauge fixed on a piece of T6 bar inside the concrete and the other a PL60 gauge fixed on the cube surface, both similar to actual gauges in the beam. Dummy gauges were common to all channels.

The logging system was programmed to give the actual strain in the gauge with an accuracy of one micro strain. For load cell readings Plessy 7-Pin plugs

were used. The connection is shown in Fig. 3.8. The computer output storage was available on a floppy disk and also gave a printed copy.

3.10 Testing of the Beam

3.10.1 Loading Arrangement

Since the connection behaviour to be investigated represents a continuous beam, and the longitudinal scale factor is smaller than the cross-sectional scale factor, a loading arrangement consisting of one span (precast beam) and a cantilever extension (in-situ solid box) was adopted (see Fig. 3.9) . This arrangement has the advantage that any combination of shear and bending moment in the connection can be obtained by changing the position and magnitude of both the span load P and the cantilever load Q.

This arrangement is also useful when a high shear force is required in the connection while avoiding a premature flexural failure in either the support or midspan sections. Loading was applied with a 300kN jack through a 610mm(24") deep steel 'I' section spreader beam to distribute the total load into span and cantilever loads. The total load was applied in 25kN increments. For each load strain readings (mechanical and electrical) and deflections were taken and also inclined cracking load and crack width were noted where appropriate up to final failure of the beam. Plate 3.3 and Fig. 3.10 show a photograph and a diagrammatic view of the testing rig together with two types of loadings including their bending moment and shear force diagrams.

3.10.2 Shear Span to Effective Depth Ratio

The connection was investigated for its capacity to transfer the maximum possible shear force in the precast beam allowed by the code (nearly all codes of

practice limit the maximum shear force in a concrete section by that required for a web crushing failure).

Each side of the connection (precast or in-situ beam) was designed separately to resist the maximum shear force and the connection was tested to see whether it was capable of producing this shear resistance in either part. This rather high shear force necessitated a shear span to effective depth of between 2.8 to 3.7 for the test rig and loading arrangement. The effect of shear span to effective depth ratio upon the shear strength of monolithic reinforced or prestressed concrete beam is found[44,59] to be insignificant when its value is greater than 3.0 .

3.11 Range of Variables Investigated in the Test Program

Differences in the test beams were mainly in the connection details which can be summarised as follows:

a) The first detail considered was a connection with a 300mm overlapping length in which the in-situ concrete nibs contained shear reinforcement and all reinforcing bars and prestressing strands in the precast beam were projected to a length of 1.00 metre into the in-situ concrete . This detail is similar to those used recently in some U.K. motorway bridges as mentioned in section 1.2.7 (see also Fig.3.2b.

b) To examine the effect of dowel action of the projecting bars from the precast beam into the in-situ concrete. In previously constructed bridges (see section 1.2.7) the bars from the M-beams were continued by means of couplers into the in-situ concrete. In this test the dowel action of these projecting bars, from the M-beam itself and also the continuity bars in the top flange, was eliminated by sleeving them at the interface. This sleeving was 50mm long and was 15mm thick around each bar as shown in Fig. 3.11. All other details were exactly as in case (a).

c) To evaluate the effectiveness of the in-situ nib shear reinforcement, in this test no shear reinforcement was installed in the overlapping in-situ concrete. In addition to that , the stirrups in the end of the precast beam had the same spacing as the stirrups in the rectangular section adjacent to the end of prestressed beam. The reason for this was to see the effect upon the shear transfer capacity of the joint if the overlapping zone (consisting of precast and in-situ concrete) was designed for shear as a monolithic rectangular section (similar to the crosshead in practice).

d) In practice, the distance between the end of the M-beam and the support may vary, making the negative bending moment at the connection high when it is near the support or low when it is near the point of contraflexure, while the shear force is more or less the same (specially for point loading). In this test the connection was subjected to a higher bending moment whilst the same shear force remained as before. Other details were as in case (c) i.e. no stirrups provided in the in-situ concrete nibs.

e) The embedment length is an economical consideration. If we can reduce its length some material will be saved. It was decided to try only 100mm embedment in this test instead of the 300mm used before. The in-situ concrete nibs had two T6 stirrups in this test. Since the same mould (for 300mm embedment) was used it was decided to leave 200mm of the precast beam unused from the other end to allow 100mm embedment.

f) This test was also performed with 100mm embedment length but the difference from case (e) was the absence of stirrups in the in-situ nib to investigate the necessity of the stirrups for small embedment lengths.

g) It was felt during the test program that the top flanges of the M-beam, in spite of their small width, may have considerable effect upon the shear transfer capacity of the connection. In addition to that a simulation of the initially suggested tapered end block[3,4,5] was needed.

That end block (although not used in practice because of economy and its

unproven behaviour) is formed by a gradual widening of the web and eliminating the top flange to form a simple inverted 'T' beam section. This section was to be continued along the connection (see Fig. 3.12 and also Fig. 2.4b). To avoid making a new mould, an easy simulation was achieved by placing two small pieces of polystyrene underneath the top flanges of the M-beam along the whole of the embedded length prior to casting in-situ concrete (see Fig. 3.13). These pieces were taken out before testing the beam. In this test the in-situ nib was reinforced with nominal shear reinforcement.

h) It was observed from the test on the connection having the feature explained in (g) above that in fact the shear transfer capacity of the connection reduces substantially. It was thus decided to improve the strength of such connection (i.e. for inverted 'T' sections without top flanges) by different means. In this test the connection was stressed transversely with four 9.8mm 7-wire strands. Ducts of 10mm diameter were accordingly made in the web of the precast M-beam and its overlapping in-situ concrete nibs. 15mm steel bearing plates were used on each side to distribute transverse loads uniformly (see plate 3.4). Cylindrical load cells were used to measure the post-tensioning force in each strand and the ducts were left ungrouted for the testing.

i) Instead of transverse prestressing (as in (h) above) it was decided to use horizontal bars passing through the M-beam's web and into the in-situ concrete nibs. These web shear connectors comprised 10mm Dia. mild steel bars (i.e. approximately the same diameter as the strands in the transverse post-tensioning test).

Four ducts were made in the web of the M-beam by placing pieces of 10mm dia. mild steel bars covered with polythene tape inside the mould. These bars were taken out after demoulding (see Fig. 3.14a). Before casting the in-situ concrete, 10mm mild steel connectors were threaded into the web and the ducts were grouted in order to be able to develop the full dowel action. Both sides of the bars were bent to avoid possible bond failure during the test. It should also be

mentioned that the top flange effect was eliminated as in tests explained in (g) and (h) above to represent a simple inverted 'T' beam.

j) In the tests without the top flange effect (i.e cases g,h,i above), from all existing bars in the precast beam (a total of 13) only 4T8 projected into the in-situ concrete for possible positive bending moment during the lifting in the test and also provided for shrinkage and support settlement in practice.

In this final test it was decided to leave all 13 bars projecting 1.0 metre into the in-situ concrete. This was to observe the contribution of dowel forces to the shear transfer capacity where there is no other means of shear transfer capacity acting.

3.12.1 Designation of the Beams

A coding system was used for the beams which can be seen in the beam test photographs. At the right hand side of each designation the serial numbers from 1 to 10 can be seen. Other letters have the following meanings:

E30 : Embedment length is 300mm (30cm)

E10 : Embedment length is 100mm (10cm)

WTF : Connection without top flange

Other letters refer to reinforcement detail in the connection, loading arrangement, special features such as transverse prestressing, web shear connectors etc. . Table 3.1 shows a summary of the different connection details used throughout the investigation.

3.13 Complementary Dowel Shear Tests

3.13.1 Test Specimen

As explained in 3.11(i) test No. 9 (see table 3.1) consisted of web shear connectors with the top flange effect eliminated. To obtain more information about

the effectiveness of this type of connection, especially the effect of bar size and strength, bond between precast beam web and in-situ concrete and different curing conditions, it was decided to design a dowel-interface shear test specimen.

This specimen comprises a 100x100x100mm cube representing the precast beam web. A bar was fixed inside the cube horizontally before casting leaving a projected length of about 70mm from each side (see Fig. 3.15a).

A 300x300x100mm mould was made for the concrete representing the in-situ part. A 100x100x30mm piece of polystyrene was placed at the middle of this mould, and the concrete cube was fixed over that and the mould was filled with concrete (see Fig. 3.15b). Specimens made in this manner can be tested for shear in a simple compressive test machine (see Fig. 3.15c).

3.13.2 Range of Variables

In general the following variables were investigated:

1) Bar size , changing from 10mm to 16mm

2) Bar strength, mild or high yield steel

3) Curing in wet conditions

4) Curing in dry conditions

5) Natural bond between cube and surrounding concrete

6) Eliminating the bond by covering the cube with polythene sheet.

For each bar size or strength, all the above conditions (3,4,5,6) were examined. The concrete mixes were similar to those used in the main beams for both precast and in-situ parts. Table 3.2 shows a summary of details and conditions for the 28 specimens tested in this part of the investigation.

3.14 Control Tests

Control specimens were made from the concrete used for each precast and

in-situ beam. These included cubes and prisms for the determination of compressive strength and modulus of elasticity respectively. They were cured in the same conditions as the test beams.

The control specimens were tested soon after the main tests. These tests were carried out in accordance with BS1881 : 1970[65] . Table 3.3 shows the average test results . The following tests were carried out:

3.14.1 Compressive Strength Test

For each precast beam six 100x100x100mm concrete cubes were tested, three at the time of prestressing transfer and the others shortly after the main beam test. Nine concrete cubes were taken from the in-situ beam concrete (three from each batch) and were tested after the main test.

3.14.2 Modulus of Elasticity

The modulus of elasticity tests were carried out on 100x100x500mm prisms taken from precast and in-situ beam concrete. Strain measurement was by an 8" DEMEC gauge fixed on two sides of the column.

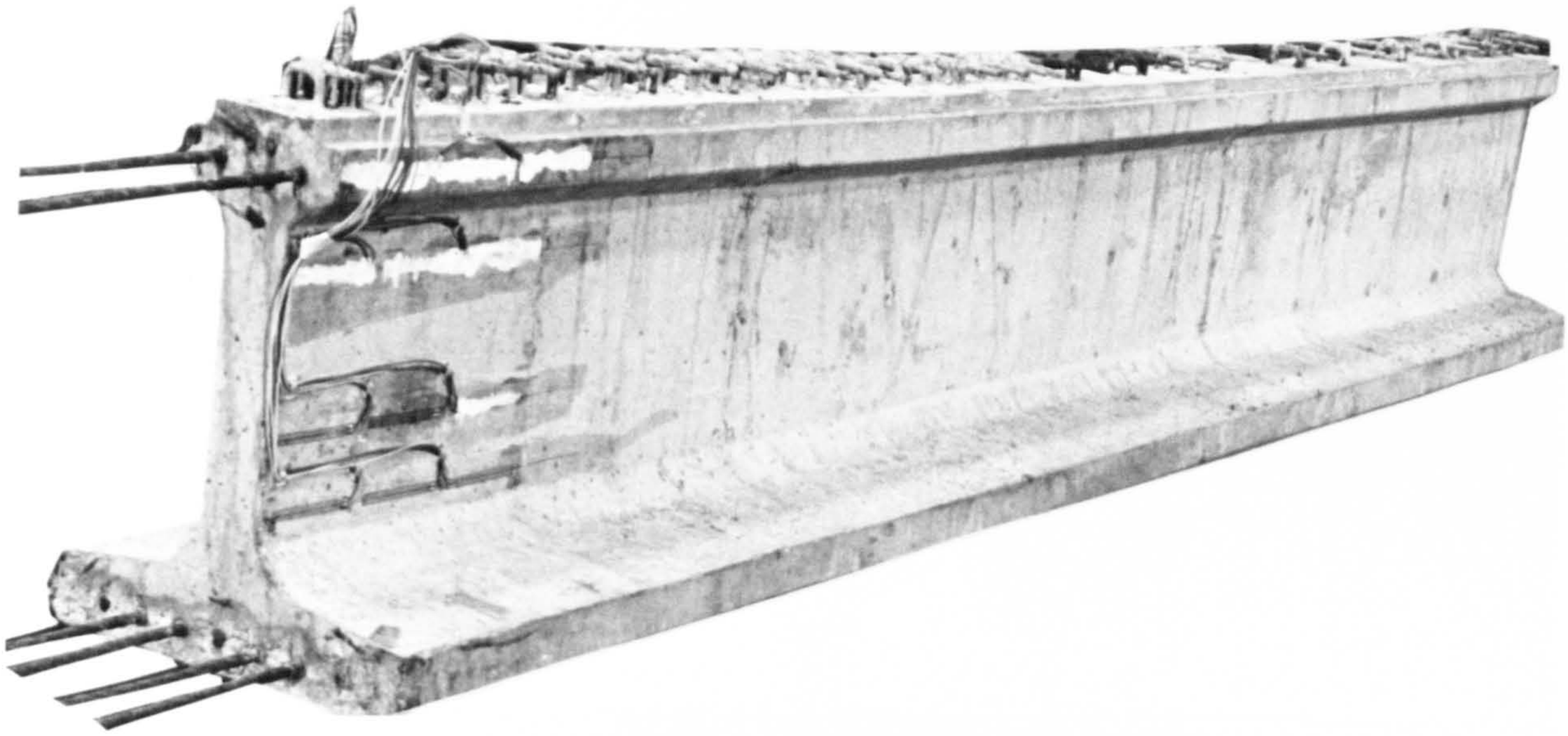

Plate 3.1 Gauged Precast Beam Before Casting In-situ Concrete

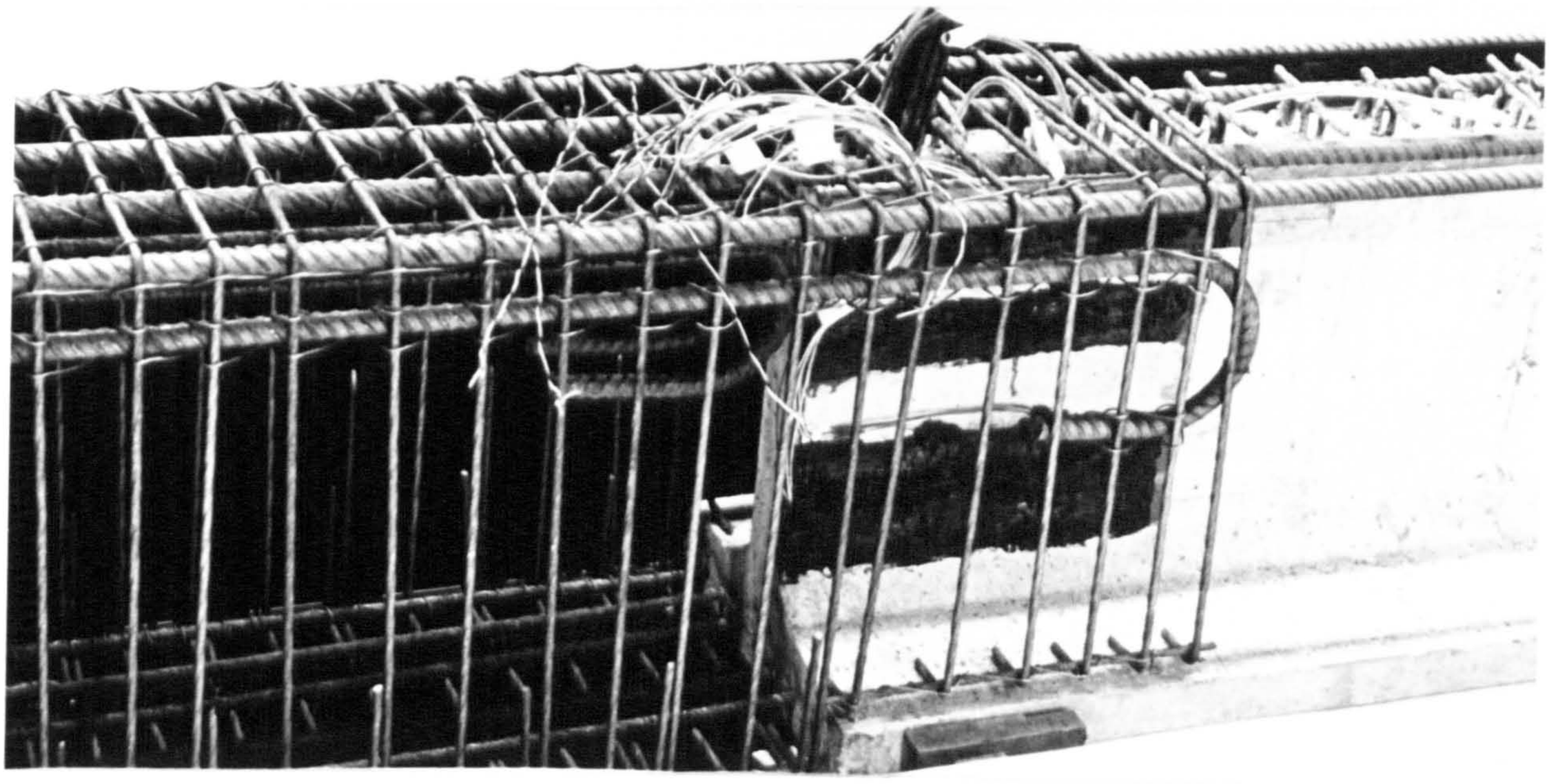

Plate 3.2 The Connection Prior to Casting of In-situ Concrete

Plate 3.3 Transverse Prestressing at the Connection

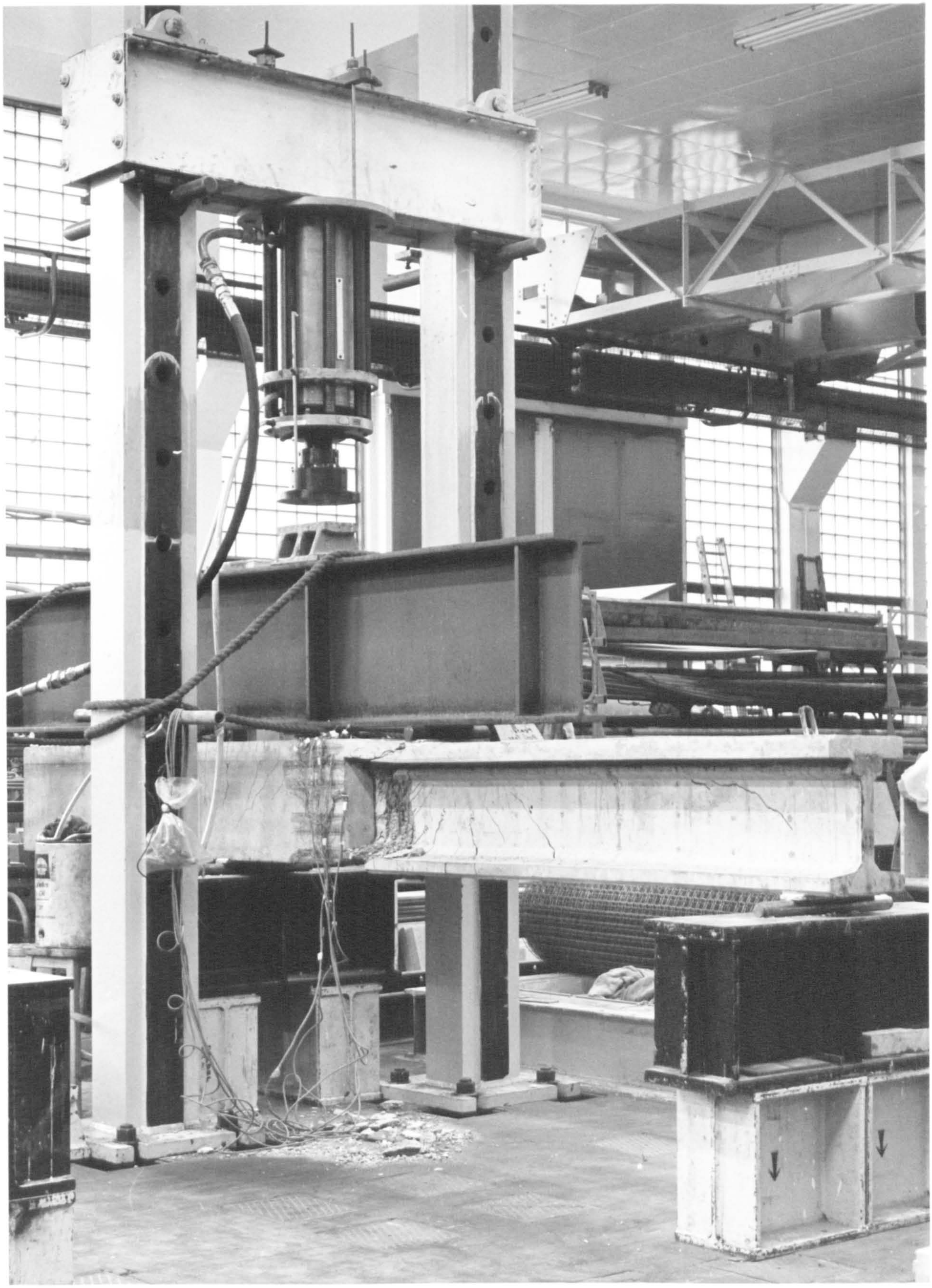

Plate 3.4 General View of the Test Rig

Test No.	Beam's Code	Embedment length mm	Top Flange Effect	No. & size of projecting bars	Nib's Stirrups	Loading Type	Additional Consideration
1	E30AA1	300	Existed	7 Strands+6T8	6T6	A	—
2	E30AA2	300	Existed	7 strands+6T8	6T6	A	All Projected bars were Sleeved
3	E30AB3	300	Existed	4T8	NIL	A	—
4	E30BC4	300	Existed	4T8	NIL	B	Higher Bending Moment at the Connection
5	E10CC5	100	Existed	4T8	NIL	C	—
7	E10CD7	100	Existed	4T8	2T6	C	—
6	WTFCC6	300	Eliminated	4T8	4T6	A	Elimination of Top Flanges Effect
8	WTFPCC8	300	Eliminated	4T8	4T6	A	Transverse Prestressing at the Connection
9	WTFCC9	300	Eliminated	4T8	4T6	A	Provision of Web Shear Connectors
10	WTFDCC10	300	Eliminated	7 Strands+6T8	4T6	A	All the Bars Projected to the Insitu Beam

Table.3.1 General Information of the Connection Details

Natural Bond		Debonded	
Wet Curing	Dry Curing	Wet Curing	Dry Curing
R10	R10	R10	R10
R12	R12	R12	R12
R16	R16	R16	R16
T10	T10	T10	T10
T12	T12	T12	T12
T16	T16	T16	T16
PLAIN	PLAIN	PLAIN	PLAIN

Table 3.2 Different Dowel Bars Tested at Various Bond and Curing Conditions

Test No.	Beam Ref.	Precast Prestressed Beam			In-situ Beam & Nibs	
		Average Compressive Strength N/mm^2		Modulus of Elasticity kN/mm^2	Compressive Str. at the Time of Testing N/mm^2	Modulus of Elasticity kN/mm2
		At Prestress Transfer	At the Time of Testing			
1	E30AA1	43.2	68.3	34.0	43.2	29.5
2	E30AA2	48.5	72.0	34.5	41.0	29.0
3	E30AB3	42.4	65.0	34.1	54.0	31.0
4	E30BC4	42.0	66.5	33.8	54.7	32.0
5	E10CC5	46.5	67.2	33.5	52.1	31.6
6	WTFCC6	44.1	69.1	33.4	54.8	31.7
7	E10CD7	47.0	68.1	34.0	56.9	32.9
8	WTFPCC8	45.2	67.5	33.7	53.8	31.5
9	WTFCC9	46.9	64.2	33.6	54.5	32.5
10	WTFDCC10	45.7	62.5	33.0	57.7	34.0

Table 3.3 Concrete Control Test Results

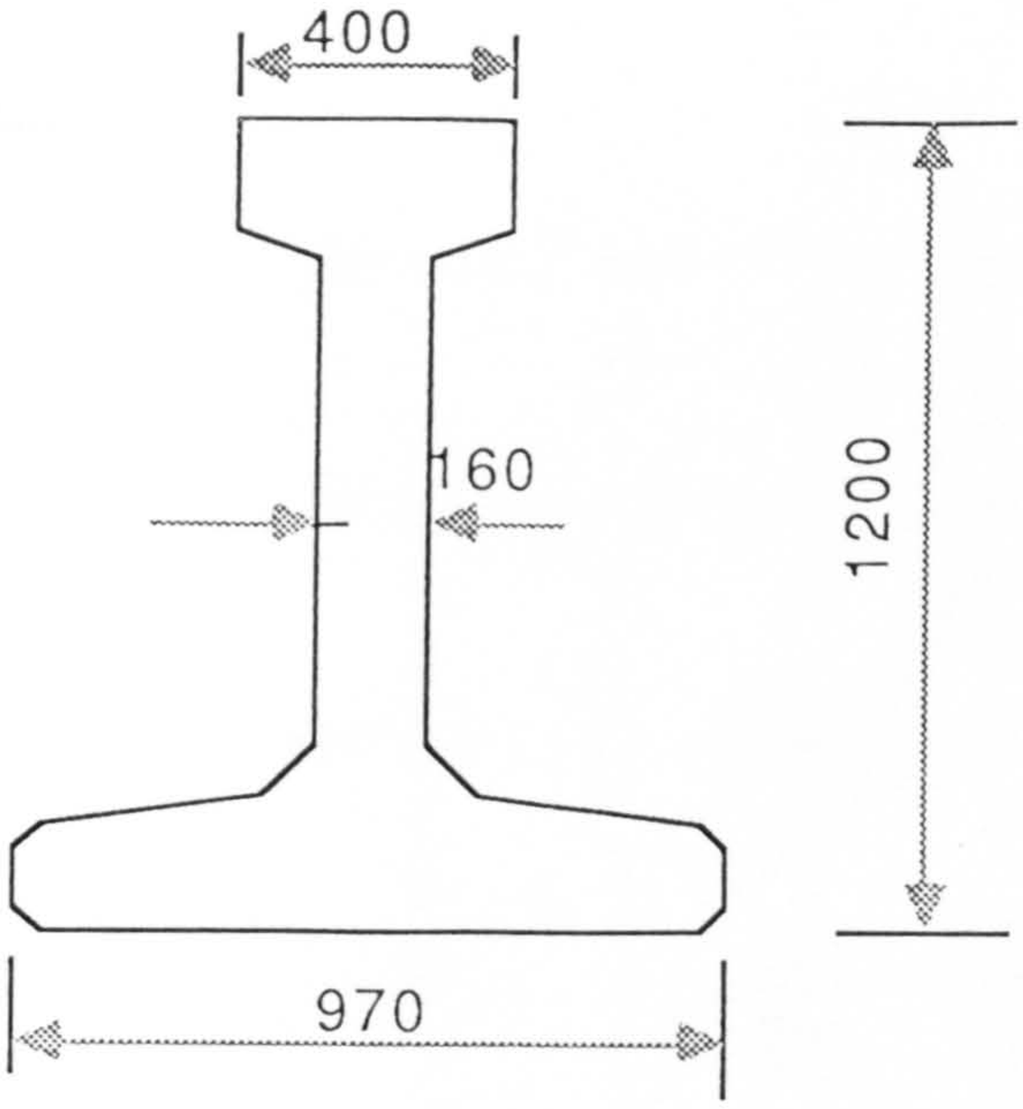

a) 'M8' Prototype

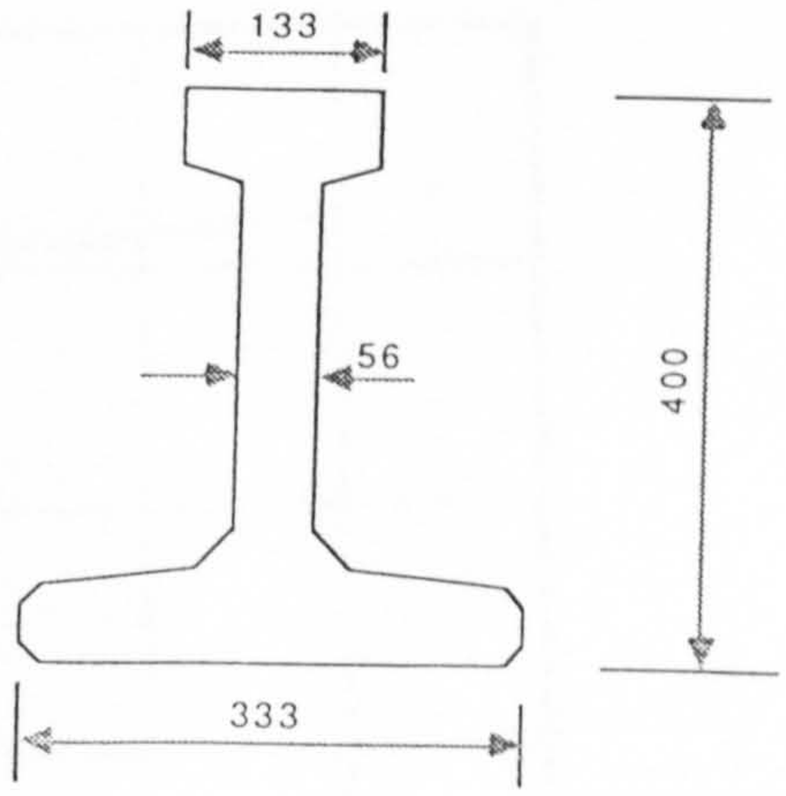

b) 'M8' 1/3 Scale Model

FIG. 3.1 Prototype and Model Dimensions

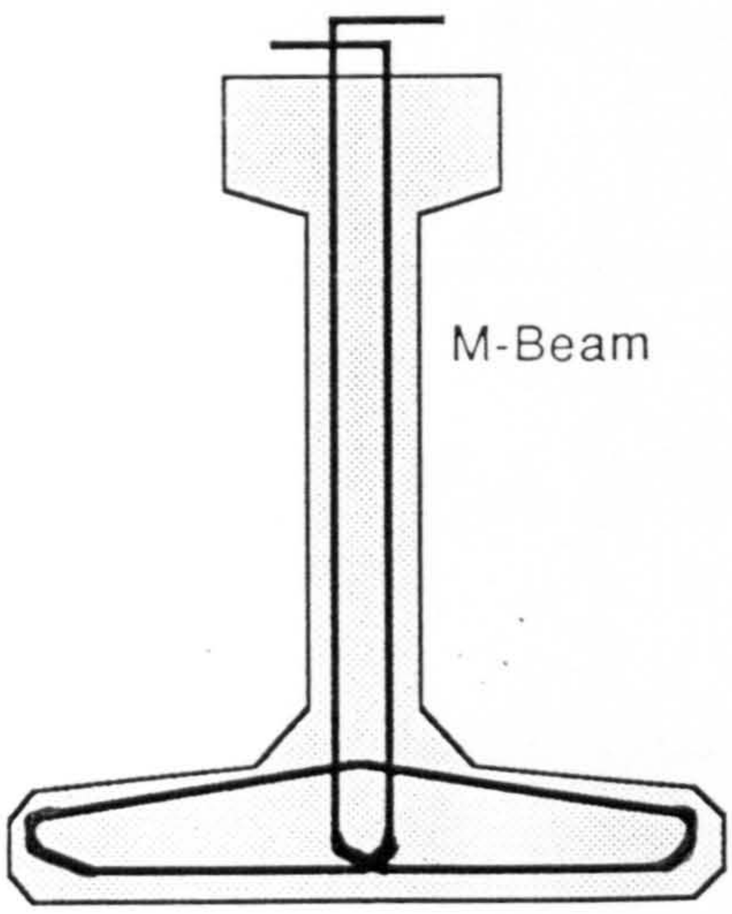

a) Stirrup in the M-Beam

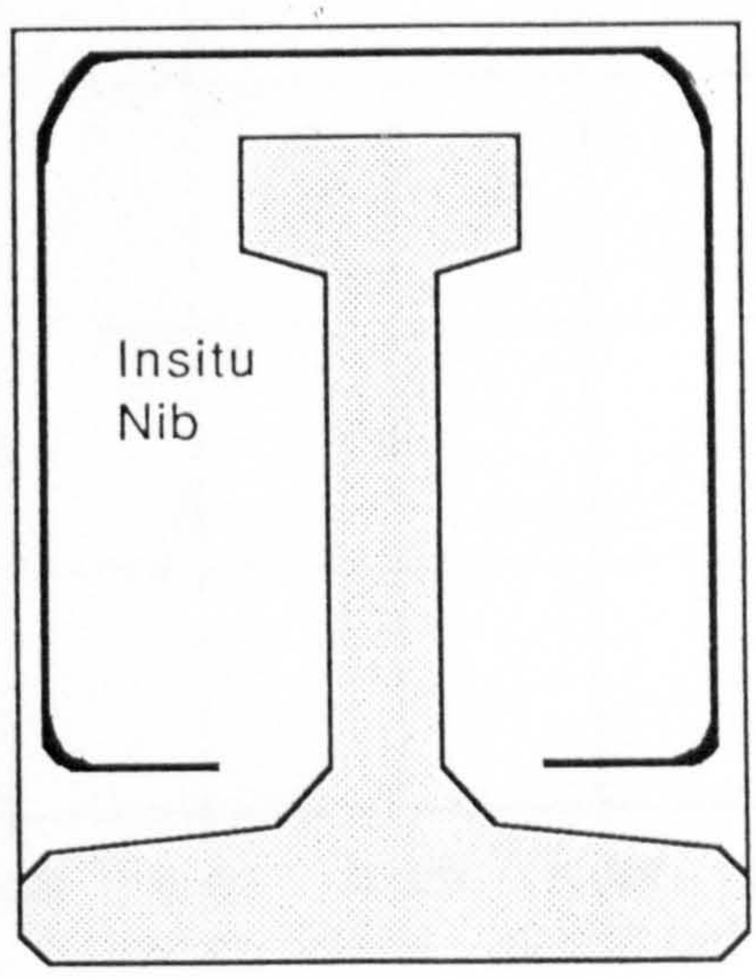

b) Stirrup in the Insitu Nibs

FIG. 3.2 Details of Stirrups for M-Beam and Insitu Nibs

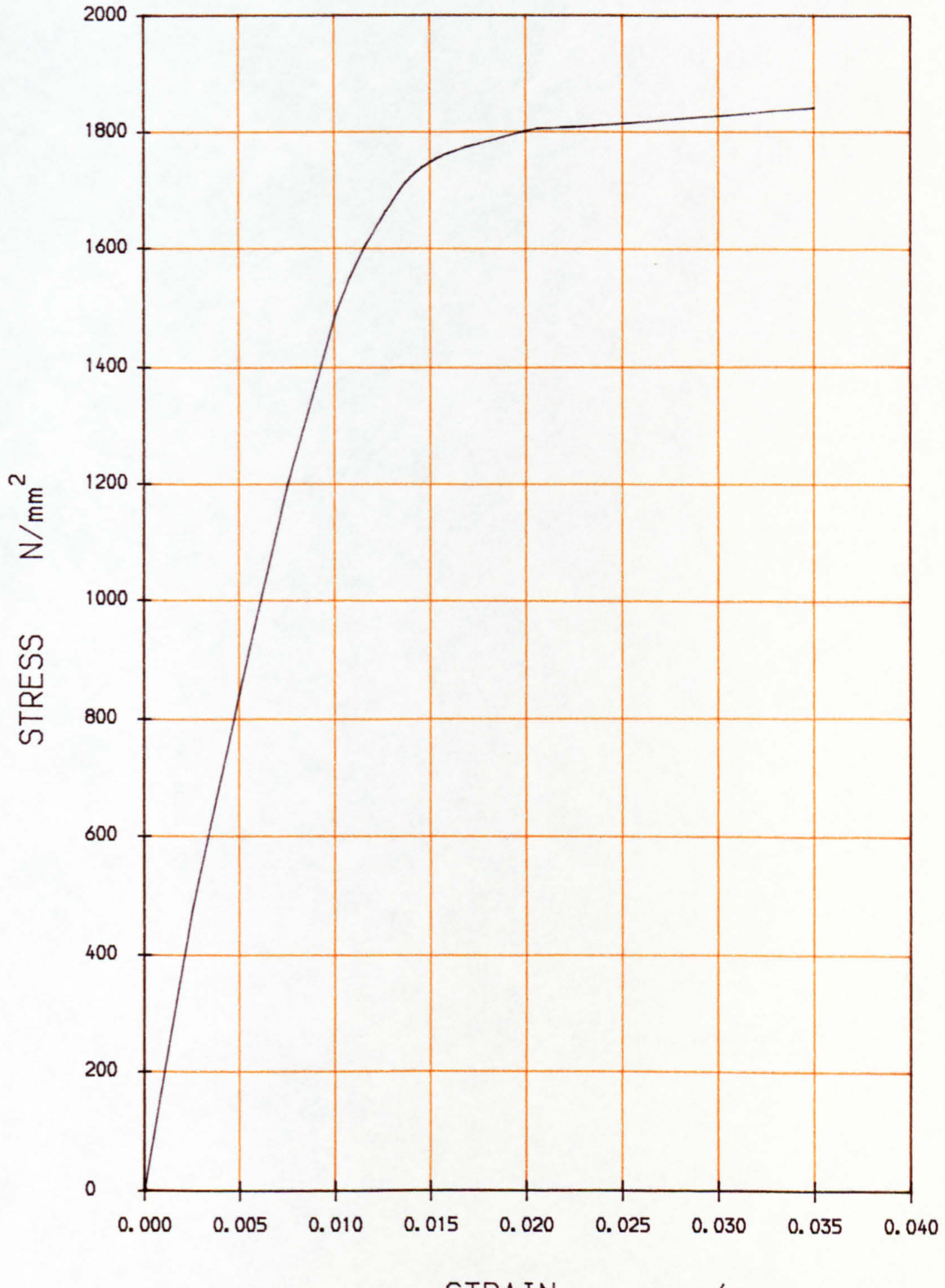

FIG. 3.3a STRESS-STRAIN CURVE FOR 8mm, 7 WIRE STRAND

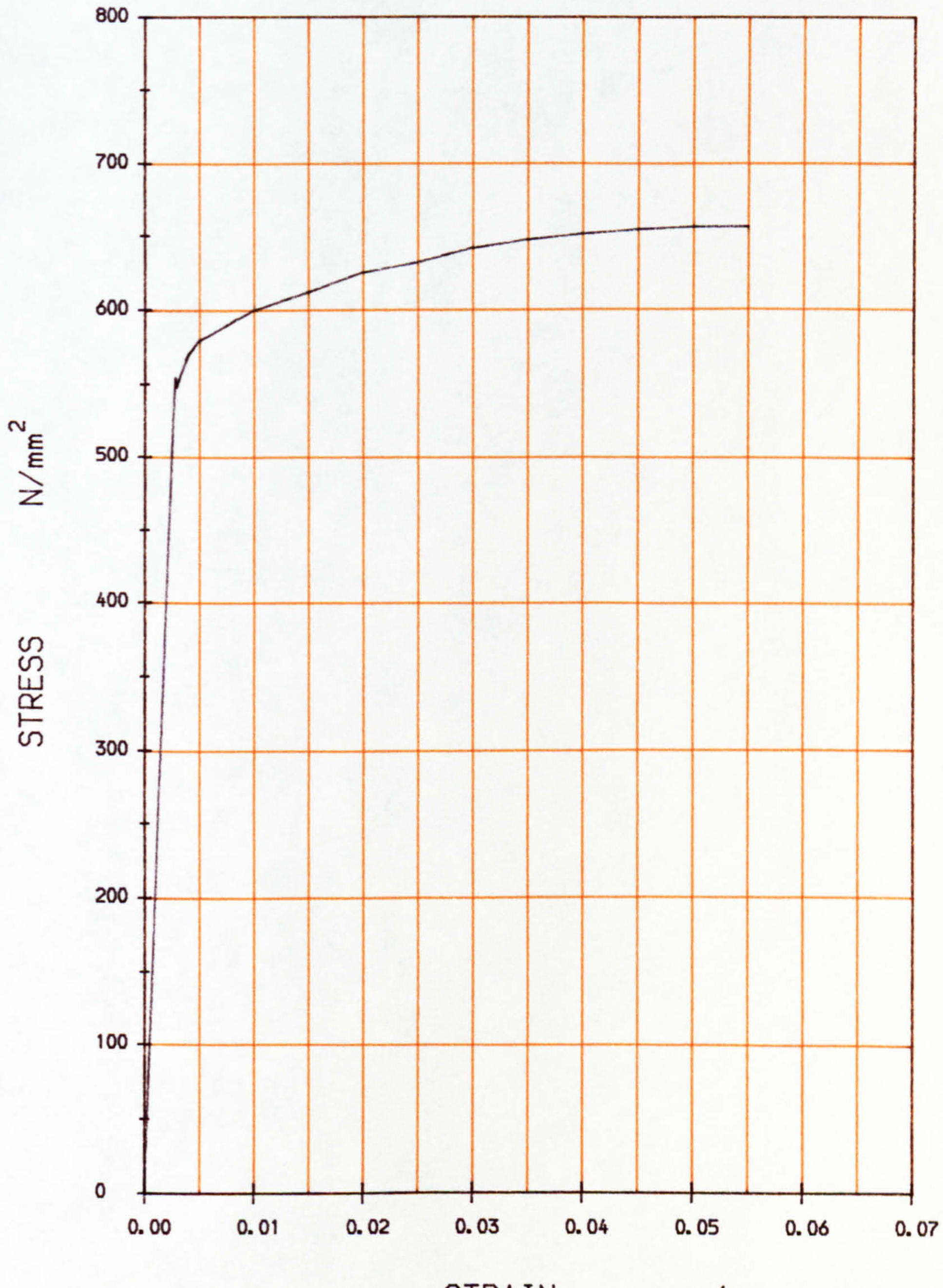

FIG. 3.3b STRESS-STRAIN CURVE FOR 6mm H.Y. BAR

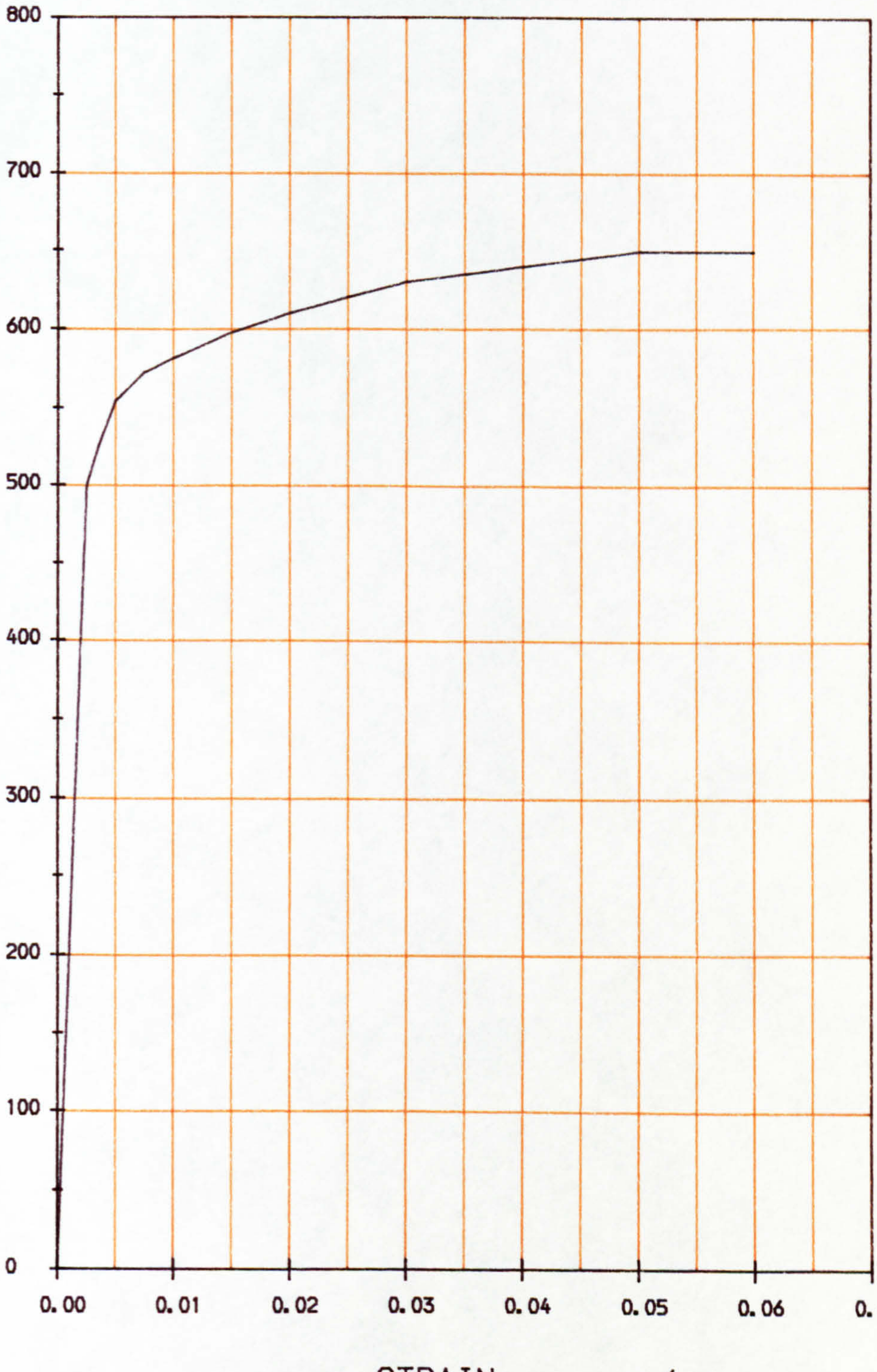

FIG. 3.3c STRESS-STRAIN CURVE FOR 8mm H.Y. BAR

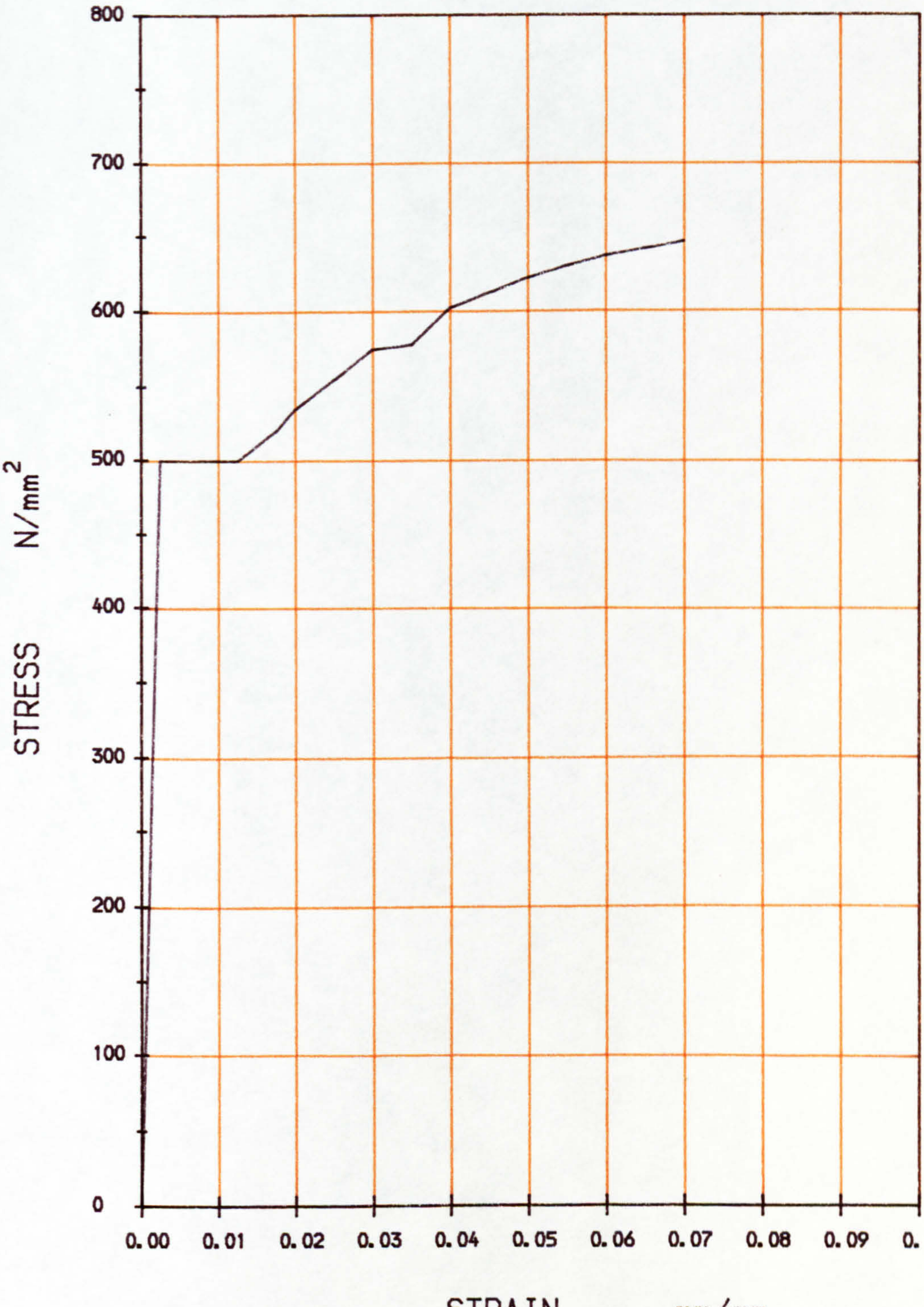

FIG. 3.3d STRESS-STRAIN CURVE FOR 16mm H.Y. BAR

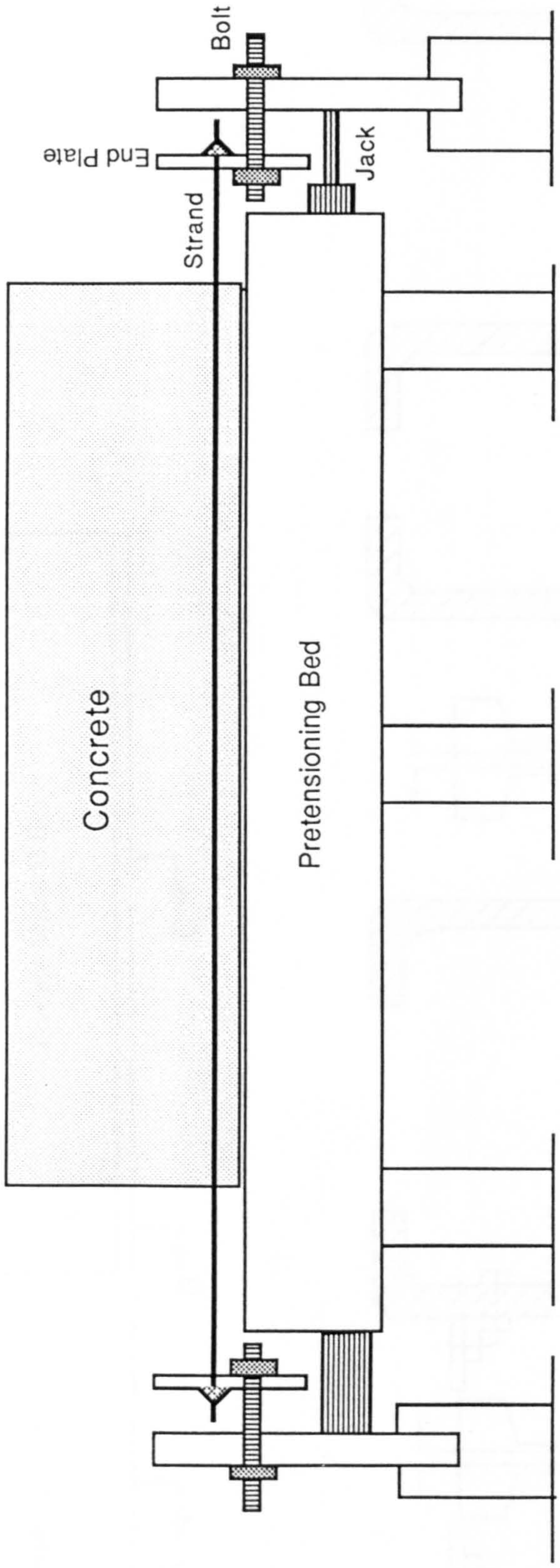

FIG. 3.4 Pretensioning Operation

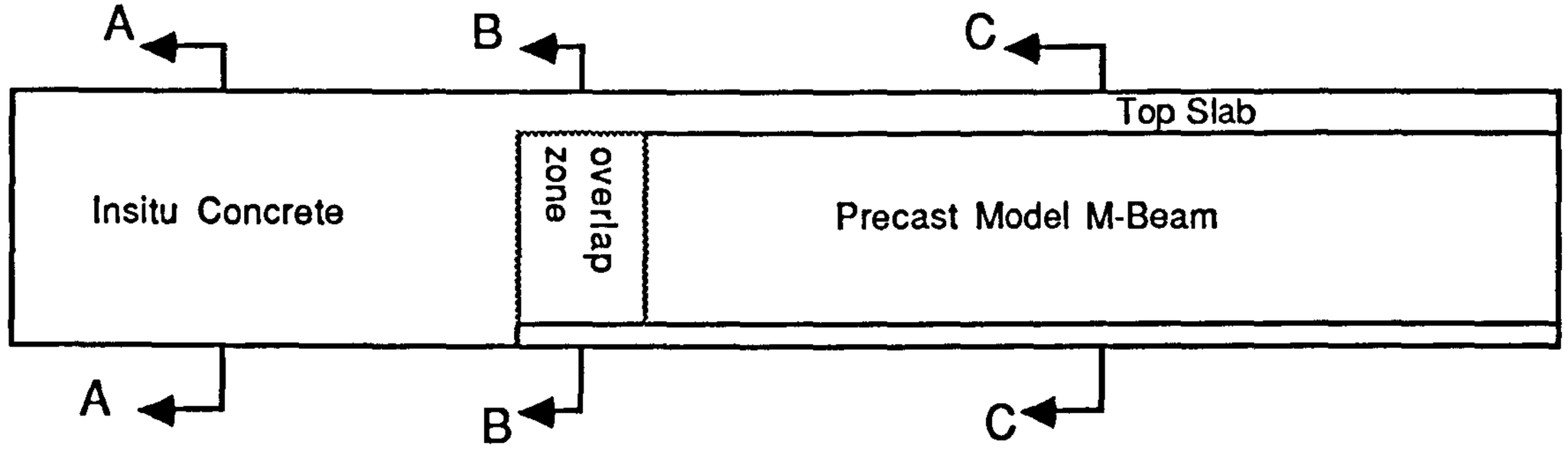

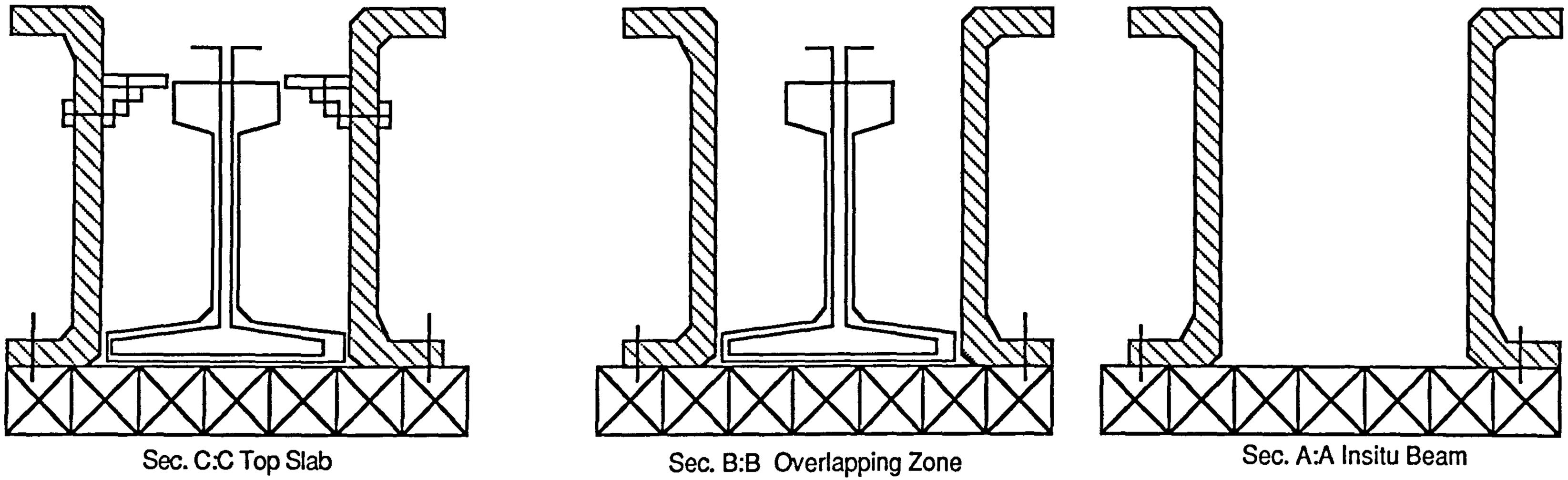

FIG. 3.5 Moulds to Connect Precast and Insitu Parts

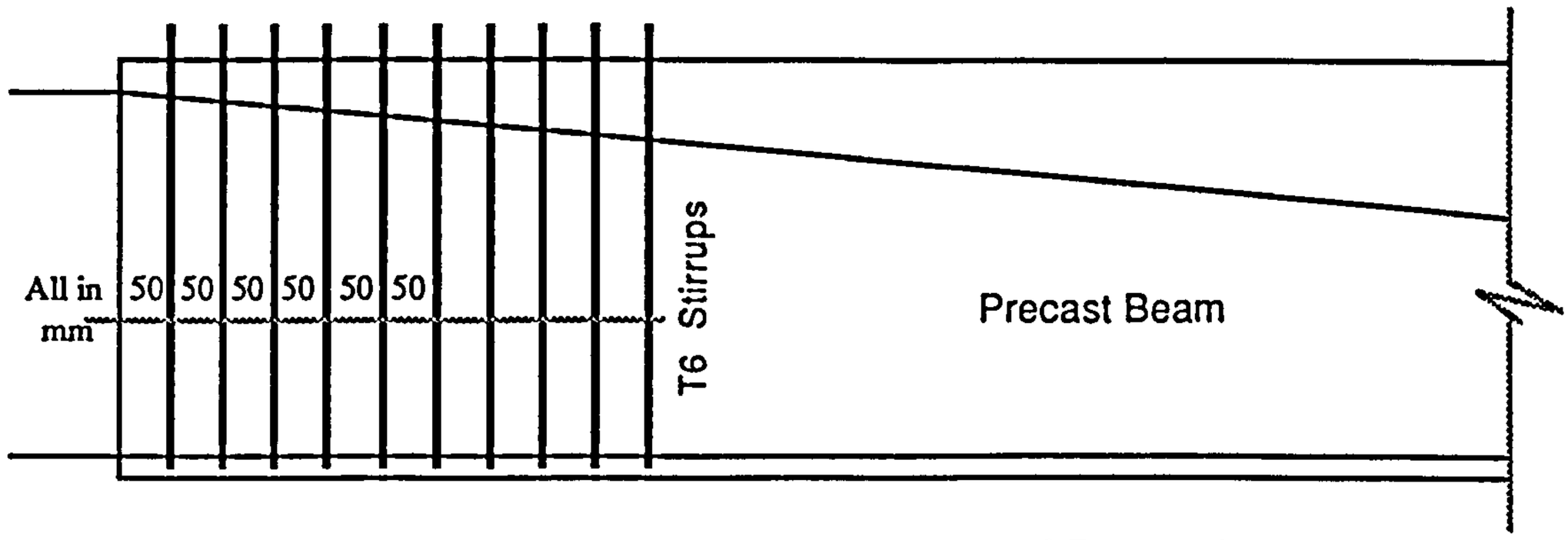

Fig.3.6a Stirrup Arrangement in the Embedment Part of Precast Beam E30AA1 ,E10CC5 and E10CD7 (but no Projected Bars into In-situ Concrete for Tests 5,7)

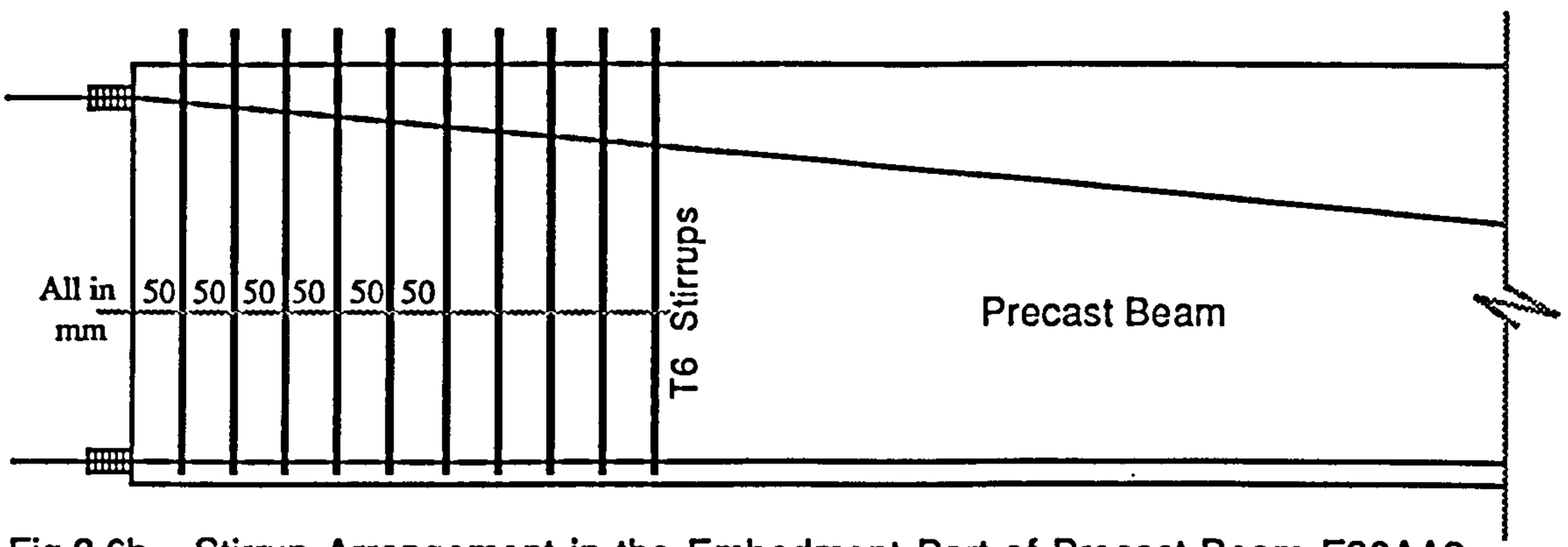

Fig.3.6b Stirrup Arrangement in the Embedment Part of Precast Beam E30AA2 Sleeving of the Projecting Bars

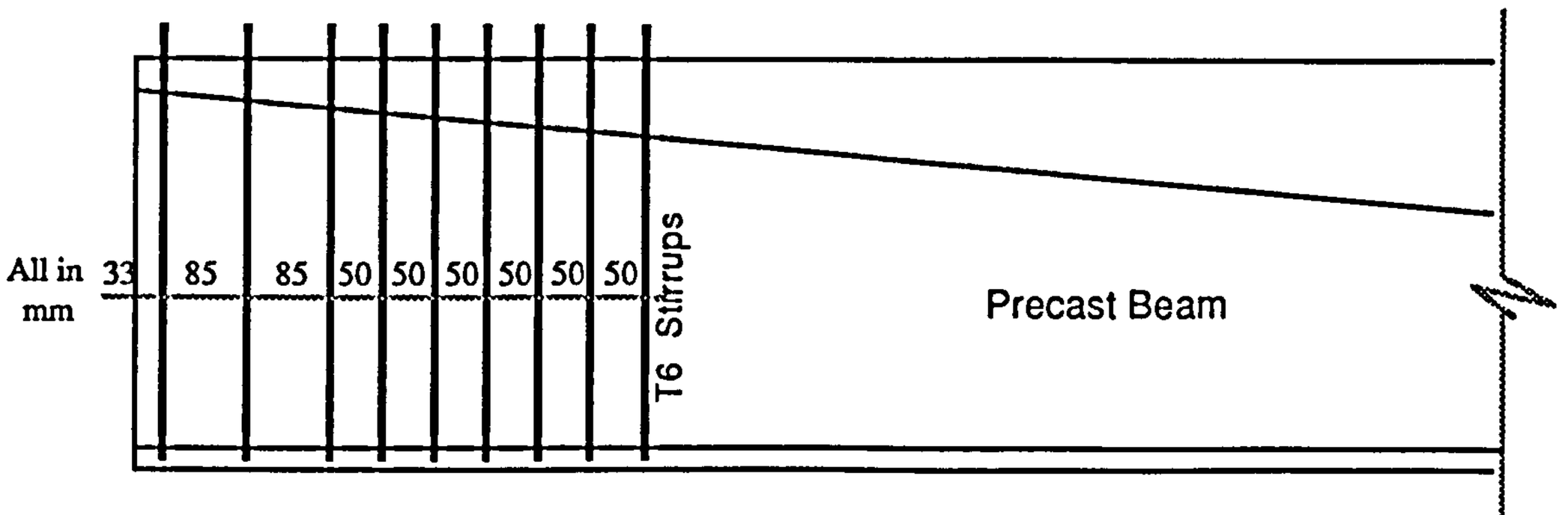

Fig.3.6c Stirrup Arrangement in the Embedment Part of Precast Beam Beams : E30AB3, E30BC4, WTFCC6, WTFPCC8,WTFCC9 (For WTFDCC10 All the bars Projected into In-situ concrete)

Fig 3.6a,b,c Stirrup Arrangement in the Precast Beam at the Connection

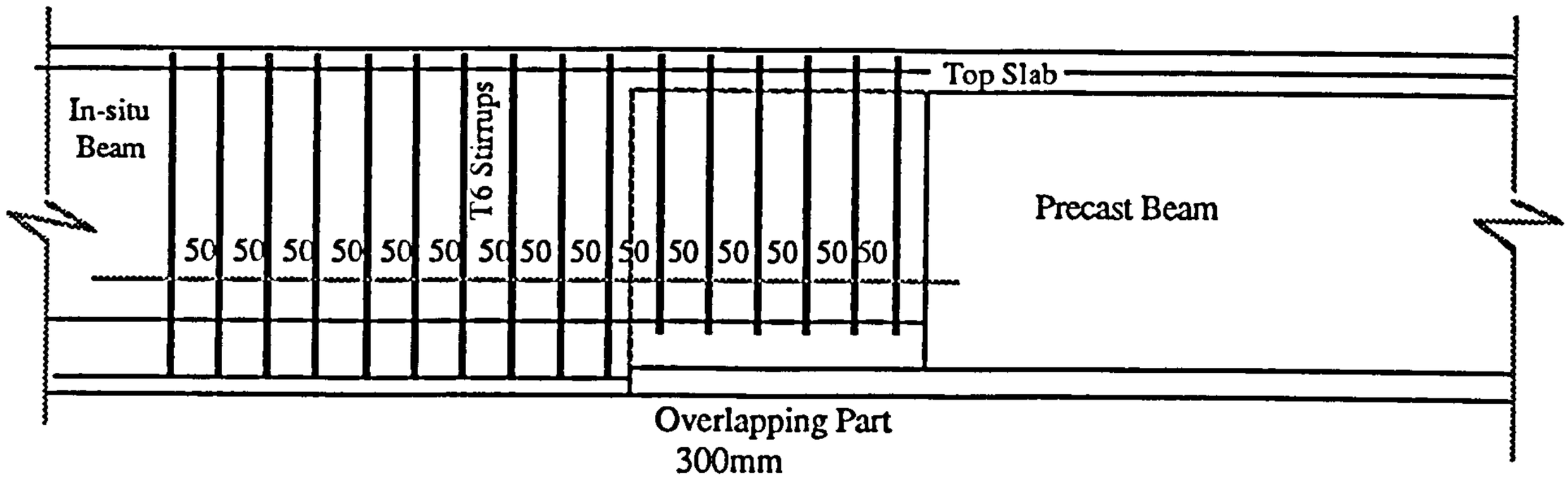

Fig. 3.6d Stirrup Spacings in the In-situ Nibs and In-situ beam
Tests E30AA1 and E30AA2

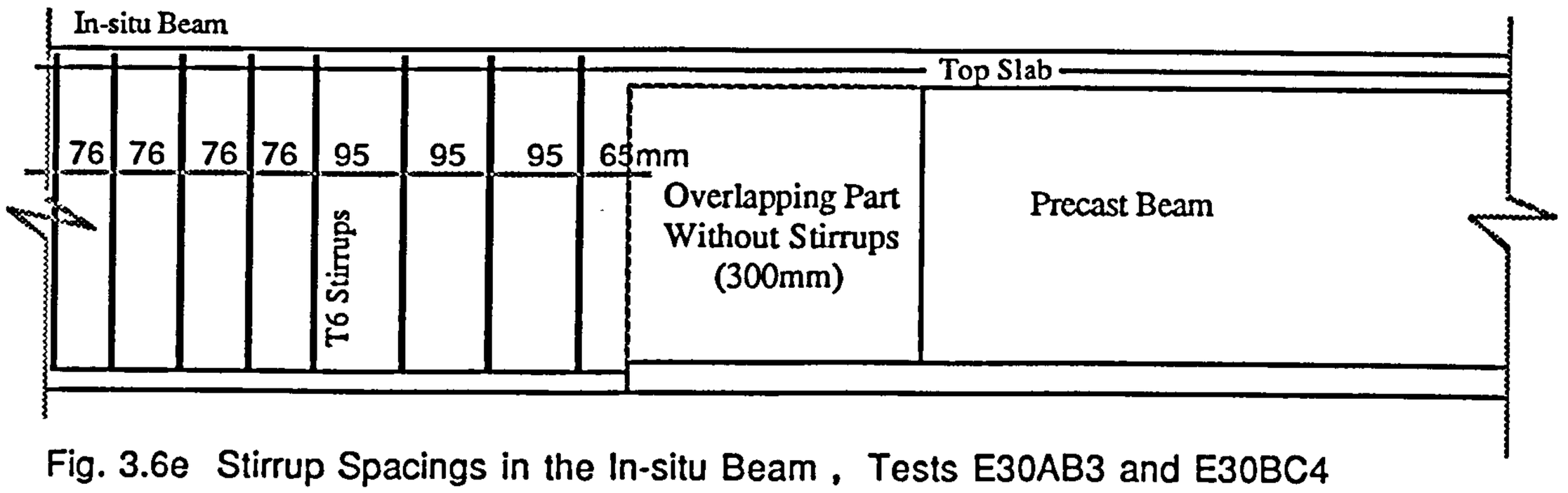

Fig. 3.6e Stirrup Spacings in the In-situ Beam , Tests E30AB3 and E30BC4
(Without Stirrups in the Nibs)

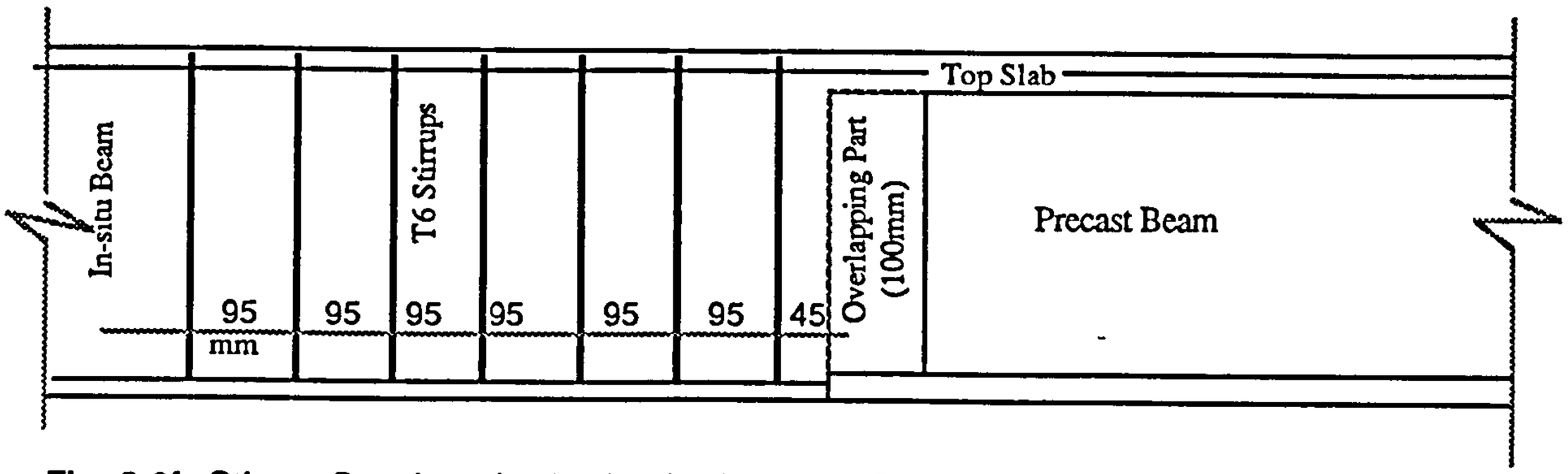

Fig. 3.6f Stirrup Spacings in the In-situ Beam , Tests E10CC5
(Without Stirrups in the Nibs)

Figs. 3.6 d,e,f Stirrup Spacings in the In-situ Beam and Nibs

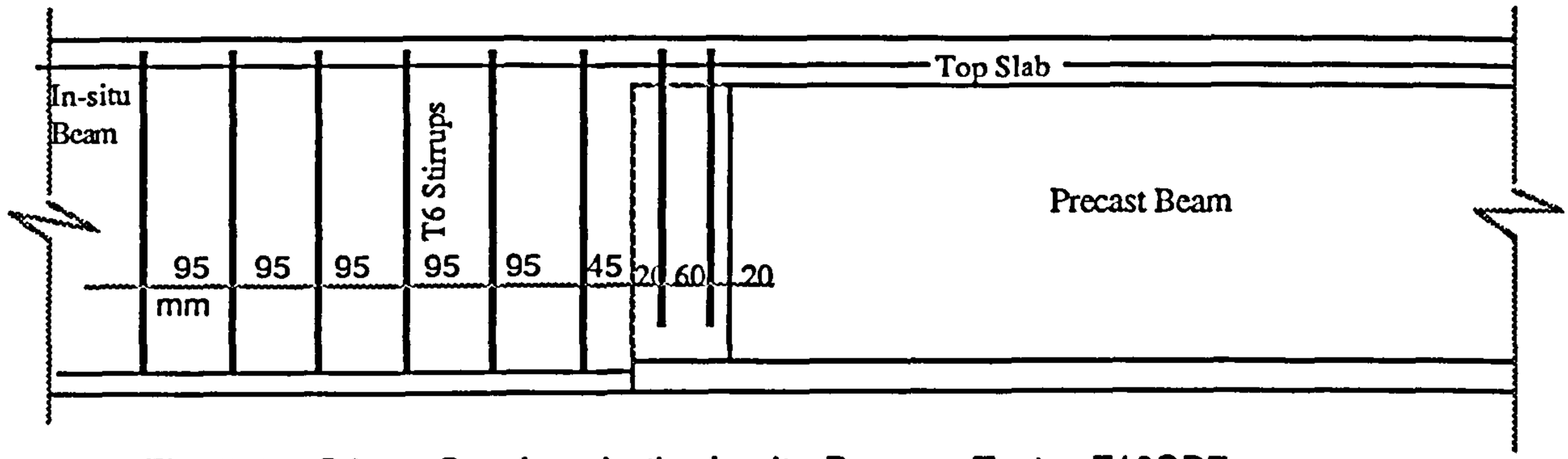

Fig. 3.6g Stirrup Spacings in the In-situ Beam , Tests E10CD7
(With Stirrups in the Nibs)
(100mm Overlap)

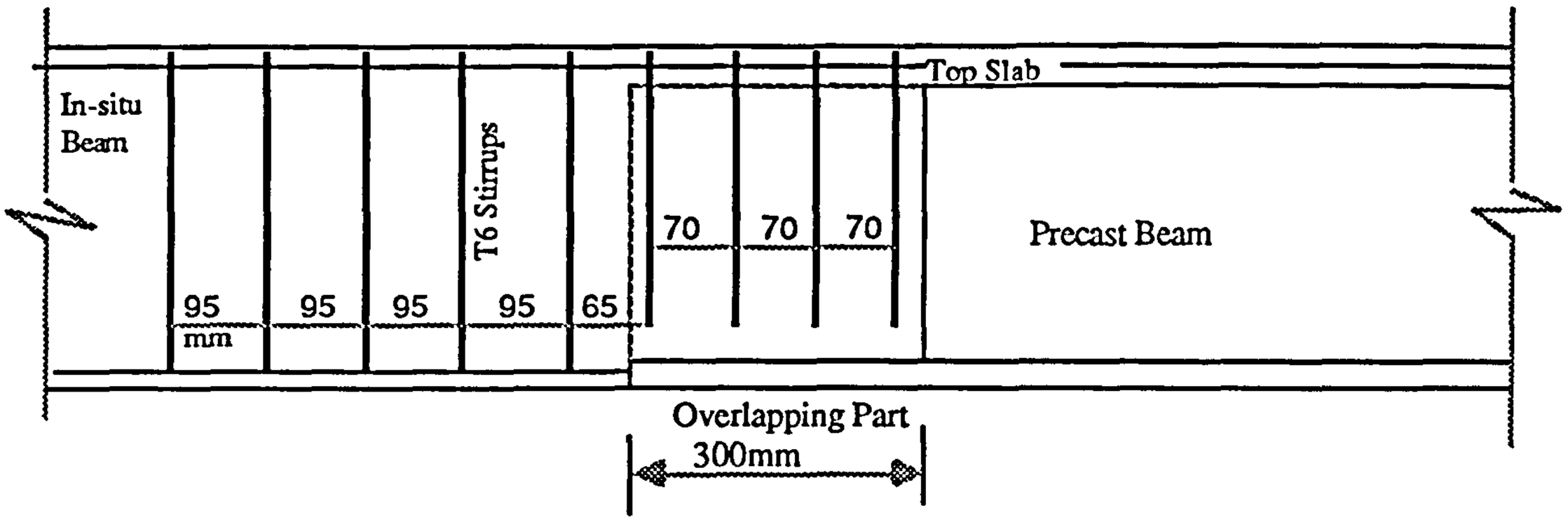

Fig. 3.6h Stirrup Spacings in the In-situ Beam and Nibs
Tests WTFCC6,WTFPCC8,WTFCC9 and WTFDCC10
(All without Top Flange Effect in the Connection)

Figs.6.3 g,h Stirrup Spacings in the In-situ Beam and Nibs

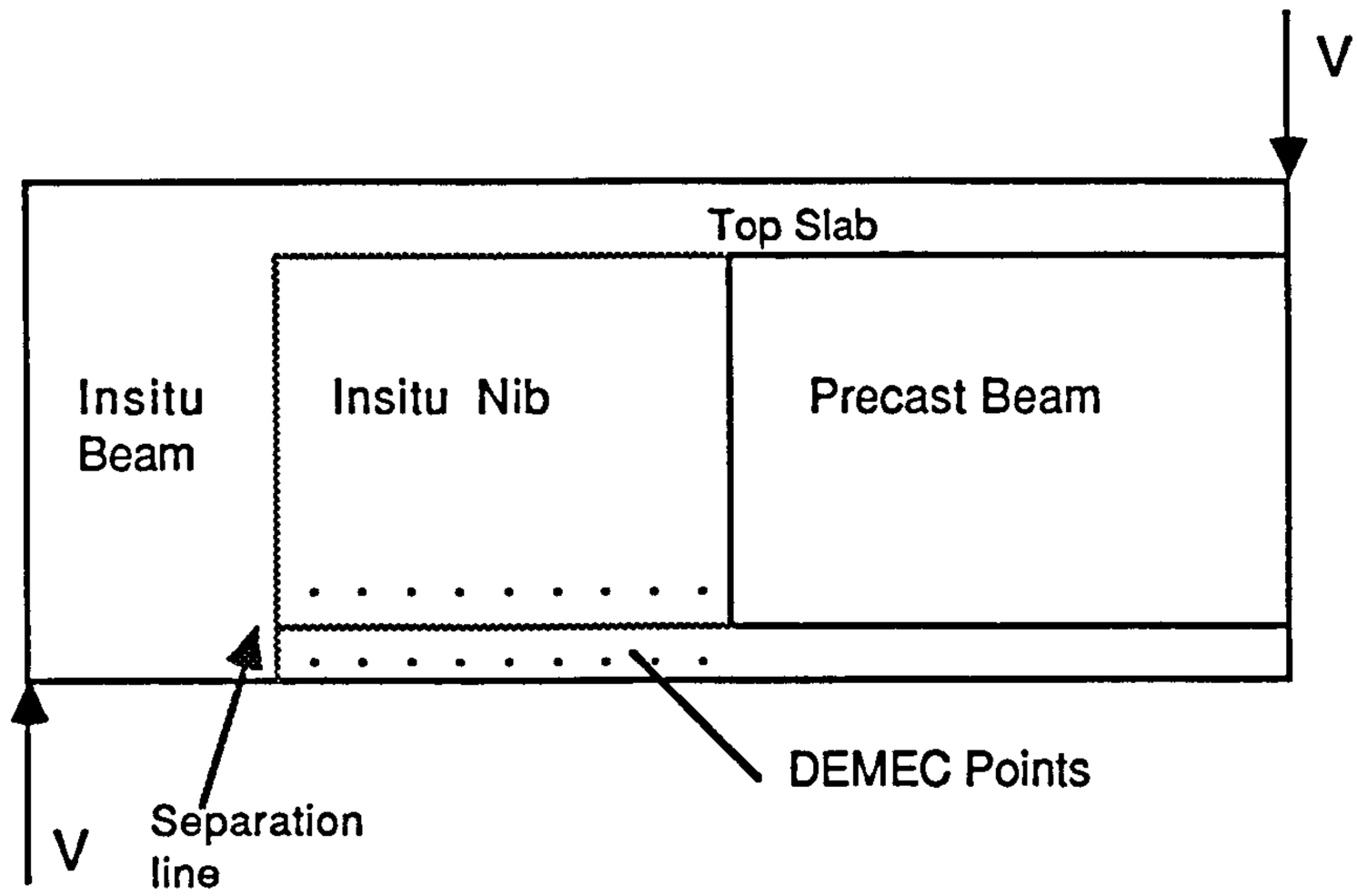

FIG. 3.7 Position of DEMEC points to Measure Vertical Separation

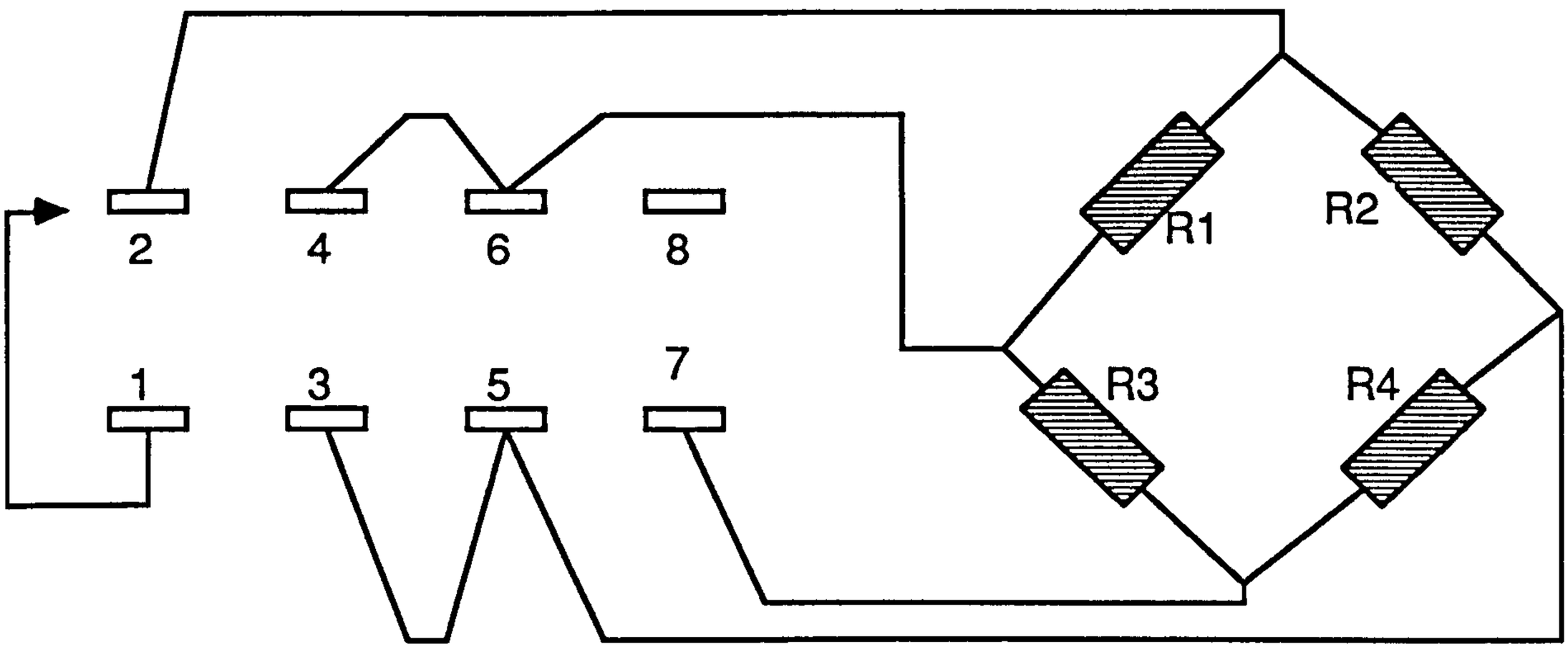

FIG. 3.8 Load Cell Connection to 7-Pin Plug

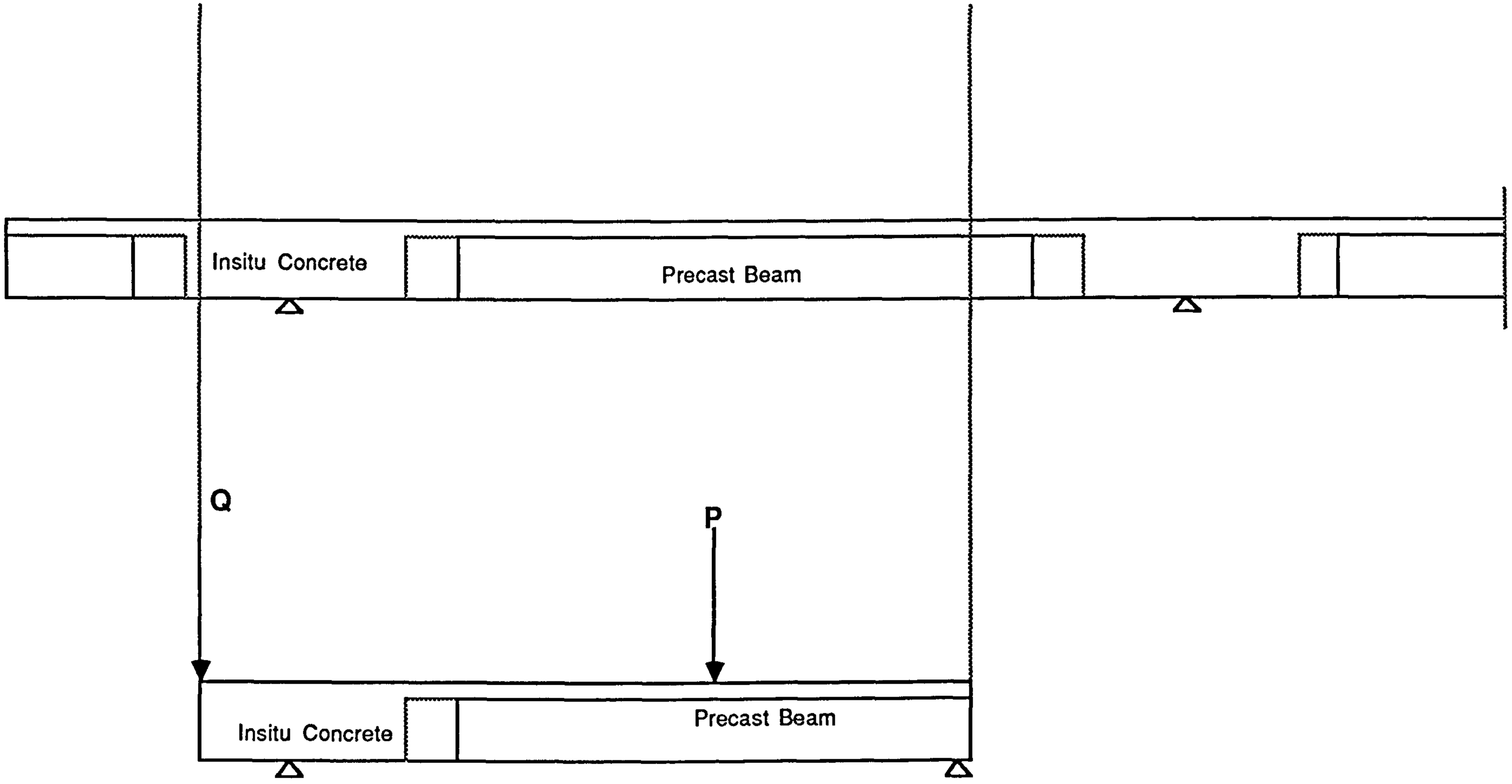

FIG. 3.9 Simulation for the Testing arrangement

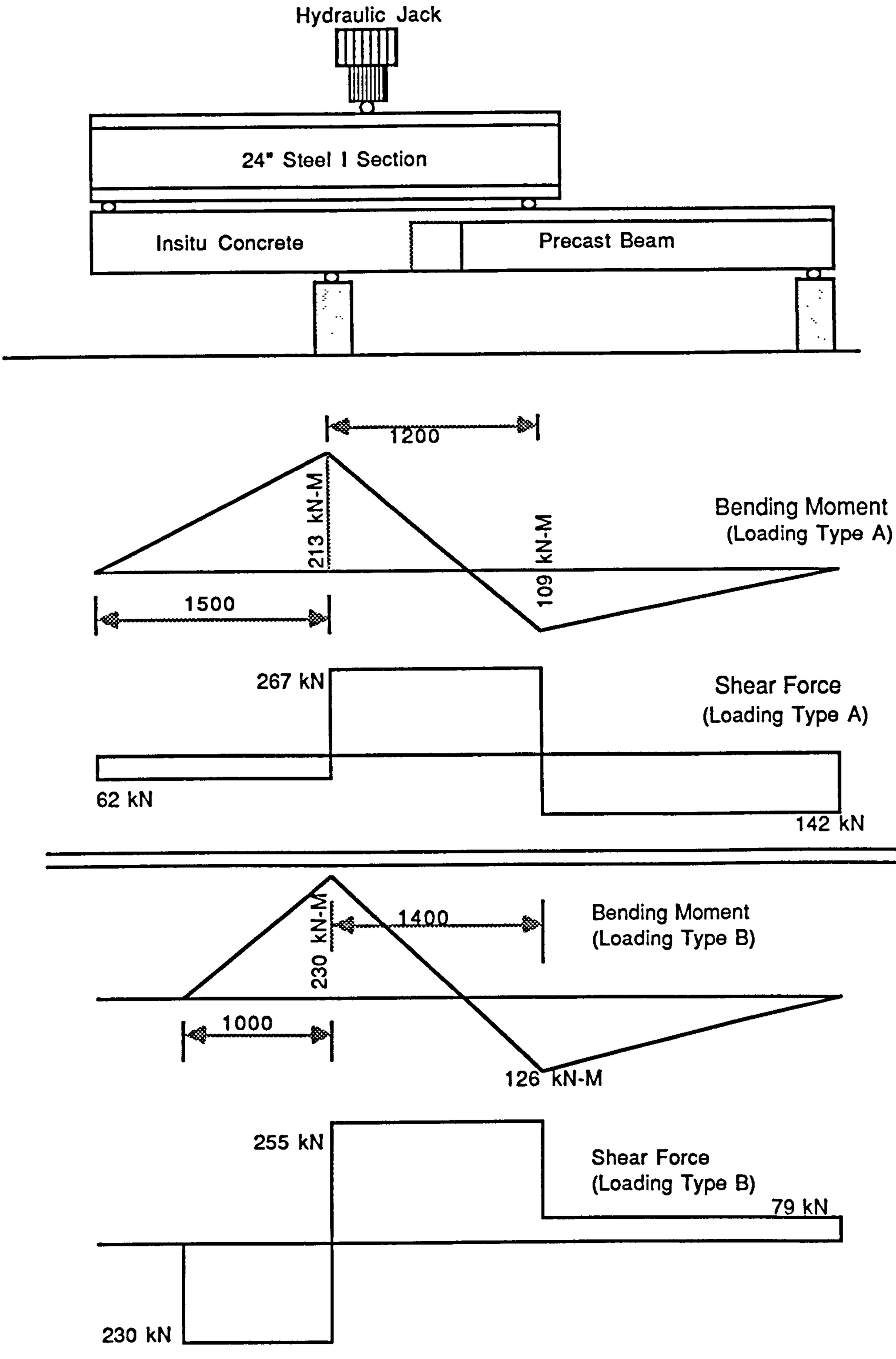

FIG. 3.10 Typical Loading Arrangement

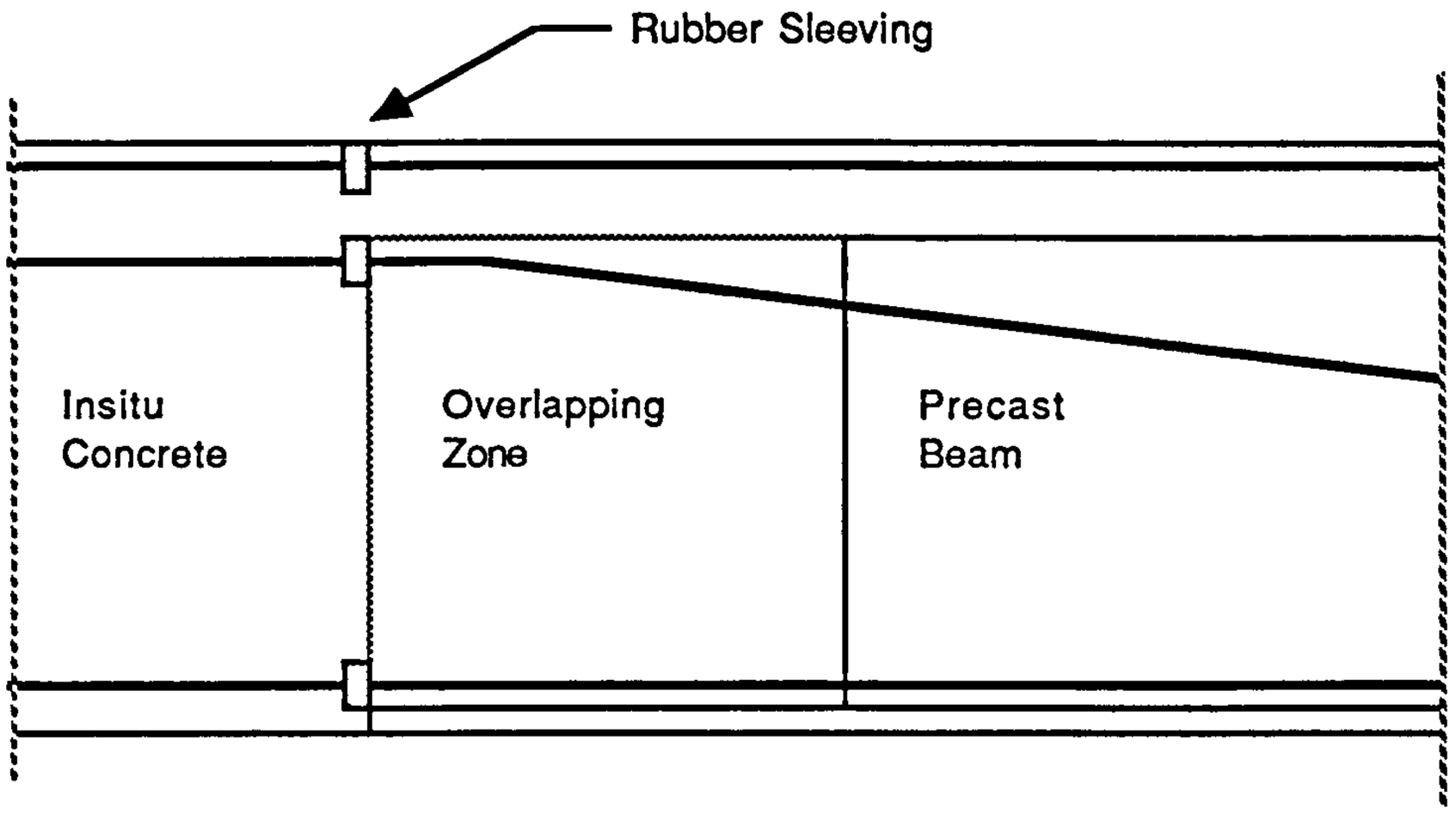

FIG. 3.11 Elimination of Dowel Effect by Sleeving the Projecting Bars at the Interface

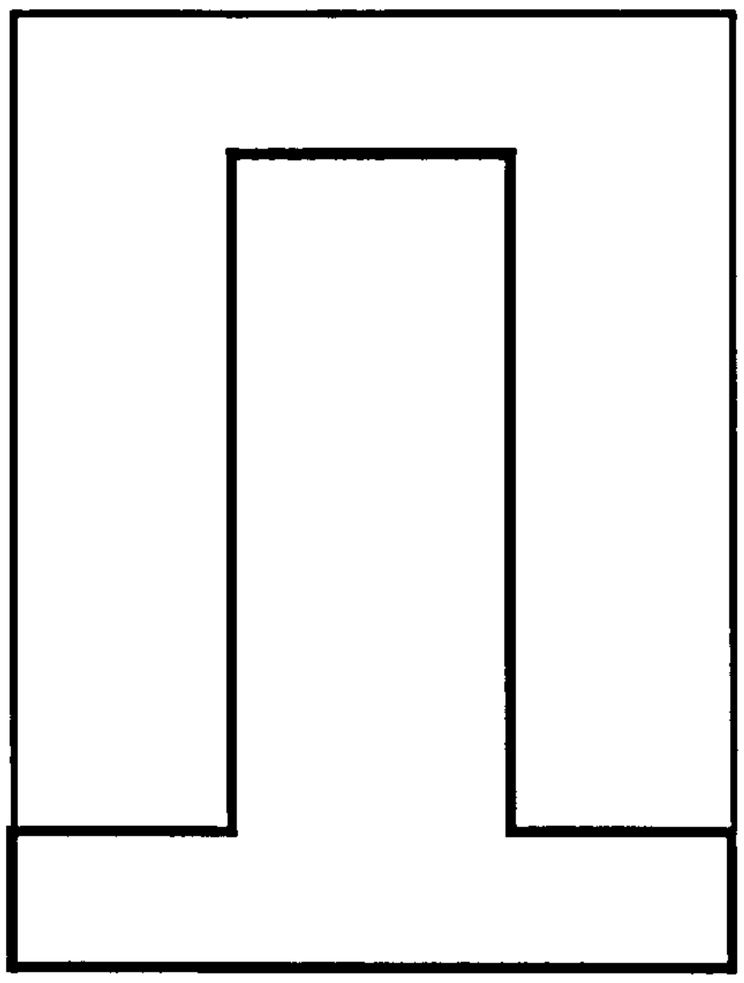

FIG. 3.12 Initially Proposed End Block (Ref. 3)

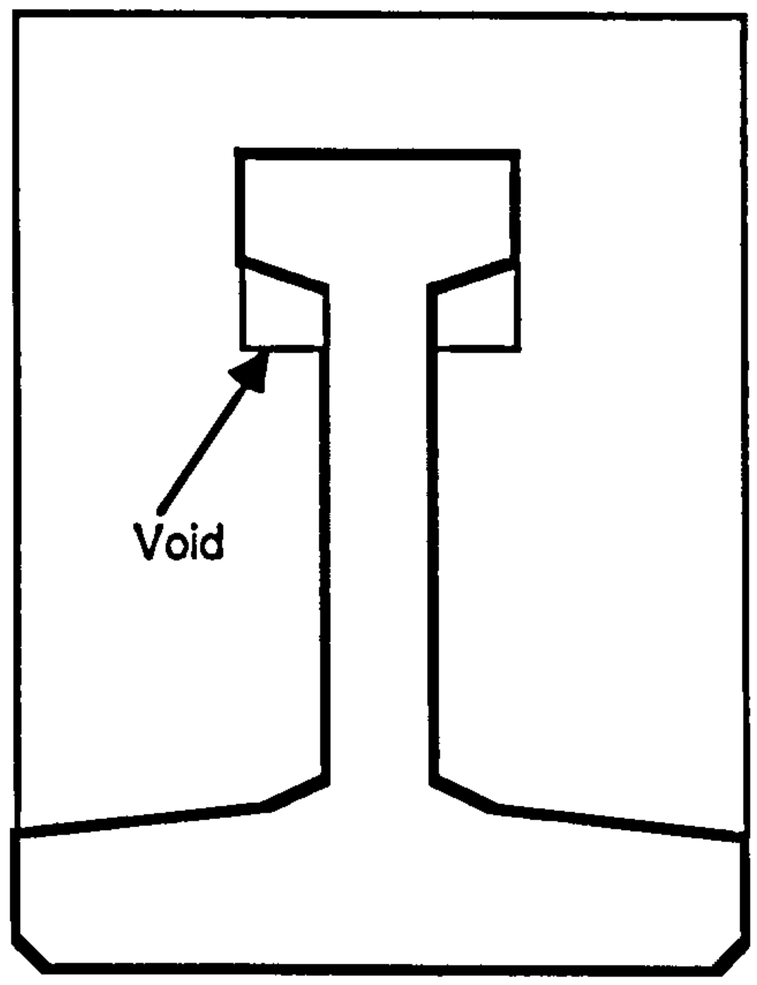

FIG. 3.13 Simulation of End Block or Top Flange Elimination

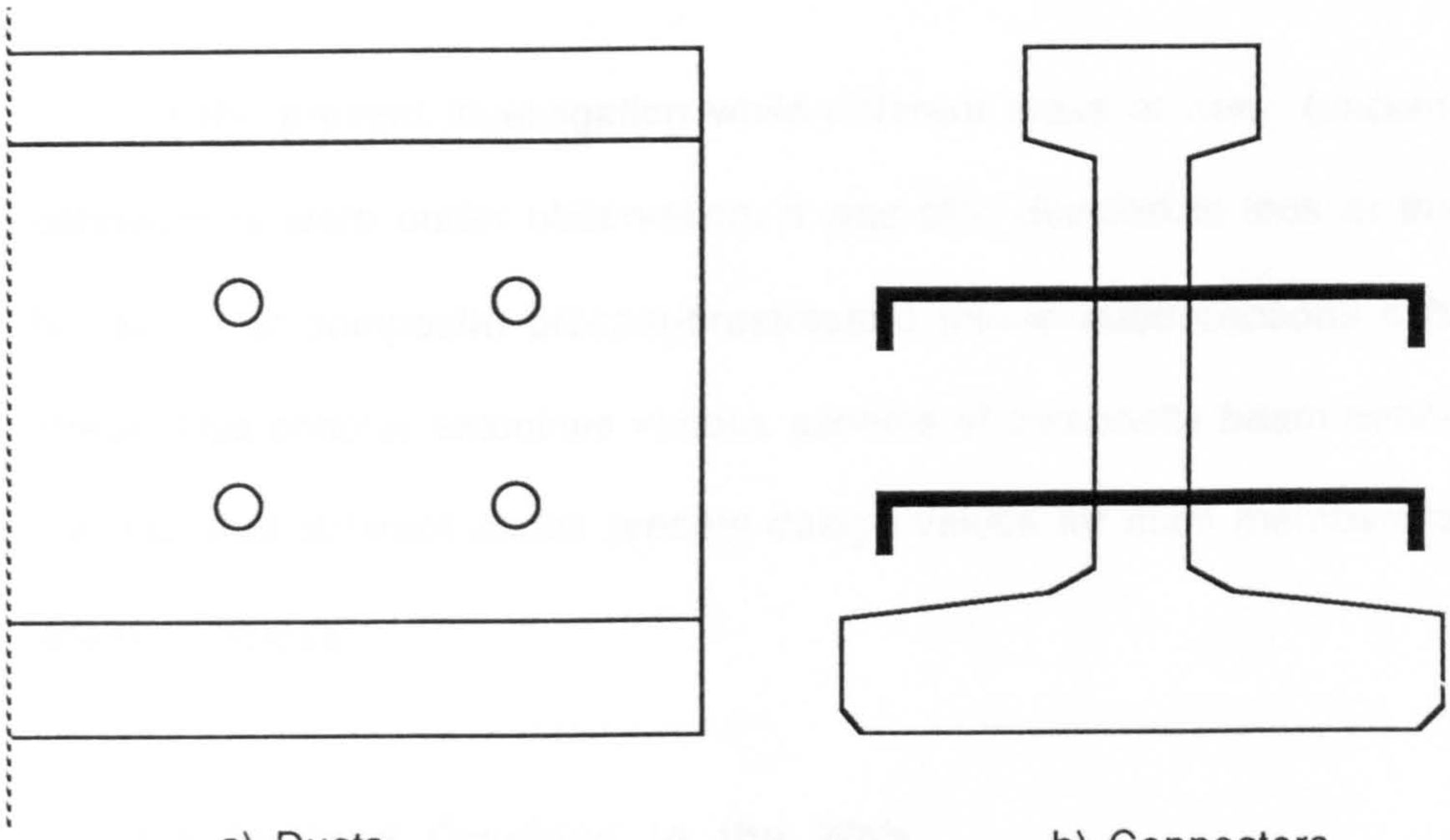

FIG. 3.14 Position of the Web Shear Connectors

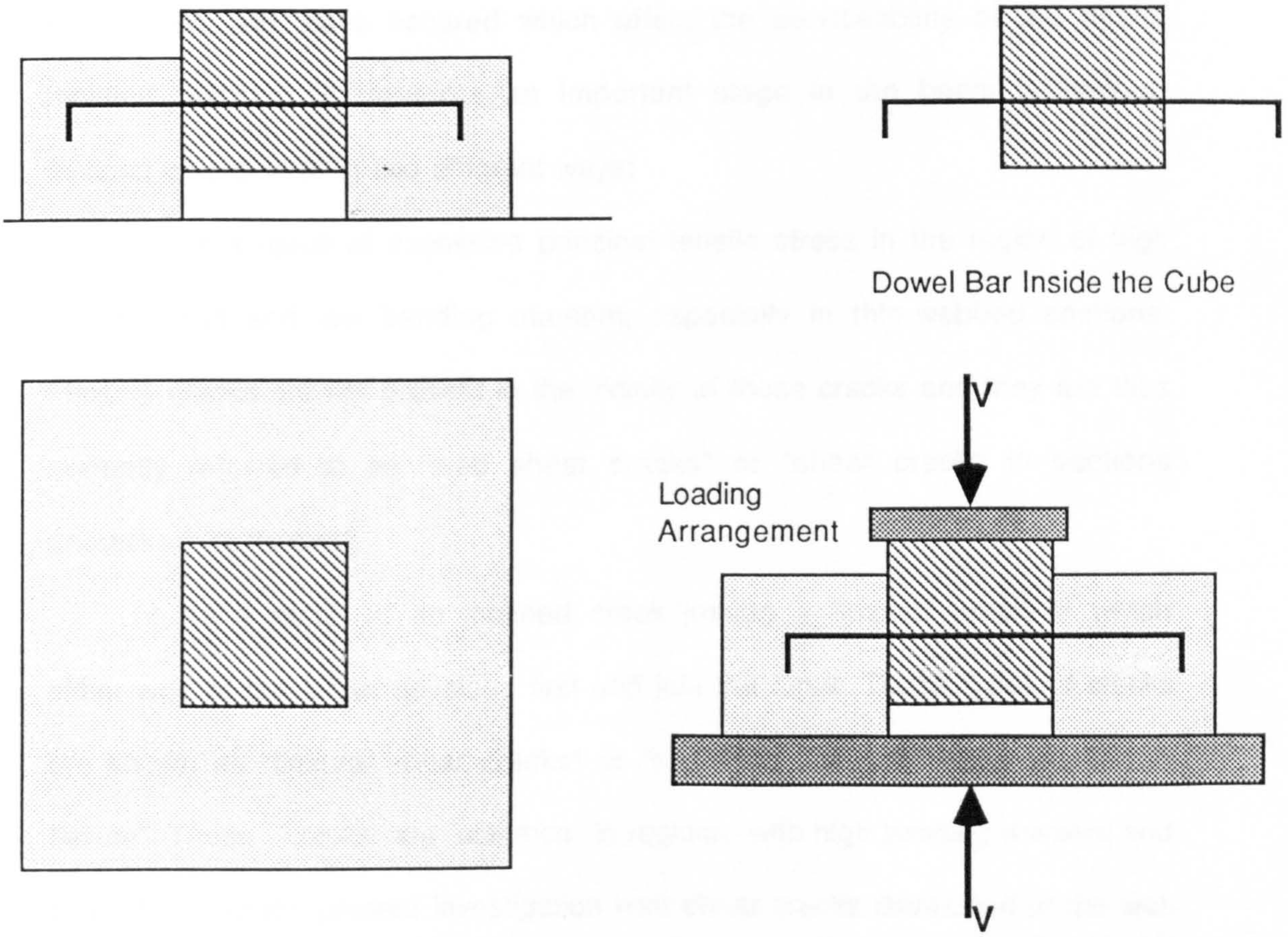

FIG. 3.15 Details of the Dowel Shear Test Specimen

CHAPTER FOUR

GENERAL BEHAVIOUR OF COMPOSITE BEAMS SUBJECTED TO SHEAR

In the present investigation while different types of new (unconventional) connections were under observation, it was also decided to look at the general behaviour of composite precast-prestressed thin-webbed sections subjected to shear. This chapter examines various aspects of composite beam behaviour and the way that different codes present design values for such members subject to shearing forces.

4.1 Inclined Cracking in the Web

After the occurrence of inclined cracks, the prestressed beam ceases to behave elastically and transforms to a complex statically indeterminate system. This implies several permanent deformations such as crack width, deflection , steel strain, etc. have occured which affect the serviceability of the beam. Inclined cracking is therefore an important stage in the beam behaviour. Inclined cracks form in two different ways:

a) As a result of excessive principal tensile stress in the region of high shear stress and low bending moment, especially in thin-webbed sections. Flexural cracks are not present in the vicinity of these cracks and they are thus normally referred to as "web shear cracks" or "shear cracks in sections uncracked in flexure".

b) As a result of an inclined crack joining a flexural crack in which either type of crack can develope first and join the other. These types of cracks are known as "flexural shear cracks" or "shear cracks in sections cracked in flexure". These cracks are common in regions with high bending moment and shear force. In the present investigation web shear cracks developed in the web of the precast section between the loading point and the continuous support

whereas flexure-shear cracks developed mainly near the continuous support in the in-situ section where high bending moment and shear force were present.

The web shear cracking load can be determined from the principal tensile stress caused by the combination of normal and shear stresses in the section. These include vertical shear stress, flexural stress, longitudinal and vertical prestress. The principal tensile stress can be calculated from basic elastic theory:

$$f_t=0.5(f_x+f_y)+\sqrt{0.25(f_x-f_y)^2+v^2} \qquad \text{.....(4.1)}$$

in which f_x is the prestress f_{cp} and f_y is the vertical prestress. Assuming $f_y=0$ and knowing that for a rectangular section at the centroid $v=1.5V/bh$:

$$V_{co}=0.67bh\sqrt{f_t^2+f_t f_{cp}} \qquad \text{.....(4.2)}$$

In British Codes a reduction factor of 0.8 (BS8110) or 0.87 (BS5400) is applied to prestress.

$$V_{co}=0.67bh\sqrt{f_t^2+0.8f_t f_{cp}} \qquad \text{(BS8110)} \qquad \text{.....(4.3)}$$

This equation applies to the centroid axis of the section where shear stress is maximum and normal stress is minimum. For other points shear stresses are smaller while normal stresses are larger and thus these two effects tend to compensate each other and the equation is generally taken as the critical condition. However, for a flanged section the top of the web may be a more critical location. In all test beams web shear cracks developed in the prestressed beam web half way between the top and bottom flange. The reason for this is that because of the loading arrangement, the bending moment is very small in that region (near the contraflexure point), and the critical point for principal tensile stress is at the centroid of the section. It has been suggested by Tay[62] that at the mid-span of long simply supported beams where the bending moment is maximum, shear stress at the base of web is still considerable while prestress diminishes, so the highest principal tensile

stress occurs at the base of web. Near the support, however, this maximum principal tensile stress occurs at the junction of the web and the top flange.

4.1.1 Different Codes Prediction of Web Cracking Shear

4.1.1.1 British Codes, BS8110[27], BS5400[68] and CP110[64]

All These British Codes give similar expressions for web shear cracking load. The beams tested all had inclined pretensioned strands and the above Codes allow the vertical component of prestressing force (Vp) to be added to the web cracking load. It should be noted here that all the Codes allow these expressions to be used similarly for either monolithic or composite beams. In BS8110 and CP110:

$$Vcr=0.67bh\sqrt{f_t^2+0.8f_t f_{cp}}+V_p \qquad \text{.....(4.4)}$$

where f_t is the concrete tensile strength, $f_t=0.24\sqrt{f_{cu}}$. In BS5400 a reduction factor of 0.87 is applied to prestress instead of 0.8.

Experimental values (obtained from the present investigation) and the British Code predictions can be seen in tables 4.1 and 4.2.

4.1.1.2 CEB-FIP Model Code[72]

The European Code predicts the web shear cracking load as :

$$V_{cr}=\beta_1\tau_{RD}\,k(1+50\rho)bd+V_p \qquad \text{.....(4.5)}$$

where $k=1.6-d>1.00$ metre (Depth effect), τ_{RD}=basic shear strength

$\beta_1=1+M_0/M_{sdu}<2.0$ .....(Prestress or axial compression effect)

where M_0 is the decompression moment at transfer and M_{sdu} is the

maximum design moment in the shear region under consideration. ρ is the stirrups ratio: $\rho=A_{sv}/bd\leq 0.02$

Correspondingly web shear cracking loads for all beams have been obtained for the above code formulae and tabulated in table 4.1 . All safety factors have been kept in the calculations and these values have been compared to the observed web shear cracking loads in table 4.2, expressed as the ratio of experimental to calculated values. The observed mean safety factor for CEB-FIP is 1.5 while for the British Code it is 1.21 in comparison with their adopted strength safety factor of 1.25 for concrete in shear.

4.1.1.3 Building Code Requirements for Reinforced Concrete ACI 318-77[71] and ACI 318-83[81]

The ACI Code prediction for web shear cracking load is based on a simple expression:

$$V_{cr}=bd\phi(0.29\sqrt{f'_c}+0.3f_{cp})+V_p \qquad \text{(S.I)}.....(4.6)$$

Assuming that $f'_c=0.8f_{cu}$

$$Vcr=bd\phi(0.27\sqrt{f_{cu}}+0.3f_{cp})+V_p \qquad \text{(S.I)}.....(4.7)$$

$\phi=0.85$.....ACI strength reduction factor

This expression is actually a simplification of the formula obtained from equating the principal tensile stress at the centroid to the tensile strength of concrete.

$$v_{cr}=\sqrt{f_t^2+f_t f_{cp}}=f_t\sqrt{(1+f_{cp}/f_t)}$$

v_{cr} is the maximum shear stress at the centroid which is theoretically 1.5 times the average shear stress (in the elastic range). British Codes allow

for this by using the factor 0.67 in the Eqn. 4.4. The ACI assumes that the tensile strength of concrete is :

$$f_t=0.33\sqrt{f'_c}=0.295\sqrt{f_{cu}} \qquad \text{(S.I)}.....(4.9)$$

This value ($0.295\sqrt{f_{cu}}$) is smaller than ($0.36\sqrt{f_{cu}}$) suggested by the British Codes. To include the factor of 0.67 (ratio of average to maximum shear), ACI has reduced the value of f_t from $0.33\sqrt{f'_c}$ (or $0.295\sqrt{f_{cu}}$) to $0.29\sqrt{f'_c}$ (or $0.26\sqrt{f_{cu}}$) which, with a ratio of 0.29/0.33=0.87, is about 30% greater than 0.67.

$$v_{cr}=f_t\sqrt{1+fcp/f'_t}=0.29\sqrt{f'_c}\sqrt{1+fcp/0.29\sqrt{f'c}} \qquad \text{(S.I)}.....(4.10)$$
$$\approx 0.29\sqrt{f'_c}+0.3f_{cp} \qquad \text{(S.I)}$$

ACI thus gives larger values for the web shear cracking loads resulting from the above mentioned reasons.

For the beams tested here, ACI predictions are almost unsafe (see tables 4.1 and 4.2) . These are on average 26% larger than the values predicted by the British Codes and the mean observed safety factor is 0.96 as shown in table 4.2. It is concluded and confirmed by the test results here that the British code approach is more reasonable and gives a more acceptable margin of safety.

4.1.1.4 Standard Specification for Highway Bridges (AASHTO)[73]

AASHTO suggests that the shear force carried by concrete in prestressed beams is as follows:

$$V_c=0.06f'_cbjd\leq 180bjd \qquad \text{(PSI)}.....(4.11)$$

or:

$$V_c=0.0481f_{cu}bjd\leq 1.266bjd \qquad \text{(SI)}.....(4.12)$$

where b is the web width and jd is the lever arm.

It can be seen from the above expressions that the magnitude of prestress is not considered in the calculation, and the limiting maximum shear carried by concrete and based a concrete strength of f_{cu}=1.266/0.0481=26 N/mm^2 is expected to give conservative results. The experimental web cracking shear has been compared to AASHTO values in table 4.1 and 4.2. A mean safety factor of 2.06 is observed when using this code.

4.1.1.5 Australian Standards: SAA Prestressed Concrete Code[70]

The Australian code limits the principal tensile stress in the beam to the tensile strength of concrete taken as:

$$f_t=0.33\phi\sqrt{f'_c}=0.295\phi\sqrt{f_{cu}} \qquad \text{(SI)}.....(4.13)$$

where ϕ is as in 4.1.1.3

which is similar to the ACI assumption in this respect. It does not explain which location in the beam web is to be examined for the principal tensile stress and so the exact theoretical equation for the principal tensile stress at the centroid was used (Eqn.4.4 but without applying the factor 0.8). Calculated values have been compared with observed web cracking shear (see tables 4.1 and 4.2) indicating an observed safety factor of 1.05 . It is not clear in this code whether the vertical component of prestressing force should be added to the web cracking shear and if it is ignored a safety factor of 1.3 would be obtained as in table 4.3.

4.1.2 Inclination of the Prestressing Strands

Most of the Codes allow the increasing effect of the vertical component of prestressing force on the shear resistance though this is not well clear in CEB-FIP and Australian Codes. The effect of the vertical component of prestressing has been ignored in all Codes approach and compared with the

experimental values. Results have been tabulated in table 4.3 showing that all Codes have sufficient margin of safety if this effect is ignored.

4.1.3 Effect of Percentage of Shear Reinforcement on Web Cracking Shear

Some investigators including Olesen et al[74] and Balsooriya[66] have suggested that web reinforcement percentage only has a slight effect on the web cracking shear. The web reinforcement percentage was not a variable for the present investigation but since a rather high amount of stirrups (2.0%) was used and no significant change in web cracking shear was seen in comparison with other investigators, it may be concluded that this variable has no appreciable effect.

4.1.4 Effect of Shear Span to Effective Depth Ratio on the Web Cracking Shear

The shear span to effective depth ratio was not considered as a major variable in this investigation but was changed from 3.72 in beams E10CC5 and E10CD7 to 2.8 in all other beams. In general it has been accepted that this factor can affect the ultimate shear strength of concrete beams but its effect on the inclined cracking load has not been given the same attention. Arthur[75] concluded that in pretensioned I-beams without web reinforcement, the inclined cracking shear decreases rapidly with an increase in a_v/d when this ratio is less than 3.0. For a_v/d ratios greater than 3.0 This change is less significant. Olesen et al[74] and Balasooriya[66] suggested that the shear span to effective depth ratio had no effect on the inclined cracking strength.

In the present investigation, no significant change was observed in the inclined cracking load of beams with different a_v/d ratios which is in agreement

with Olesen[74] and Balasooriya[66] results. Tay[62] compared some investigators' results for this effect and concluded that in general a_v/d ratio has no significant influence on the web cracking shear for av/d ratios ranging between 1.5 to 4.0.

4.2 Principal Strains and Stresses

4.2.1 Theoretical Values

At any point of cross-section, the state of stresses can be defined knowing the magnitude of longitudinal stresses, (including bending stress, axial stress or prestress), vertical normal stress (e.g vertical prestress) and shear stress. The magnitude of principal stresses and strains can be obtained using the classical elastic theory provided the elastic modulus and Poisson's Ratio are known.

$$\sigma_1,\sigma_2=0.5(\sigma_x+\sigma_y)\pm\sqrt{0.25(\sigma_x-\sigma_y)^2+v^2} \qquad \text{.....(4.14)}$$

$$\varepsilon_1=\sigma_1/E-\nu\sigma_2/E=1/E(\sigma_1-\nu\sigma_2) \qquad \text{.....(4.15)}$$

$$\varepsilon_2=\sigma_2/E-\nu\sigma_1/E=1/E(\sigma_2-\nu\sigma_1) \qquad \text{.....(4.16)}$$

In this elastic analysis it has been assumed that the concrete is an homogeneuous material, behaving elastically and having the same modulus of elasticity in compression and tension. These assumptions are reliable when obtaining principal strains or stresses before inclined cracking, which is normally associated with relatively small strains or stresses, but after inclined cracking this analysis may not be reasonable.

4.2.2 Experimental Principal Strains and Stresses

Strains were measured at specific points on the web, in three directions

(horizontal,vertical and 45° directions). These measurements were either with a mechanical or electrical rosette gauge arrangement. With the mechanical gauge, a 100mm DEMEC extensiometer was used (see Fig. 4.1a) and with the electrical gauges three 60mm (TML-PL60) gauges were fixed on the web so that the centre point of each gauge located at the required point (see Fig. 4.1b). The actual stresses in an element parallel to the longitudinal axis can be seen in Fig. 4.1c. To define the complete stress field in any point of the web, in addition to horizontal and vertical strain measurement an arbitrary direction for the strain measurement can be chosen, which was -45° as in Figs. 4.1a and 4.1b.

In any direction θ, :

$$\varepsilon_\theta=0.5(\varepsilon_x+\varepsilon_y)+0.5(\varepsilon_x-\varepsilon_y)Cos2\theta+0.5\gamma_{xy}Sin2\theta \qquad .....(4.17)$$

and the principal strains :

$$\varepsilon_1=0.5(\varepsilon_x+\varepsilon_y)+0.5\sqrt{(\varepsilon_x-\varepsilon_y)^2+\gamma^2_{xy}} \qquad .....(4.18a)$$

$$\varepsilon_2=0.5(\varepsilon_x+\varepsilon_y)-0.5\sqrt{(\varepsilon_x-\varepsilon_y)^2+\gamma^2_{xy}} \qquad .....(4.18b)$$

Directions for the strain measurements were: 0° , 90° , –45° so:

$$\varepsilon_x=\varepsilon_0 \quad ,\varepsilon_y=\varepsilon_{90} \ , \ \varepsilon_\theta=\varepsilon_{-45} \ , \ \theta=-45° \qquad .....(4.19a)$$

From Eqn. 4.17 the only unknown value i.e. γ_{xy} will be obtained and hence from Eqn. 4.18a and 4.18b principal strains can be calculated:

$$\gamma_{xy}=-2[\,\varepsilon_{-45}-0.5(\,\varepsilon_0+\varepsilon_{90}\,)]=\varepsilon_0+\varepsilon_{90}-2\,\varepsilon_{-45} \qquad .....(4.19b)$$

$$\varepsilon_1=0.5(\varepsilon_0+\varepsilon_{90}\,)+0.5\sqrt{(\varepsilon_0-\varepsilon_{90})^2+(\,\varepsilon_0+\varepsilon_{90}-2\,\varepsilon_{-45}\,)^2} \qquad .....(4.20a)$$

$$\varepsilon_2=0.5(\varepsilon_0+\varepsilon_{90}\,)-0.5\sqrt{(\varepsilon_0-\varepsilon_{90})^2+(\,\varepsilon_0+\varepsilon_{90}-2\,\varepsilon_{-45}\,)^2} \qquad .....(4.20b)$$

Having determined the principal strains (ε_1, ε_2), the values of principal

stresses (σ_1,σ_2) relating to these strains can be calculated using the fundamental elastic deformation equation:

$$\sigma_1=E_c(\varepsilon_1+\nu\varepsilon_2)/(1-\nu^2) \qquad \text{.....(4.21)}$$

$$\sigma_1=E_c(\varepsilon_2+\nu\varepsilon_1)/(1-\nu^2) \qquad \text{.....(4.22)}$$

It should be mentioned that in Eqn. 4.20, ε_0 is the sum of apparent longitudinal strain measured and the amount of prestrain caused by the prestressing force which is:

$$\varepsilon_{cpx}=f_{cp}/E_c \qquad \text{.....(4.23)}$$

In the vertical direction , the effect of horizontal prestrain will be :

$$\varepsilon_{cpy}=-\nu f_{cp}/E_c \qquad \text{.....(4.24)}$$

The values of E_c for the tested beams were obtained using BS1881[65] method for concrete prisms and the value of Poisson's ratio found by determining the ratio of transverse strain to longitudinal strain.

All the above calculations were produced by a specially written computer programme and the principal strains or stresses were plotted against the shear force in the section considered and have been shown in Figs.4.2 through 4.9. Each page of graphs includes principal strains (upper half) and principal stresses (lower half) for both tensile (positive) and compressive (negative) cases. The inclined cracking shear has been marked in each curve.

4.2.2.1 Measured Tensile Strains and Stresses

Tensile strains are relatively small and change linearly with the applied shearing force (see fig. 4.2 for example). There is always a small tensile principal prestrain (resulting from the compressive prestrain) amounting

about 40 micro strains . The departure from linearity of principal tensile strains or stresses appears at a load slightly bigger than the inclined cracking load. The reason for this is that the position of the first detected inclined crack has not been within the rosette gauge measurement area. It can be seen that after inclined cracking, strain or stress increases sharply and elastic equations are not valid after this point. The amount of strain under which the inclined crack has occurred, excluding prestrain, was about 80 to 120 micro strain. Assuming that concrete behaves linearly in tension up to the tensile cracking with same modulus of elasticity as in compression and using British code values of tensile strength and modulus of elasticity:

$f_t=0.36(f_{cu})^{0.5}$ (tensile strength) (SI).....(4.25)

$E_c=9100(f_{cu})^{0.33}$ (modulus of elasticity) (SI).....(4.26)

Cracking strain of concrete will be :

$\varepsilon_{cr}=f_t/E_c=39.5\times10^{-6}(f_{cu})^{0.17}$ (SI).....(4.27)

For the tested beams this equation gives a strain of about 80 micro strain which is comparable with the measured values (80 to 120) although those are generally larger than the calculated values. One reason for this could be that the concrete stress-strain curve may not be linear near the tensile strength of concrete . It has been suggested by Domone[76] that only up to about 60% of the tensile strength the relationship is linear and this seems to be in agreement with the present test results.

Principal tensile stress changes with principal tensile strains and at the time of inclined cracking experimental stresses (calculated by using the measured strains in three different directions) ranged from 2.2 to 4.5N/mm^2. The well-known tensile strength equation $f_t=0.36\sqrt{f_{cu}}$ gives a comparable value of about 3.0N/mm^2 for the type of concrete used in the tests.

4.2.2.2 Principal Compressive Strains and Stresses

In compression, up to between one third and half the compressive strength, concrete behaviour is elastic and nearly linear. This means that even when some parts of the concrete are cracked in tension, other parts which are in compression may well still be within their elastic range. It can be seen from the graphs of principal strains or stresses (Figs. 4.2 to 4.9) that generally the compression curves of stress or strain remain linear for a larger range of loading than for the tensile cases. However, since the calculation of principal compressive strain and stress are also dependent on the tensile strain measurements, the compression curves depart from linearity before reaching their linear limits in pure compression alone.

The effect that prestressing has on the principal stress or strain has already been considered by assuming its equivalent prestrain in equations 4.17 to 4.22. Note that in Figs. 4.2 to 4.9 for zero load, there is always a small principal tensile strain due to the Poisson's Ratio effect.

4.3 Post Cracking Behaviour

After inclined cracking a substantial redistribution of forces takes place in the section causing a change in its behaviour. The most important mechanism which has been proposed to analyse reinforced concrete sections is the truss analogy.

4.3.1 Truss Analogy

The behaviour of thin-webbed beams with stirrups, having a regular pattern of inclined cracks, may be considered as a truss in which the concrete compression zone is the top cord, the main longitudinal bars act as the tensile

bottom cord, and concrete struts between the cracks act as diagonal compressive elements with stirrups as the vertical tension members.

This analogy was first proposed by Ritter[19] in 1899 and then deveoped by Morsch[20] in 1903. He assumed that the total shear was carried by stirrups with no contribution from the concrete in a shear carrying capacity. The shear capacity can then be expressed as a function of web reinforcement:

$V_s=kbdrf_{yv}$ (classical truss analogy) .....(4.28)

k is a value relating to the directions of inclined cracks (θ) and stirrups(α)

$k=(\cot\alpha+\cot\theta)\ \sin^2\alpha$ .....(4.29)

$r=A_{sv}/bS_v$ .....(4.30)

It was found by other investigators 21,44 that concrete does contribute to the shear capacity and can be added to the ultimate shear carried by the stirrups thus forming the modified truss analogy:

$V_u=V_c+V_s$ (modified truss analogy) .....(4.31)

4.4 Stress in Stirrups

4.4.1 Importance of Stirrup Strain Measurement

Detailed knowledge of actual steel stress can provide a better understanding of the internal behaviour of reinforced concrete structures. In the case of shear, strain (stress) measurement in the stirrups is helpful with regard to (a) design criteria for web reinforcement,(b) inclined crack width and (c) fatigue strength of stirrups.

a) Most of the shear tests have been undertaken to observed failure behaviour. If web reinforcement is provided, stress measurements are desirable to verify a rational theory of shear strength.

b) Thin-webbed sections such as 'I' or 'T' sections which are used widely in precast concrete construction, may show inclined cracking under service load

and these cracks can sometimes be wider than flexural cracks. Stirrup strain measurement is of great importance to study and predict these inclined crack widths.

c) Stress in the stirrups can substantially increase under the fatigue loading. More detailed knowledge of stress developement can be obtained by observation of stress behaviour of stirrups.

It was discussed with reference to the modified truss analogy that the total shear stress carried by the section is:

$$v=v_c+rf_{sv} \qquad \text{.....(4.32a)}$$

or $$f_{sv}=(v-v_c)/r \qquad \text{.....(4.32b)}$$

where v_c is the shear stress at the inclined cracking limit, and several investigators including Leonhardt[59] have confirmed this. In accordance with these test results, nearly all Codes of practice propose formulae for the design of web reinforcement. These are of the basic form:

$$V_s=V_u-V_c \qquad \text{.....(4.33)}$$

i.e the ultimate shear V_u considered in the classical truss analogy can be reduced by V_c which corresponds to the shear cracking load and it means that the stress in the stirrup depends on the concrete sheare strength.

4.4.2 Experimental Results of Strain in Stirrups

Stirrup strain was measured at a point positioned approximately at the level of the centroid of the section in order to obtain the maximum tensile strain in the stirrups. The gauged stirrups were located in the overlapping part of the connection as well as in the adjacent in-situ or precast sections.

The behaviour of the stirrups in the overlapping region was influenced substantially by the detailing and modifications at the connection. These will be

discussed fully in the next two chapters relating to different types of connections. In this chapter the behaviour of stirrups located either in the precast or in-situ sections only will be considered.

Tensile stresses in the stirrups were obtained using measured strain and calculating the appropriate stress from the experimental stress-strain relationship explained previously.

Figs. 4.10 to 4.19 show the relationship between experimental stirrup stress and applied shear force in the section for either the precast (Figs. marked a) or the in-situ part (Figs. marked b) of the specimen.

These figures consist of several curves corresponding to different longitudinal positions of stirrups. These positions have been marked numerically both on the curve and on the beam. The experimental inclined cracking shear has also been marked on each set of curves.

It can be seen from these curves that in general up to the inclined cracking shear, the stress in the stirrup is very small and almost zero. When the concrete web cracks, the stirrups begin to take the shear and the tensile stress in the stirrups continue to increase nearly linearly until failure.

It should be noted that the limiting shear force carried by the concrete in prestressed beams depends on the tensile strength of the concrete and the level of prestress. Several experimental expressions have been proposed for the shear carried by the concrete and generally this depends upon the :

a) Concrete strength

b) Percentage of main reinforcement

c) Effective depth

d) Level of prestress

It has been observed experimentally that after the occurrence of inclined cracking, the limiting concrete shear strength (Vc) can still be maintained until the failure. The reason for this is that this value may be equal to the sum of other effects which carry the shear force (i,e concrete compression zone,

aggregate interlock and dowel action) after inclined cracking . In other words the shear carried by the uncracked concrete is transferred to other effects after the inclined cracking.

The stress in the stirrups has been compared with Eqn. 4.28 (classical truss analogy) and Eqn. 4.31 (modified truss analogy) and the results plotted in Figs. 4.20 and 4.21 for both the precast and in-situ parts of the beam. It should be mentioned that a 45° crack inclination has been assumed for Eqns. 4.28 and 4.31 and plotted in those figures. This assumption is true for reinforced beams but for prestressed beams this angle can be slightly less than 45° which is not normally considered in design and hence a slightly higher stirrup stress may be obtained.

It can be seen from these graphs (Figs. 4.20 and 4.21) that the modified truss analogy (Eqn. 4.31) gives an accurate or slightly conservative result up to half the failure shear load but for larger loads it seems to be slightly unsafe. The reason for this can be explained by the way that in concrete beams without web reinforcement, shear mechanisms (especially aggregate interlock) can function as long as the crack width is not excessive. Hence in the presence of stirrups, this action will exist provided the the stirrup strain is small. This means that near failure the assumed concrete shear strength (v_c) can actually reduce, resulting in an increase in the stirrup's stress. Such behaviour is more significant in beams with a relatively high ratio of web reinforcement auch as those tested in the present investigation.

The loading and support arrangement as discussed in a previous chapter represent a continuous beam. It has been previously suggested by Leonhardt[77] that shear carried by concrete (v_c) at the inner supports of continuous beams is smaller than that for simply supported beams and values of $v_c=f'_c/22$ and $v_c=f'_c/16$ have been proposed for continuous and simple span structures

respectively. The straight lines indicating the modified truss analogy on Figs. 4.20 and 4.21 are based on the BS8110 prediction method for concrete shear strength. If the above mentioned decrease in concrete shear strength in continuous beams is accepted, the experimental stirrup stress would be closer to the modified truss analogy.

In current Codes of practice, for design of shear reinforcement there is no difference between simple span and continuous beams and it is proposed here that in continuous beams for the failure condition, the classical truss analogy could be used conservatively.

4.4.3 Stirrup Stress Behaviour under Load Removal and Reloading of the Beam

All beams, except one (E30BC4), were tested in a static loading condition. In test E30BC4 however, the load was applied up to the design service limit and then it was reduced to zero. In the second cycle the load was gradually increased up to failure. The stirrup strain (stress) was measured in both cycles and plotted against the applied shear as shown in Figs. 4.13a,b and 4.22a,b.

Generally, no significant stress was developed by the stirrup in the first cycle until inclined cracking of the web had occurred, whereupon the stress increased from zero to about 120 N/mm^2.

On load removal after inclined cracking the stirrup stress did not fall below a certain residual stress. In the second cycle, the stirrup stress remained unchanged up to approximately half the inclined cracking load and then increased nearly linearly up to failure.

In contrast to laboratory specimens, actual structures (especially bridges) are mainly subjected to load repetitions or changing load positions. In order to simulate real conditions, it is desirable in a shear test to measure the

stirrup stress not only during a single loading but to study also the influence of subsequent load cycles.

The residual stress in the stirrup seems to be due to inelastic behaviour and unrecoverable deformation in concrete and hence in the stirrup, although the actual stress in the stirrup at the time of load removal may be well below its elastic limit.

Several investigators including Ruhnau[78] have observed the influence of repeated loading on the stirrup stress. Ruhnau tested five reinforced concrete beams of rectangular and 'I' sections . Four beams were subjected to several load repetition cycles and the fifth beam loaded only twice (similar to one tested here) . Test results revealed that a substantial residual stress (15% to 30% of the yield stress) existed and it was suggested that the stirrup stress increased under repeated loading. A comparison of the test results with both the theoretical truss and modified truss analogies indicated that neither of these equations was acceptable for predicting stirrup stress under repeated loading and he therefore proposed the alternative equation:

$$f_{sv}=k_1+k_2v/\rho_v \qquad \text{(PSI)}.....(4.34)$$

where k_1 and k_2 were empirical coefficients, $\rho_v=A_{sv}/bS_v$ and $v=V/bz$.

The values of k_1 and k_2 were thought to depend mainly on the previous loading and it was suggested that k_1 should range from 4000 Psi to 28000 Psi and k_2 from 0.45 to 0.6 .

4.4.3.1 Calculation of Stirrup Stress

It can be seen from Fig. 4.22a that in the second cycle neither classical nor modified truss analogies are capable of predicting the actual value of stress in the stirrup. The experimental results represents a bilinear curve starting

from a residual stress at zero load and continuing approximately evenly up to about half the initial inclined cracking load and then increasing at a higher rate. This part of the curve is located between curves for the two above mentioned truss analogies.

Using classical truss analogy the stirrup stress is:

$$f_{sv}=VS_v/(dA_{sv}) \qquad \text{.....(4.35)}$$

But by the modified truss analogy:

$$f_{sv}=(V-V_c)S_v/(dA_{sv}) \qquad \text{.....(4.36)}$$

The equation 4.34 proposed by Ruhnau[78] predicts a residual stress of k_1. It also takes into account the change in the slope of the curve by inserting the term k_2 but it doesn't consider the bilinear shape of the curve. This effect has been considered in a mathematical model proposed by Tay et al[79].

Since in most cases the ultimate shear resistance of structures subjected to cyclic loading is required, it is proposed that the classical truss analogy may be used with a sufficient margin of safety. It can be seen in Fig. 4.22b that in the rectangular section of the in-situ beam, after the second cycle of loading, there is no residual stress in the stirrup and the modified truss analogy can thus give a safe prediction of the stirrup stress. The reason is that in the first loading cycle the maximum shear was the service shear of the precast section which is smaller than that for the in-situ part. Thus the stirrup stress has recovered to some extent and the shear resisted by the concrete is maintained in the second cycle.

4.5 Failure Mode in Precast Prestressed M-Beam

4.5.1 Web Crushing

Seven beams failed in a web crushing mode which is sometimes referred to as web compression, web distress or inclined compression. This failure

occured in the web of the precast M-beam between the loading point and the continuous support (see plate 5.6 for example). This mode of failure may be described by considering the previously mentioned truss analogy with the concrete struts acting between successive inclined cracks as compressive members of the truss. Obviously these concrete struts have limited compressive strength and the shear strength of a section is thus not solely controlled by the amount of shear reinforcement as it is possible for the concrete struts to fail under the compression forces before the stirrups can develop their full tensile strength.

Considering the above mentioned reasons for web crushing, it can be seen that this mode of failure occurs mostly in thin-webbed sections under high shear force in which a high amount of shear reinforcement has been provided, and it is in fact an upper limit to the shear carrying capacity of a section. The shear strength of a beam will not be increased beyond that upper limit even by increasing the shear reinforcement.

In prestressed concrete, thin-webbed 'I' or 'T' sections are commonly used. The prestressing itself will increase the compressive stress in the struts and thus the importance of the web crushing mode of failure in prestressed concrete is quite clear. The web crushing problem has received comparatively little attention in reinforced concrete, since the width of webs is usually sufficient to produce web crushing failure.

In Codes of practice, therefore, the web crushing limit is defined as a maximum nominal shear stress that the beam can carry. In the following section different code limits and their comparisons with the present experimental results will be discussed.

4.5.2 Code Provisions for Web Crushing

4.5.2.1 BS8110 :1985[27] , BS5400 :1978[68] , CP110 : 1972[64]

The current British code BS8110 limits the maximum shear stress in a concrete section as:

$$v_{max}=0.8\sqrt{f_{cu}}<5.0 \text{ N/mm}^2 \qquad \text{(SI)}.....(4.37)$$

which includes a safety factor of 1.25.

These values are slightly larger than those suggested by the previous code CP110 :1972 and current bridge code BS5400 : Part 4 in which the following limits are recommended :

$$v_{max}=0.75\sqrt{fcu}<4.75 \text{ N/mm}^2 \qquad \text{(SI)}.....(4.38)$$

which includes the same safety factor.

The corresponding maximum shear force, V, is obtained by multiplying v_{max} by bd (effective cross-section area for shear). For the case of web voids such as in post-tensioned members, grouted or ungrouted, there is no recommendation to allow for the reduction in web width. Guidance on the application of the CP110 code in the C&CA handbook[80], suggests that for ungrouted ducts, the actual width of concrete is used and for grouted ducts the actual concrete width plus one third of duct width should be considered in calculating the maximum shear strength.

In BS5400, it is recommended that the web width should be reduced by the duct diameter or two-thirds of the duct diameter for ungrouted and grouted members respectively.

4.5.2.2 ACI 318-83[81]

The current American code gives a maximum limit for the shear force

carried by the shear reinforcement equal to : $(8\sqrt{f'_c})bd$ .....in (Psi)

or: $(0.67\sqrt{f'_c})bd=(0.6\sqrt{f_{cu}})bd$ .....in (SI) units

so the maximum total allowable shear stress in a concrete section will be:

$$v_{max}=v_c+ 8\sqrt{f'_c} \quad \text{(Psi)} \quad (4.38a)$$

or: $v_{max}=v_c+ 0.67\sqrt{f'_c}=v_c+ 0.6\sqrt{f_{cu}}$ (SI).....(4.38b)

where v_c is the shear stress carried by the concrete section and prestressing effect obtained in accordance with the section 11.4 of this code. There is no recommendation on the reduction of section width in the case of web holes in post-tensioned members.

4.5.2.3 CEB-FIP Model Code : 1978[72]

There are two (standard and accurate) methods to determine the maximum allowable shear force in the section to prevent web crushing. The standard method limits the shear force in sections with vertical stirrups to :

$$V_{R2}=0.3f'_cbd \quad .....(4.39)$$

in which b is the web width and in case of bars or tendons passing through the web, b should be replaced by a reduced value b_{red} if the bar diameter is greater than b/8 .

$$b_{red}=b-0.5\Sigma\phi \quad .....(4.40)$$

where ϕ is the bar diameter and $\Sigma\phi$ is the total web width engaged by the bars (which is not necessarily equal to the sum of the diameters in case of grouped bars). The b_{red} should be obtained for the most unfavourable level.

Using the CEB-FIP accurate method, the maximum shear force will be :

$$V_{R2}=0.3f'_cbdSin2\theta \quad \text{.....(4.41)}$$

where b is determined as in the standard method and θ is the direction of inclined cracks or concrete struts but: $3/5 \leq \cot\theta \leq 5/3$

4.5.2.4 Australian Standards , SAA Prestressed Concrete Code : 1978[70]

Protection against web crushing failure in the Australian code is provided by limiting the maximum shear carried by the stirrups to : $V_s=(0.58\sqrt{f'_c})bd$. Adding the shear carried by the concrete V_c, the maximum total allowable shear carried by the section :

$$V_{max}=V_c+(0.58\sqrt{f'_c})bd = V_c+(0.52\sqrt{f_{cu}})bd \quad \text{(SI).....(4.42)}$$

in which b has been defined as the effective width of the web though there is no definition for effective width to see whether the duct width should be deducted or not.

4.5.2.5 Standard Specification for Highway Bridges (AASHTO)[73] : 1977

The American bridge code limits the maximum shear carrying capacity of a concrete section to:

$$V_u=(4.75\sqrt{f'_c})bd \quad \text{(Psi).....(4.43a)}$$

or: $V_u=(0.397\sqrt{f'_c})bd=(0.355\sqrt{f_{cu}})bd \quad \text{(SI).....(4.43b)}$

Again there is no inclusion for the effect of possible ducts in the web. This code gives a much more conservative result than ACI in this respect.

4.5.2.6 Danish Standards "Structural Use of Concrete"[69] : 1986

Two different limits are given in the Danish Code for different types of stirrup arrangements:

a) For vertical stirrups:

$$v_{max}=0.25f_{cd}\leq 6 \text{ N/mm}^2 \qquad \text{.....(4.43c)}$$

b) For 45° inclined stirrups:

$$v_{max}=0.35f_{cd} \leq 7 \text{ N/mm}^2 \qquad \text{.....(4.43d)}$$

where f_{cd} is the characteristic design compressive strength of concrete.

4.5.3 Comparison of Code Predictions With Observed Web Compression Strength

Table 4.4a,b shows a comparison between calculated web compression strengths as discussed in previous sections and the experimental values. The experimental values have been divided by the calculated values to obtain the actual observed safety factors . The mean values have also been calculated for all code predictions.

It can be seen from this table that all British Codes (BS8110,BS5400 and CP110) and the Danish Code underestimate the web crushing strength for the type of beams tested in this investigation and their observed safety factors lie between 2.0 and 2.66 in comparison with typical material or strength safety factors of 1.5 , 1.25 , and 1/0.85=1.17 suggested by different Codes. The American , Australian and European (CEB_FIP) Codes give closer predictions in which these mean values are 1.47 , 1.69 , and 1.60 respectively.

It should be noted that the web crushing strength is partly affected by the shear span to effective depth ratio. It has been observed by Bennett[67] and Balasooriya[66] that a reduction in shear span to effective depth ratio will lead to

an increase in the web crushing strength. The shear span to effective depth ratio in this investigation was relatively low, varying from 2.8 to 3.72. It can also be seen that generally for smaller shear spans, larger web crushing strengths were apparent.

In the Codes there is no inclusion of shear span in predicting the web crushing strength and it is likely that their suggestions are based on the worst cases i.e. for larger shear spans. It was observed by Tay[62] that in some cases, with larger shear spans than those tested here, CEB-FIP and ACI were severely unsafe while CP110 gave closer predictions. It can thus be concluded that British and Danish Codes give closer predictions for high shear span to effective depth ratios while ACI, CEB and Australian Codes are more suitable for smaller ratios.

It has been suggested in some Codes e.g CEB, that the web holes such as post-tensioning ducts either grouted or ungrouted should be deducted completely or partly from the web width. This has been investigated and confirmed by Clarke and Taylor[18] in a series of tests on concrete prisms with different type of holes in respect of size, direction, bars and grouting. In tables 4.4a,b for calculation of web crushing shear, the effect of prestressing strands passing through the web has been considered only when using CEB method. It is notable that where Codes allow for the effect of ducts they only refer to grouted or ungrouted ducts in post-tensioned members and it is disputable whether this could be considered for pretensioned members. If British Codes considered this effect, more conservative results would be produced.

It is probable that when a bar, or group of bars, passes through the web of a beam which is subjected to inclined compression, these bars can transmit the entire compressive force provided there is natural bond between bars and concrete, as with pretensioned bars bonded with concrete.

4.5.4 Proposed Mathematical Equation for Web Crushing Strength

The truss analogy implies that the amount of required shear reinforcement depends on the shear stress carried by the concrete and the steel tensile strength:

$$V-V_c=(dA_{sv}f_{sv})/S_v \quad , \quad r=A_{sv}/bS_v \qquad \text{.....(4.44a)}$$

$$v-v_c=(\ V_u-V_c)/bd=rf_{sv} \qquad \text{.....(4.44b)}$$

For the case of relatively small shear spans, where the failure is controlled by crushing of the web, the above equations can not predict the actual shear at failure. The reason is that in this case the following factors will apply, as has been observed in this investigation and also by others[8,66].

a) The ratio of shear span to effective depth will itself influence the web crushing strength.

b) The shear reinforcement may not be fully utilized in this type of failure and thus the stirrup ratio can not be increased indefinitely.

The shear span effect can be inserted in the left hand side of equation 4.44b . The right hand side then may be a function of rf_{sv} rather than rf_{sv} itself.

$$(a/d)(V-V_c)/bd=f(rf_{sv}) \qquad \text{.....(4.45)}$$

and at failure $V=V_u$:

$$(a/d)(V_u-V_c)/bd=\ f(rf_{yv}) \qquad \text{.....(4.46)}$$

It can be seen from equations 4.45 and 4.46 that the shear span is inversely proportional to the shear force V or V_u . For small shear spans, the direction of compressive struts i.e inclined crack direction, is controlled by the position of the nearest point load to the support. This direction is the line joining loading point to the support. Mattock and Kaar[8] related the shear

strength to the sine of the angle between that line and the horizontal. They introduced a mathematical model which was discussed in chapter two.

To find a mathematical form for the right hand side of equation 4.45, for every loading stage the experimental shear force (V) and stirrup stress(f_{sv}) have been used to plot the left hand side of the equation against (rf_{sv}). A mean curve was drawn to approximate all the points. For simplicity this was taken as a parabolic curve rather than higher orders. The equation of this curve is:

$$(a/d)(V-V_c)/bd=3.9(rf_{sv})-0.151(rf_{sv})^2 \quad .....(SI).....(4.47)$$

Furthermore a conservative lower bound line was drawn to give a simplified relation, and the following equation represents that line (see the green line in Fig. 4.23).

$$0.45(a/d)(\ V-V_c)/bd=rf_{sv}$$

or: $$Asv=0.45(a/d)(V-V_c)S_v/df_{sv}=p(\ V-V_c)S_v/df_{sv} \quad .....(4.48)$$

It can be seen that Eqn. 4.48 has an extra parameter (p) in comparison with the conventional equation: $A_{sv}=(V-V_c)S_v/df_{sv}$

The value of p is :

$$p=\ 0.45(a/d)\leq 1.0 \quad \text{or:} \quad a/d \leq 2.2 \quad .....(4.48a)$$

This means that for the type of beams tested here, if the shear span to effective depth ratio is less than 2.2, the required area of shear reinforcement may be reduced.

4.5.4.1 Condition at Failure

For the failure condition experimental values of ultimate shear (V_u) and stirrup stress (normally f_{yv}) have been plotted in conjunction with the proposed equation in Fig. 4.24. The web crushing results from some other

investigators have also been shown in that figure. It should be mentioned here that at web crushing failure, the stirrup stress is not necessarily equal to its yield value.

To find the actual stirrup stress at web crushing, the web crushing shear force V_u should be obtained experimentally or by using the maximum permitted shear force given in the codes and then by using the curve or simplified line of Fig. 4.23, the actual value of (rf_{sv}) will be found. For a specific condition of web crushing, the value of (rf_{sv}) is a constant, so by increasing the stirrup ratio (r), the stress (fsv) will be reduced without affecting the strength. This means that shear reinforcement can not be utilized above a certain ratio.

4.5.4.2 Effect of Concrete Strength

It was mentioned in section 4.5.2 that the web crushing strength is dependent upon the concrete strength, and some codes have assumed it to be related to the square root of compressive strength. The proposed equation (Eqn. 4.47) does not include concrete strength but it is for an average cube strength of $67N/mm^2$ throughout the tests. It is then reasonable to change the web crushing strength by a factor $(\sqrt{f_{cu}})/(\sqrt{67})=\sqrt{f_{cu}}/8.2\ N/mm^2$.

$$(a/d)(V-V_c)/bd=(\sqrt{f_{cu}}/8.2)[3.9(rf_{sv})-0.151(rf_{sv})^2] \quad .....(4.49a)$$

or: $$(8.2/\sqrt{f_{cu}})(a/d)(V-V_c)/bd=3.9(rf_{sv})-0.151(rf_{sv})^2 \quad .....(4.49b)$$

(Both Eqns. 4.49a,b are in SI units). The simplified lower bound line becomes:

$$0.45(a/d)(V-V_c)/bd=(\sqrt{f_{cu}}/8.2)\ rf_{sv} \quad \text{(SI)}.....(4.50a)$$

$$A_{sv}=(3.7/\sqrt{f_{cu}})(a/d)(V-V_c)S_v/df_{sv} \quad \text{(SI)}.....(4.50b)$$

The reduction factor to the conventional equation will then be:

$$p = (3.7/\sqrt{f_{cu}})(a/d) \leq 1.0 \qquad \text{(SI)}.....(4.51)$$

4.6 Enhanced Shear Strength near the Support

At the support, or loading point region of a beam, the reaction or external load produces a compressive bearing effect within the beam depth. The affected part can be obtained by drawing 45° dispersal lines from the supports or loading points. The affected area from each side of the support or load will be equal to the beam's depth.

This bearing compressive stress is similar to vertical prestressing which in turn reduces the principal tensile stress and hence increases the shear strength, and is why shear cracks are rarely observed in these regions.

4.6.1 Code Provisions for Enhanced Shear Strength

Most Codes of practice allow for the increased shear strength near the supports by assuming a constant shear force from a certain point to the support or increasing the concrete shear strength, irrespective of the shear force diagram, near the support. These recommendations are similar for either simple or continuous supports.

4.6.1.1 British Code BS8110 : 1985[27]

It has been explained that shear failure in the beams without stirrups normally occurs on a plane inclined at an angle of approximately 30° to the horizontal but if the angle of failure plane is forced to be inclined more steeply than this (because the section considered is close to a support or for other reasons), the failure shear is increased, and this enhancement of shear strength may be taken into account when designing sections near the support by

increasing the design concrete shear strength v_c to $v_c(2d/a_v)$ [but not greater than the $0.8\sqrt{f_{cu}}$ or $5N/mm^2$ whichever is the lesser]. This enhancement may be applied to any section closer than 2d to the face of support or concentrated load. The total required area of shear reinforcement will be :

$$\Sigma A_{sv}=a_v b(v-2dv_c/a_v)/0.87f_y \geq 0.4ba_v/0.87f_y \qquad .....(4.52)$$

which should be provided within the middle three-quarters of a_v.

In the simplified method it is recommended that the design shear stress may be calculated at a section at a distance of the effective depth, d, from the face of the support.

4.6.1.2 British Bridge Code BS5400: Part 4 :1978[68]

According to this code, enhancement of shear strength may be allowed for at sections within a distance $a_v<2d$ from the face of a support, front edge of a rigid bearing or centreline of a flexible bearing. This enhancement should take the form of an increase in the allowable shear stress ζv_c to $\zeta v_c(2d/a_v)$ but not greater than $0.75\sqrt{f_{cu}}$ or $4.75N/mm^2$.

ζ_s=depth factor=max.$[\sqrt{(500/d)}$, 0.70)] .....d in millimetre

a_v=distance of section considered to the support

4.6.1.3 CEB-FIP Model Code[72] : 1978

The European code adopts a less conservative and possibly unsafe design method for shear near supports. It suggests that shear stress within a distance 'd' from the face of a direct support need not be checked.

4.6.1.4 Australian Standards, SAA Prestressed Concrete Code[70] : 1978

According to the Australian code, the calculated value of shear reinforcement at sections within a distance of h/2 (half the beam depth) should be continued to the support.

4.6.1.5 Danish Standards "Structural Use of Concrete"[69]

The Danish code assumes a reduced shear force within a distance of jd (internal lever arm) from the support and having a constant value equal to the shear force at that distance. This method is similar to the simplified method of BS8110.

4.6.2 Experimental Results of Enhanced Shear Strength and Proposed Method

The Increased shear strength of sections near the supports was observed experimentally by the measurement of stirrup stresses in the vicinity of continuous supports. The stirrup spacings were dictated by the shear force required to be transferred between the precast and in-situ concrete. Stirrup strains were obtained by using electrical resistance strain gauges fixed to the middle of all stirrups placed near the support. The stresses were then obtained by using the experimental stress-strain relationship for the 6mm high yield deformed bar.

Experimental stirrup stresses were plotted against their distances from the support. Typical curves can be seen in Figs. 4.25 to 4.28 for some of the tests. Each figure consists of a number of curves representing a certain loading level indicated by 'R' (the ratio of load to the failure load). The curve with R=1.0 represents the failure condition.

Consideration of the stirrup stress variation along the beam over the support reveals that in general the stirrups at or very close to the support remain more or less unstressed right up to the failure. For stirrups further from the support higher stresses were observed increasing approximately linearly with their distances from the support up to a certain point from which the stress in the stirrup stays approximately constant. For the failure load after that point all the stirrups read their yield stress.

It can be seen from the curves that at a distance of about 250mm to 350mm, the stresses in the stirrups become constant or equal to their yield value (for the failure load). Comparing these distances with the effective depth (i.e 430mm) shows that the enhancing effect of the support on the shear strength starts from a distance of about 0.6d to 0.8d from the support. An average value of 0.7d may thus be selected.

Assuming a linear relationship between stirrup stress and its distance from the support (as experimental results show), the proposed mathematical equation will be:

$$f_s=(f_y/0.7d)x \quad \text{.....for:} \quad x\leq 0.7d \quad \text{.....(4.52a)}$$

$$f_s=f_y \quad \text{.....for:} \quad x>0.7d \quad \text{.....(4.52b)}$$

where x is the stirrup distance from the support (see also Fig. 4.29).

The above equation is for a constant shear force acting in the support region and it can be seen that while stirrups located further than 0.7d from the support have their full yield stress, the stirrups located within 0.7d from the support do not develope their full tensile strength. This means that there is a reserve of shear strength in this region. The unused strength of the stirrup (Δf_s) is :

$$\Delta f_s=f_y-f_s=f_y-(f_y/0.7d)x=fy(1-x/0.7d) \quad \text{for: } x\leq 0.7d \quad \text{.....(4.53)}$$

This reserve of stirrup tensile strength is capable of increasing the shear

strength of the beam as follows:

$$\Delta v = r\,(\Delta f_s) = r f_y (1 - x/0.7d) \qquad \text{for: } x \leq 0.7d \qquad \text{.....(4.54)}$$

Adding this extra shear strength to the conventional expression for shear strength:

$$v_u = \Delta v + (v_c + r f_y) = v_c + (\Delta v + r f_y) = (v_c + \Delta v) + r f_y \qquad \text{.....(4.55)}$$

It can be seen from the above equation (Eqn. 4.55) that the increased shear strength can be expressed as an imaginary increase in the shear carried by stirrups or shear carried by concrete. For practical purpose the value of Δv can be taken as its average between x=0 and x=0.7d:

$$x=0 \quad \Rightarrow \quad \Delta v = rfy$$

$$x=0.7d \quad \Rightarrow \quad \Delta v = 0$$

$$(\Delta v)_{av.} = 0.5 r f_y \qquad \text{.....(4.56)}$$

and the ultimate increased strength:

$$v_u = 0.5 r f_y + (v_c + r f_y) = v_c + 1.5 r f_y = (v_c + 0.5 r f_y) + r f_y \qquad \text{.....(4.57)}$$

For the beams tested here $r f_y = 1.94$ N/mm^2 while the average value of v_c is equal to 0.80 N/mm^2 so the increased concrete strength will be:

$$v'_c = v_c + \Delta v = 0.81 + 1.94(1 - x/0.7d) \qquad \text{.....(4.58)}$$

v'_c=Increased concrete strength

with an average value of : $(v'_c)_{av.} = 1.78$ between x=0 and x=0.7d which is 2.2 times greater than the concrete shear strength v_c.

4.6.3 Comparison of Experimental Results with Different Code Predictions

In general Codes of Practice have two different methods of predicting the enhanced shear strength near the supports. One approach is to increase the

concrete shear strength by a factor relating to the distance between the section considered and the support, and the enhancement is limited to a certain length from the support. This method is used by the British Codes BS8110 and BS5400. The second approach is to reduce the shear force near the support to the shear force at a point located at a certain distance from the support. This point will usually have a smaller shear force in the case of uniformly distributed loading. This method is used as a simplified method in BS8110 and also in Australian and Danish Codes. The first method is more accurate as seen from the experiments while the second method is simple and practical.

With reference to the first method, the experimental increased shear strength was attributed to an increase in the concrete shear strength v_c and Eqn. 4.58 was derived. A comparison was made between this equation and BS8110 or BS5400 prediction in table 4.5. Test results show that British Codes overestimate the increased shear strength of the beams tested here. This overestimation is for both the length of the beam from support over which the shear is increased (2d) and also its magnitude (see table 4.5).

There is no explanation in the Codes whether this enhancement is applied for continuous structures and has been suggested by Leonhardt[77] that the concrete shear strength in a continuous beam is smaller than that of simply supported beam with an order of 16/22=0.72.

The present observation proves this matter to some extent but it seems that more research is required in this area. In a continuous beam flexural cracks will appear at the top of the beam and penetrate downwards. If the shear force is high at the support (which is usually the case), these flexural cracks extend steeply towards the support to form the flexural-shear cracks. In this case a reduction in the beam's shear strength could be expected.

Using the second approach of the Codes, including the simplified method of BS8110, Australian and Danish Codes in which a reduced shear force is assumed from a distance of d, h/2 or jd respectively seems to be safer for the case of

continuous beams, especially the Australian code in which the assumed distance ($h/2 \cong 0.6d$) is close to the observed value of $0.7d$.

The European Code (CEB-FIP) recommends that the shear stress should not be checked within a distance 'd' from the support irrespective of the shear force magnitude in that region. This seems an illogical approach, at least for continuous beams, and could be unsafe and dangerous.

Table 4.1 Experimental and Calculated Values of Web Cracking Shear

Beam Designation	Cube Strength N/sq. mm	Eff. Prestress at the Centroid N/sq. mm	Vertical Component of Prestress (kN)	Experimental Web Cracking Shear (kN)	Predicted Values by Different Codes				
					BS8110 : 1985 BS5400 : 1984 CP110 : 1972	CEB-FIP Model Code : 1978	ACI 318-83	Standard Spec. for Highway Bridges AASHTO : 1977	Australian Standards Prestressed Concrete Code: 1978
E30AA1	68.3	6.2	17.0	87.9	76.7	60.7	96.8	44.4	88.3
E30AA2	72.0	6.1	16.7	98.3	77.0	62.1	97.1	44.1	88.7
E30AB3	65.0	6.1	16.7	92.7	75.1	65.3	94.8	44.1	86.5
E30BC4	66.5	5.9	16.2	67.7	74.2	57.2	93.5	43.6	85.6
E10CC5	67.2	5.9	16.2	94.3	74.4	64.8	93.5	43.6	85.8
E10CD6	69.1	6.0	16.4	56.8	75.6	65.0	95.2	43.8	87.1
WTFCC7	68.1	6.1	16.7	94.3	76.0	62.7	95.8	44.1	87.5
WTFPCC8	67.5	6.0	16.4	103.2	75.2	57.2	94.6	43.8	86.6
WTFCC9	64.2	6.1	16.7	97.6	75.0	58.9	94.5	44.1	86.3
WTFDCC10	62.5	5.9	16.2	92.0	73.1	59.0	92.2	43.6	84.3

Note : The Vertical Component of Prestress has been Added to Calculated Design Values

Table 4.2 Ratio of Observed to Calculated Values of Web Cracking Shear (Vertical Component of Prestress Included)

	$\frac{V_{cr.,Test}}{V_{cr.,Cal.}}$ All Safety Factors Included in Calculated Values				
Test Code	BS8110 BS5400 CP110	CEB-FIP	ACI 318-83	Standard Spec. for Highway Bridges (AASHTO)	Standars Asso. of Australia
E30AA1	1.14	1.44	0.90	1.98	0.99
E30AA2	1.27	1.57	1.00	2.21	1.10
E30AB3	1.23	1.41	0.97	2.08	1.07
E30BC4	0.90	1.16	0.71	1.52	0.79
E10CC5	1.25	1.43	1.00	2.12	1.09
E10CD6	0.74	0.86	0.60	1.28	0.65
WTFCC7	1.23	1.49	0.98	2.12	1.07
WTFPCC8	1.36	1.78	1.08	2.32	1.19
WTFCC9	1.29	1.64	1.03	2.19	1.13
WTFDCC10	1.24	1.53	0.99	2.07	1.09
MEAN*	1.21	1.50	0.96	2.06	1.05

* Test WTFCC6 has not been taken into account due to premature failure of the connection

..Table 4.3 Ratio of Observed to Calculated Values of Web Cracking Shear (vertical Component of Prestress Not Included)

	$\frac{V_{cr.,test}}{V_{cr.,cal.}}$ All Safety Factors Included in Calculated Values				
Different Codes / Test No.	BS8110 BS5400 CP110	CEB-FIP	ACI 318-83	Standard Spec. for Highway Bridges (AASHTO)	Standard Asso. of Australia
E30AA1	1.47	2.01	1.1	3.20	1.23
E30AA2	1.63	2.16	1.22	3.58	1.36
E30AB3	1.58	1.90	1.18	3.38	1.32
E30BC4	1.16	1.65	0.87	2.47	0.97
E10CC5	1.62	1.94	1.21	3.44	1.35
E10CD6	0.95	1.16	0.72	2.07	0.80
WTFCC67	1.59	2.05	1.19	3.44	1.33
WTFPCC8	1.75	2.52	1.32	3.76	1.47
WTFCC9	1.67	2.31	1.25	3.56	1.40
WTFDCC10	1.61	2.15	1.21	3.36	1.35
MEAN	1.56	2.07	1.17	3.35	1.30

* Test WTFCC6 has not been taken into account due to premature failure of the connection

Table 4.4a. Predicted Web Crushing Strength by Different Codes

Beam Designation	Concrete Cube Strength N/sq.mm	Shear Span/Eff. Depth	Experimental Web Crushing Strength (kN)	Predicted Web Crushing Strength by the Codes (kN) (All Safety Factors Included)					
				BS8110 : 1985	BS5400 : 1984 CP110 : 1972	CEB-FIP Model Code : 1978	ACI 318-83	Australian Standards Prestressed Concrete Code: 1978	Danish Standard 1986
E30AA1	68.3	2.8	312	120.4	114.38	187.3	203.9	180.0	144.5
E30AA2	72.0	2.8	309	120.4	114.38	198.0	207.7	183.3	144.5
E30AB3	65.0	2.8	267	120.4	114.38	178.6	200.0	176.1	144.5
E30BC4	66.5	3.25	255	120.4	114.38	182.6	200.0	176.8	144.5
E10CD7	68.1	3.72	297	120.4	114.38	186.6	203.4	179.3	144.5
WTFPCC8	67.5	2.8	348	120.4	114.38	185.3	202.0	178.4	144.5
WTFCC9	64.2	2.8	329	120.4	114.38	176.0	199.2	175.2	144.5

Table 4.4b. Ratio of Observed to Calculated Web Crushing Strength(Observed Safety Factor)

Beam Designation	Concrete Cube Strength N/sq.mm	Shear Span/Eff. Depth	Experimental Web Crushing Strength (kN)	Ratio of Observed to Calculated Design Web Crushing Strength					
				BS8110 : 1985	BS5400 : 1984 CP110 : 1972	CEB-FIP Model Code : 1978	ACI 318-83	Australian Standards Prestressed Concrete Code: 1978	Danish Standard 1986
E30AA1	68.3	2.8	312	2.59	2.72	1.66	1.53	1.73	2.15
E30AA2	72.0	2.8	309	2.56	2.70	1.56	1.48	1.68	2.13
E30AB3	65.0	2.8	267	2.21	2.41	1.50	1.33	1.56	1.91
E30BC4	66.5	3.25	255	2.11	2.29	1.38	1.27	1.44	1.76
E10CD7	68.1	3.72	297	2.46	2.59	1.57	1.46	1.65	2.05
WTFPCC8	67.5	2.8	348	2.89	3.04	1.86	1.72	1.95	2.40
WTFCC9	64.2	2.8	329	2.73	2.87	1.73	1.53	1.87	2.27
MEAN (Safety Factors Included)				2.50	2.66	1.60	1.47	1.69	2.09
MEAN (Safety Factors Removed)				2.0	2.12	1.07	1.25	1.43	1.40

Table 4.5. Values of Increased Concrete Shear Strength (Proposed Eqn.)in Comparison with BS8110

d=Effective Depth

Distance of the Section From the Support, x	0	0.25d	0.5d	0.7d	d	1.5d	2d
BS8110 Increased Shear Str. N/sq. mm	6.25	6.25	3.23	2.32	1.61	1.07	0.81
Increased Shear Str. by Proposed Eqn. (Eqn. 4.58), N/sq. mm	2.75	1.29	1.46	0.81	0.81	0.81	0.81

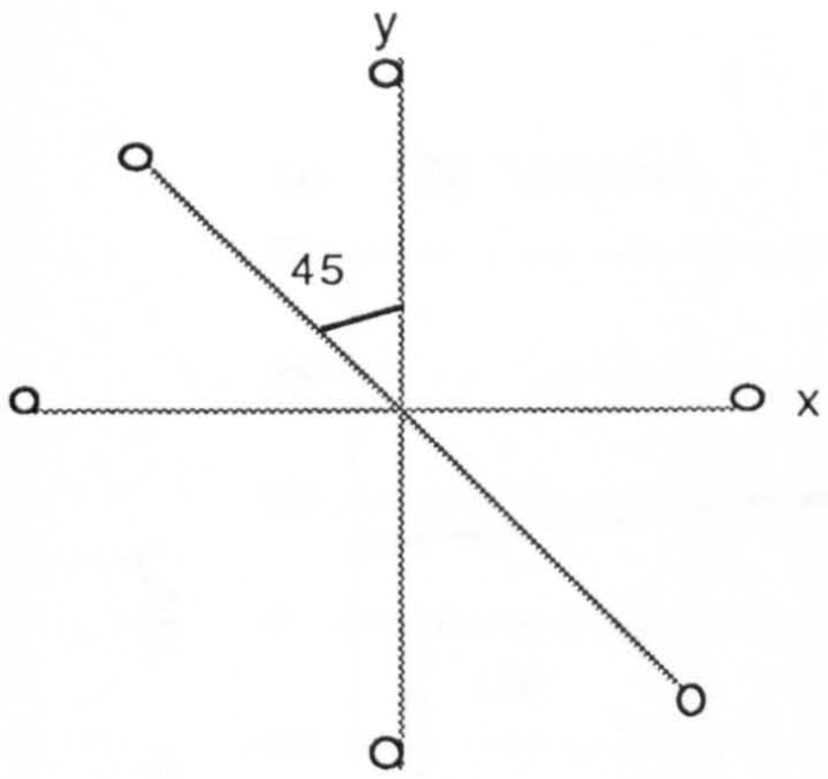

a) 100mm DEMEC Rosette

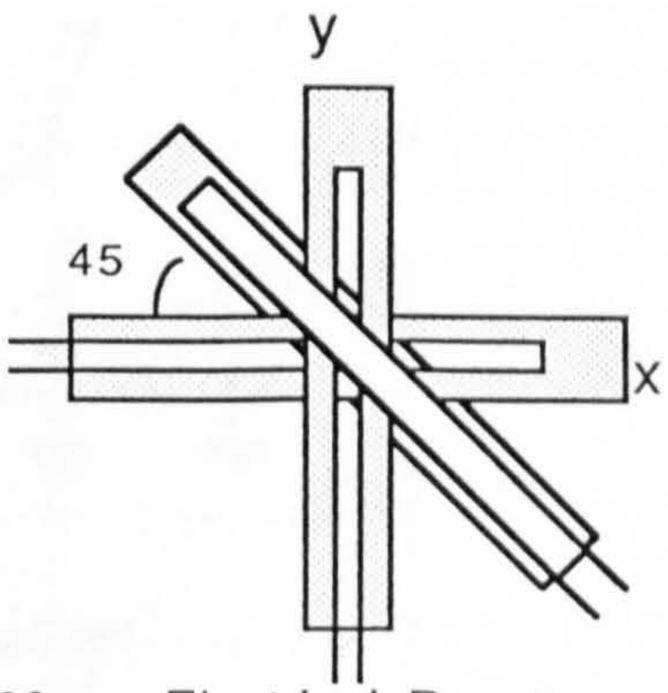

b) 60mm Electrical Rosette

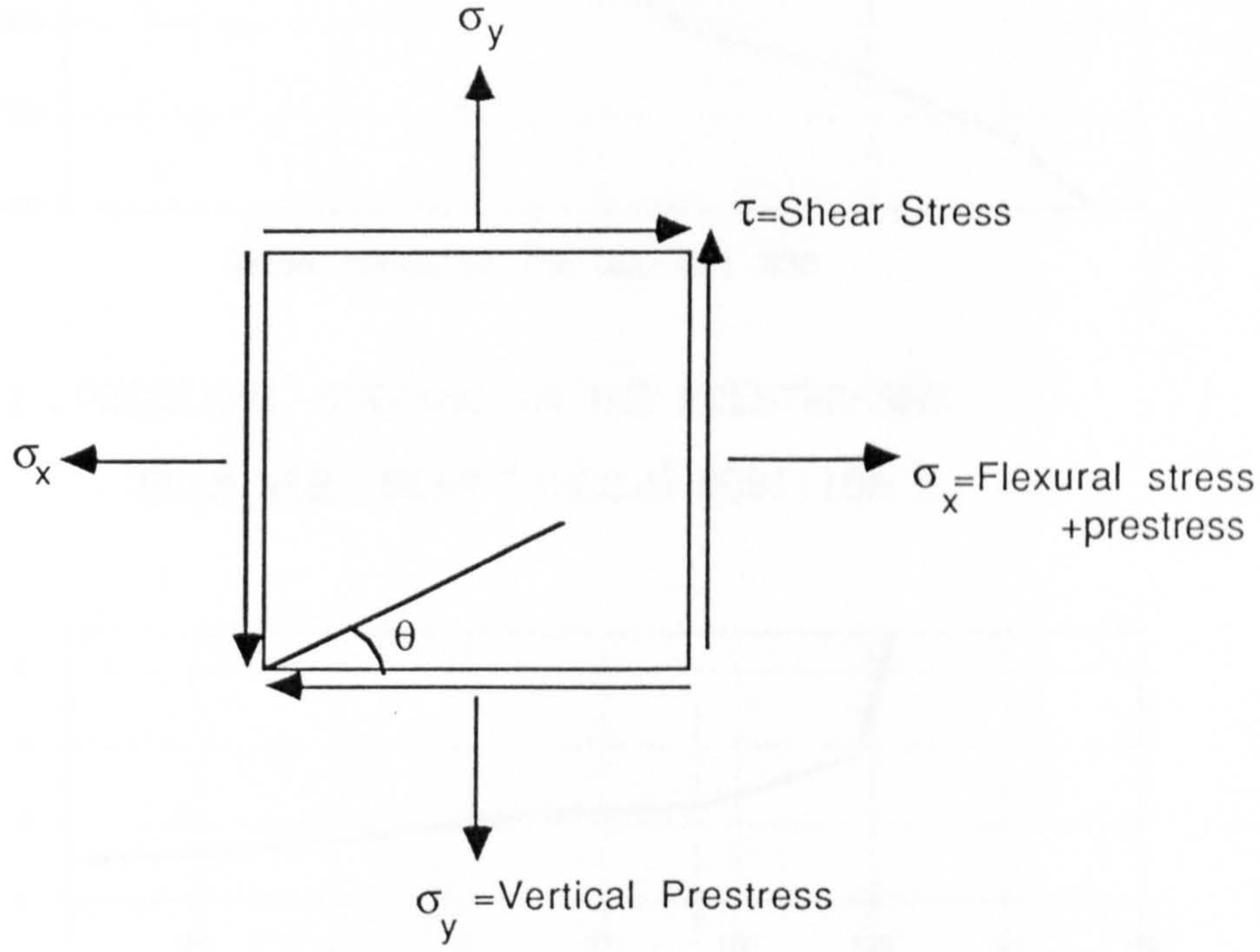

c) Stresses in the Section

FIG. 4.1 Gauge Arrangement to Determine Principal Stresses

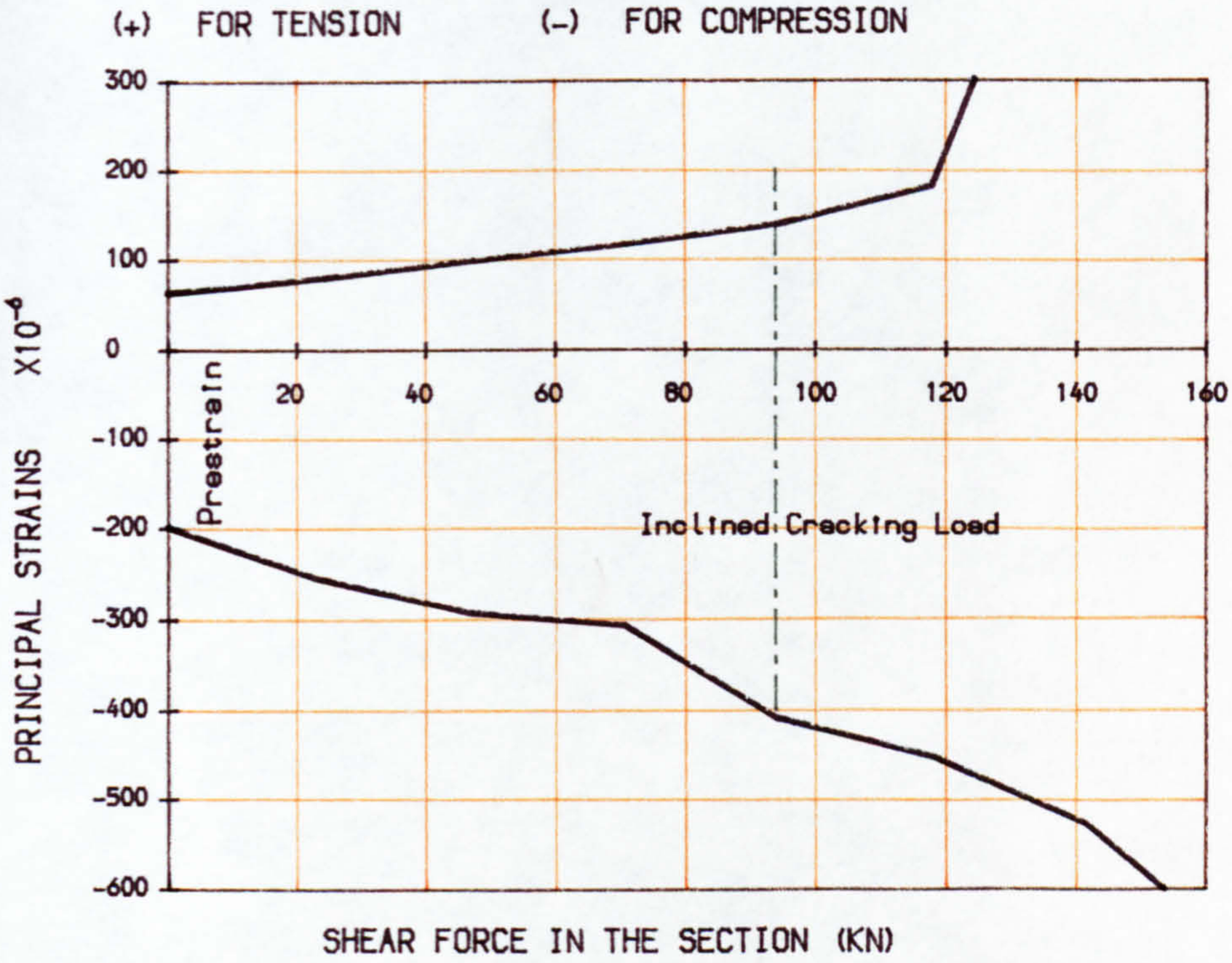

FIG 4.2 .PRINCIPAL STRAINS IN THE PRESTRESSED BEAM WEB. BEAM E10CC-5 POSITION 2

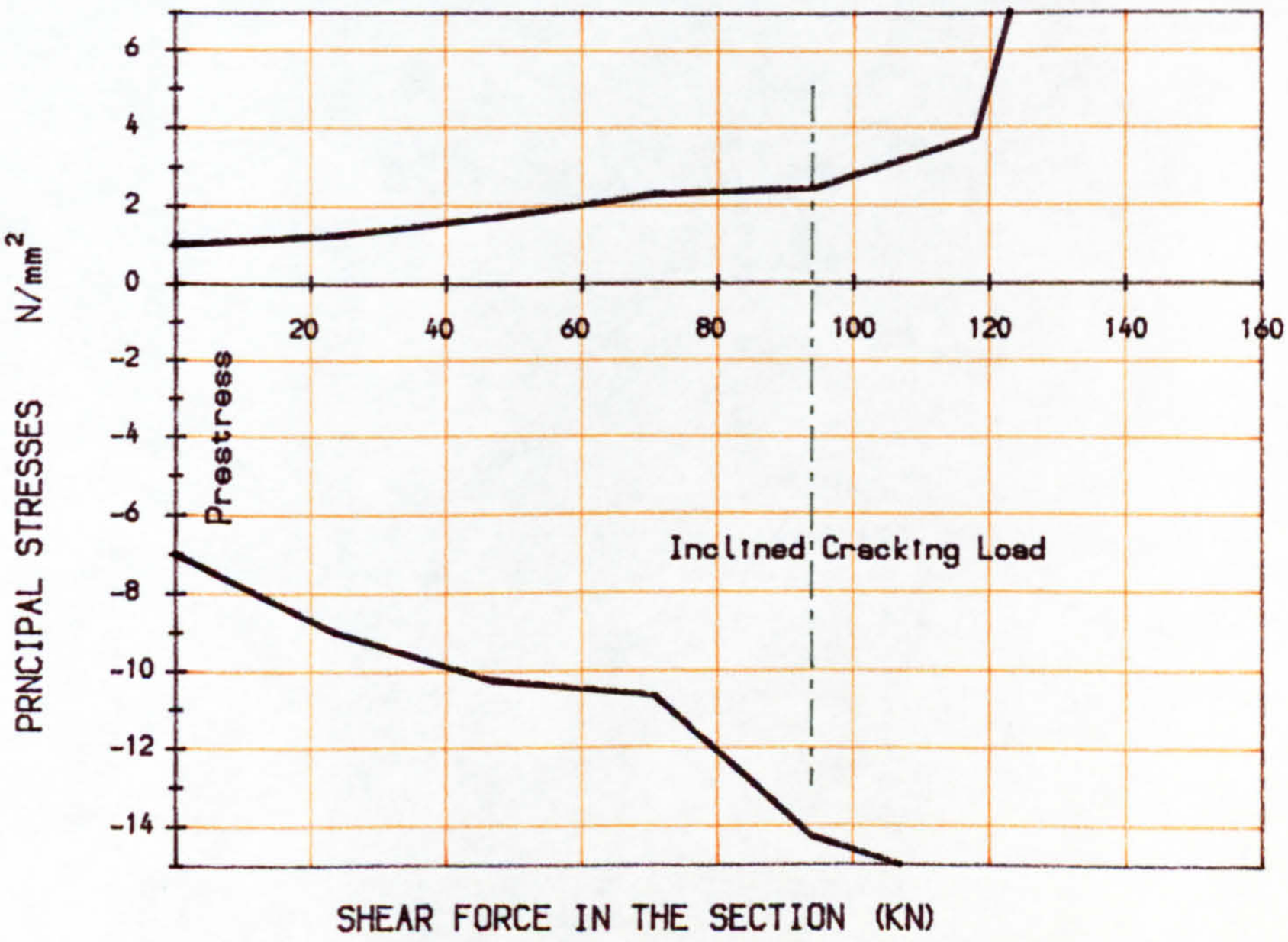

FIG 4.3 .PRINCIPAL STRESSES IN THE PRESTRESSED BEAM WEB. BEAM E10CC-5 POSITION 2

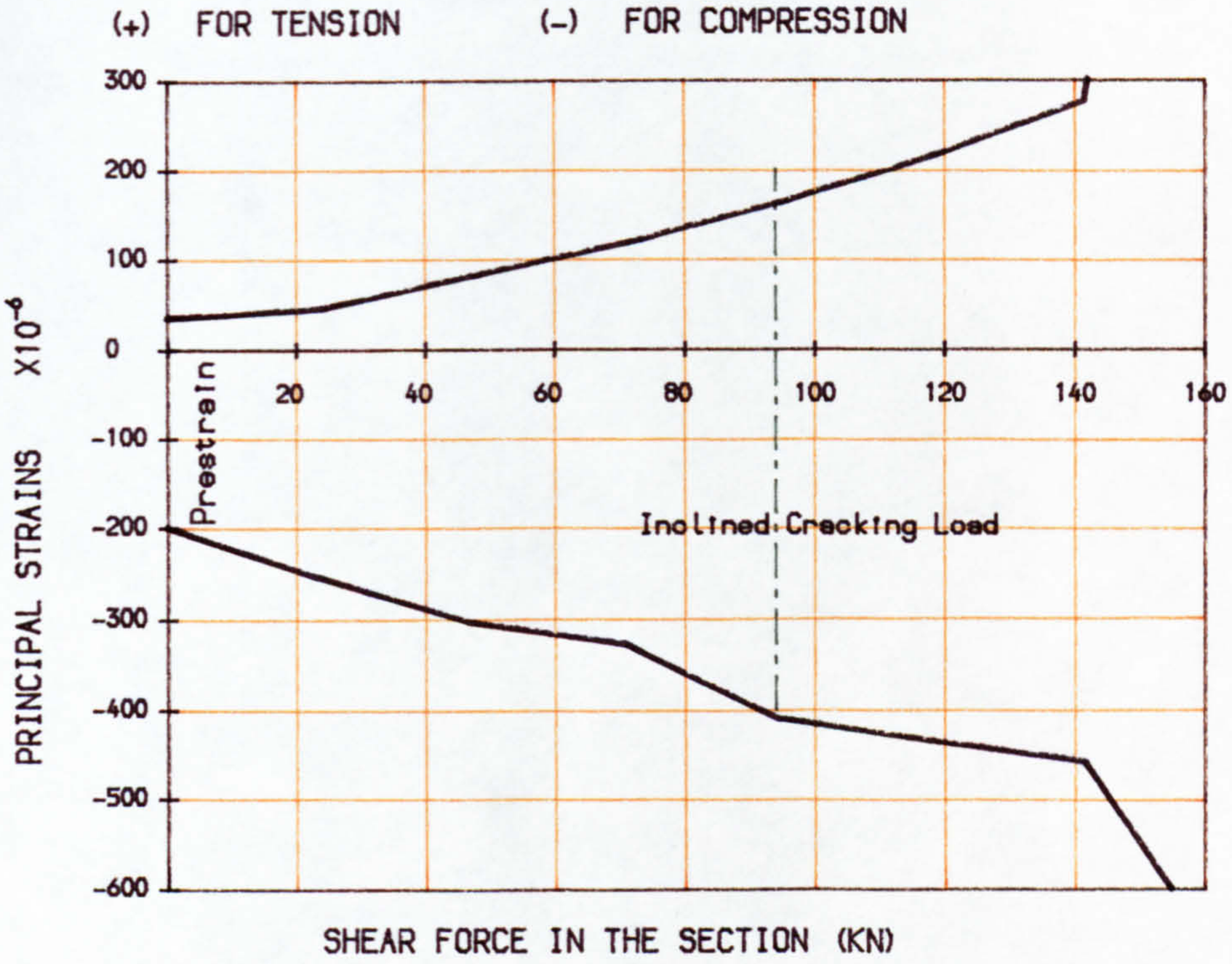

FIG. 4.4. PRINCIPAL STRAINS IN THE PRESTRESSED BEAM WEB. BEAM E10CC-5 POSITION 1

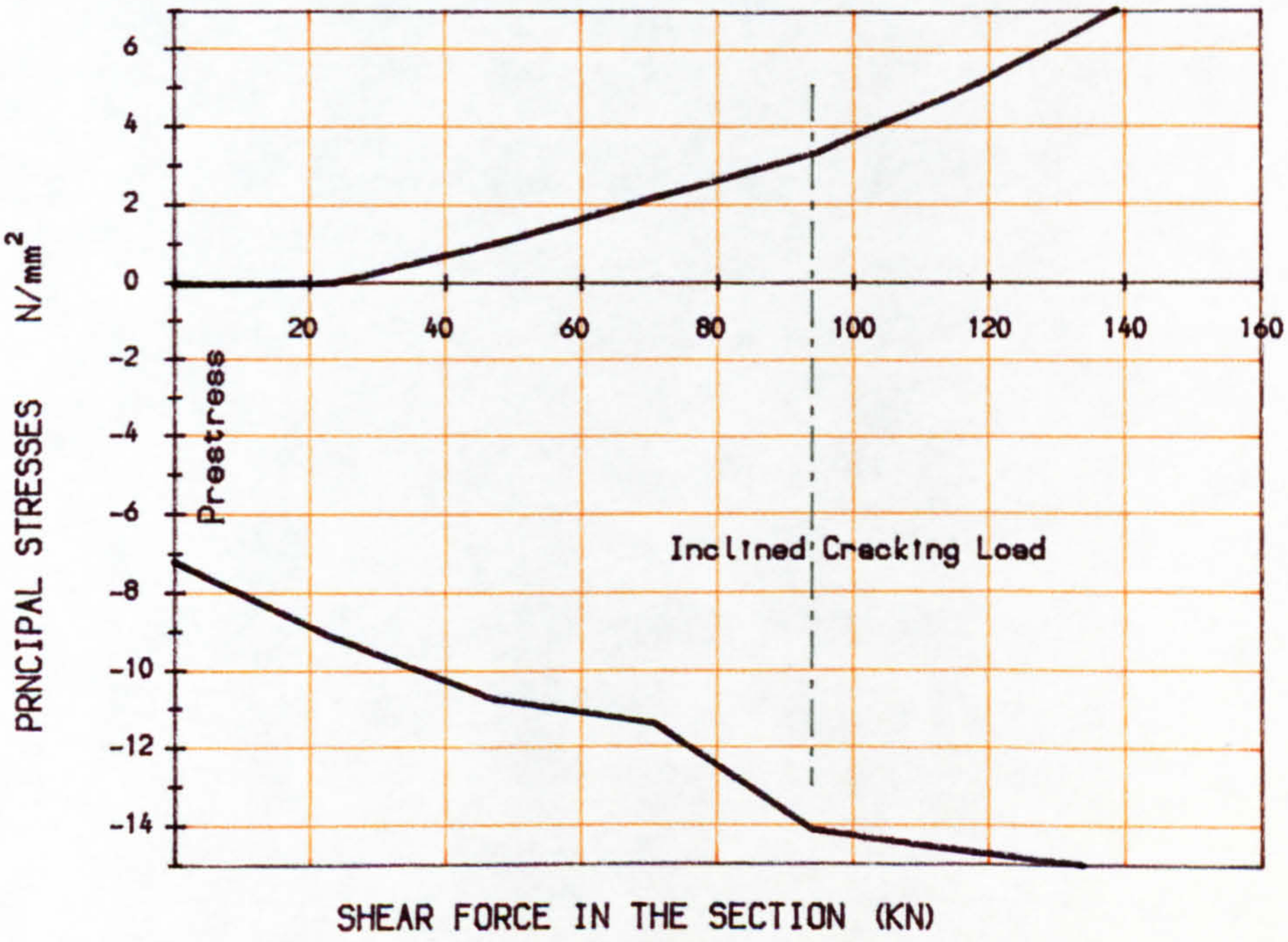

FIG. 4.5 . PRINCIPAL STRESSES IN THE PRESTRESSED BEAM WEB. BEAM E10CC-5 POSITION 1

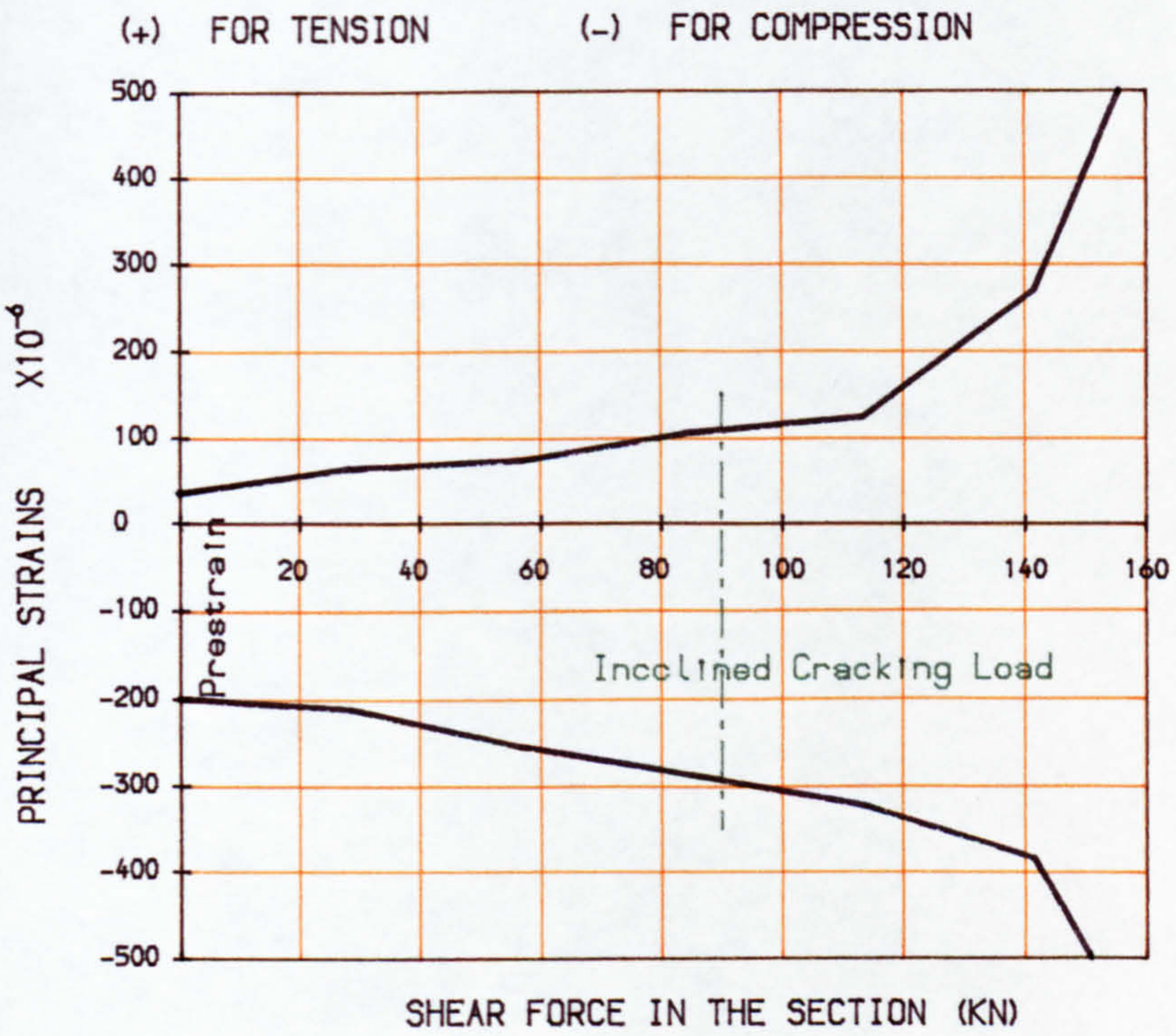

FIG. 4.6. PRINCIPAL STRAINS IN THE PRESTRESSED BEAM WEB. BEAM E30AA-1 POSITION 2

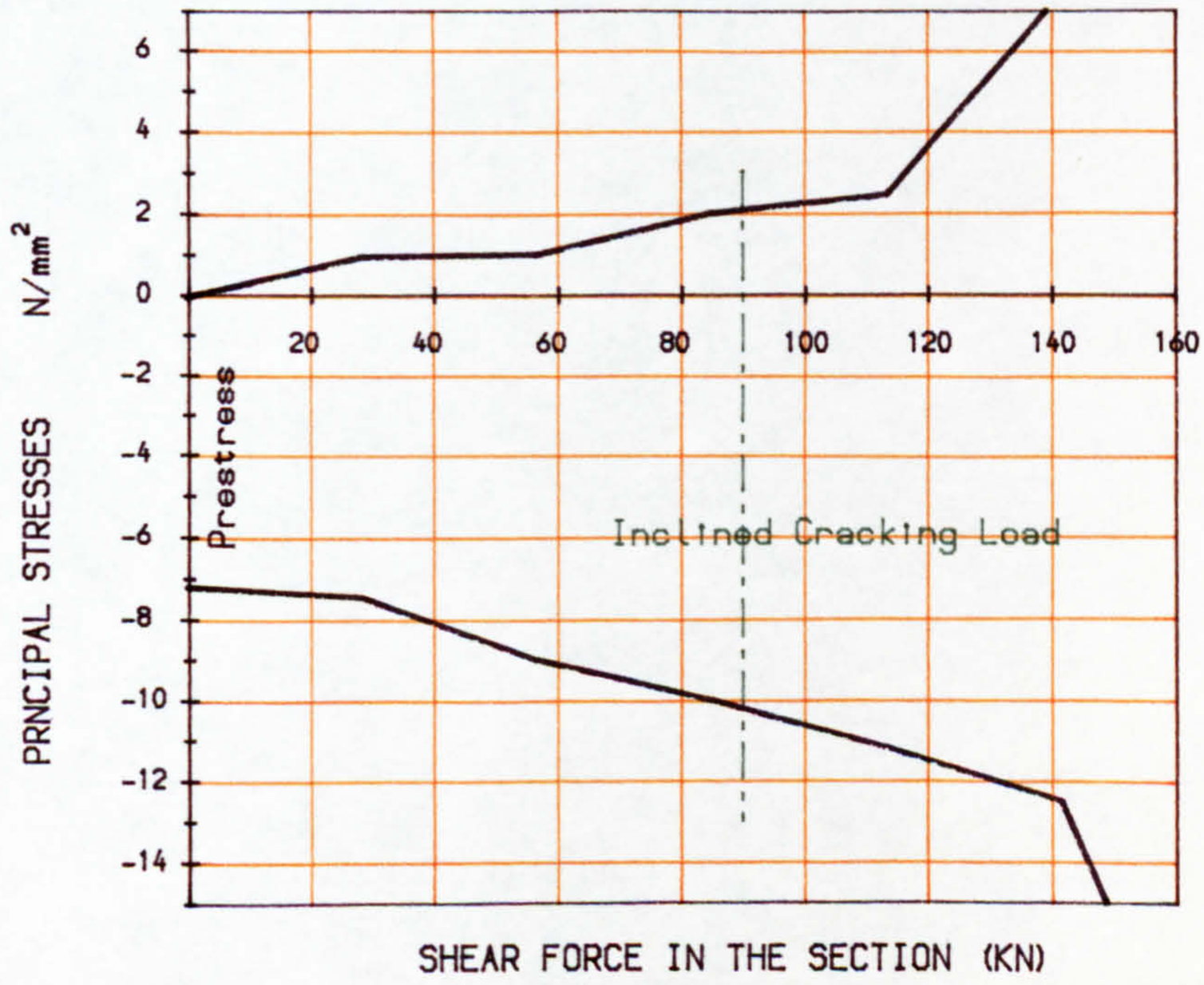

FIG. 4.7 . PRINCIPAL STRESSES IN THE PRESTRESSED BEAM WEB. BEAM E30AA-1 POSITION 2

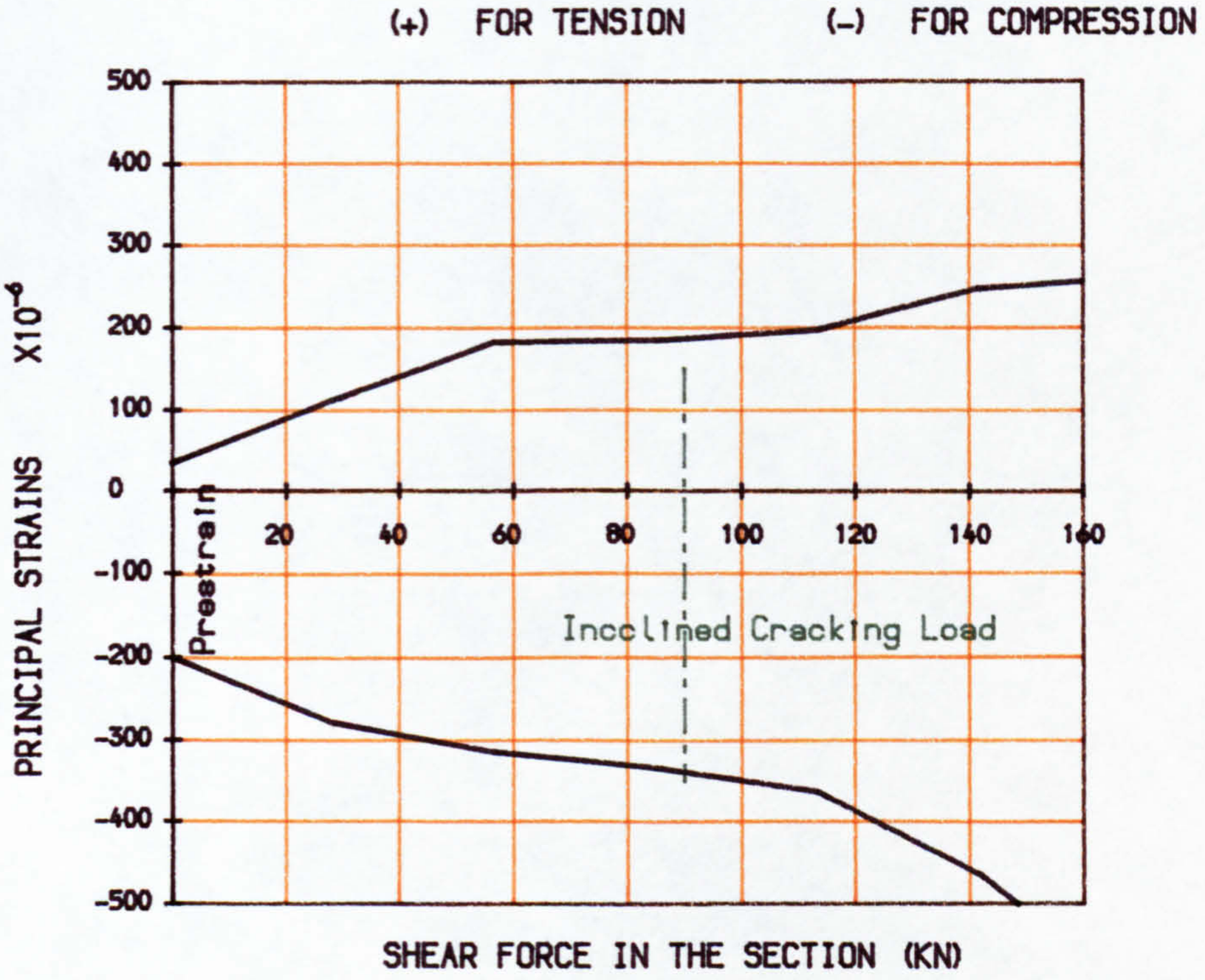

FIG. 4.8. PRINCIPAL STRAINS IN THE PRESTRESSED BEAM WEB. BEAM E30AA-1 POSITION 1

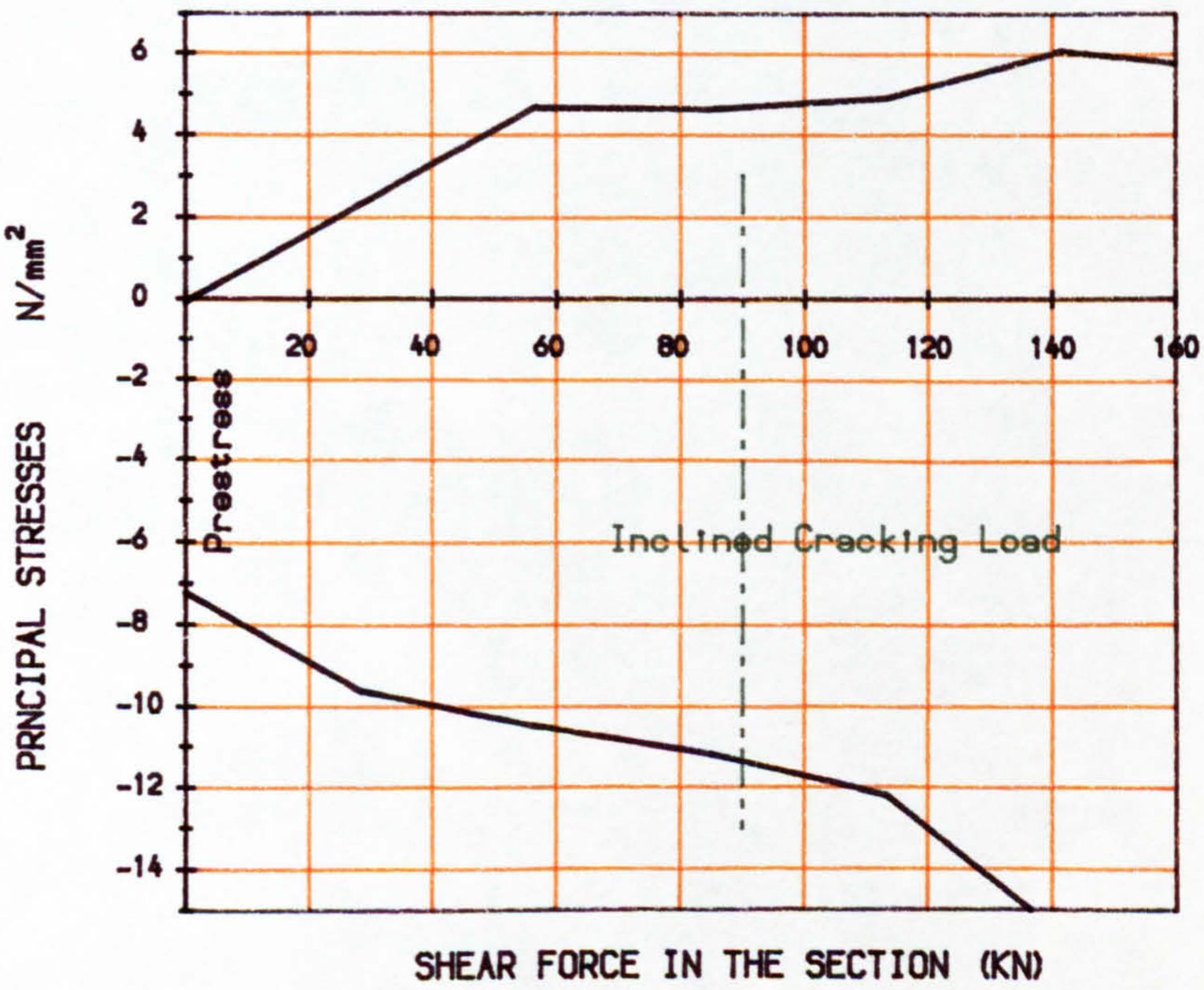

FIG. 4.9 . PRINCIPAL STRESSES IN THE PRESTRESSED BEAM WEB. BEAM E30AA-1 POSITION 1

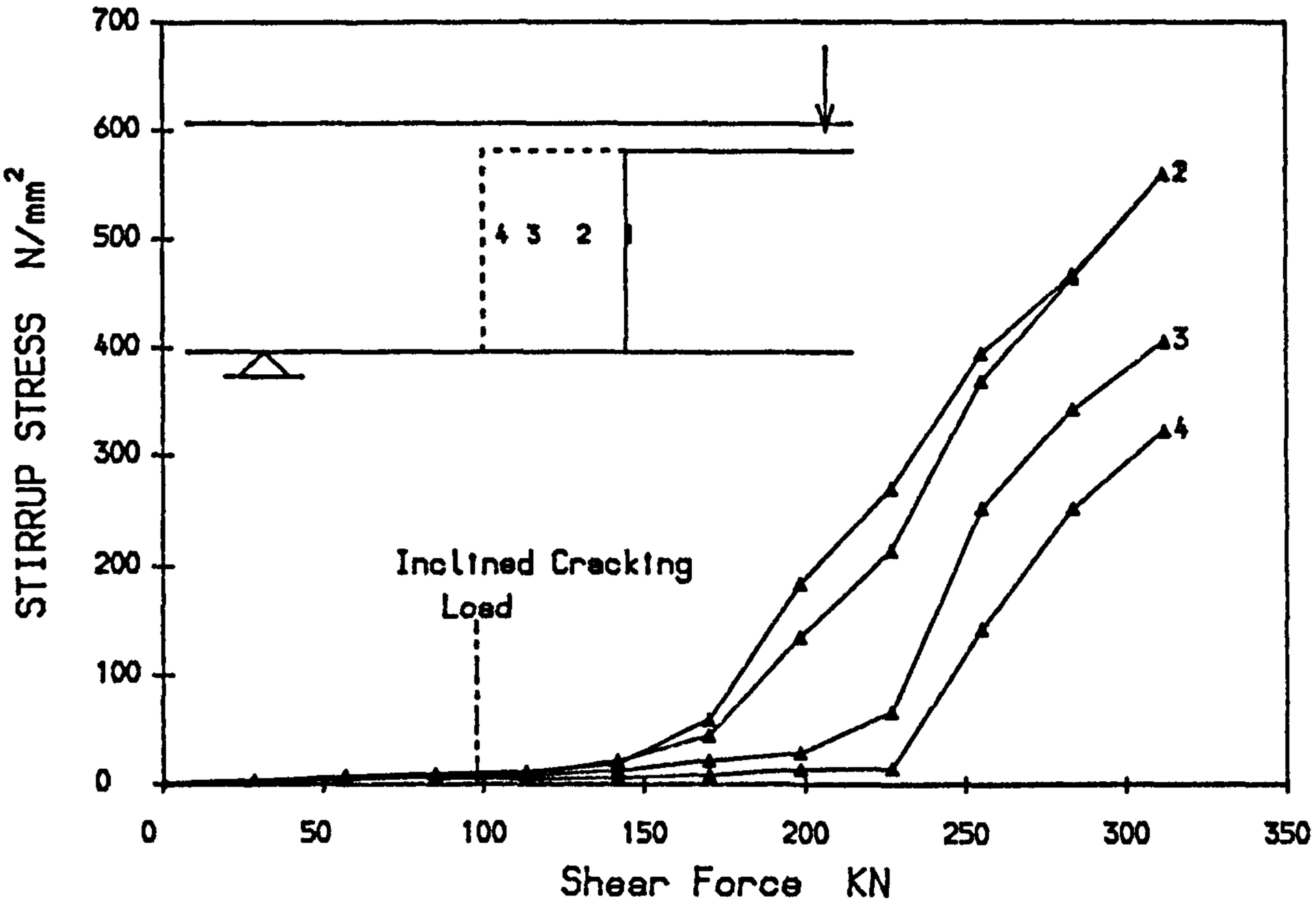

FIG. 4.10a STIRRUP STRESS V.S SHEAR FORCE IN THE PRECAST PART OF E30AA-1

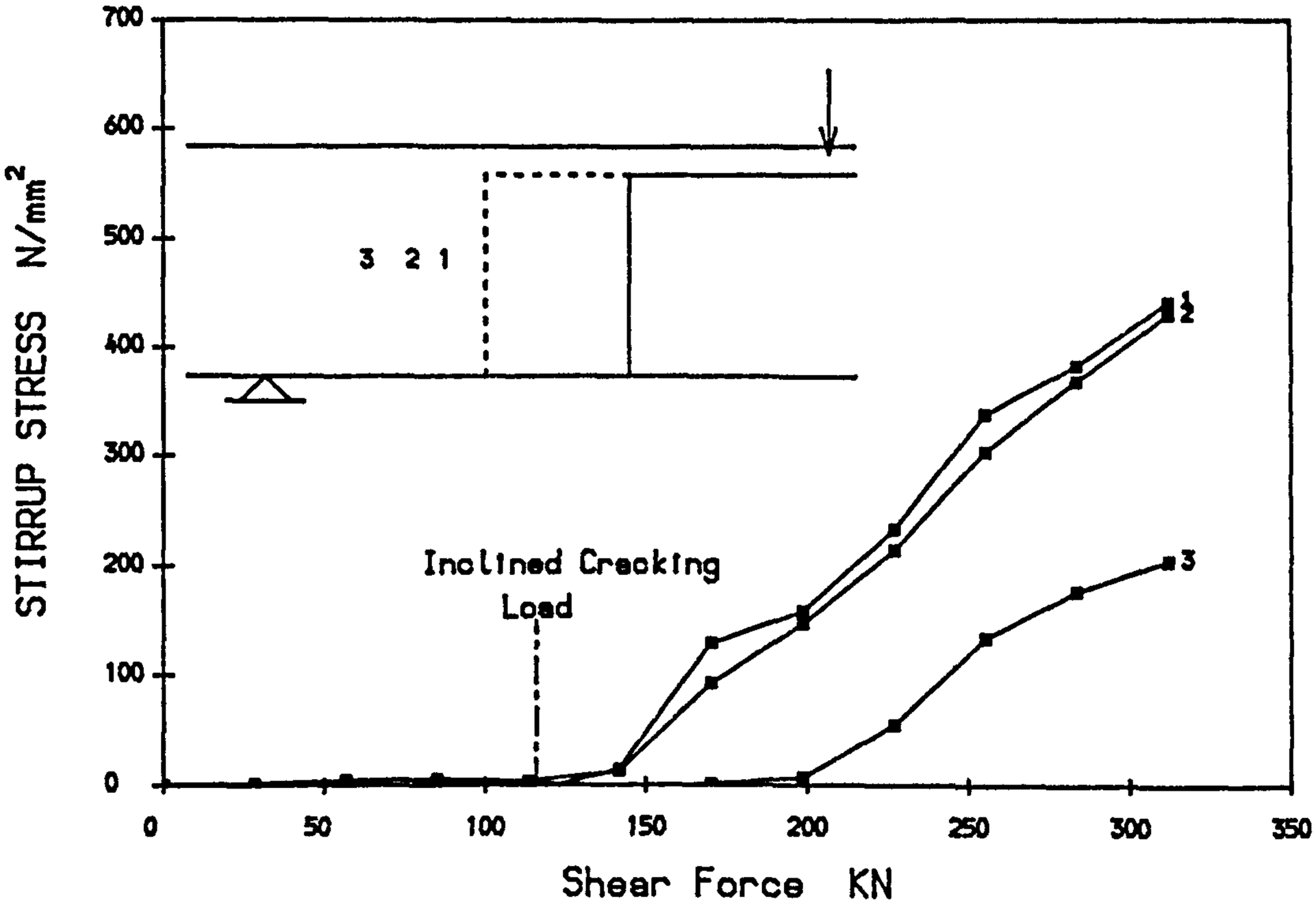

FIG. 4.10b STIRRUP STRESS V.S SHEAR FORCE IN THE IN-SITU PART OF E30AA-1

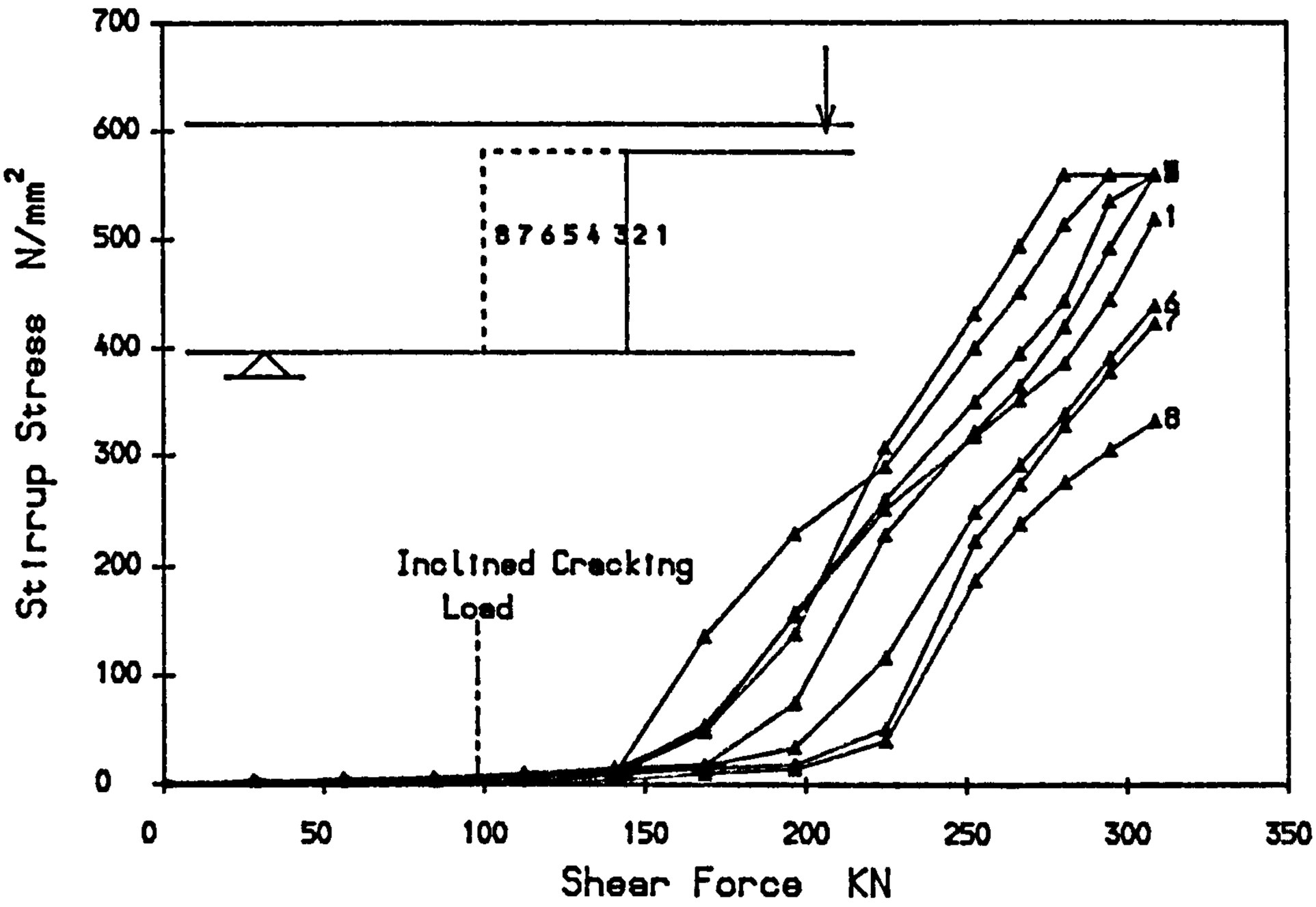

FIG. 4.11a STIRRUP STRESS V.S SHEAR FORCE IN THE PRECAST PART OF E30AA-2

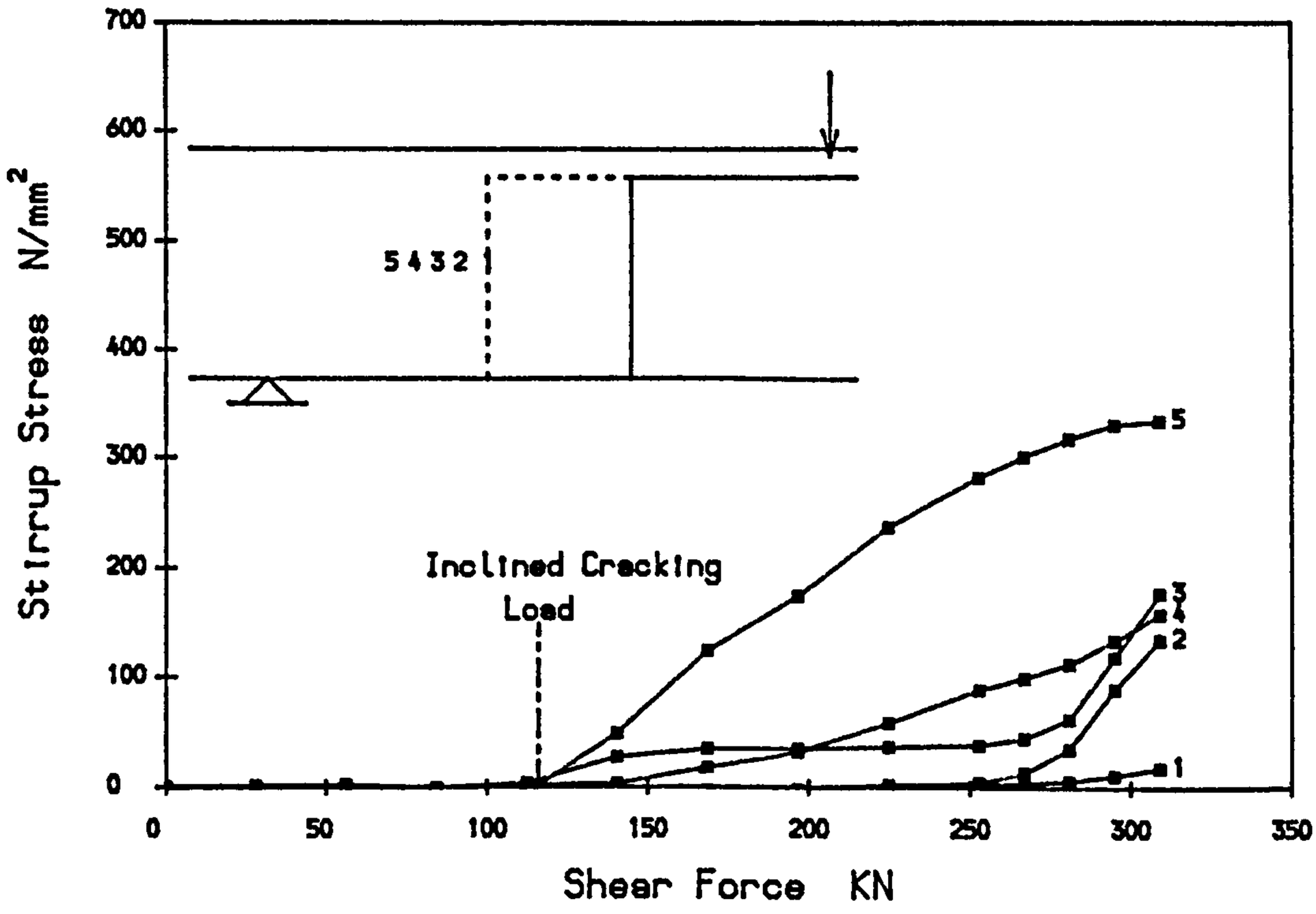

FIG. 4.11b STIRRUP STRESS V.S SHEAR FORCE IN THE IN-SITU PART OF E30AA-2

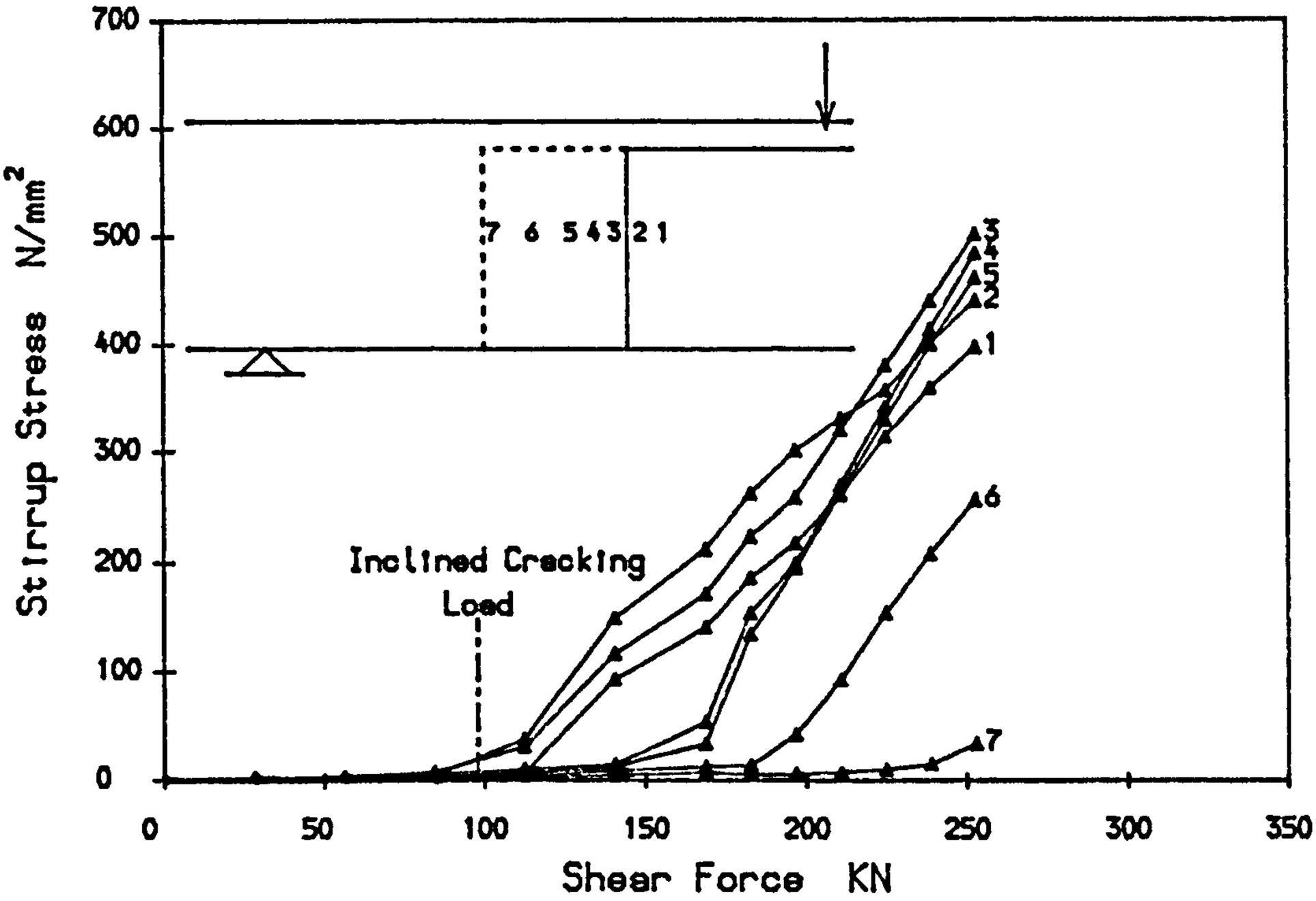

FIG. 4.12a STIRRUP STRESS V.S SHEAR FORCE IN THE PRECAST PART OF E30AB-3

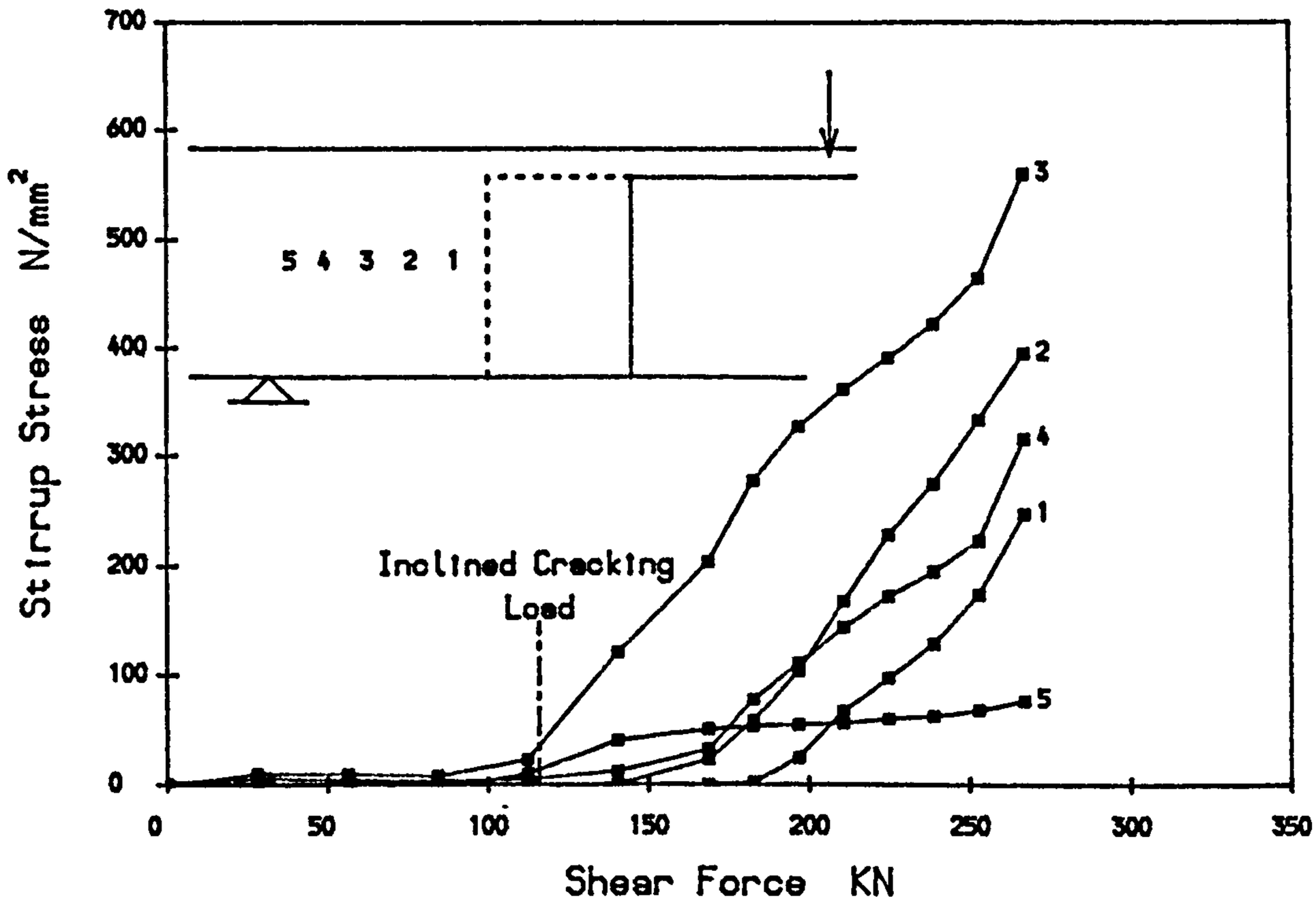

FIG. 4.12b STIRRUP STRESS V.S SHEAR FORCE IN THE IN-SITU PART OF E30AB-3

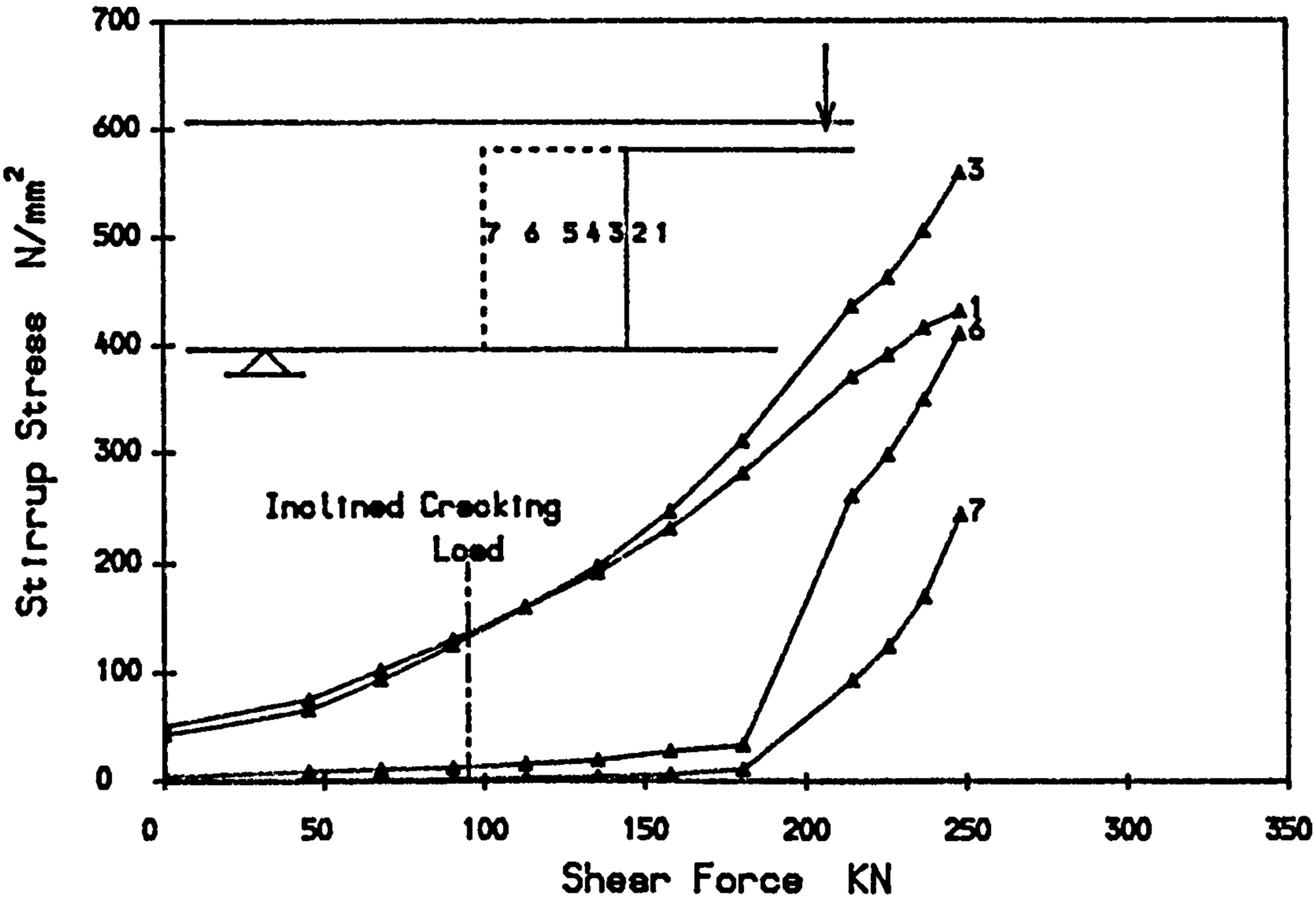

FIG. 4.13a STIRRUP STRESS V.S SHEAR FORCE IN THE PRECAST PART OF E30BC-4 (Final Loading)

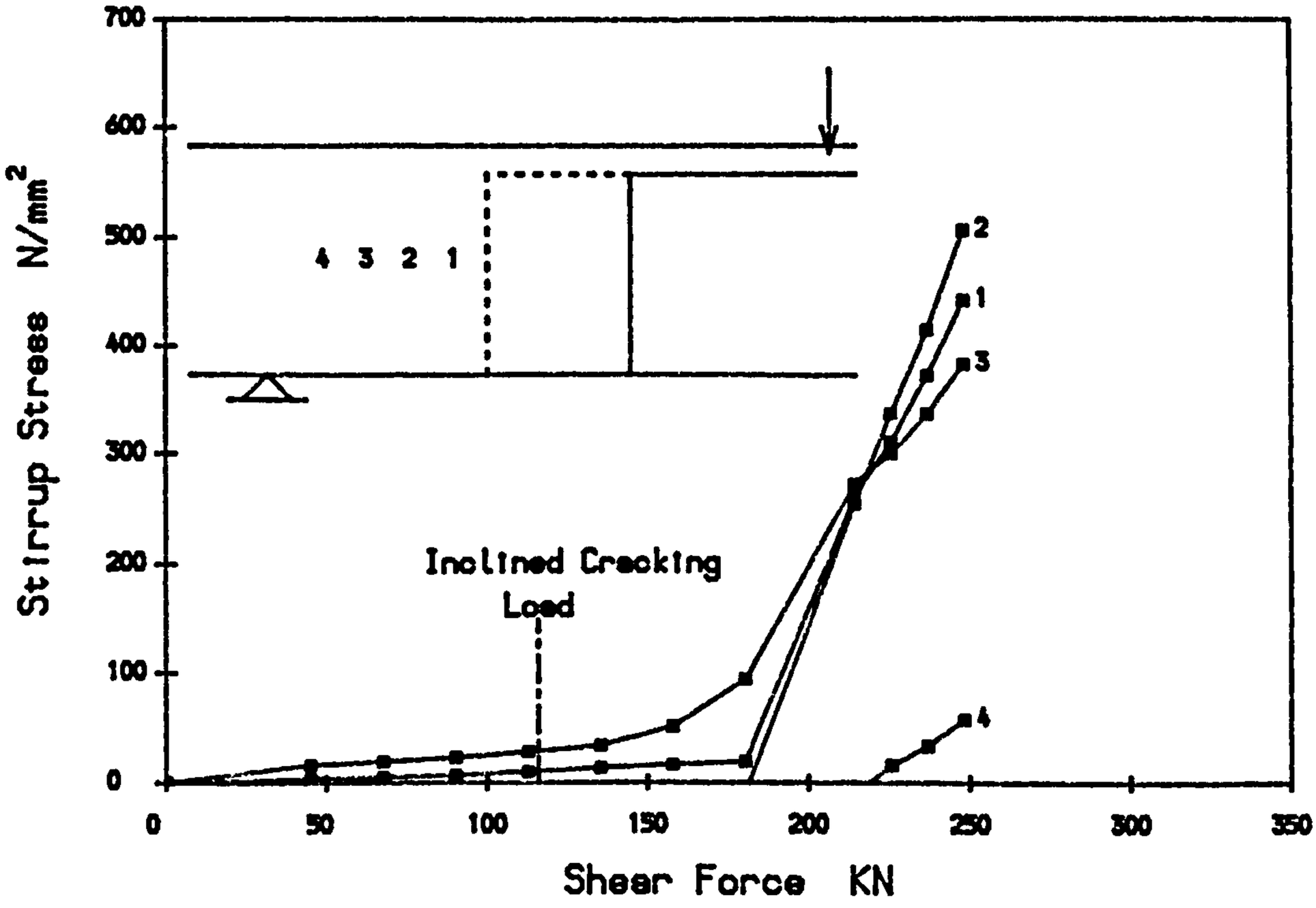

FIG. 4.13b STIRRUP STRESS V.S SHEAR FORCE IN THE IN-SITU PART OF E30BC-4 (Final Loading)

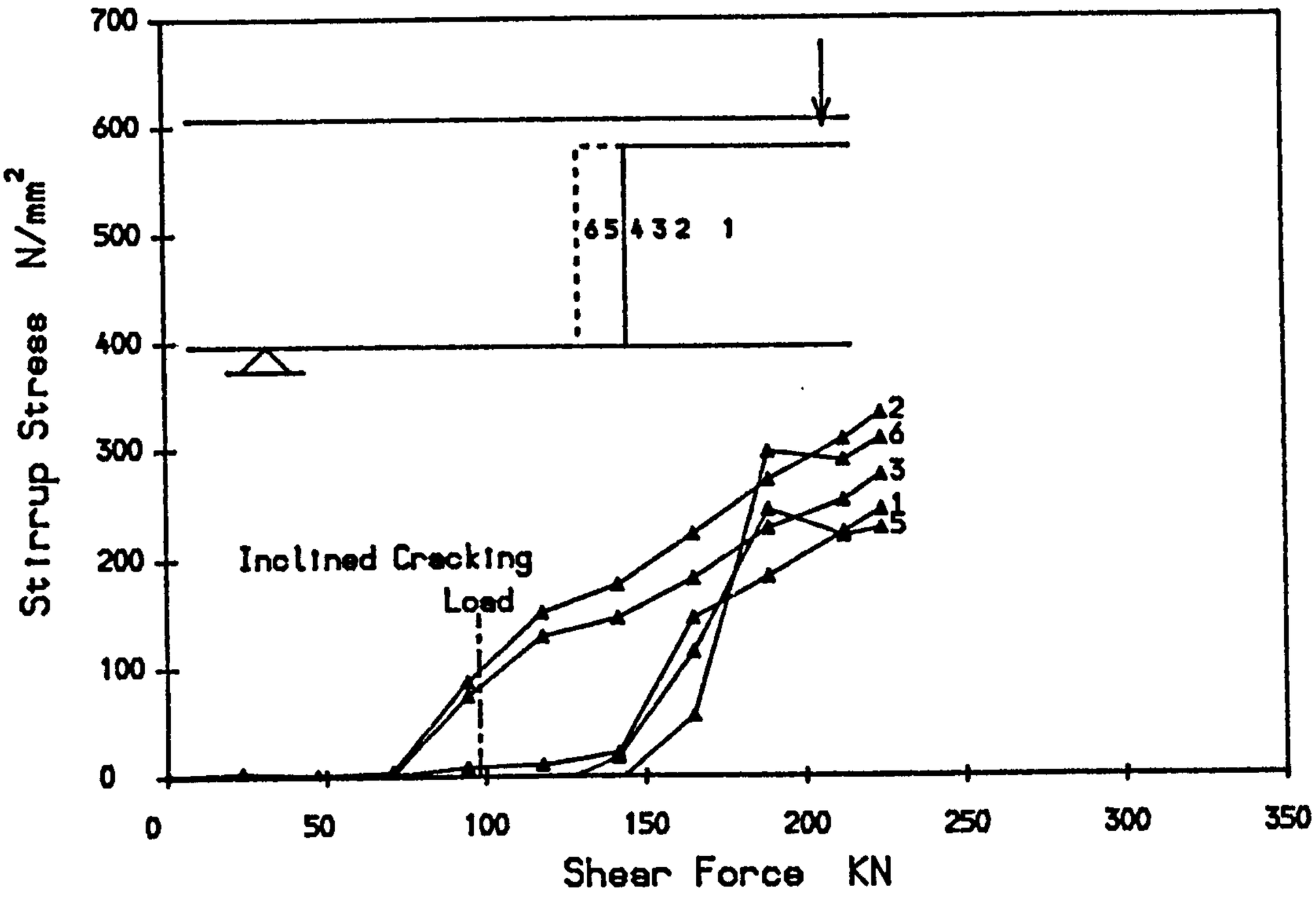

FIG. 4.14a STIRRUP STRESS V.S SHEAR FORCE IN THE PRECAST PART OF E10CC-5

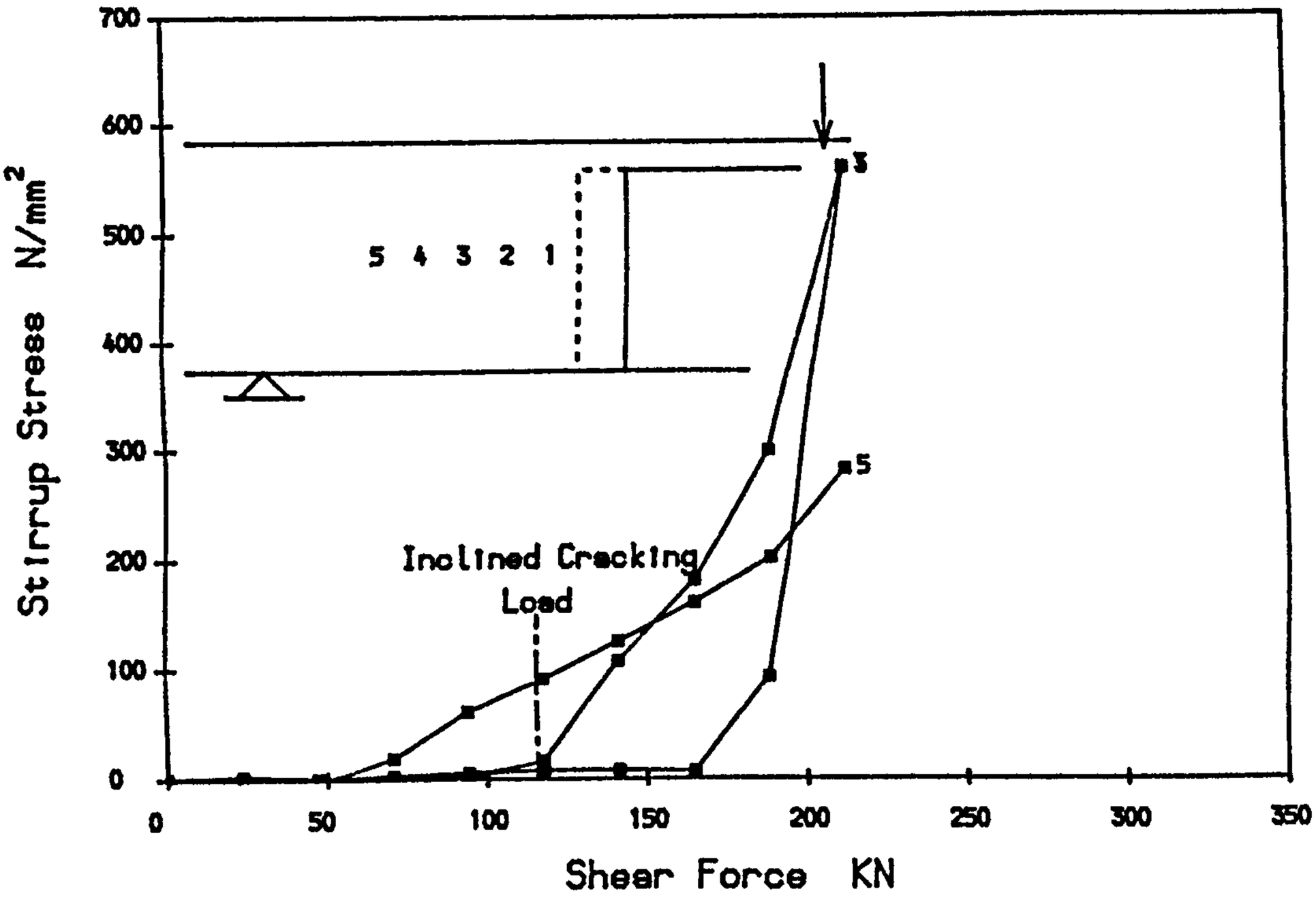

FIG. 4.14b STIRRUP STRESS V.S SHEAR FORCE IN THE IN-SITU PART OF E10CC-5

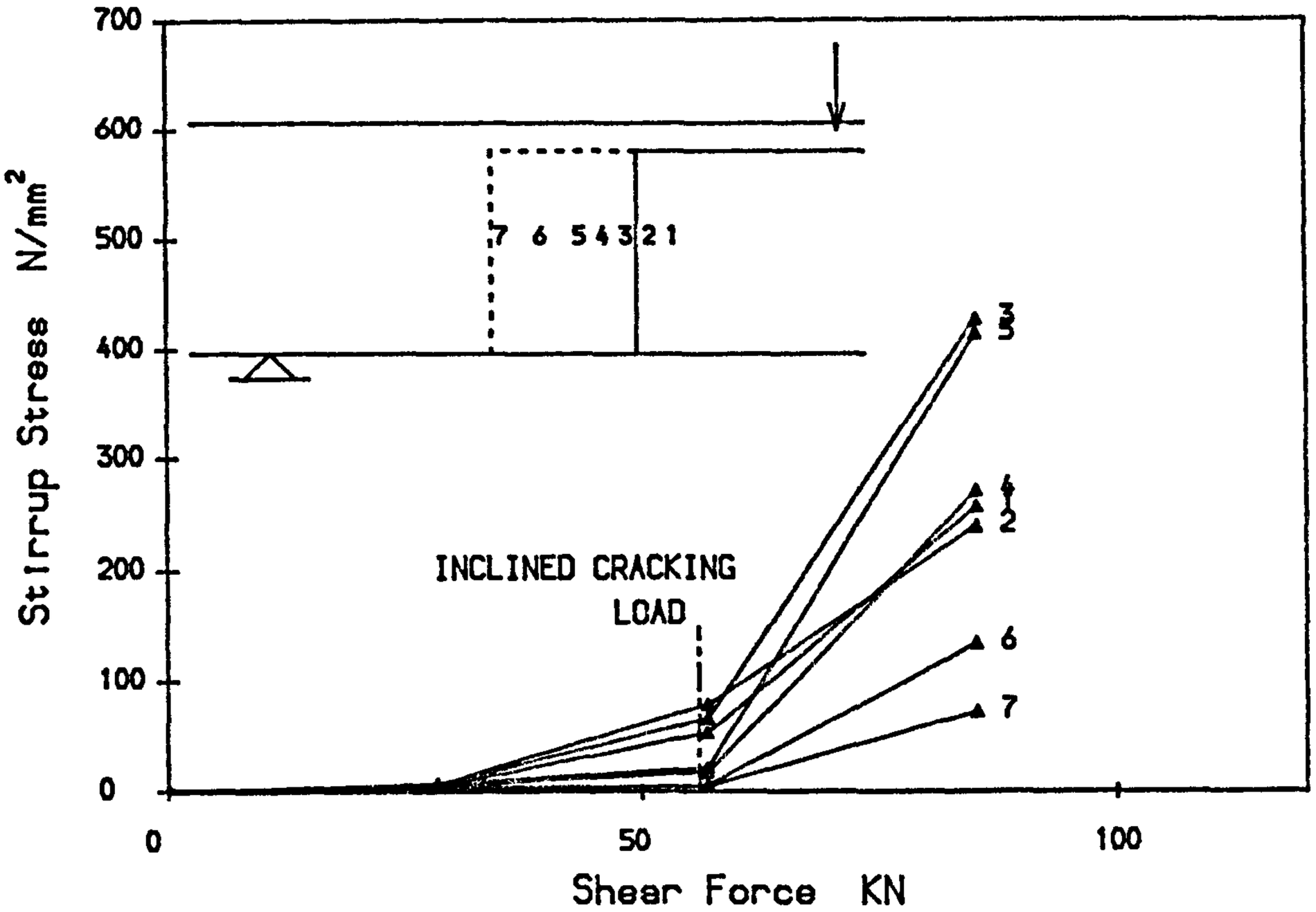

FIG. 4. 15a STIRRUP STRESS V.S SHEAR FORCE IN THE PRECAST PART OF WTFCC-6

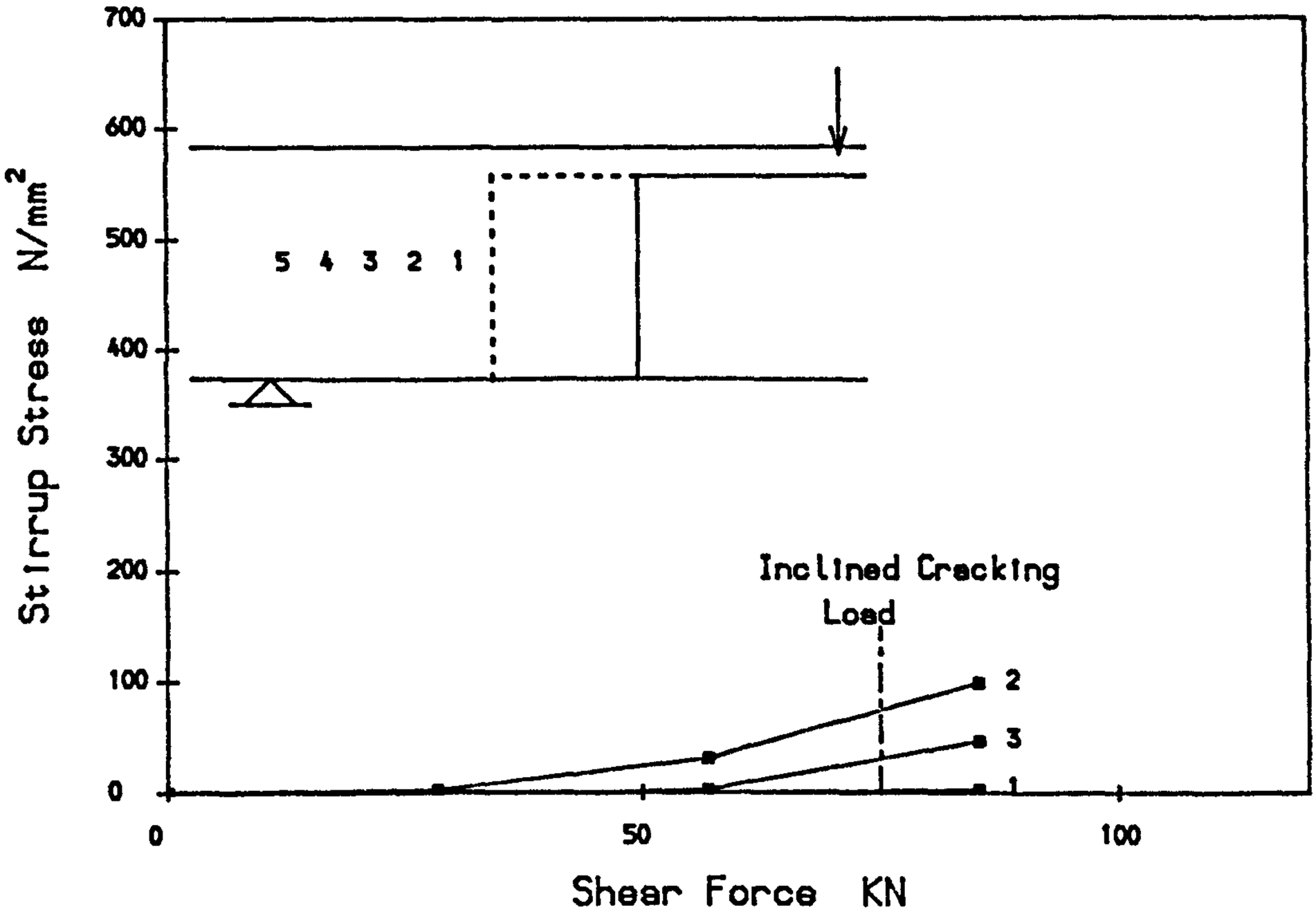

FIG. 4. 15b STIRRUP STRESS V.S SHEAR FORCE IN THE IN-SITU PART OF WTFCC-6

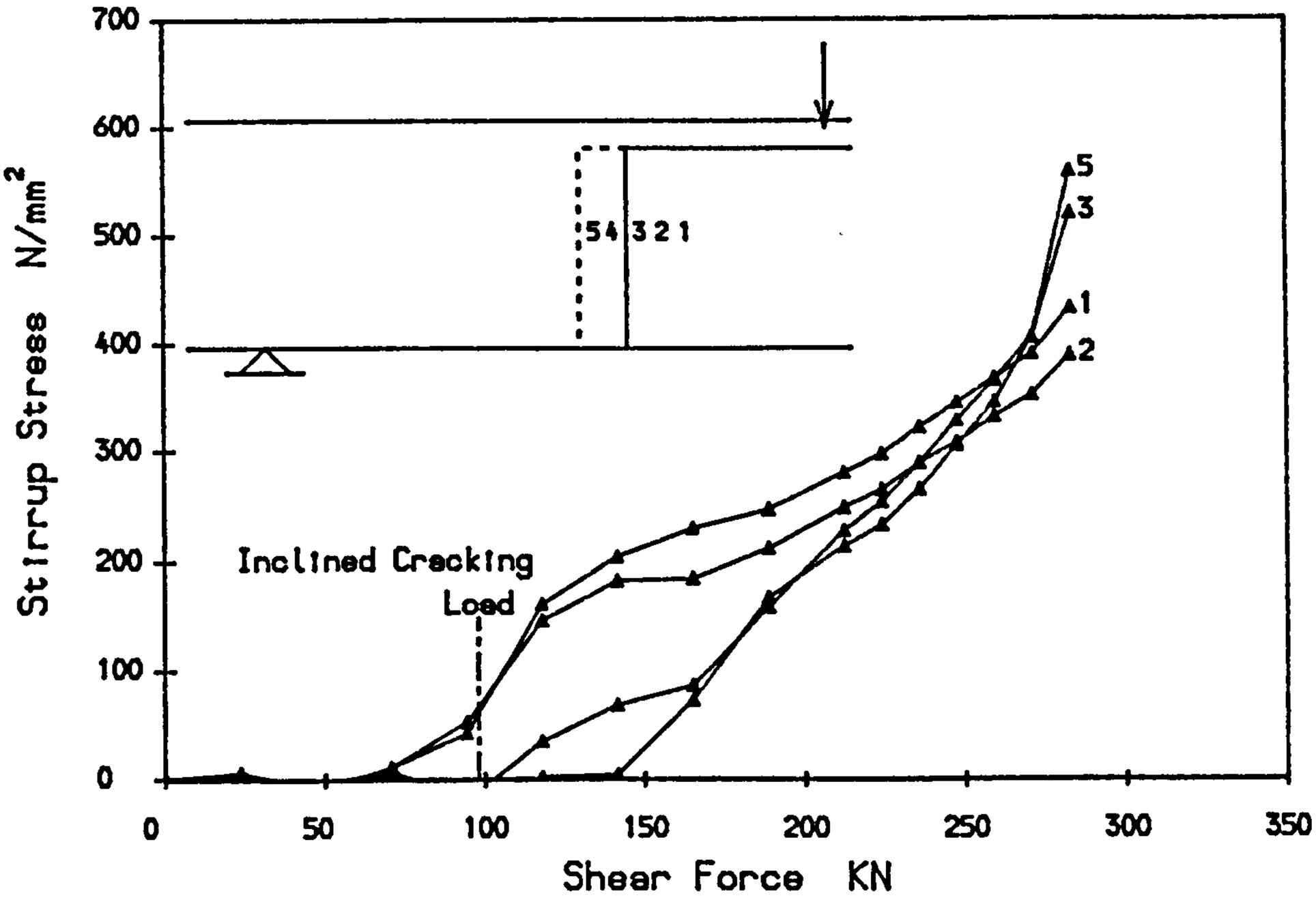

FIG. 4.16a STIRRUP STRESS V.S SHEAR FORCE IN THE PRECAST PART OF E10CD-7

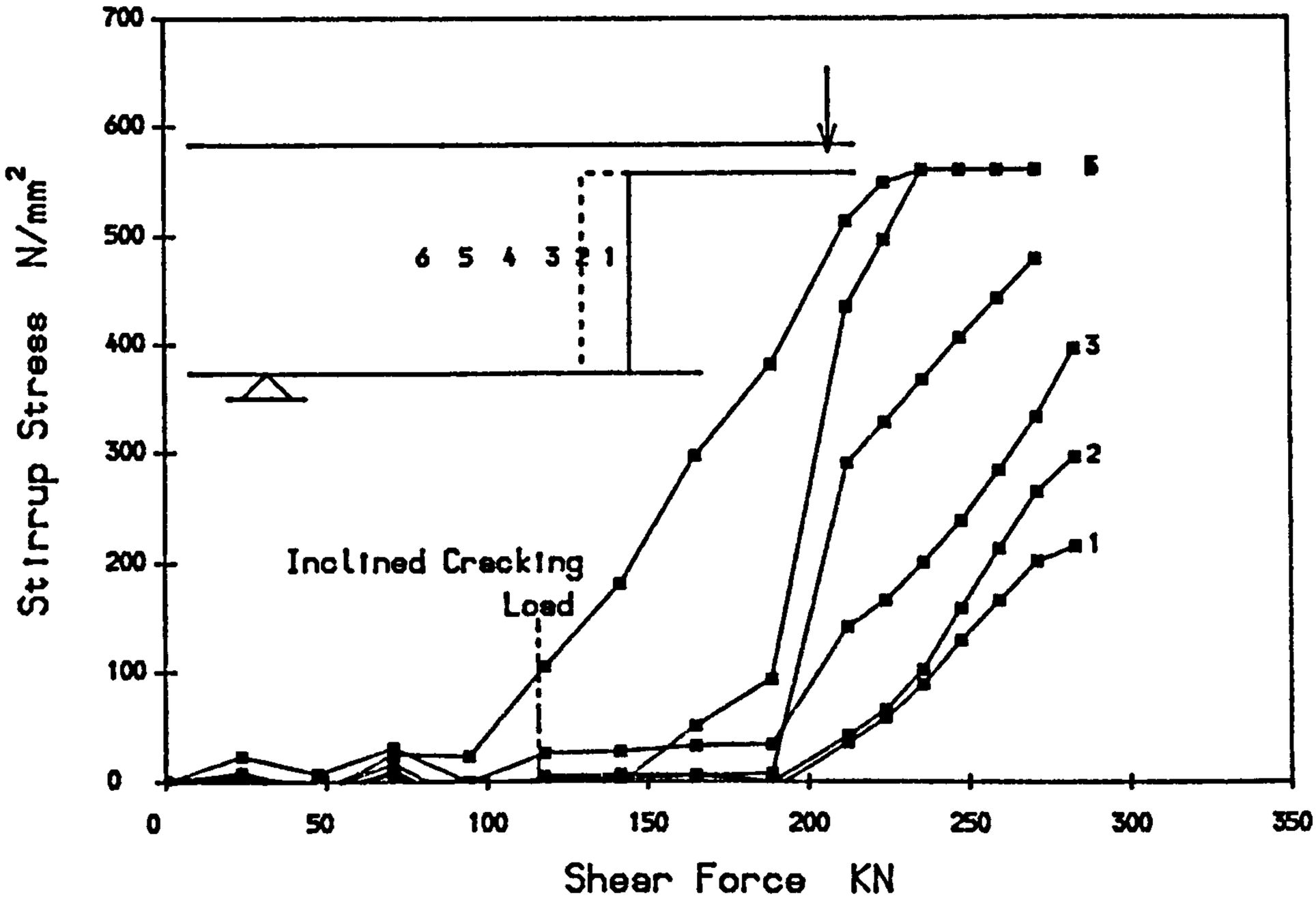

FIG. 4.16b STIRRUP STRESS V.S SHEAR FORCE IN THE IN-SITU PART OF E10CD-7

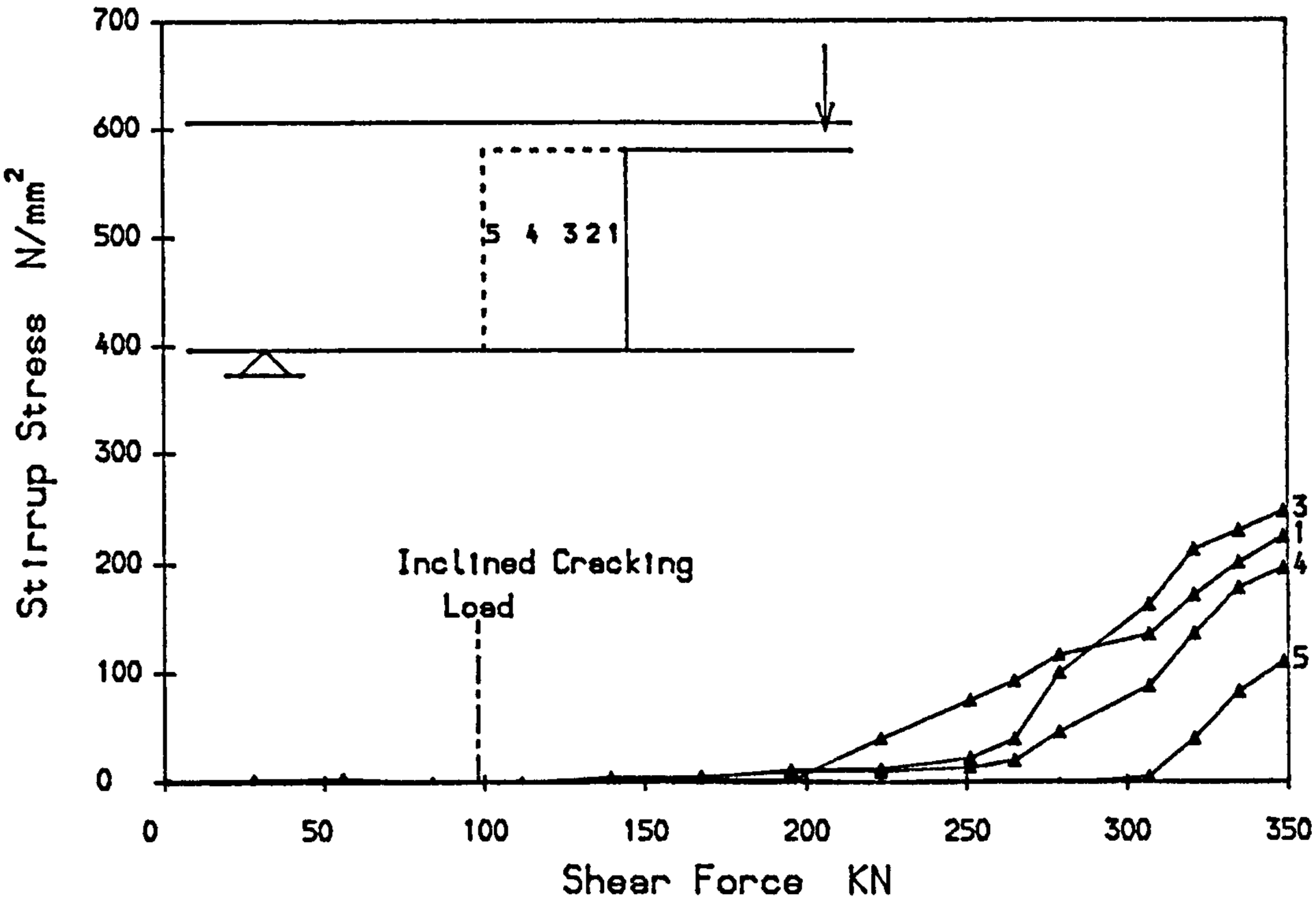

FIG. 4.17a STIRRUP STRESS V.S SHEAR FORCE IN THE PRECAST PART OF WTFPCC-8

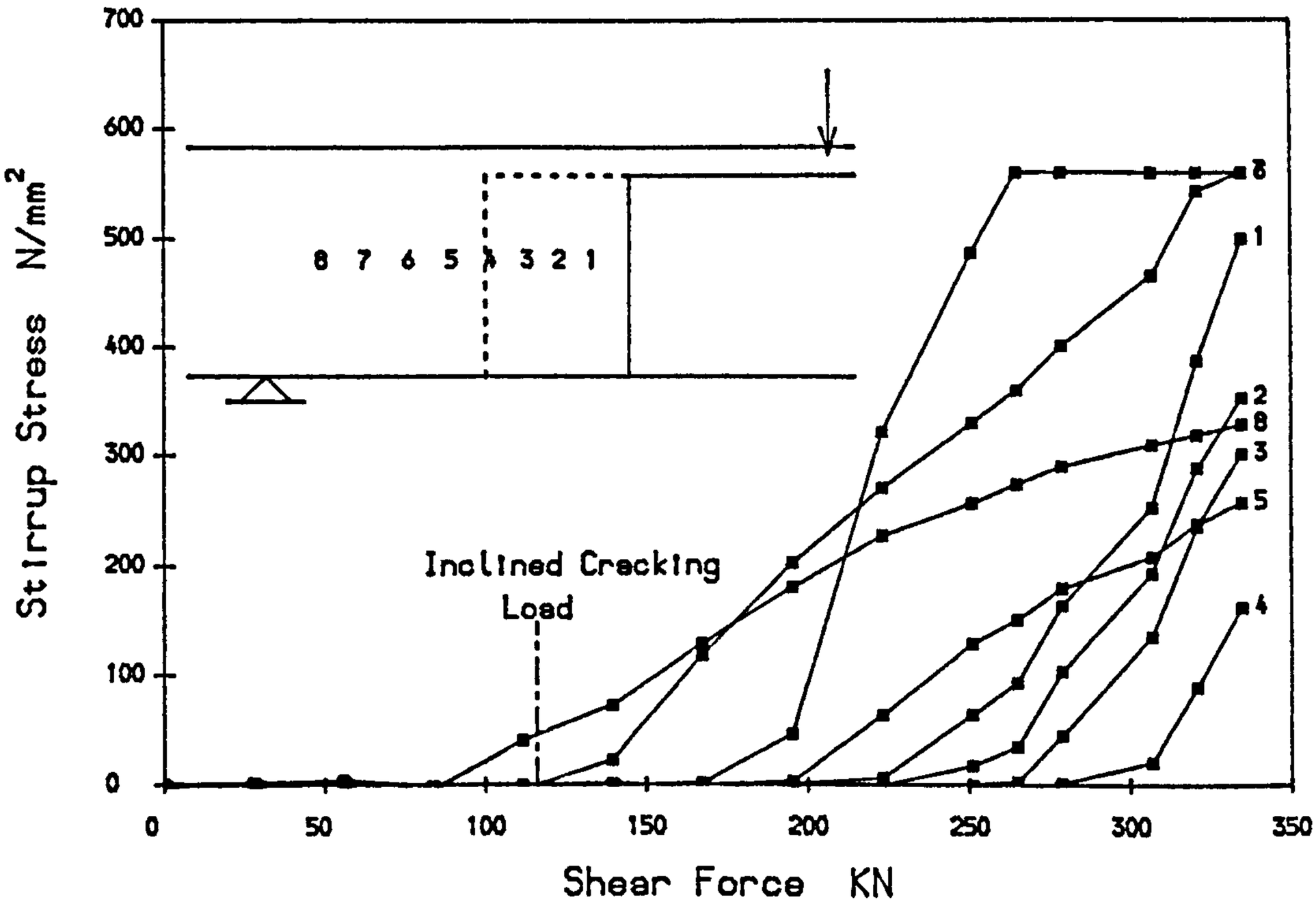

FIG. 4.17b STIRRUP STRESS V.S SHEAR FORCE IN THE IN-SITU PART OF WTFPCC-8

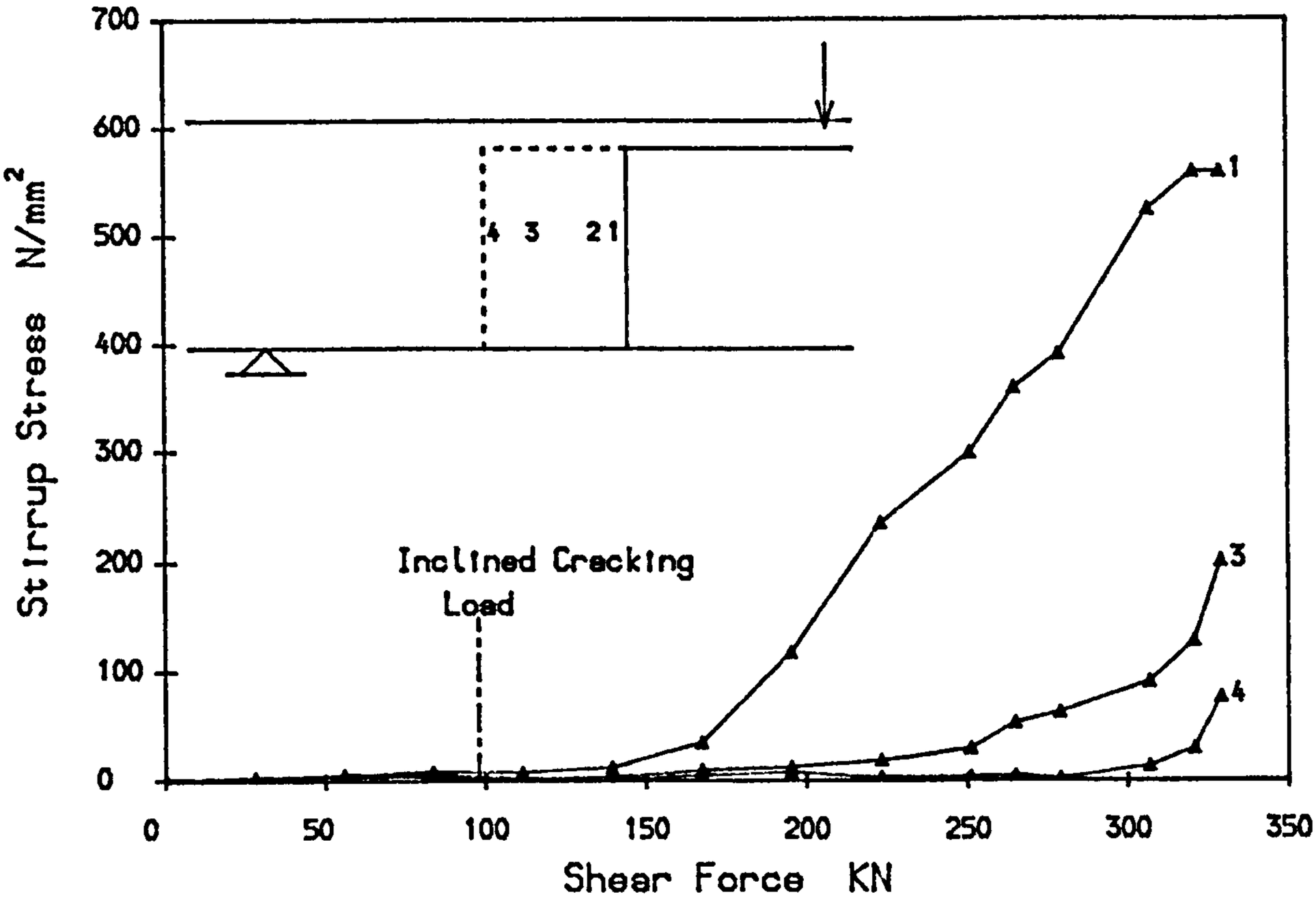

FIG. 4.18a STIRRUP STRESS V.S SHEAR FORCE IN THE PRECAST PART OF WTFCC-9

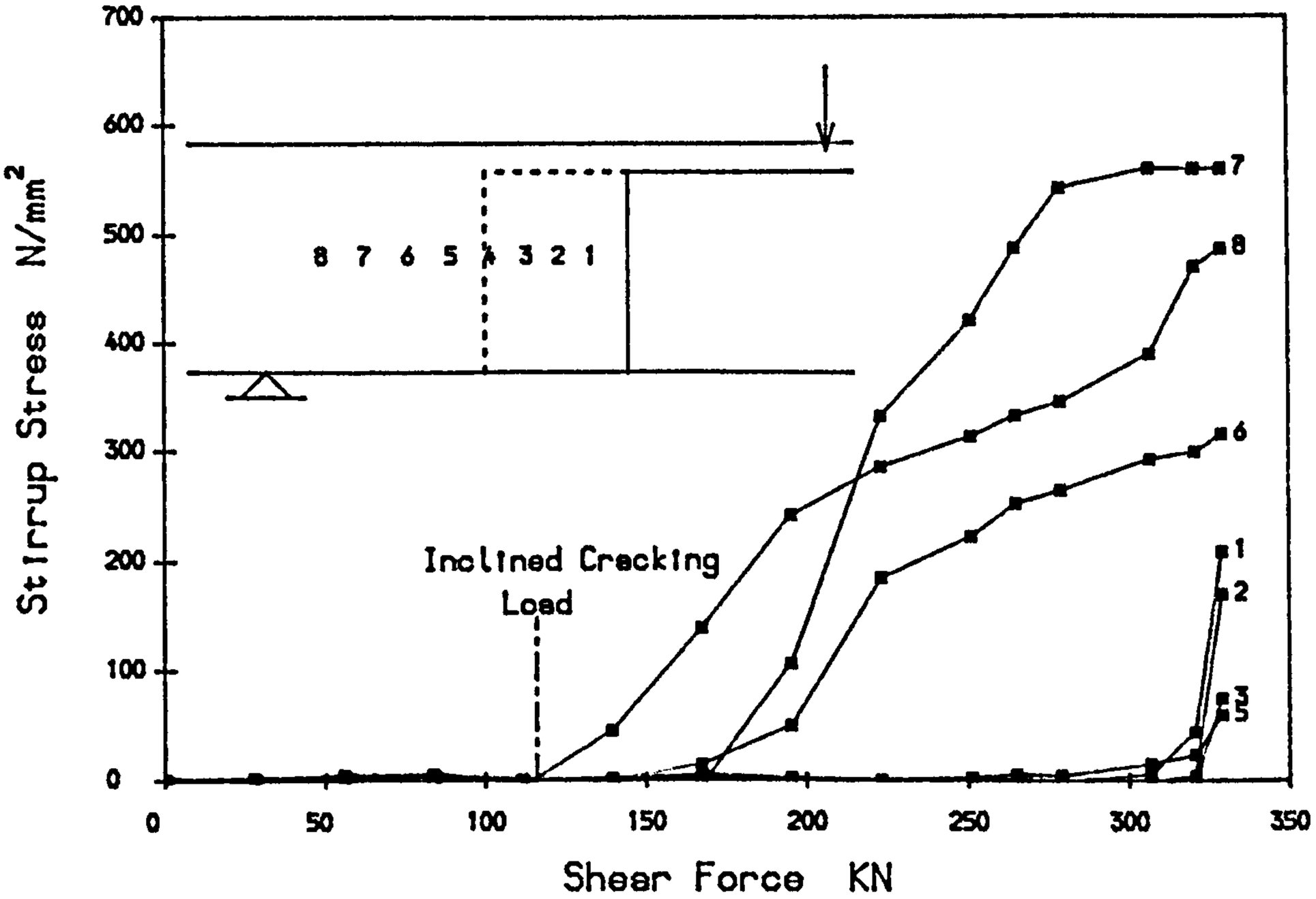

FIG. 4.18b STIRRUP STRESS V.S SHEAR FORCE IN THE IN-SITU PART OF WTFCC-9

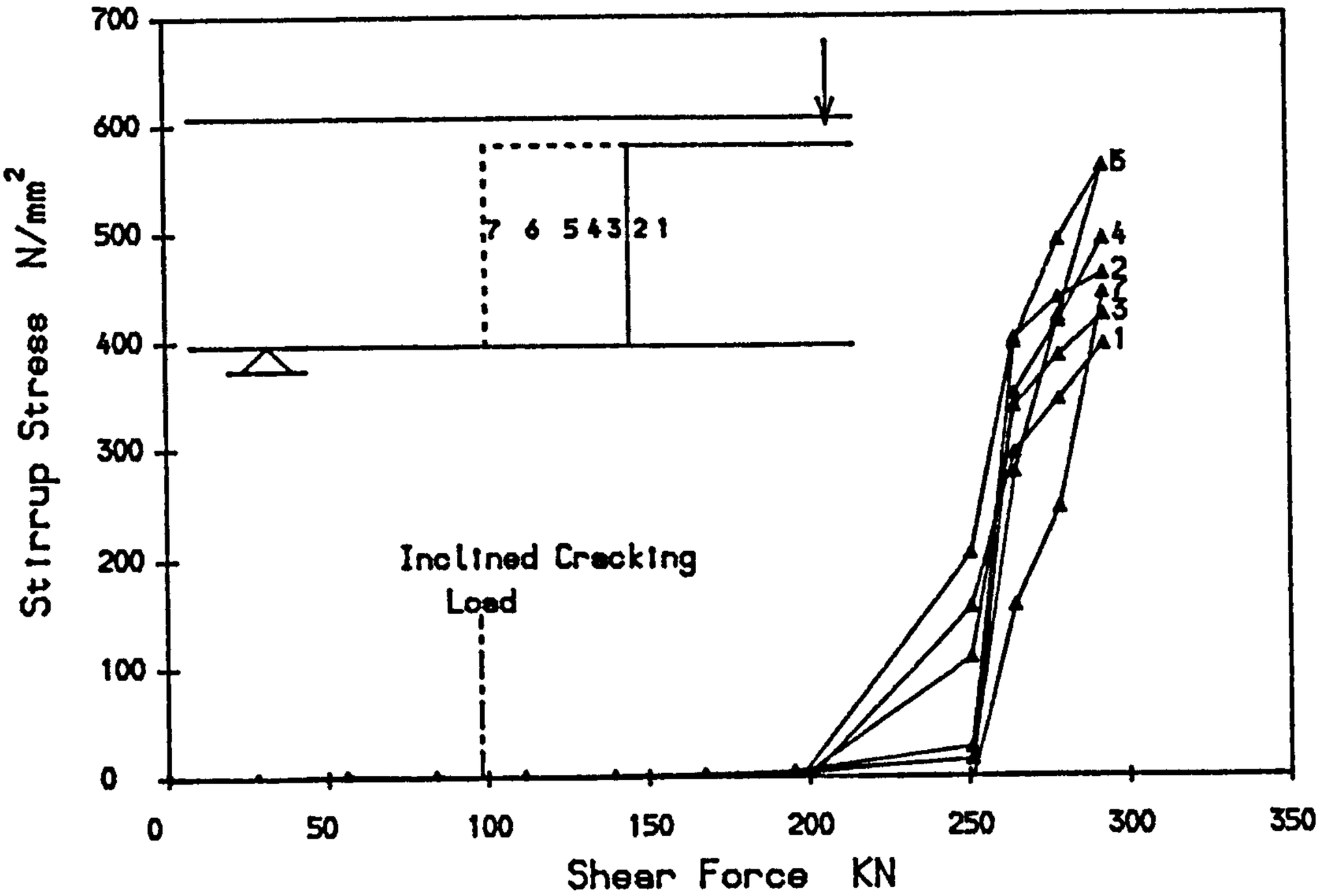

FIG. 4.19a STIRRUP STRESS V.S SHEAR FORCE IN THE PRECAST PART OF WTFDCC-10

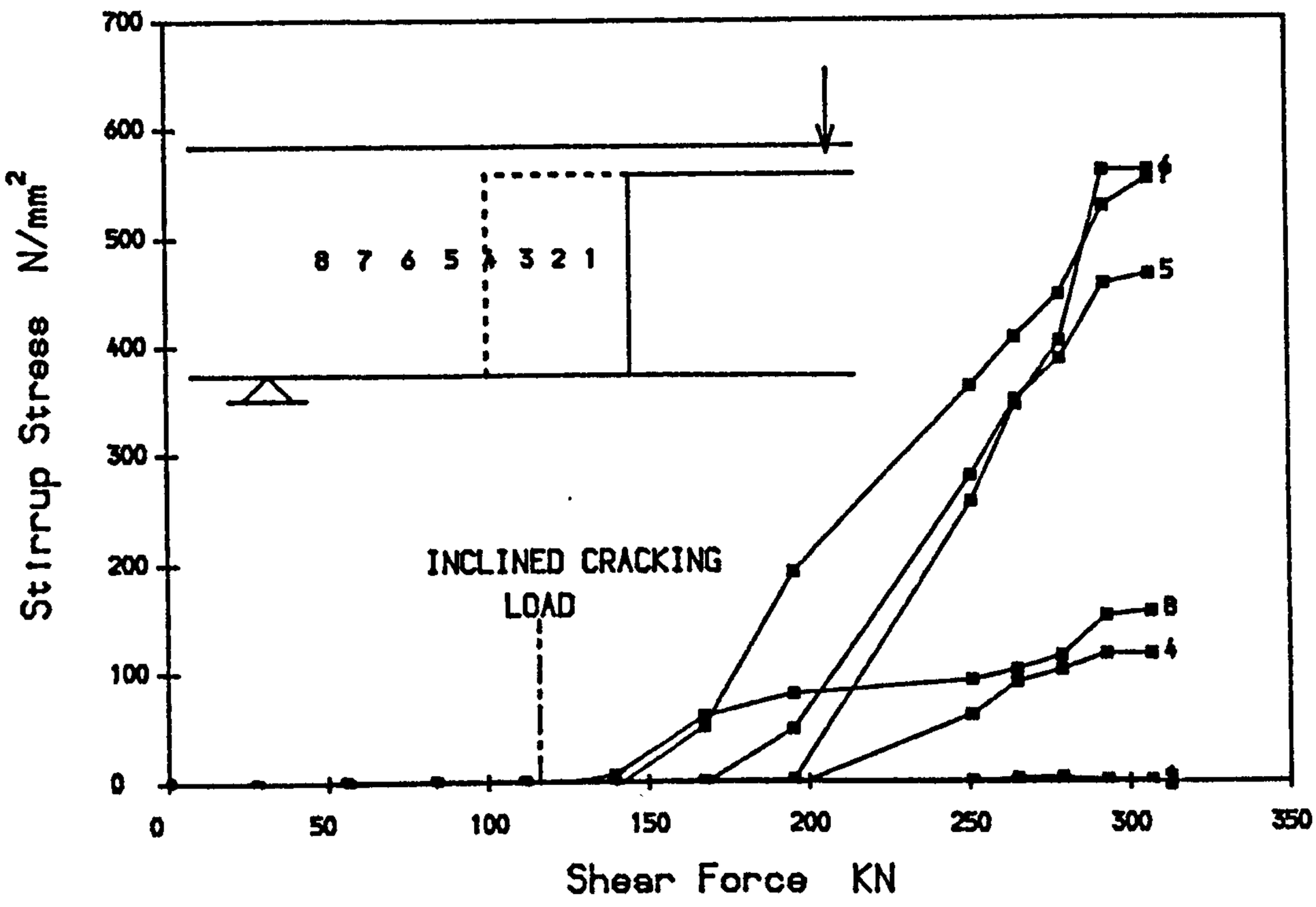

FIG. 4.19b STIRRUP STRESS V.S SHEAR FORCE IN THE IN-SITU PART OF WTFDCC-10

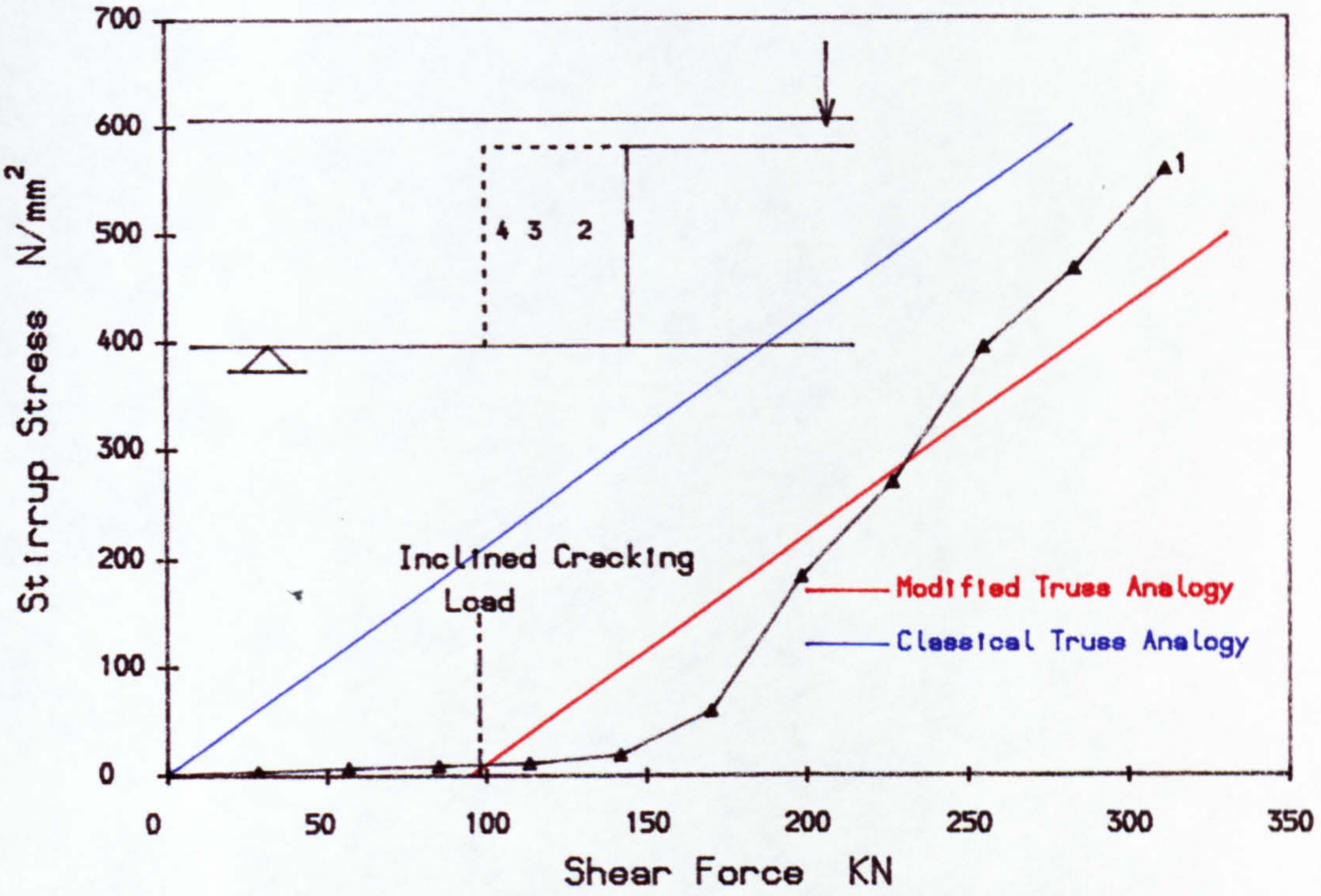

FIG. 4.20a STIRRUP STRESS IN COMPARISON WITH TRUSS ANALOGY (Precast Part of E30AA-1)

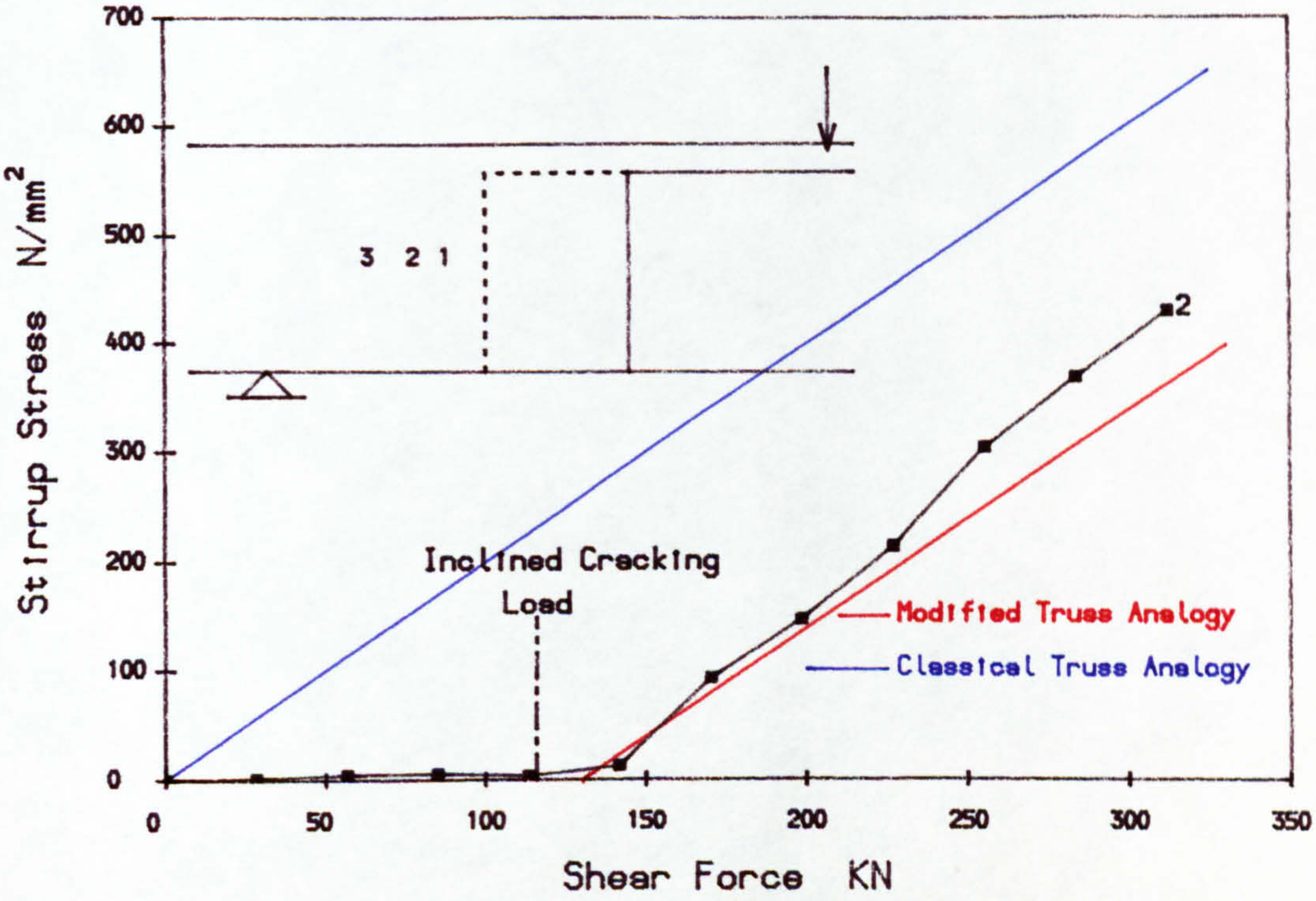

FIG. 4.20b STIRRUP STRESS IN COMPARISON WITH TRUSS ANALOGY (In-Situ Part of E30AA-1)

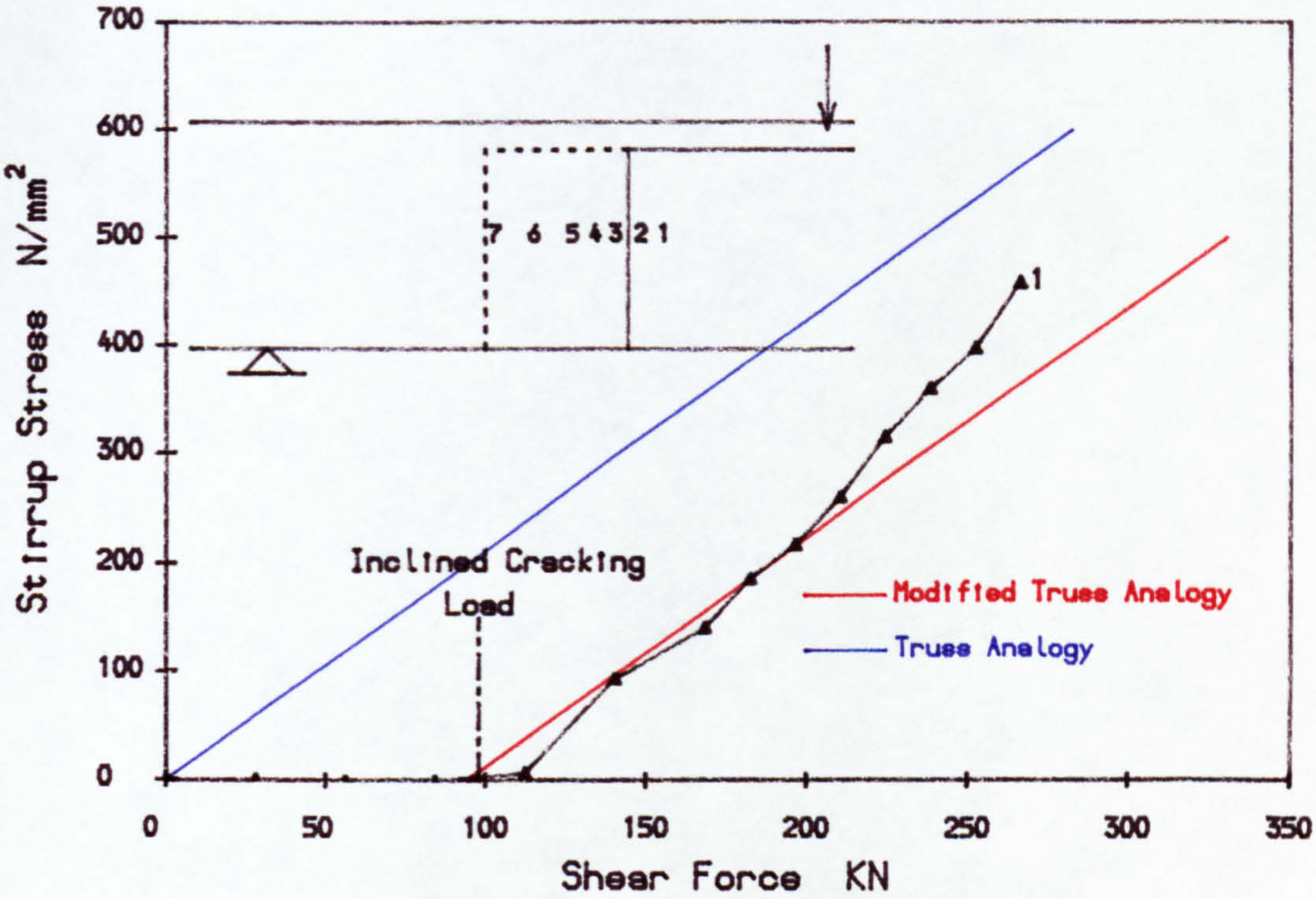

FIG. 4.21a STIRRUP STRESS IN COMPARISON WITH TRUSS ANALOGY (Precast Part of E30AB-3)

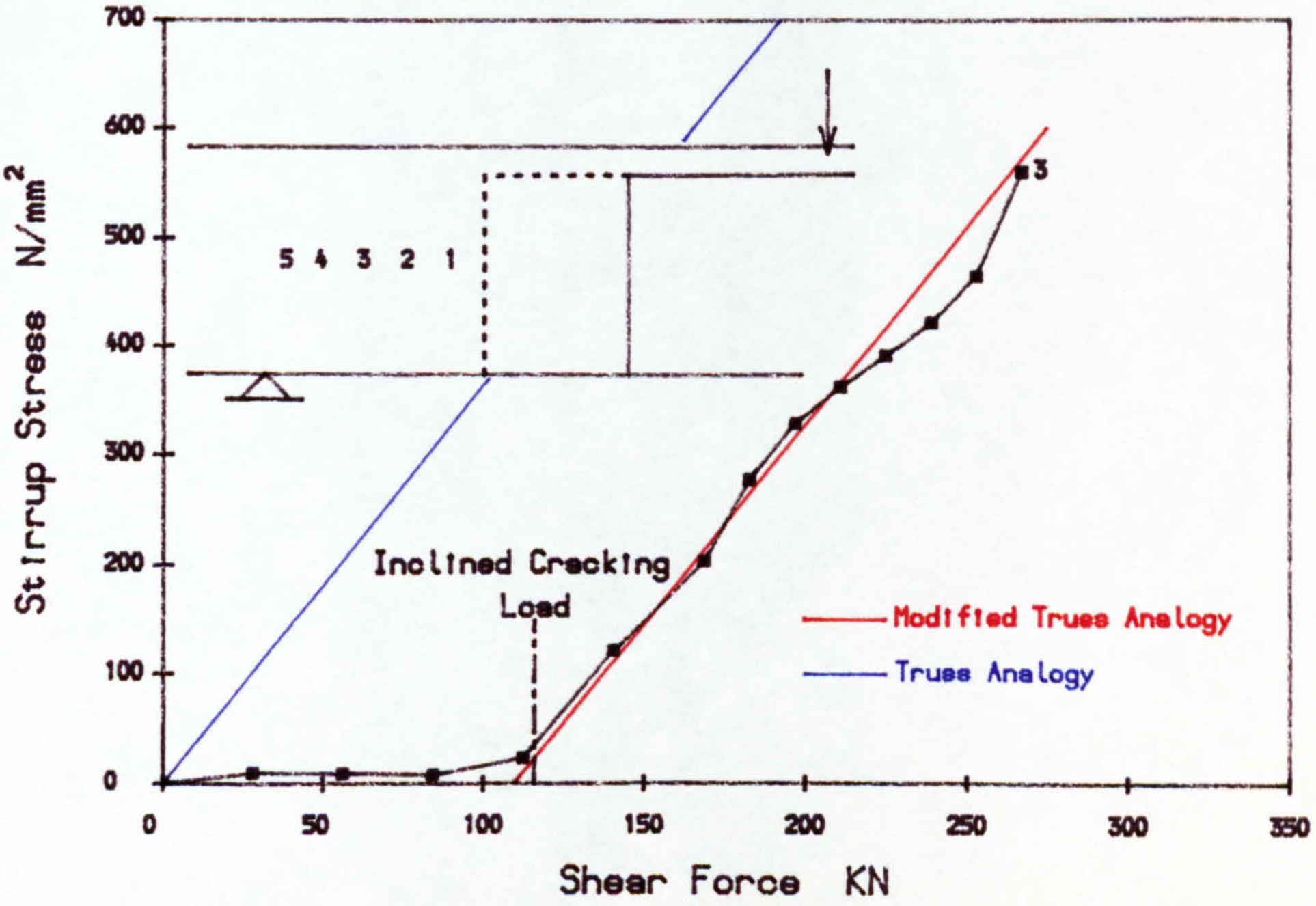

FIG. 4.21b STIRRUP STRESS IN COMPARISON WITH TRUSS ANALOGY (In-Situ Part of E30AB-3)

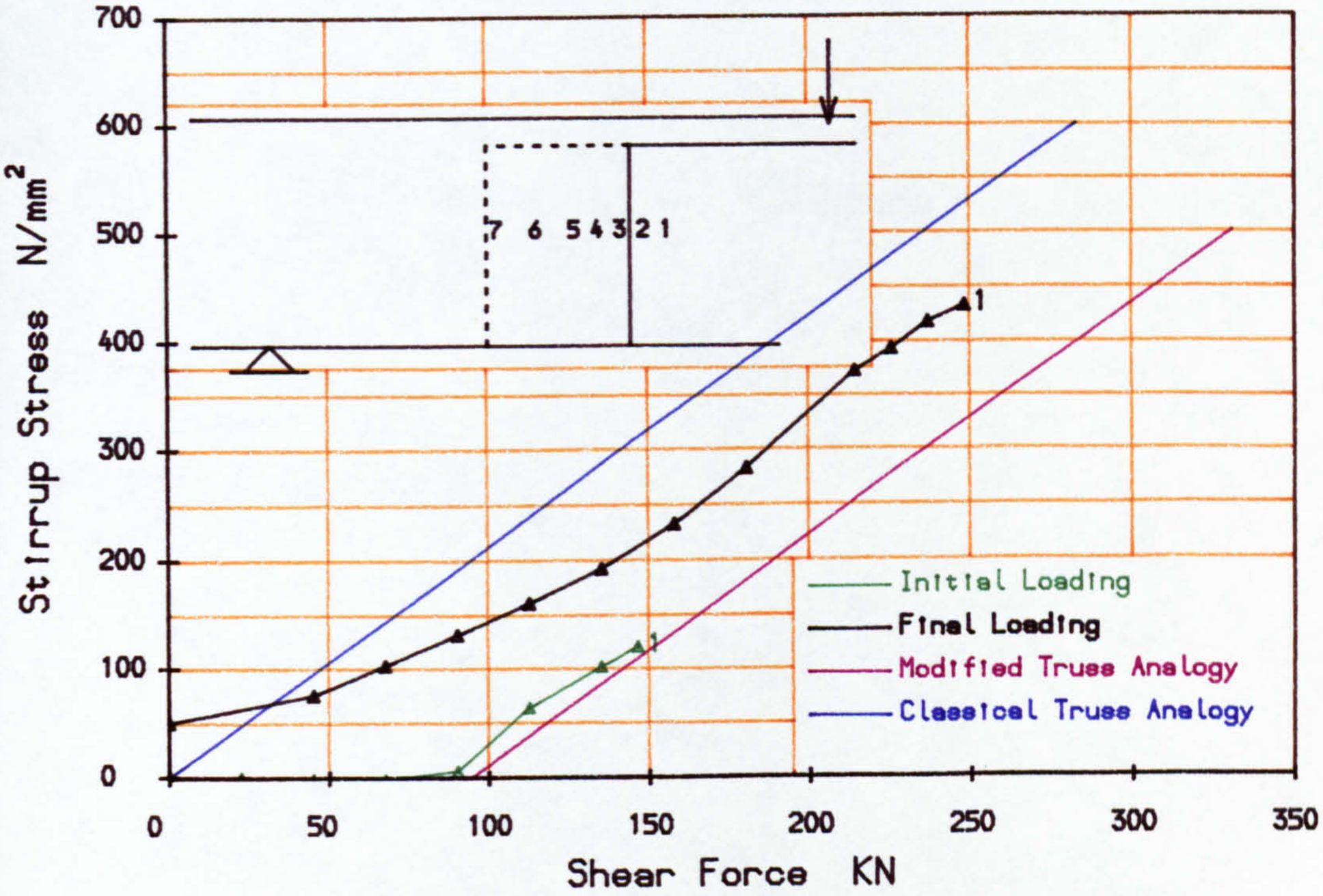

FIG. 4.22a STIRRUP STRESS V.S SHEAR FORCE IN THE PRECAST PART OF E30BC-4

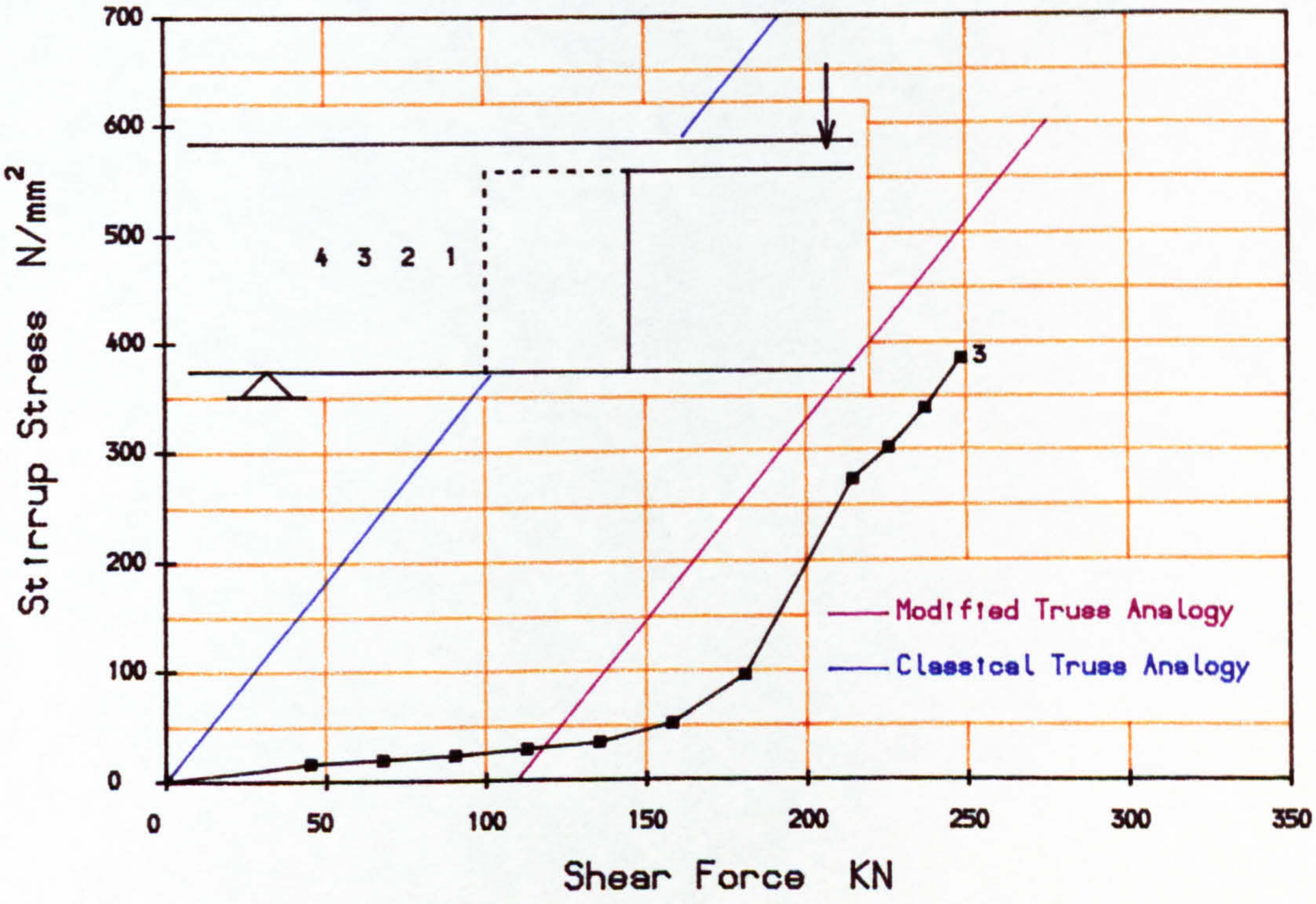

FIG. 4.22b STIRRUP STRESS V.S SHEAR FORCE IN THE IN-SITU PART OF E30BC-4 (FINAL LOADING)

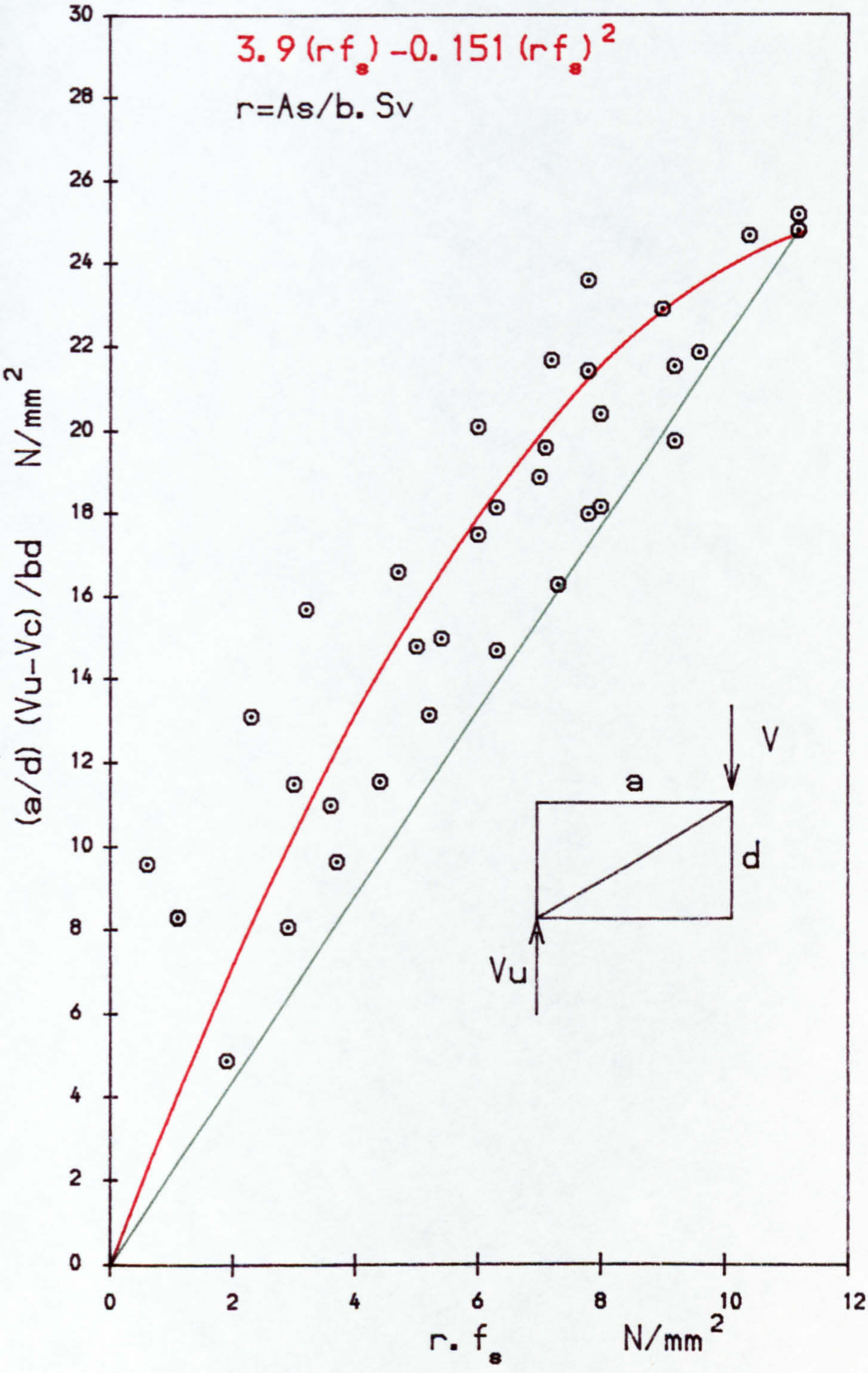

FIG. 4.23 VARIATION OF STIRRUP INDEX WITH SHEAR FORCE AND SHEAR SPAN

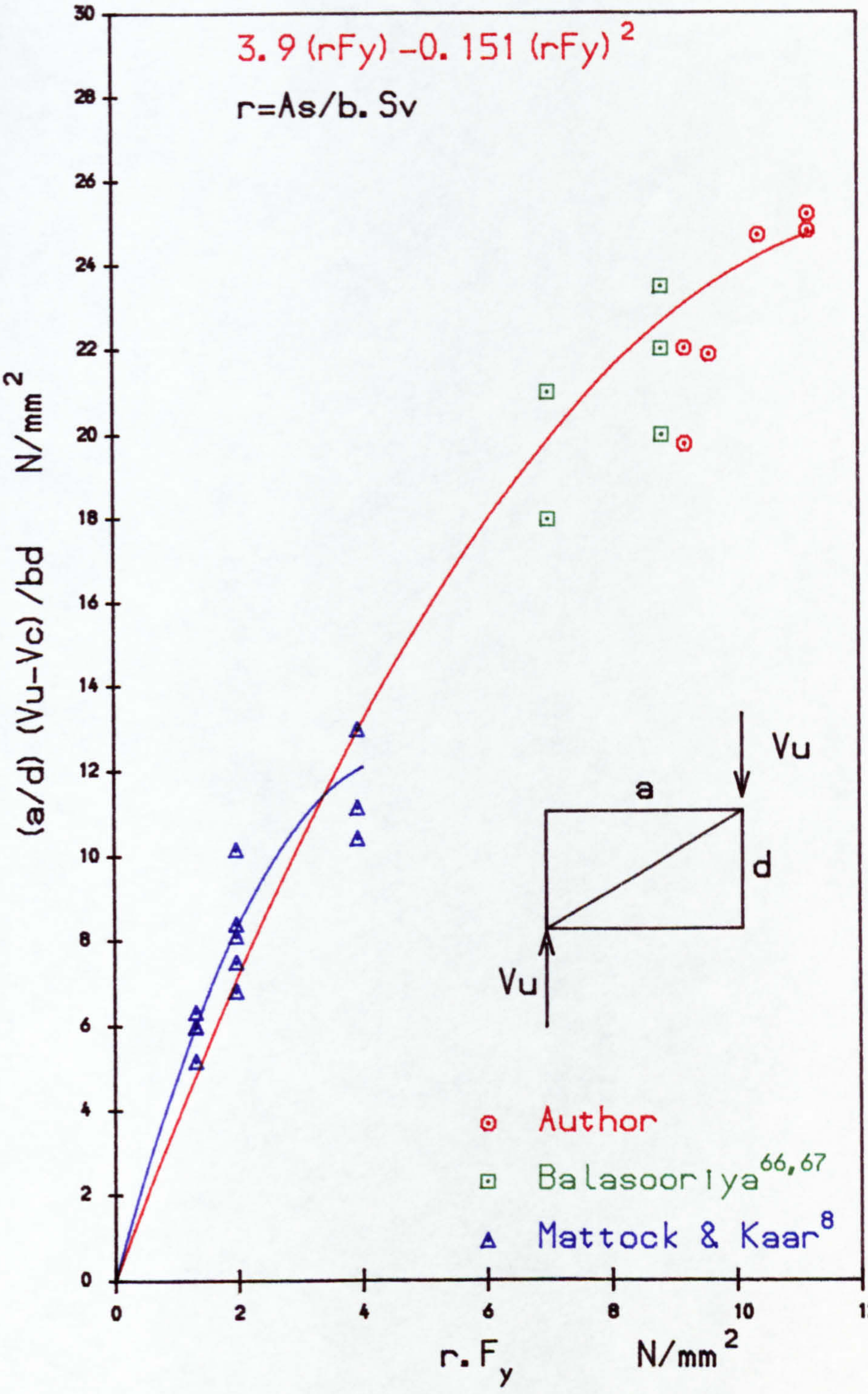

FIG. 4.24 VARIATION OF WEB CRUSHING STRENGTH WITH SHEAR SPAN RATIO AND REINFORCEMENT INDEX

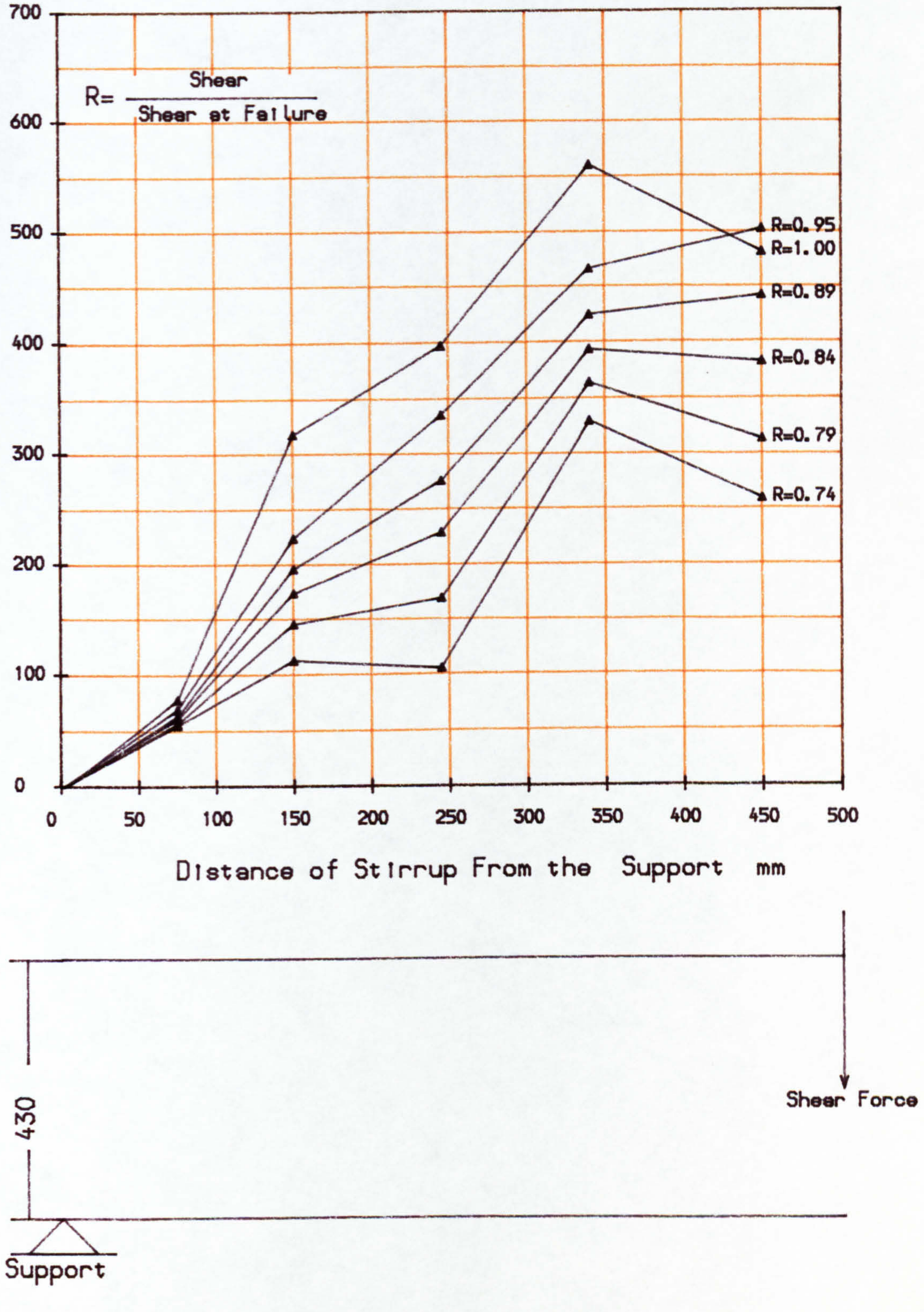

FIG. 4.25. STIRRUP STRESS NEAR THE SUPPORT- E30AB-3
(ENHANCED SHEAR STRENGTH)

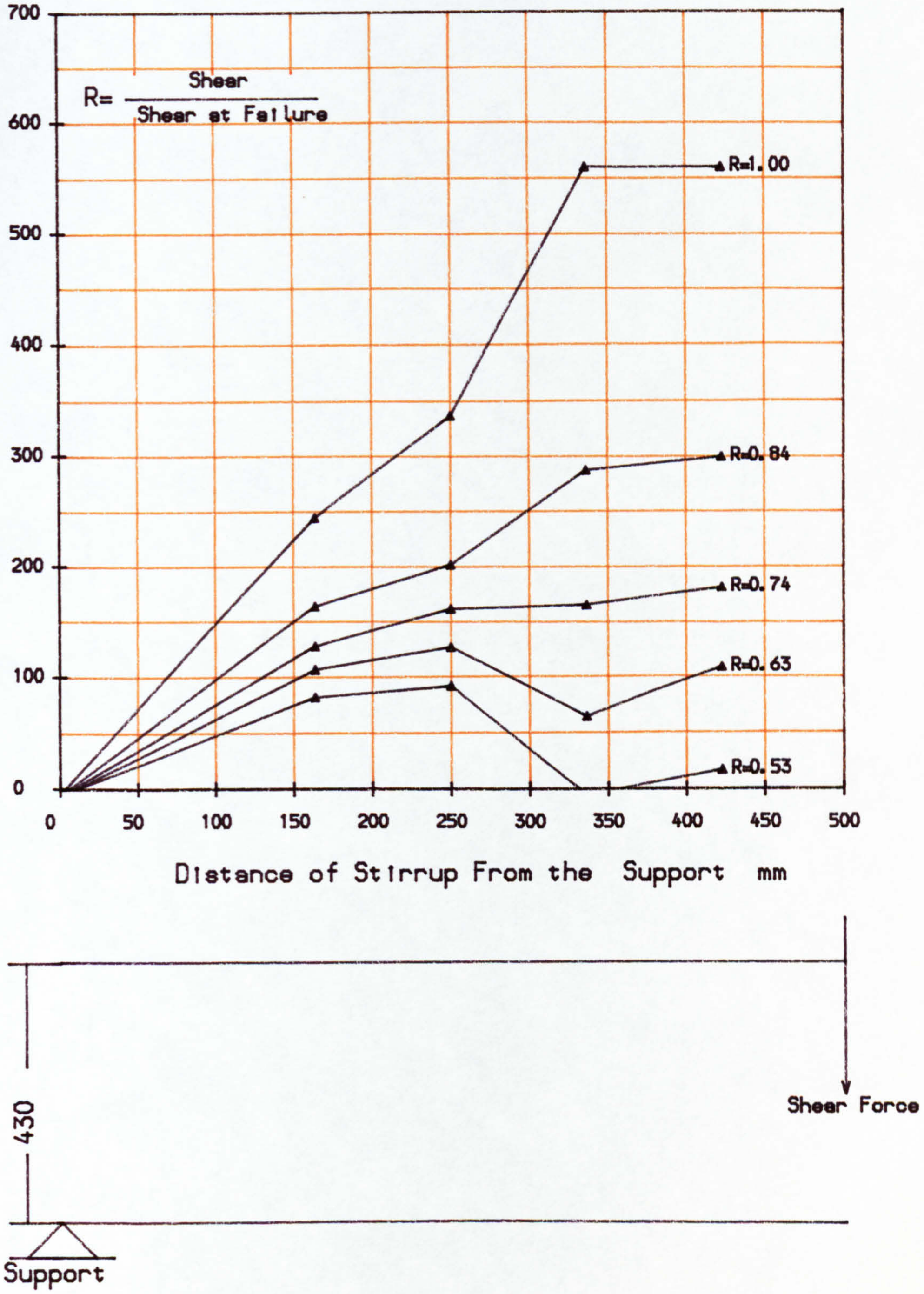

FIG. 4.26 STIRRUP STRESS NEAR THE SUPPORT- E10CC-5
(ENHANCED SHEAR STRENGTH)

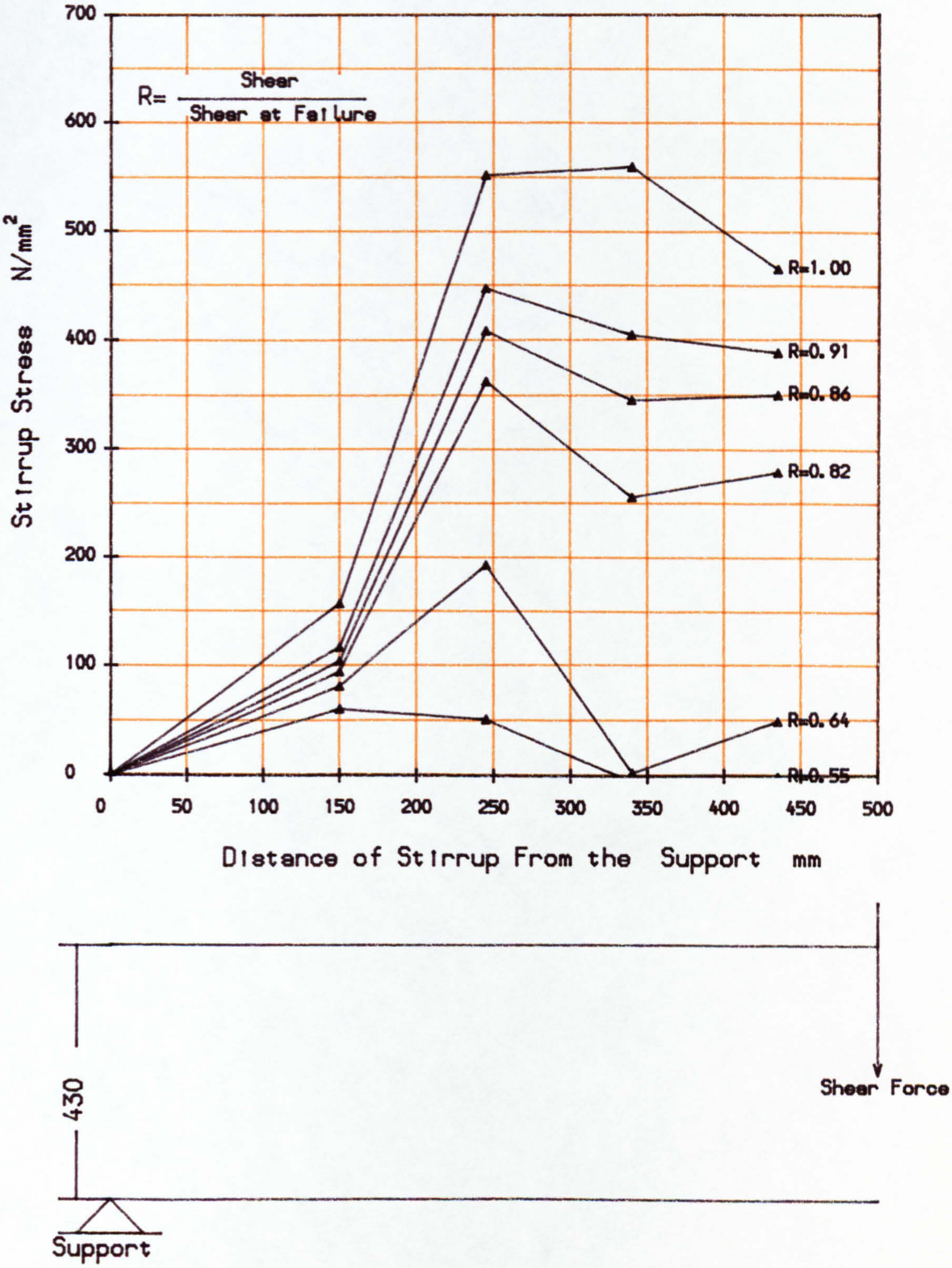

FIG. 4.27. STIRRUP STRESS NEAR THE SUPPORT -WTFDCC-1 0
(ENHANCED SHEAR STRENGTH)

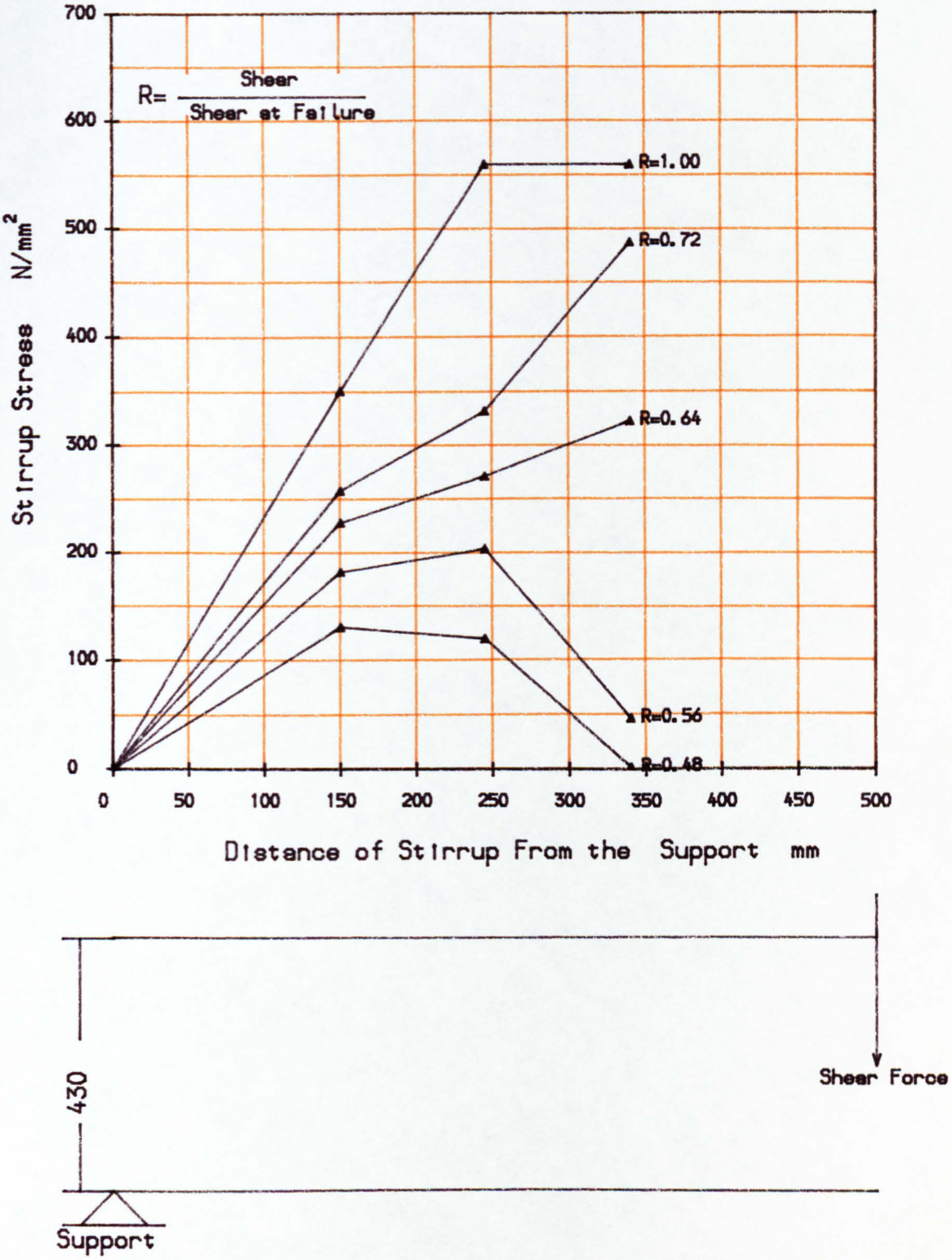

FIG. 4.28. STIRRUP STRESS NEAR THE SUPPORT - WTFPCC-8
(ENHANCED SHEAR STRENGTH)

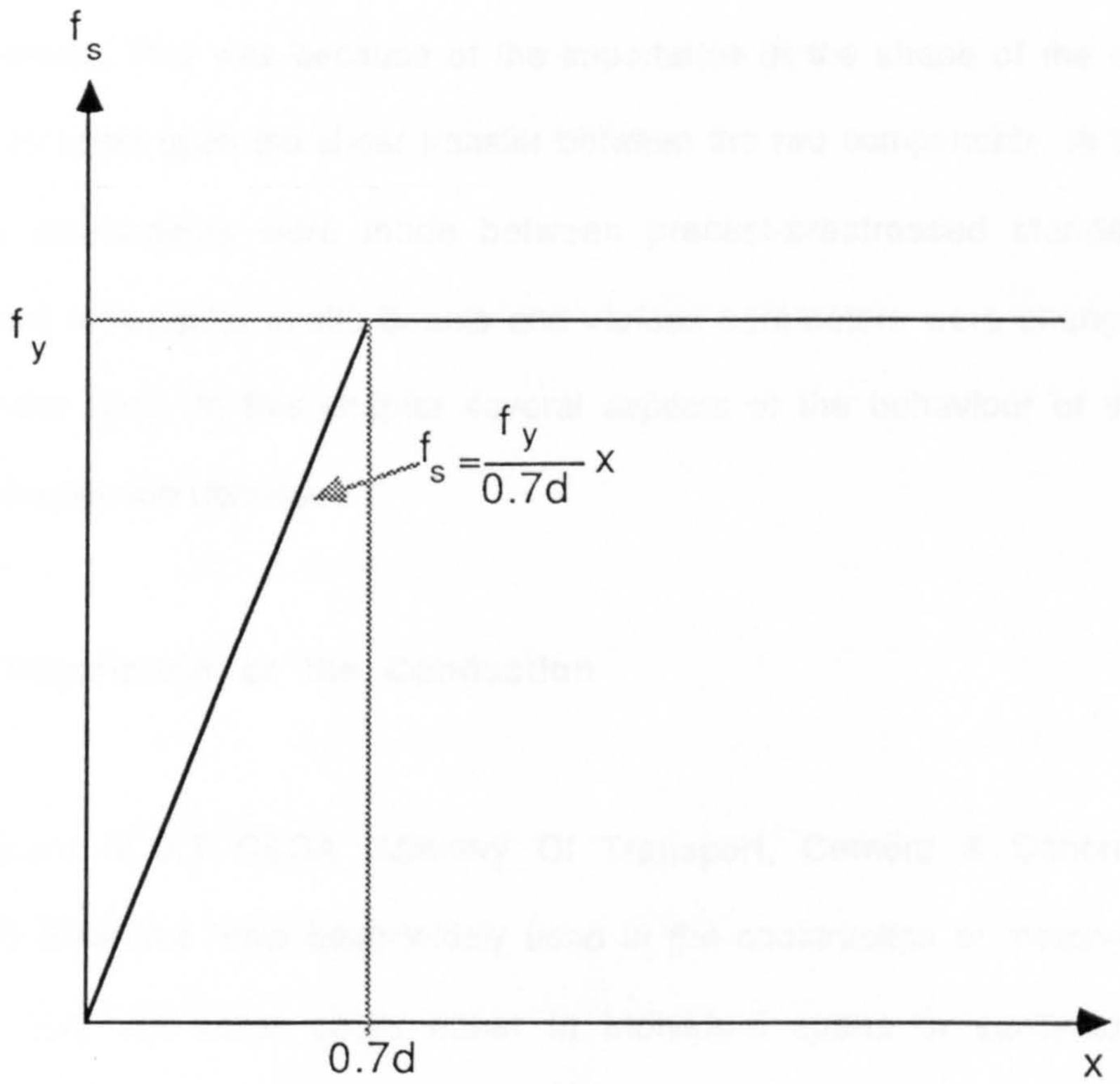

FIG. 4.29 Experimental Stirrup Stress V.S. Distance of Stirrup from the Support

CHAPTER FIVE

SHEAR TRANSFER MECHANISM FOR BEAMS WITH TOP FLANGES

5.1 General

As explained in chapter three, the complete test program was divided into two major series. This was because of the importance of the shape of the top flange and its effect upon the shear transfer between the two components. In the first series connections were made between precast-prestressed standard M-beams and rectangular in-situ beams and various parameters were changed throughout the tests. In this chapter several aspects of the behaviour of this type of connection are discussed.

5.2 Description of the Connection

Standard M.O.T C&CA (Ministry Of Transport, Cement & Concrete Association) M-beams have been widely used in the construction of motorway bridges in U.K. for some years either in individual spans or continuous structures. The type of connection which was tested here was an unconventional (new) joint in continuous structures as described in the introductory chapter in Sec. 1.2.7 (see also Fig.1.7). Relatively few bridges have been constructed using this method. The negative bending moment over the supports can easily be transferred by providing continuity bars in the top deck slab, but the mechanism of shear transfer raises many questions.

Although the test beams were 1/3 scale M8, in this part of the programme no attempt was made to change the geometrical shape of the model M-beam in the joint region.

5.3 Parameters Investigated

Experimental variations mainly concentrated on details of the connection including its reinforcement and dimensions, though in one case the moment/shear combination was changed.

5.3.1 Change of Shear Reinforcement

At the connection between the two components one of the most important features is the shear reinforcement in the in-situ concrete surrounding the M-beam. This concrete on each side of the web of the M-beam is referred to as "concrete nibs". In previous construction work of this type, designers have provided a large amount of stirrups in these nibs which is a difficult job to undertake in practice. It was thus decided to examine the need for this reinforcement. The effect of reinforcing bars, or strands, projecting from the end of M-beam into the in-situ concrete was also examined. This is important because if we can eliminate or reduce the necessity for these projected bars, the precast beams will be easier to make and transport, the labour work on site will be less and there will be no corrosion problem if the beams are stored on site.

5.3.2 Change of Dimensions

In this part of the tests the only geometrical change was the length of embedment of the end portion of the M-beam. If this length can be reduced without losing the strength, then again economy could be achieved.

5.3.3 Change of Moment/Shear Combination

In one case the loading arrangement enabled a higher bending moment to be produced at the connection in order to see the effect upon the shear transfer capacity.

5.4 Mechanism of Shear Transfer at the Connection

In the conventional method of continuous precast prestressed composite construction precast beams are supported permanently on the piers and in-situ concrete is cast over the beams and supports transmitting the shear force to the supports. In contrast, since the new method comprises precast elements supported away from the piers through the in-situ concrete crosshead, one has to make sure that the shear force can be transferred from the precast beams to the crosshead and then to the supports. Consider such a connection as in Fig. 5.1 without any additional shear connection. The shear force acting at the right hand side of the connection (where the M-beam is situated) tends to move the M-beam downwards relative to the in-situ crosshead and its nibs. This movement is carried (i.e the shear force is transferred from the M-beam to the in-situ nibs) by means of three different mechanisms:

a) Mechanical interlock between the bottom surface of the M-beam's top flange and the in-situ nibs. A part of the shear force, V_1, (half at each side) is transferred by this mechanism (see Fig. 5.1c,d). The significance of this mechanism will be discussed in a later chapter.

b) The bond between the in-situ concrete nibs and the M-beams web provides this mechanism of shear transfer. A total value of bond force V_2 (half at each side) is transferred by this effect.

c) The third mechanism is provided by the top slab over the M-beam

which is cast together with the nibs and crosshead. This part is equivalent to the shear capacity of the top slab. The contribution of this mechanism is assumed to be V_3 (see Fig. 5.1c,d). If the connection transmits the total shear force V then:

$$V=V_1+V_2+V_3 \qquad \text{.....(5.1)}$$

The completion of the first and second parts of the test programme revealed the importance and contribution of each mechanism in the total shear transfer capacity of the connection. In general it was seen that the second part (V_2) is dependent on the roughness of the M-beam's web and the shrinkage of the in-situ concrete nibs. Since the M-beam's web is usually quite smooth and the in-situ concrete is subject to shrinkage, this part of the shear transfer mechanism cannot provide a reliable effect (this topic was examined in a complementary test program on small specimens, and is discussed in chapter seven).

5.5 Test Details

The beams tested in this part of the investigation comprise six different connections between precast prestressed M-beams and in-situ concrete. Two point loads were applied through a span-cantilever arrangement which is capable of producing high shear and bending moment in the connection (see Fig. 3.10 for bending moment and shear force diagrams).

In the first four tests the embedment length in the connection was 300mm which is 1/3.3 of the prototype embedment length (1000mm). Two other tests had 100mm embedment length at the connection representing an embedment length of 300mm in prototype. Other details, test specifications, calculated and experimental results are shown in table 5.1.

5.6 General Procedure for Evaluation of the Shear Transfer Capacity of The Connection

The connection between precast and in-situ concrete is acceptable if its shear capacity is greater than the shear strength of either precast or in-situ beams, which means that a premature failure in the connection does not occur. In addition to that, the connection must be serviceable i.e cracks, separation between components and the rotation at the joint are within accepted limits.

5.7 Experimental Results

The first test had exactly the same construction details in the connection as in the prototype. These include overlapping length and stirrups in the in-situ nibs. Both precast and in-situ beam stirrups were continued through the overlapping zone with their original spacings so the amount of stirrups in this zone was equal to the sum of both.

The deck was designed with the precast section having a lower shear strength than the in-situ section (see table 5.1). This was to ensure failure occured in one side of the connection so that the failure mode could be seen clearly (i.e without a simultaneous failure in the precast and in- situ beams). Load was increased in about 20 intervals and a web crushing failure occured in the precast section (see plate 5.6).

The failure shear force was close to the calculated shear resistance of the precast beam and it can thus be concluded that the connection was able to transfer the whole design shear force. It can also be seen in plate 5.6 that the connection overlap zone has remained unaffected after the failure.

5.7.1 Stirrup Stress

The stress in the stirrups in each section of the beam can be used as a means to evaluate the amount of shear force carried by that section. Strains were measured for all stirrups positioned in the overlapping zone both in the precast beam and in-situ nibs. These strains were then converted to stresses using experimental stress-strain curves for the stirrup reinforcement.

5.7.2 Variation of the Stirrup Stress Within the Connection

In Fig. 5.2 the experimental stirrup stresses have been plotted against their positions in the connection (positions are expressed as the distances from the support). Different colours have been used to distinguish between precast beam and in-situ nib stirrups. These curves have been produced for different loading stages expressed as the ratio of load to failure load (R).

For the precast beam, stresses continue to decrease along the overlapping length as the stirrups become nearer to the precast beam's end. As an example, for a shear force equal to 73% of the shear force at failure, the stirrup stress decreases from 270N/mm^2 (for stirrup outside the connection) to 210, 70 and 10 N/mm^2 (for those stirrups located inside the connection). The smallest stress being for the stirrup positioned at the end of precast beam. This indicates that the shear force transfers gradually from the precast beam to the in-situ nibs. To obtain the distribution of forces from the precast section to the in-situ nibs it is possible to use the experimental stirrup stress (f_s) in the following equation:

$$V_p=V_c+rf_sbd \qquad \text{.....(5.2)}$$

in which V_p is the amount of shear force in the precast section at the position of

the stirrup having a stress of f_s. This equation could be used for all stirrups within the overlapping zone to obtain the shear force diagram of the precast beam along its embedment length. This has been shown for the beam E30AA1 at a load equal to 73% of failure load (see Fig. 5.3b).

It should be mentioned that in obtaining the shear force diagram it has been assumed that the shear force carried by the precast beam at its end (inside the connection) is zero. At first it was thought that part of the total shear is carried by the dowel action of projecting bars from the end of precast beam into the in-situ concrete, but as it will be discussed later, in a later test the dowel action was eliminated and it was revealed that in fact for this type of connection in which there is a top flange effect, the dowel forces do not act. In the next chapter the importance of the dowel action of projecting bars can be seen when the precast beam in the connection has no top flanges.

5.7.3 Distribution of Forces Between the Two Parts of Connection

The shear force diagram produced for the precast beam inside the connection can be converted to an equivalent distributed load by differentiating the shear force (i.e. q=-dV/dx). This distribution consists of two different uniform amounts (see Fig. 5.3c). 55% of the shear force is transmitted through 250mm (83%) of the connection length. The remainder of the shear force (45%) is transferred through a 50mm (17%) length of the end of the precast beam into the in-situ nibs.

The distribution of forces between the two parts were obtained for other loading stages and also for tests E30AA2 , E30AB3 and E30BC4 . They were similar to the results from E30AA1.

The embedment part of the precast beam was removed from the connection by carefully breaking the concrete nibs and it was seen that the diagonal cracks

had penetrated into the connection but these cracks reduced for smaller distances from the end of the precast beam.

It is thus seen that for an embedment length of 300mm, a considerable proportion of the shear force is transferred through a small length of the end of the precast beam. This lead to the conclusion that it could be possible to use a smaller embedment length than 300mm. Two tests were thus undertaken in this manner and their results will be discussed later in this chapter.

5.7.4 The Shear Force Carried by the In-situ Nibs and the Stirrup Stress

The distributed load that was obtained from the precast beam in the overlapping zone (see Fig. 5.3c) will be transferred to the in-situ nibs surrounding the end of the precast beam. The intensity of this distributed load is low for a considerable length of the nib (250mm out of 300mm). The shear force diagram for the nibs can be obtained using that load distribution or simply by subtracting the precast beam's shear force from the total shear force in the section as shown in the upper part of Fig. 5.3b. The concrete nibs have large cross-sections relative to the precast beam (about 4.5 times in this case) and so the shear carried by the concrete is significant.

The shear force increases from zero (at the end of nibs) to about the shear strength of concrete nibs (without stirrups) within a length of 200mm (out of 300mm). This is confirmed by considering the observed shear force in the nibs obtained from strain measurement in stirrups in the nib.

In Fig. 5.2 the red lines show the stirrup stresses in the in-situ nibs and beam . There are six stirrups in the nibs and for five of them (located within 200mm from the end of the nib) the stress is almost zero. In other words in this distance the shear force carried by the nibs is less than or equal to the shear strength of concrete nibs without stirrups. This was the basis for the

tests in which no stirrups were used in the nibs and will be discussed later in this chapter.

5.8 Shear Transfer by the Projecting Bars from the Precast Beam into the In-situ Concrete

After observing that a large amount of shear force is transferred to the in-situ nibs from the end of the precast beam, it was thought that possibly the dowel action of the projecting bars had an important contribution. It was thus decided in test E30AA2 to eliminate any dowel action effect with sleeving all the longitudinal bars with soft rubber at the end of the precast beam (and also the continuity bars in the top slab) before casting the in-situ concrete (see chapter three section 3.11 for other details).

5.8.1 Ultimate Strength and Failure Mode

The beam failed by web compression in the precast beam at a load very close to the failure load of a previous test (E30AA1) with dowel action effect (see plates 5.1 and 5.7). No weakness was observed in the connection itself and it was able to transfer the design shear strength of the precast beam (see table 5.1).

5.8.2 Stirrup Stresses

Experimental stirrup stresses were plotted against their positions in the connection (see Fig. 5.4) and the same trend as the previous test (E30AA1) was observed. In the precast beam the stirrup stresses are lower for those nearer to its end and in the in-situ nibs no significant stress was observed in the stirrups up to failure. In the precast beam outside the connection the stirrup stresses

reduce slightly as they become nearer to the span loading point. This may be explained in two different ways:

a) The increas in shear strength (and hence decrease in stirrup stress) near the loading point , taking into account that the distance between the span load and starting point of the connection is approximately equal to the effective depth . This was discussed in chapter four as the enhanced shear strength near the supports and loading points.

b) The reduction in shear strength of the precast beam within the transmission length (the part of the precast beam in the connection is almost within its transmission length) which results in lower stirrup stress remote from the beam's end .

5.8.3 Inclined Tensile Strain in the Concrete within the Connection

A comparison was made between the inclined tensile strain on the precast beam embedded in the in-situ concrete nibs and the inclined tensile strain on the external surface of the in-situ nibs. Three different positions (R_1,R_2 and R_3 as in Fig. 5.5) were selected both on the precast beam and the same level of in-situ nib along the connection. Tensile strains in a direction of 45° with the horizontal were measured and have been plotted against the total shear force in the connection (see Fig. 5.5). Solid lines are for the precast beam and dotted lines for the in-situ nib. Theoretically in a monolithic rectangular section there should be no change in the strains of different points located at a specific level of the beam's depth but since the connections tested here were not monolithic, strains are not similar in each level of two parts and in fact a large difference was observed. It can be seen from these curves that near to failure the precast beam can develope a very high inclined tensile strain of about 7000

micro strain (position R_3) whilst at the same time at the same level the tensile strain in the same direction in in-situ nib is almost zero. For the precast beam itself it can be seen that although the strain at the end of beam (position R_1) is smaller than that for R_3 it is of significant value at about 1200 micro strain.

These observations again confirm the previously mentioned fact that most of the in-situ nibs are carrying only a small fraction of the shear force with a large amount of shear being transferred to the in-situ nibs near the end of precast beam.

5.9 Elimination of Projecting Bars and Stirrups in the Nibs

Since it was observed in previous tests that :

a) The stirrups in the in-situ nibs do not develope any appreciable stress (i.e. they do not participate in the load carrying capacity of the connection).

b) The elimination of dowel action (by sleeving with rubber) did not make any difference to the behaviour of connection.

It was decided in this test (E30AB3) to use neither stirrups in the in-situ nibs nor projecting bars from the precast to the in-situ beam (except four 8mm bars at the bottom which may be needed in practice for possible positive bending moment resulting from support settlement).

In this test the connection was designed such that the in-situ beam had a lower shear strength than the precast beam but in the embedded part of the precast beam the stirrups had the same spacing as in the in-situ beam, representing the stirrup arrangement as if assuming a monolithic beam.

5.9.1 Ultimate Strength and Mode of Failure

In this test the in-situ beam failed in a diagonal tension mode with a very wide crack approximately joining the support and the span loading point (see plates 5.2 and 5.8). The failure load was slightly larger than the calculated shear resistance of the in-situ beam (267kN in comparison with 262kN but see table 5.1). It can thus be concluded that the two previously mentioned major modifications (see section 5.9) did not reduce the ultimate shear transfer capacity of the connection.

The direction of the main crack (see plate 5.8) noticeably passes from the intersection of the top slab and the concrete nib. There is also another crack passing through the junction between the top flange of the precast beam and the in-situ nib. These clarify that the mechanical interlock between top flange of the precast beam and in-situ concrete has a significant contribution to the shear transfer capacity.

5.9.2 Stirrup Stress

The change of stirrup stress with respect to their position in the connection have been plotted in Fig. 5.6 . As previously stated stirrups in the connection are only placed in the precast beam (blue lines of Fig. 5.6). If the connection was cast as monolithic a constant stirrup stress distribution would be expected along the beam, but it can be seen here that in the region at the end of precast beam for up to 95% of failure load the stirrup stress is almost zero whereas in the in-situ beam stirrup stresses decrease when they are nearer to the connection. This condition can be explained as follows:

At the connection, each side (precast beam or in-situ concrete) behaves like a support for the other and as previously discussed, in chapter four, there

is an increased shear strength within a specific distance from the support resulting in lower stresses in the stirrups.

5.9.3 Concrete Diagonal Tensile Strain at 45° Inclination

Fig. 5.7 shows the experimental inclined tensile strain within the overlapping zone for each part of the connection. Again a substantial difference was found between the inclined tensile strain in the precast beam and the same level of the in-situ nibs. The explanation for this has already been given in section 5.8.3 .

5.10 Change in the Magnitude of Bending Moment at the Connection

In a multi-span continuous beam with uniformly distributed load, the point of zero bending moment lies within 7% to 10% of the span length from the supports. Assuming a span of 27 metres for our case with M-8 beams, the contraflexure points are located at about 1.9 to 2.7 metres from the supports. For this method of construction the end of the precast beam is located 2.5 metres from the support. This indicates that the connection is situated within a zone of low bending moment.

In previous tests all the reinforcing bars over the support were continued along the connection but in this test (E30BC4) the following modifications were made:

a) Some of the bars which were required to resist the negative bending moment at the support section were curtailed at the end of the precast beam.

b) The loading arrangement was changed so that a higher bending moment was produced at the connection.

These two changes resulted in the bending moment at the end of precast

beam being slightly lower than it's flexural capacity.

5.10.1 Ultimate Strength and Mode of Failure

The beam failed when the shear force in the section reached 255 kN (in comparison with the calculated shear resistance of 262 kN) and the failure mode was diagonal tension between the span load and continuous support (see plates 5.3 and 5.9).

Considering the higher applied bending moment at the connection and the lower flexural capacity of the member at the end section of the precast beam (in comparison with previous test), it was seen that flexural-shear cracks appeared at the sections closed to the precast beam's end well before the failure. However, these cracks did not appreciably reduce the shear capacity of the beam compared with previous tests, and it can thus be concluded that the connection is capable of transferring the design shear force from either part to the other. It is also worth noting that when this type of construction is used it is less likely to have the connection very close to the support (in which case the conventional type of construction could be used). Nevertheless more research work is required for the cases in which the end of the precast beam is located close to the support (say less than 300mm in the prototype).

5.10.2 Stirrup Stress In the Connection

No stirrups were used in the in-situ nibs but the others had the same spacing either in the precast beam within the connection or in the in-situ beam away from the connection. The experimental stirrup stresses are plotted against their distances from the continuous support in Fig. 5.8. The only minor difference in comparison with previous tests (see also Fig. 5.6) is that slightly

higher stirrup stresses were observed for a given level of shear force (for example at 84% of the failure load) which is probably due to more flexure-shear cracks occurring in that region.

5.11 Change of Embedment Length

It was seen in previous tests that a rather high percentage of shear force is transferred to the in-situ nibs through a small length at the end of the precast beam (see Fig. 5.3) . It was decided in this stage to examine the behaviour of connections with smaller embedment lengths. Two tests were carried out in this manner and the embedment length was selected to be 100mm (300mm in the prototype).

In the first test (E10CC5) no stirrups were used in the in-situ nibs while in the second test (E10CD7) two 6mm high yield stirrups were used in the nibs.

5.11.1.1 Experimental Results for the Test with no Stirrups in the Nib

The observed ultimate shear capacity of the beam was lower than for either the precast or in-situ parts. The beam failed at a load equal to 83% of the in-situ beam shear resistance indicating that it was a connection failure rather than the failure of components (precast or in-situ beam). The failure was sudden and brittle with a very wide crack (approx. 30mm) passing through the junction between in-situ nib and the top flange of the precast beam (see plates 5.4 and 5.10).

To illustrate the behaviour of this connection consider Fig. 5.9a in which the direction of the main crack at the time of failure has been shown. Figs. 5.9b and 5.9c are the idealized free body diagrams for in-situ nib and precast beam.

The shear force V transfers from each part to another by means of:

i) Bearing between the bottom surface of the top flange of the precast beam and the in-situ nibs, which is a distributed load having a resultant of V_1.

ii) The shear resistance of the in-situ top slab concrete over the precast beam, which is monolithic with the in-situ beam. This part is called V_3.

The bond between in-situ nibs and precast beam web is negligible due to the very smooth surface of the web and inherent shrinkage existing in practice.

It is possible to obtain an approximate value for V_3 by using geometrical dimensions and the shear strength of top concrete and V_1 is obtained by subtracting V3 from the shear at failure.

$$V_3=25 \text{ kN}$$

$$V_1=224-25=199 \text{ kN}$$

This high shear force is exerted through the top flanges of the precast beam to the in-situ nibs each having an effective area of $40\times100=4000mm^2$, implying an average bearing stress of $24.9N/mm^2$ on the concrete. Taking into account that this distribution is not uniform, and has a higher intensity near the end of the precast beam, even a higher bearing stress may exist. The effect of this force on the in-situ nibs or precast beam can be explained as follows:

a) The in-situ nib has a smaller length (100mm) in comparison to its depth (335mm), thus having a maximum shear span to effective depth of 100/335=0.3 . It is a very deep beam and is similar to a corbel (see Fig. 5.9b). The high shear force tends to spall off the nib through the corner and in fact the observed main crack at the failure indicates this clearly (see Fig.5.9b).

b) For the precast beam, the high upward reaction from the nib is applied

on the bottom surface of the precast beam's top flange which is located at about one third of its overall depth. In addition to this the first stirrup in the precast beam is located 50mm (half the embedment length) from its end and this high concentrated load could produce a high tensile stress in that stirrup (see Fig. 5.10).

5.11.1.2 Rotation at the Connection

In an homogeneous beam with constant or variable cross-section subjected to an arbitrary loading, elastic structural analysis shows that there is no sudden change in the slope of the deflection curve. Consider a connection somewhere along the beam. If this connection is completely fixed, its components do not move relative to each other and the slopes and deflections are fully compatible, but if the connection is partially fixed we could expect relative movement and rotation at the joint.

Plate 5.4 indicates how the precast and in-situ beam have rotated sharply relative to each other. This has also been schematically shown in Fig. 5.9d. In addition to this the excessive rotation at the connection has affected the deflection at the mid-span and cantilever end in comparison with previous beams (see Fig. 5.16).

5.11.1.3 Stirrup Stress in the Connection

As before there are no stirrups in the nib for this test. The distance between the last stirrup in the precast beam and the first stirrup in the in-situ beam is the same as the in-situ beam stirrup spacings (see Fig. 5.10). The stirrup stress in the precast beam (two stirrups are located within the connection) at the time of failure was well below its yield stress because its

own shear capacity was about 40% greater than the shear at which the connection failed.

With regard to the stirrup stress in the in-situ beam, truss analogy (assuming a monolithic section) would indicate a stress of about 66% of its yield value at the time of connection failure but experimental stress measurement showed that the four stirrups in the in-situ beam had attained their yield stress at that time (see Fig. 5.10). The reason for this can be explained by the large rotation of the end of the precast beam relative to the in-situ concrete tending to open the inclined crack (see plate 5.10) as much as possible which in return implies tensioning of the stirrups . Tensile strains up to 22500 micro strain (2.25%) were recorded in this test.

At the initial loading stages, and up to about 74% of failure load, the previously observed trend (smaller stresses for those stirrups which are nearer to the connection) was also observed indicating that for this loading range the in-situ nibs are supporting the precast beam from its top flanges and the connection is transferring the shear without causing any abnormal stress or deflection.

5.11.2.1 Experimental Results of Connection with Stirrups in the Nib

In this test (E10CD7) the precast beam had 100mm embedment in the in-situ concrete but in contrast to the previous test the connection also had two 6mm stirrups in the in-situ nib. The connection was able to carry the full shear force and the beam failed in a web compression mode in the precast beam without causing excessive rotation or relative movement in the connection. The improving effect is attributed to the addition of stirrups in the nibs in the following ways:

a) Improving the connection between in-situ nibs and in-situ top flange

which in turn can prevent separation between top flanges and nibs.

b) The embedded length of the precast beam cannot easily rotate inside the in-situ nibs unless putting these stirrups into tension, and so prevents the widening of inclined cracks.

5.11.2.2 Stirrup Stress

The experimental stirrup stress has been plotted for all stirrups inside and remote from the connection in Fig. 5.11. As far as the in-situ beam stirrups are concerned, up to 67% of the failure load the two stirrups located in the nibs have zero stress, bearing in mind that the cracking load is 44% of failure load and that up to this load the in-situ nibs were uncracked. It was also noted that for the same load (67% of failure load) the stirrups in the precast beam are subject to about 30% of their yield stress. For larger loads these two stirrups are under considerable tensile stress and at failure they have about 40% and 50% of their yield values for the first (nearer to the nib's end) and second stirrup respectively.

To compare this connection (100mm with stirrups) with the first two tested connections (300mm with stirrups) consider Fig. 5.4. The nib stirrups had the same spacings in this test as in tests with 300mm embedment lengths. In the latter all the stirrups in the nibs remained unstressed up to the failure while in the former they had undergone 40% to 50% of their yield stress at the time of failure. The reason may be explained in that with longer embedment lengths the intensity of distributed load from the precast beam top flanges to the in-situ nibs is low but for shorter connection lengths the same total load produces a distributed load with a significantly higher intensity.

The possibility of reducing the embedment length is beneficial from the economical point of view because for existing pier positions shorter precast

beams can be used. It was found in these tests that connections having small embedment lengths (100mm) can be used satisfactorily provided proper detailing (geometrical shape of components and stirrup reinforcement) is maintained at the connection. It has also to be mentioned here that in all the test beams precast sections were designed to be capable of carrying the maximum shear allowed by the code so that in practice the shear force which is to be transferred by the connection is equal to or smaller than the shear for which the connections were examined in the tests. More research work is required for connections having embedment lengths between 100mm and 300mm and even for those smaller than 100mm.

5.12 Deflections

For all the beams in this series deflections for mid-span and cantilever end were measured and plotted and can be seen in Figs. 5.12 to 5.17. Considering load-deflection curves for the mid-span points reveals that up to an appreciable load (generally about 60% of the failure load) the behaviour is linear, but after that non-linear behaviour occurs. The portion of the beam between the supports consists of a precast prestressed beam together with a part of in-situ reinforced concrete (which is about 1/6 of the distance between the supports). There is a point of contraflexure near to this connection making this part of the beam similar to a simply supported beam. This has a load-deflection curve similar to that of prestressed beams in which the deflection is linear up to its service load (about 60% of failure load) because the section is uncracked up to this stage and has its full flexural stiffness (EI). For higher loads the beam starts to crack gradually, from mid-span to the supports, reducing the beam's stiffness and resulting in higher deflection producing the non-linear part of the curve.

The cantilever part of the beam is reinforced concrete. The cracking load is therefore much lower than for the prestressed beams and it can be seen in Figs. 5.12 to 5.17 that for the cantilever end (dotted lines) the initial linear part for the uncracked section is very small. Comparing Fig. 5.12 with Fig. 5.13 reveals that in the former the deflections are slightly lower. This should be attributed to the elimination of dowel action in the second test. It is also noticeable that in Figs. 5.16 and 5.17 the deflection at the cantilever end is much higher than in others, which is because of considerable rotation at the connection when the embedment length was 100mm.

5.13 Vertical Separation between the Precast Beam and In-situ Nib

The vertical separation between the precast beam and in-situ concrete at the connection was measured along the junction between the top surface of the bottom flange of the precast beam and bottom surface of the in-situ nib. Pairs of DEMEC discs were fixed in a vertical direction along this region to enable this to be measured.

A substantial variation was observed in the vertical separation along the connection. The amount of separation was plotted against the location in the connection (see Figs. 5.18 to 5.23). Generally speaking, vertical separation between the two parts is very low at the end of the precast beam and is very high at the end of the in-situ nib. The reason can be attributed to the previously observed distribution of shear force within the connection in which a substantial amount of shear force is transferred from the end part of the precast beam to in-situ nib so that the load on the end of the in-situ nib is very low and therefore it can not deflect together with the precast beam, producing separation as expected. Comparing the vertical separation for the different tests produces the following points:

a) It can be seen from Fig. 5.18 that the vertical separation is zero for the first 100mm of the in-situ concrete nib while for the beam with eliminated dowel action (see Fig. 5.19) the whole length of the connection showed vertical separation with zero at the end of the precast beam.

b) In Fig. 5.20 (for the beam without stirrups in the nibs and also with minimum projecting bars at the end of precast beam) it can be seen that the end point of the precast beam has about 0.2mm separation. The same behaviour was observed in beam E30BC4 (see Fig. 5.21).

c) With the short connections (100mm embedment length), it is apparent from Figs. 5.22 and 5.23 that the two parts have been separated vertically through the whole length of the connection and these diagrams are in fact similar to those for long connections (300mm embedment length) in the 100mm length from the end of in-situ nib. This again confirms that for a long embedment length a considerable length of in-situ nib is redundant.

5.13.1 Significance of Vertical Separation

Vertical separations up to about 0.5mm and 1.9mm were observed for the service and failure loads respectively. In a reinforced or prestressed concrete beam cracks having widths equal to those figures can be quite harmful from the point of view of corrosion and freezing. Fortunately the gaps produced here as a result of separation do not give access to exposed reinforcement . For the water penetration and freezing effects, since the top surface of M-beam's bottom flange has a slope, penetrated water should be easily expelled .

5.14 Design Recommendations

If the new (unconventional) method of construction is employed for a

continuous bridge and the precast elements are M-beams or similar sections having top flanges, certain design recommendations can be suggested as a result of this part of the present investigation.

5.14.1 Design of Precast Beams for Shear

It was found that a small length of precast beam at its end (about 50mm) transfers about 50% of the shear force. Thus the shear force in the precast beam decreases very slowly within about 83% of the embedment length after which it sharply decreases along the final 17% . It is slightly conservative but convenient to design the precast section for the total shear force to be transferred (assuming that there is no relief of shear force within the connection).

5.14.2 Design of In-situ Nibs for Shear

It was observed before that in longer connections (300mm embedment lengths) the stirrups in the nibs had almost zero stresses, which was the reason for ommitting these stirrups in subsequent tests. This modification had no effect on the shear transfer capacity of these connections. It is also apparent that nibs carry relatively small shear forces along a large fraction (83%) of their length. The concrete nibs have large cross-sections in comparison with the precast beam hence their concrete shear resistance is enough to carry the shear with no need for stirrups. It is recommended here that minimum (nominal) stirrups be provided in the in-situ nibs to control possible cracking due to shrinkage and temperature change. It also helps to have a ductile rather than a plain concrete.

In connections with small embedment lengths (100mm) it is seen that the

high intensity of shear force acting on the nibs necessitated the need for a small amount of stirrups in the nib. Provision of these stirrups had an increasing effect of about 15% in the shear transfer capacity of the connection.

5.14.3 Embedment Length

Connections having embedment lengths of 300mm (900mm in prototype) behaved quite satisfactory even without stirrups in the nibs. In tests with reduced embedment (100mm) the connection was able to carry the whole shear resistance provided the in-situ nib was reinforced with stirrups. It is therefore suggested here that smaller embedment lengths can be used satisfactorily.

5.14.4 Distance of Connection from the Support

This matter is purely related to the applied bending moment at the connection. All the connections tested in this part were subject to the highest possible shear force allowed by the codes to cover any case which may arise in practice. With regard to the bending moment, it was seen that an increase in the bending moment (with the same shear force) had no significant effect on the shear capacity of the connection. In practice it is more desirable to have this type of connection well away from the support (to get the full benefit from this method of construction) for which the bending moment is likely to be small.

5.14.5 Projecting Bars from the Precast Beam

In the first test all the bars and prestressing strands projected from the

end of the precast beam into the in-situ concrete for about 1 metre. In the second test the same bars projected, but their dowelling effect was eliminated by sleeving with rubber. No significant change was observed and so it was decided to terminate all the bars and strands at the end of precast beam (except four bars at the bottom which are needed in practice to take possible positive bending moment due to creep, shrinkage and support settlement). This was done for all subsequent tests in this part of the investigation and it was seen that this feature did not affect the shear strength of the connection. In practice the bars either project from the end or they are screwed to previously fixed couplers. In the first method steel bars are exposed from the time of manufacture to the time of erection and may be subjected to corrosion, and also handling and transportation is difficult. The second method seems to be time consuming and expensive.

It is recommended here that there is no need to extend or couple all the bars in the precast beam (with top flanges) and only for the possibility of positive bending moment at the connection should the required bars be extended or coupled.

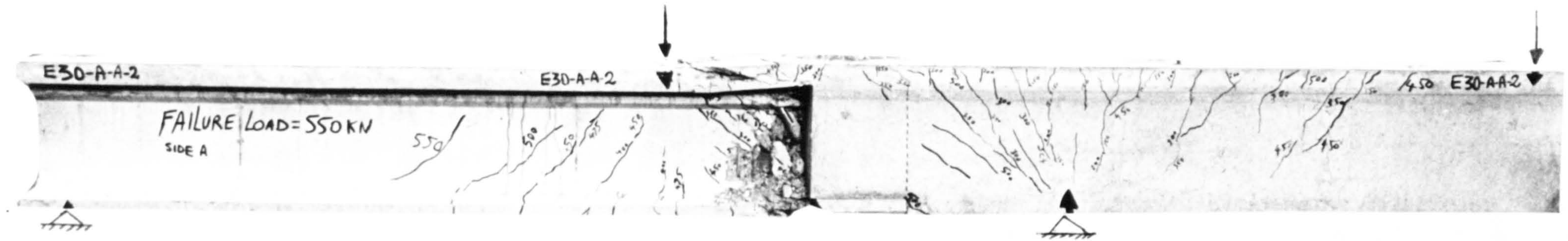

Plate 5.1 Longitudinal Elevation of Beam E30AA2 After Failure

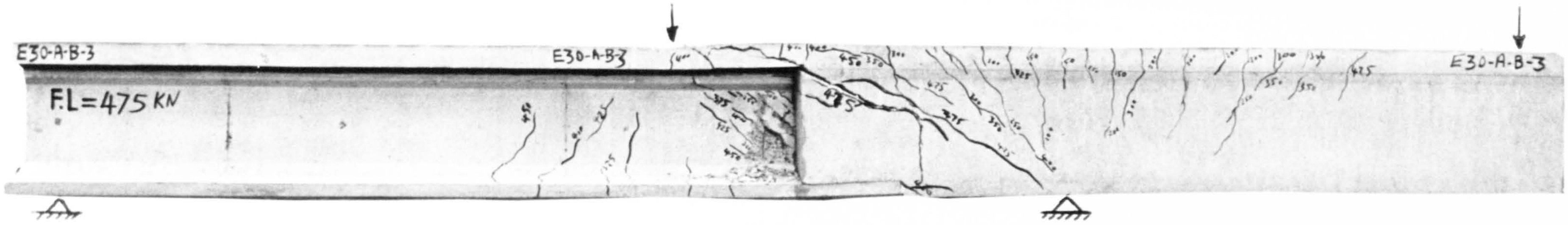

Plate 5.2 Longitudinal Elevation of Beam E30AB3 After Failure

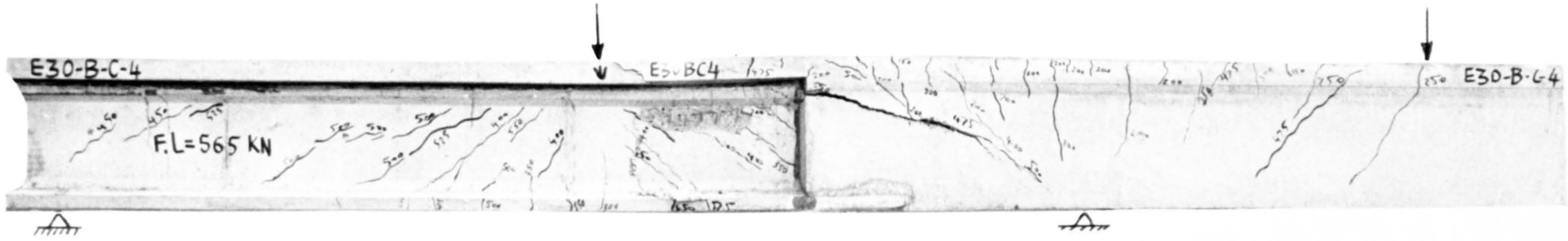

Plate 5.3 Longitudinal Elevation of Beam E30BC4 After Failure

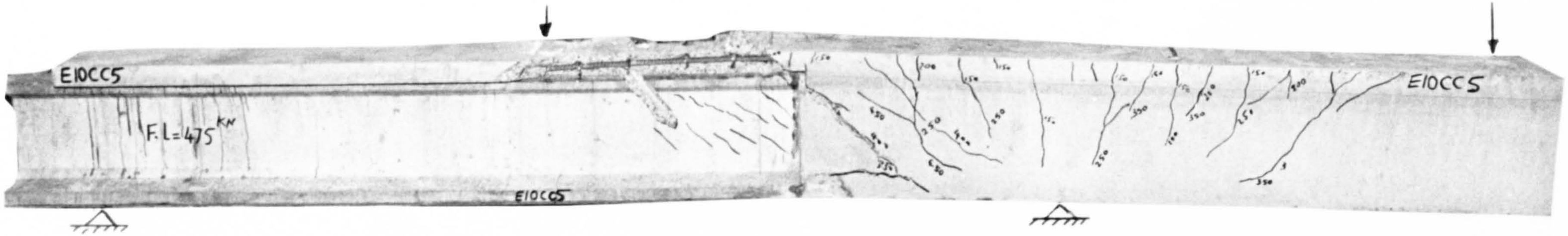

Plate 5.4 Longitudinal Elevation of Beam E10CC5 After Failure

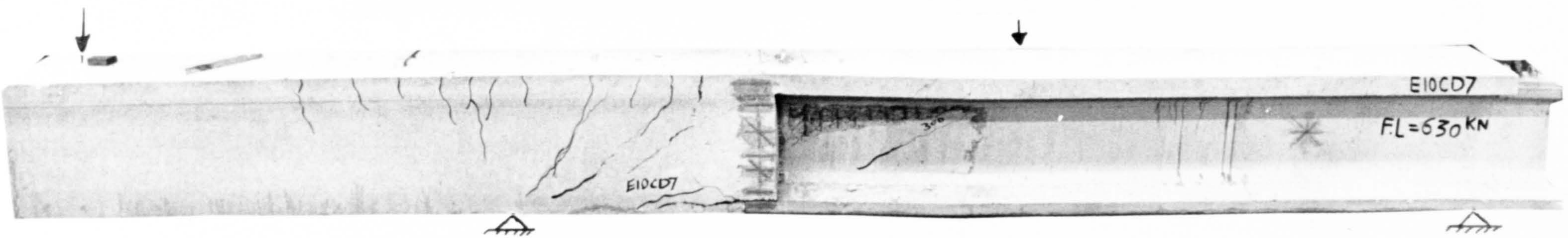

Plate 5.5 Longitudinal Elevation of Beam E10CD7 After Failure

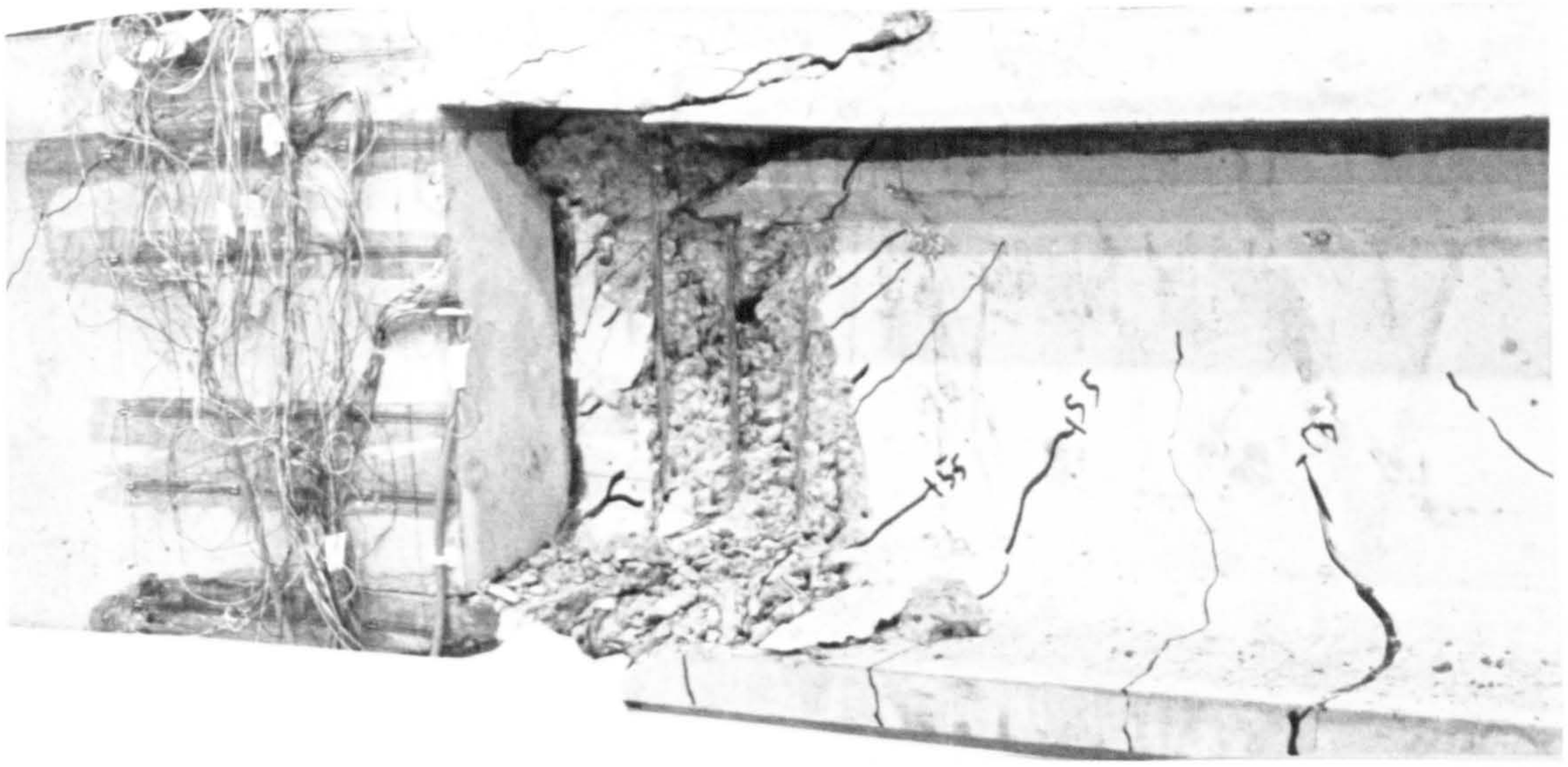

Plate 5.6 Test Similar to Prototype (With Nib Stirrups &All Bars Projected)
Condition in The Connection After Failure

Plate 5.7 Elimination of Dowel action by Sleeving the Bars(With Nib Stirrups)
Condition in The Connection After Failure

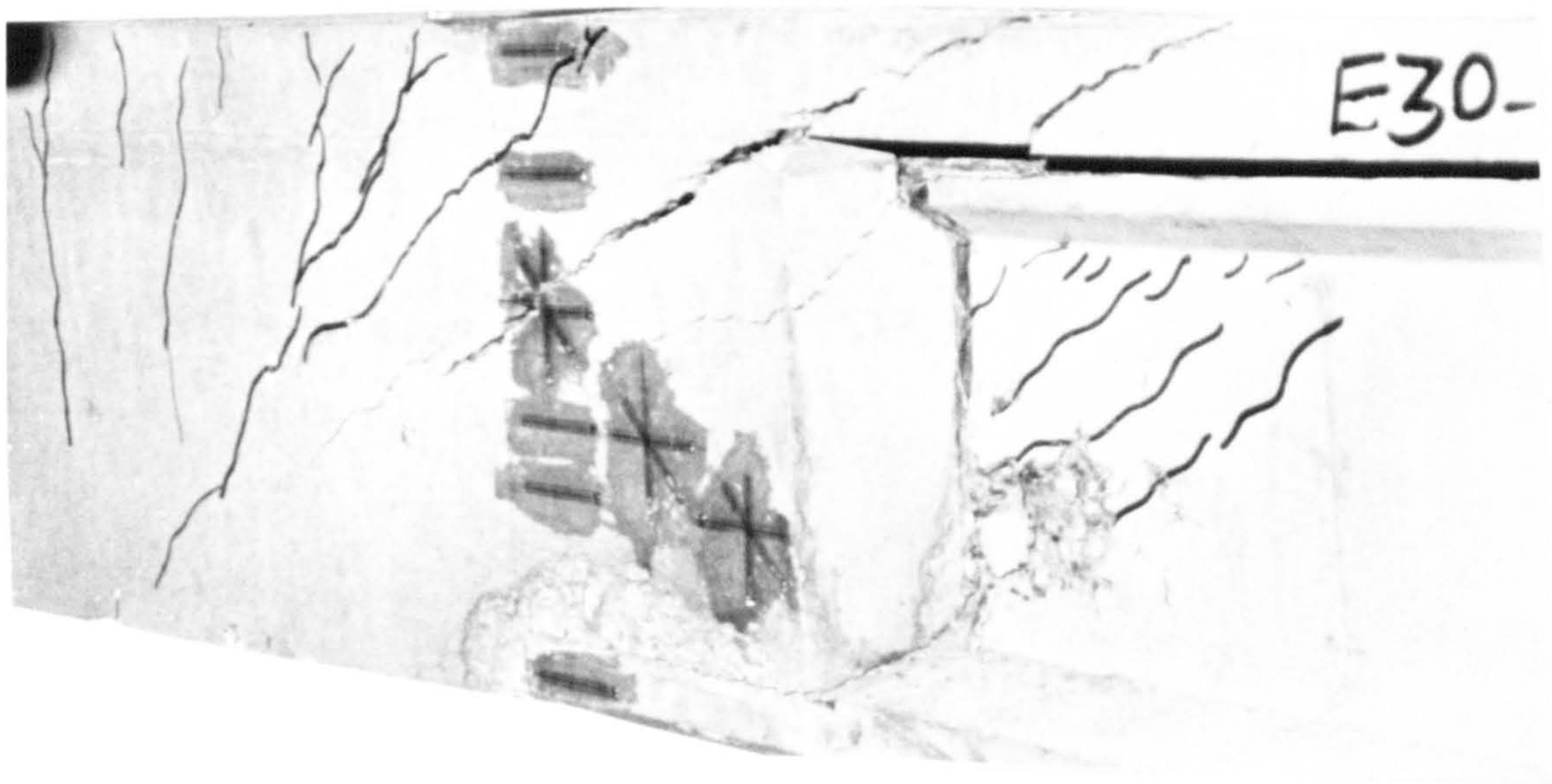

Plate 5.8 Elimination of Stirrups in the Nib
Condition in The Connection After Failure

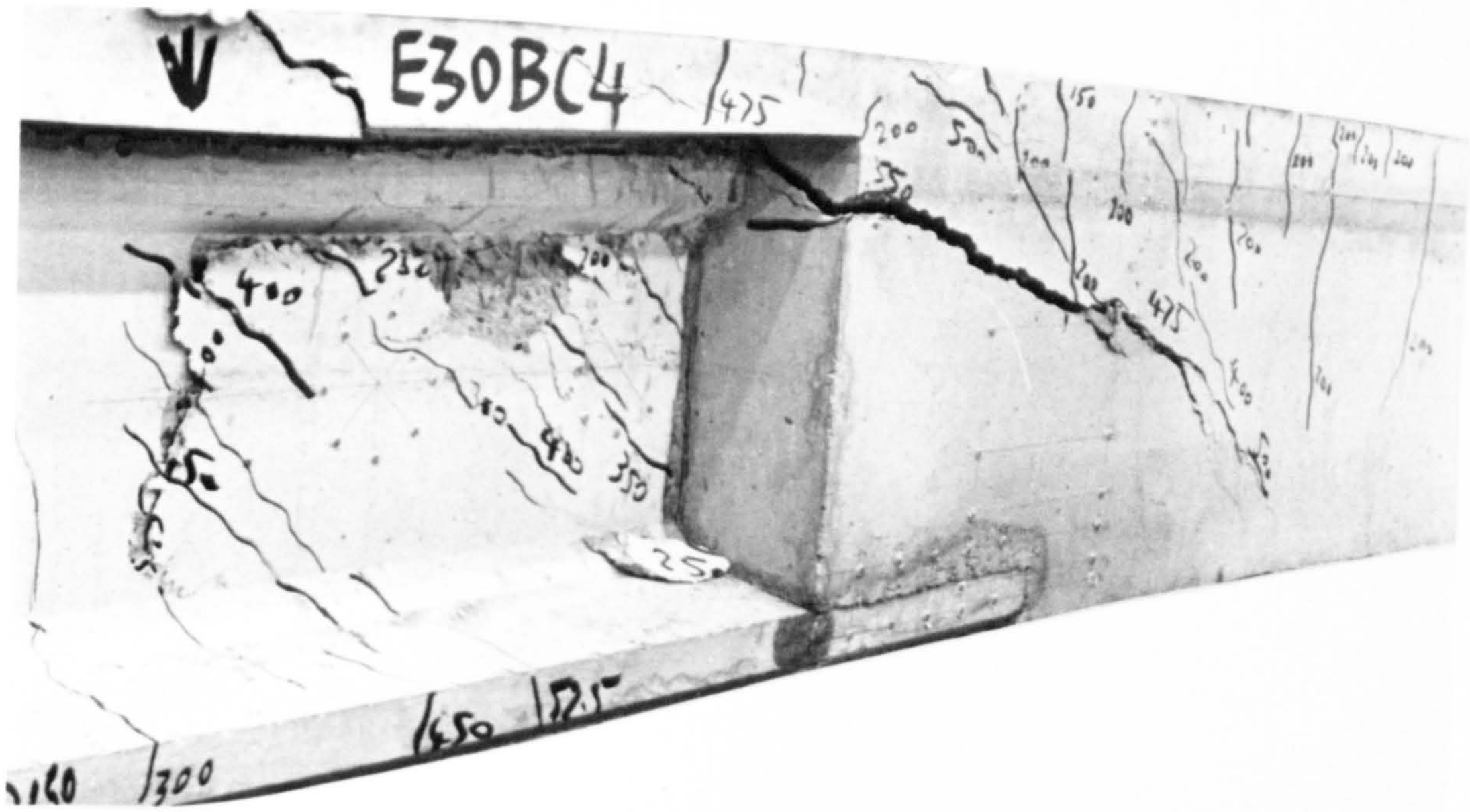

Plate 5.9 Increased Bending Moment at the Connection (without Nib Stirr.)
Condition in The Connection After Failure

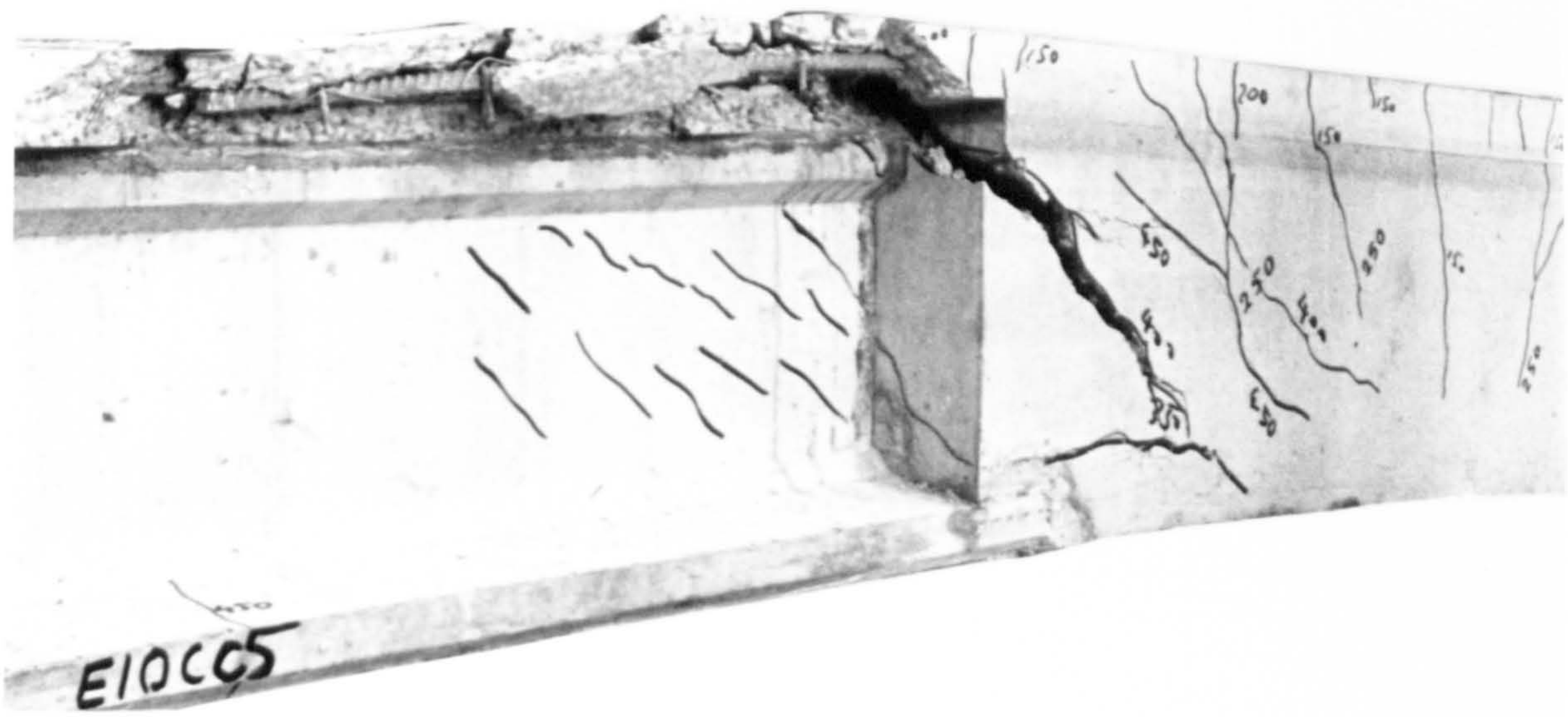

Plate 5.10 100mm Embedment Length (without Nib Stirrups)
Failure of the Connection with Large Rotation

Plate 5.11 100mm Embedment Length (with Nib Stirrups)
Condition in The Connection After Failure

Table 5.1 Beam Details, Calculated and Experimental Results
(For the connections with Top Flanges in the Beam)

	E30AA1	E30AA2	E30AB3	E30BC4	E10CC5	E10CD7
Connection length (mm)	300 mm	300mm	300mm	300mm	100mm	100mm
M-beam's Stirrups in the Conn.	T6@50	T6@50	T6@85	T6@85	T6@50	T6@50
Nib's Stirrups in the Connection	T6@50	T6@50	None	None	None	T6@50
Total Stirrup Ratio in the Conn.	0.7%	0.7%	0.2%	0.2%	0.2%	0.2%
Stirr. Ratio in the Insitu Beam Remote from the Connection	0.35%	0.35%	0.2%	0.2%	0.2%	0.2%
No. of Projecting Bars	13 bars	13 bars (sleeved)	4 bars (bottom)	4 bars (bottom)	4 bars (bottom)	4 bars (bottom)
Bending Moment	Moderate	Moderate	Moderate	High	Moderate	Moderate
Cal. Shear Resist. of M-beam (kN)	315	315	315	315	315	315
Cal.Shear Resist. of Insitu Beam Remote from the Conn	389	368	262	262	265	265
Cal. Shear Resist. of Conn. if assume Monolithic (kN)	630	608	262	262	265	465
Observed Shear Resist. (kN)	312	309	267	255	224	297
Type & Position of the Failure	Web Crush in the M-Beam	WebCrush in the M-Beam	Inclined Tension in the M-beam	Inclined Tension in the In-situ beam	Inclined Tension in the In-situ Beam +separation	Web crushing in the M-beam

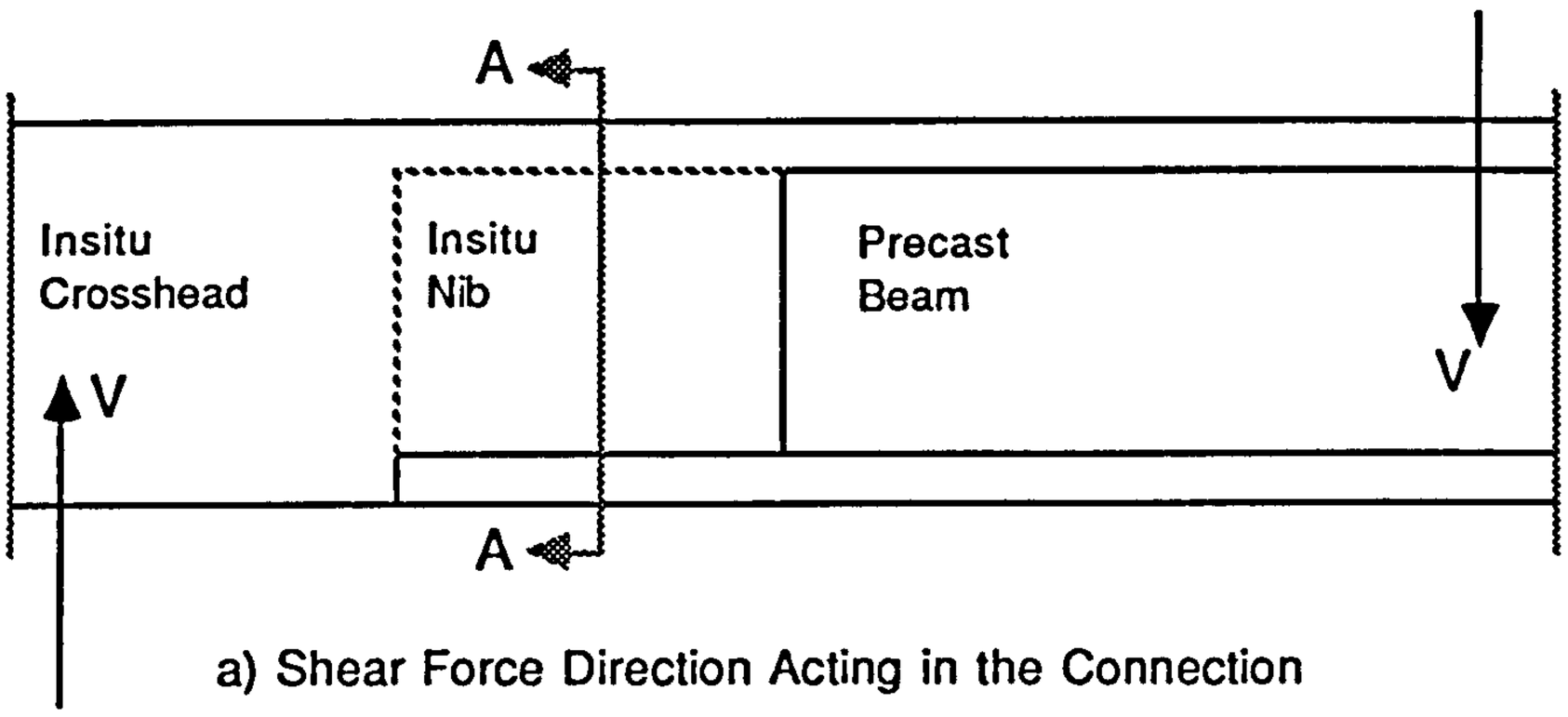

a) Shear Force Direction Acting in the Connection

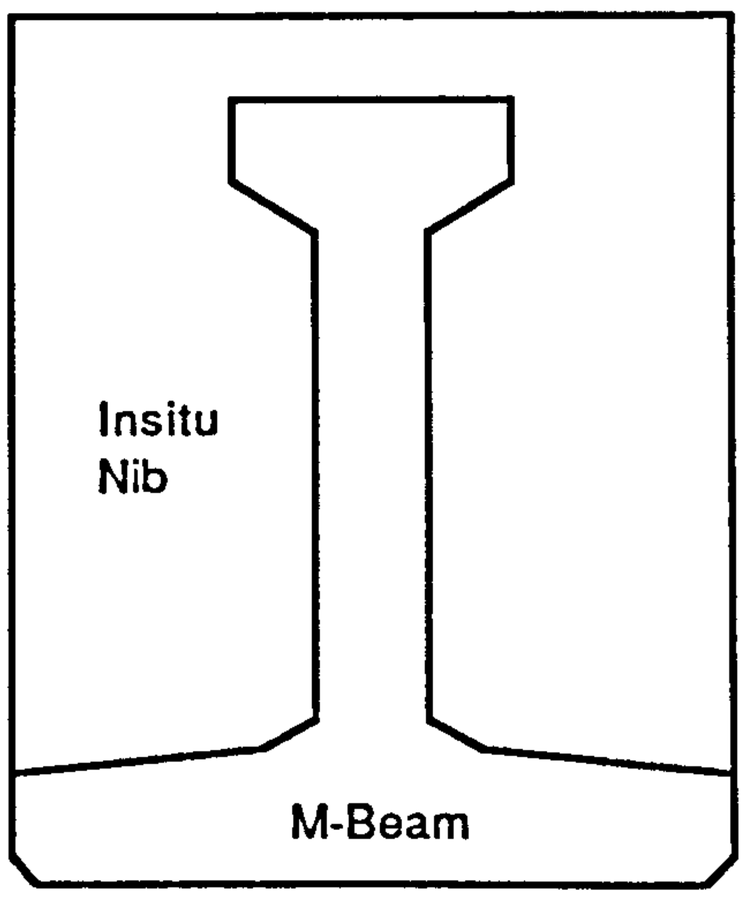

b) Section A:A

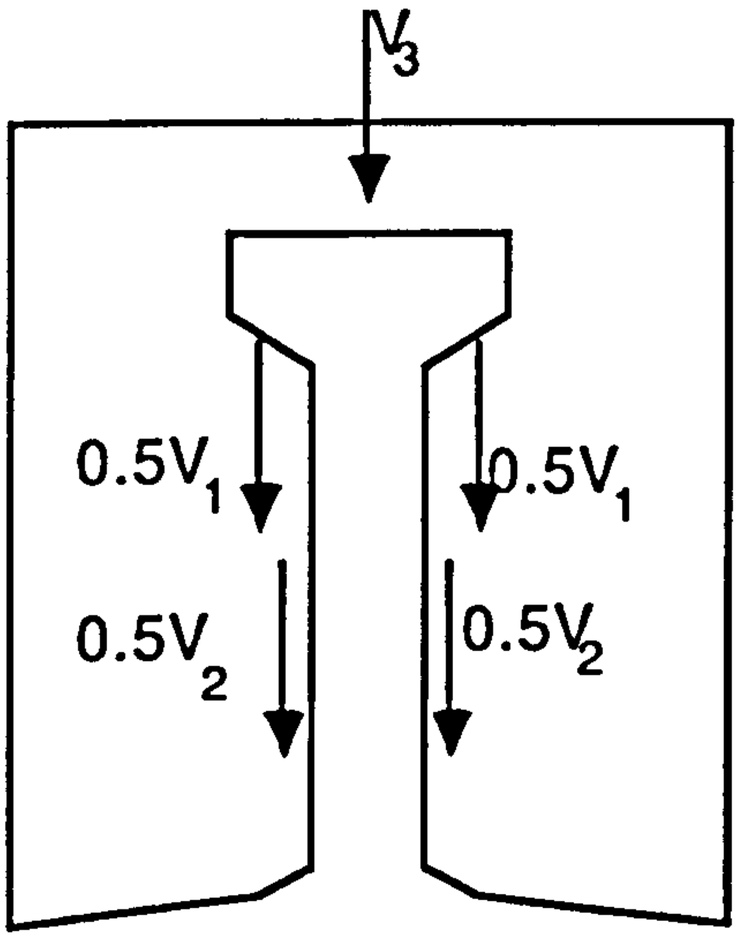

C) Free Body Diagram for Insitu Nibs Showing Shear Force Components

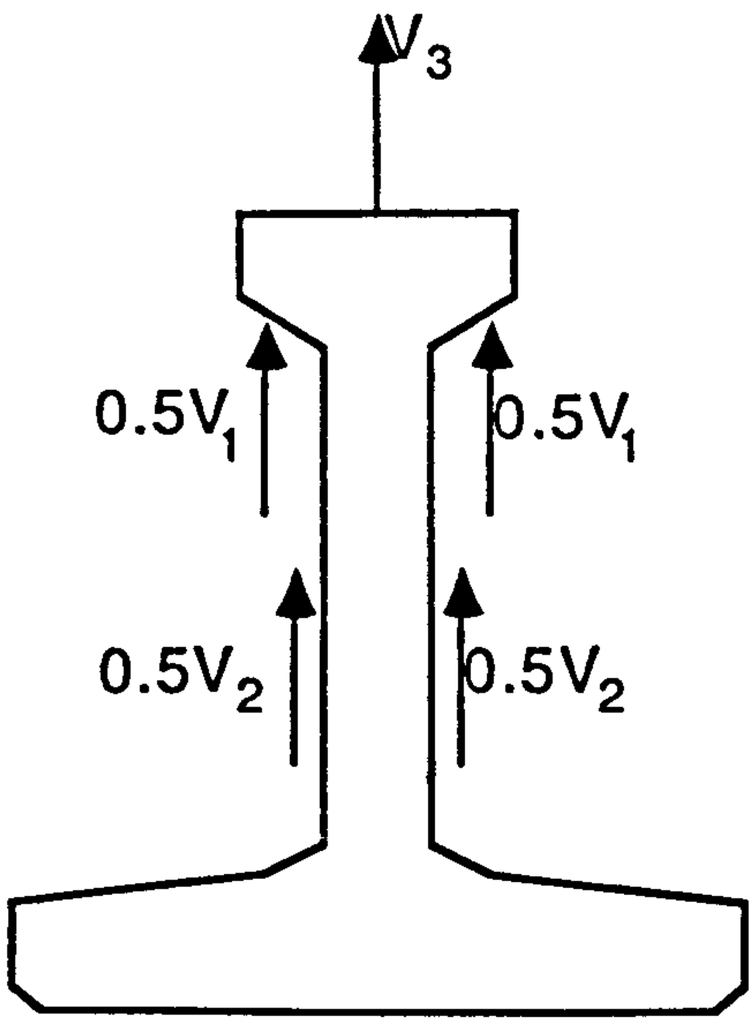

d) Free Body Diagram for M-Beam Showing Shear Force Components

FIG. 5.1 Freebody Diagram for the Connection

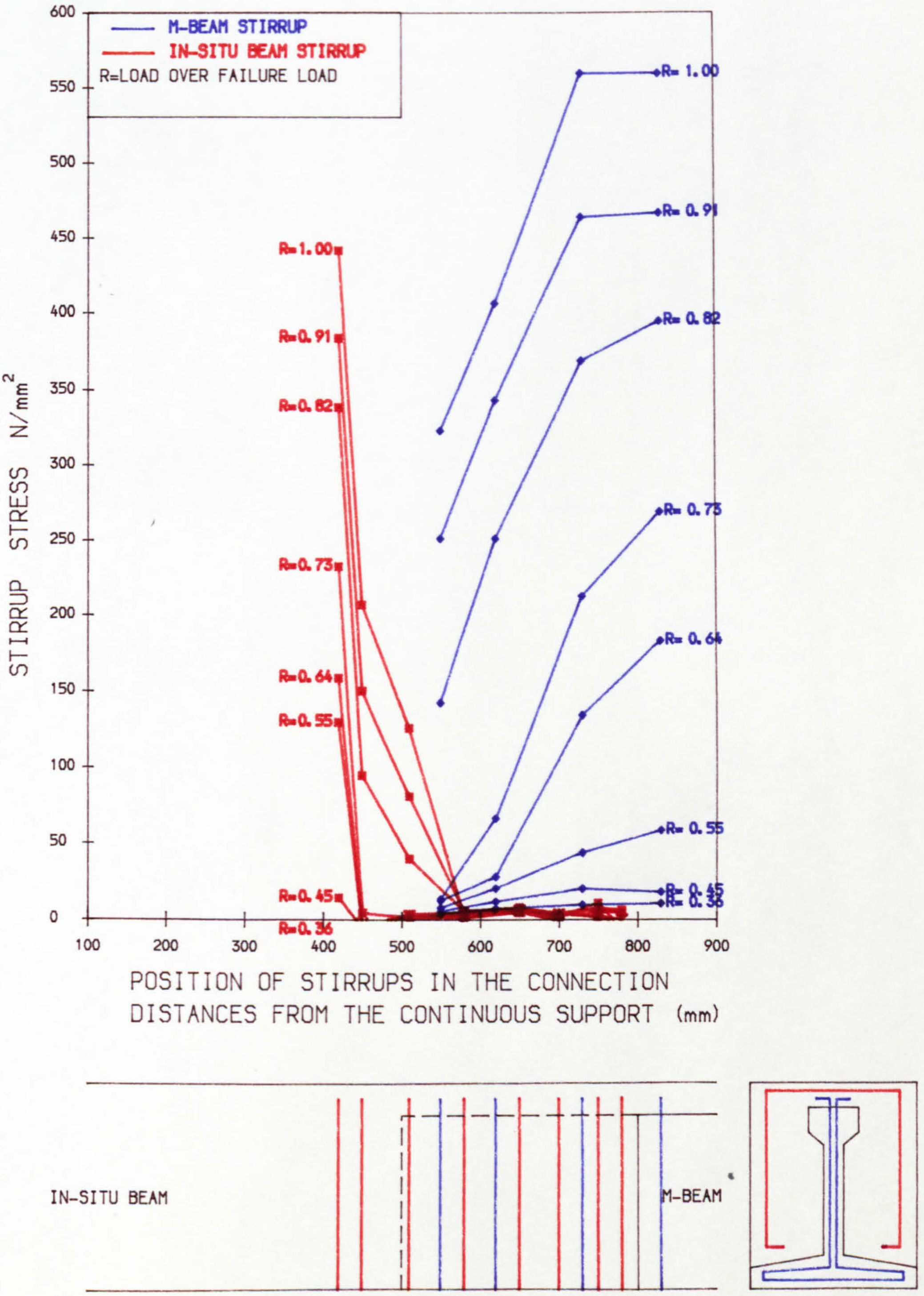

FIG 5.2 STRESS IN THE SHEAR REINFORCEMENT OF THE CONNECTION IN BEAM E30AA-1

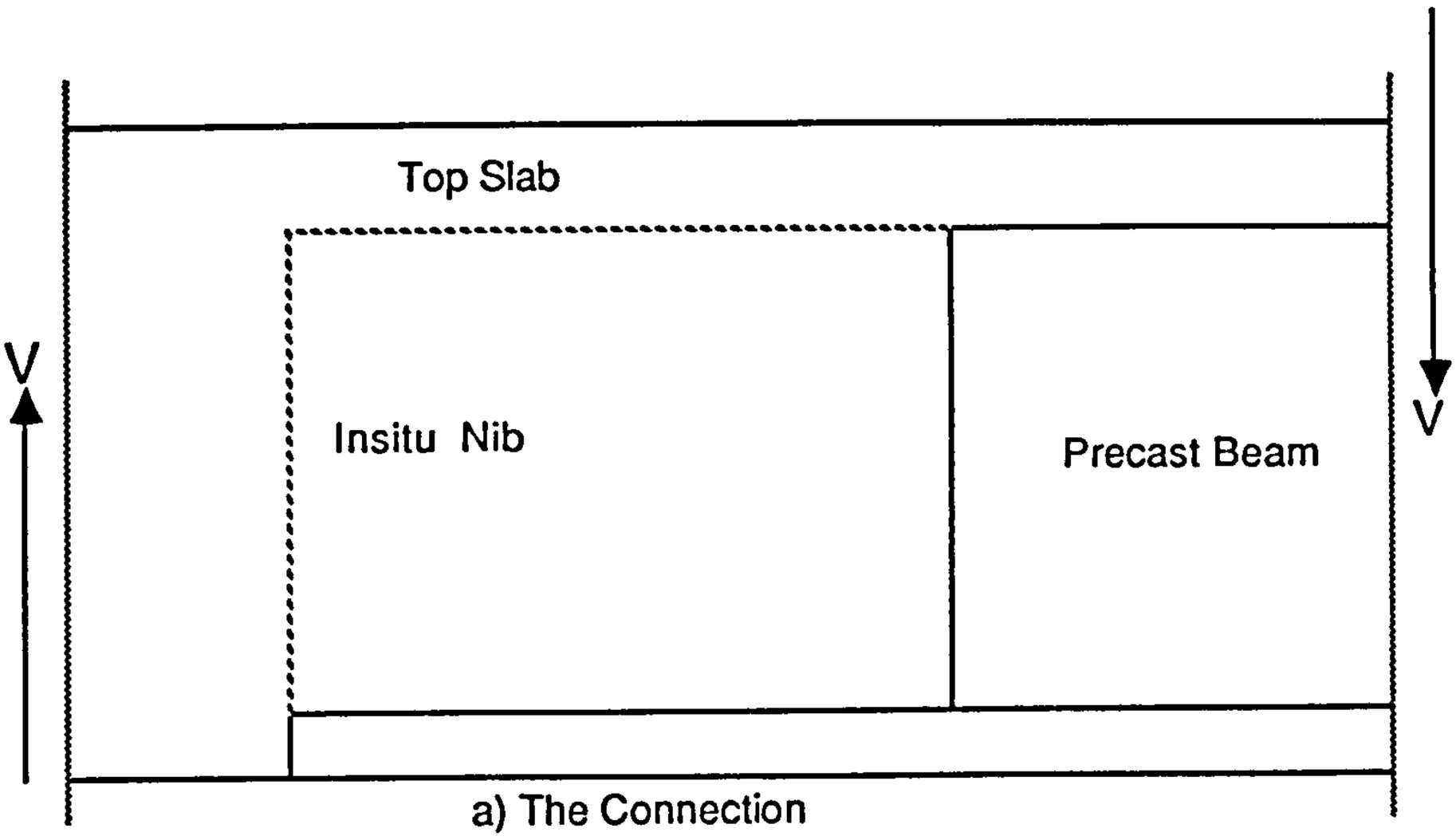

a) The Connection

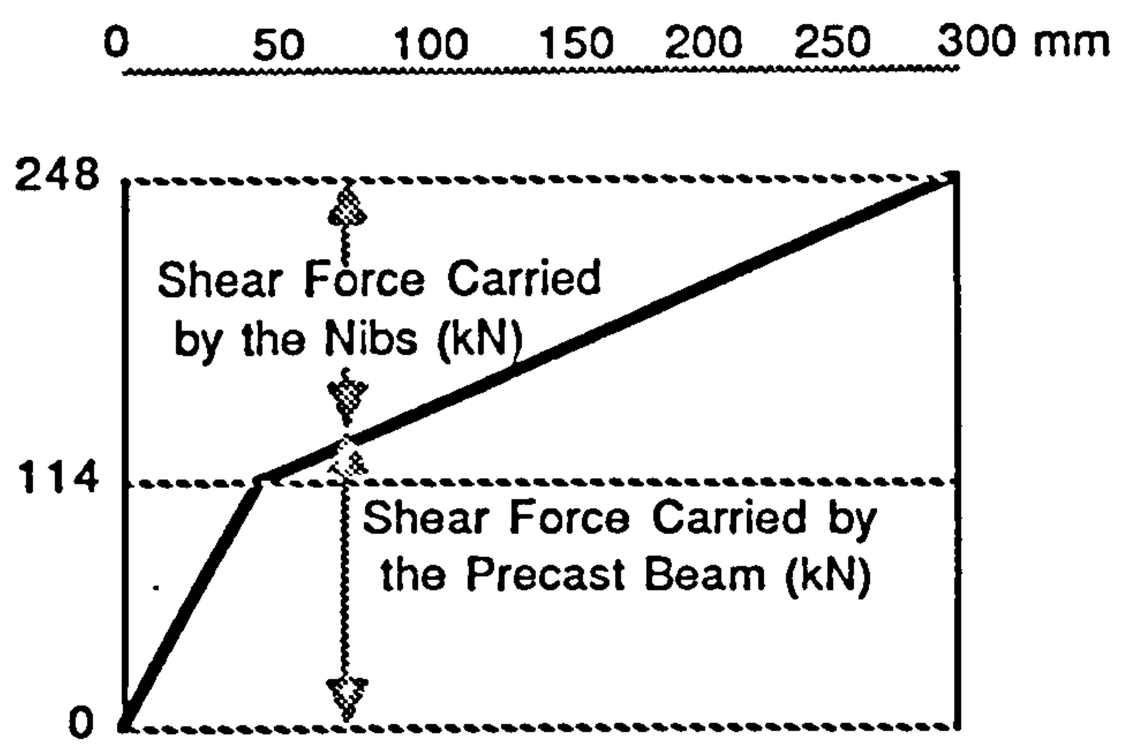

b) Shear Force Diagram Along the Embedment Length

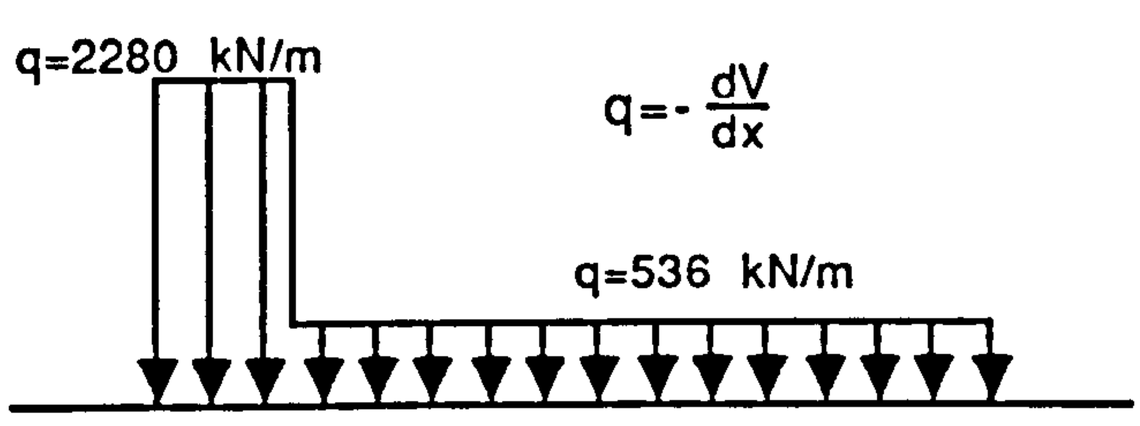

c) Equivalent Load Distribution Between Two Parts

FIG. 5.3 Load Distribution Between Two Parts in Beam E30AA1 at 70% of the Failure Load

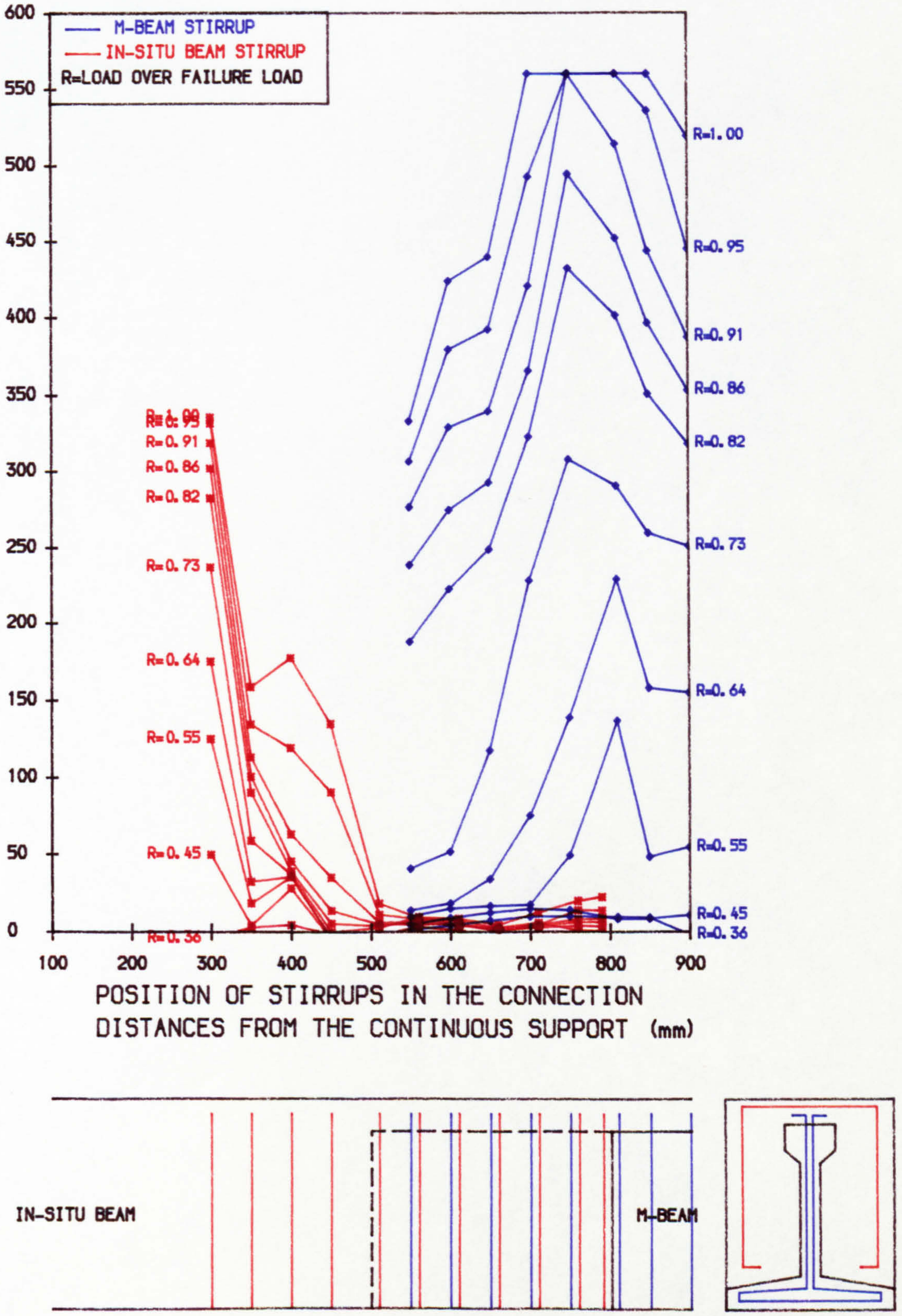

FIG. 5.4 STRESS IN THE SHEAR REINFORCEMENT OF THE CONNECTION IN BEAM E30AA-2

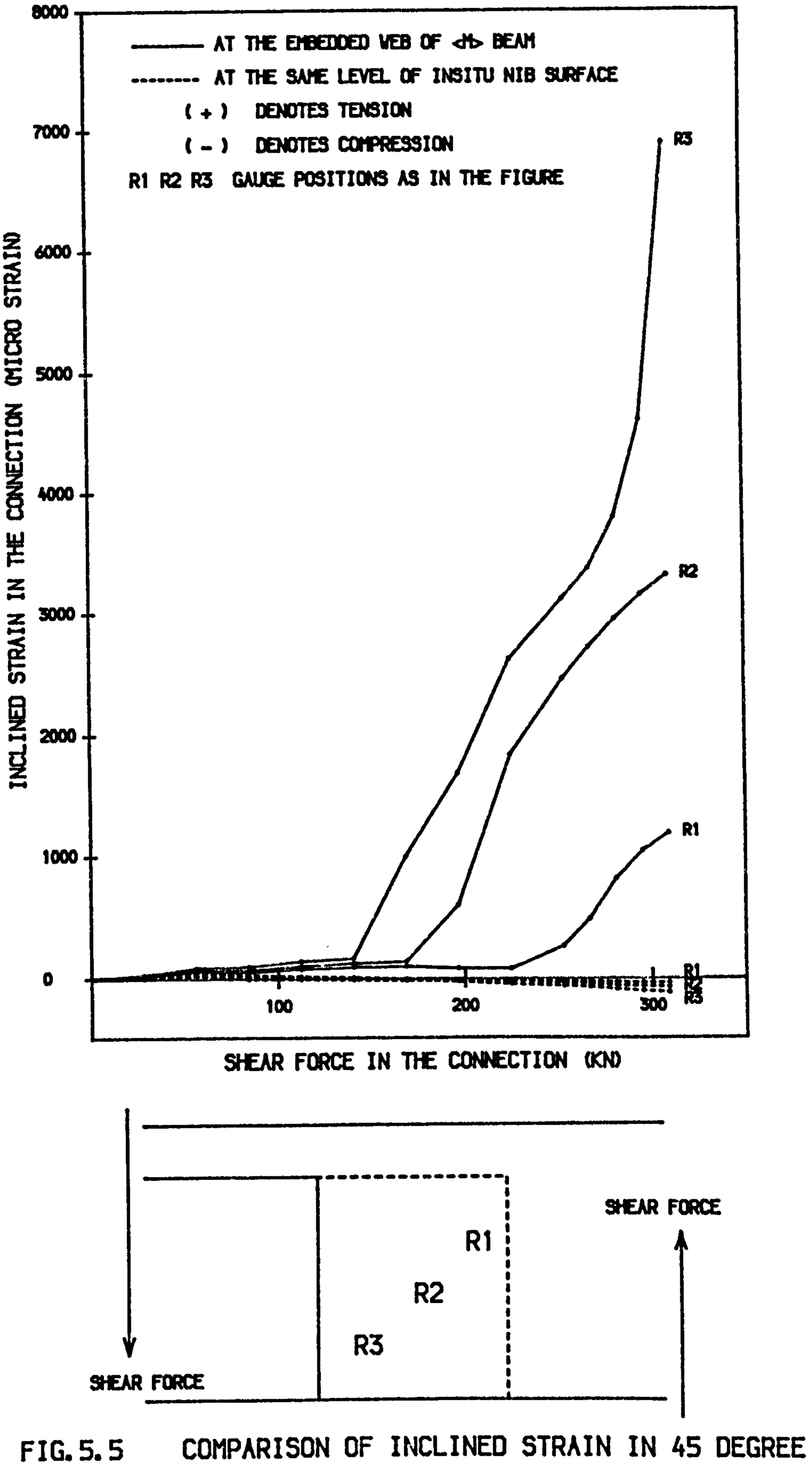

FIG. 5.5 COMPARISON OF INCLINED STRAIN IN 45 DEGREE DIRECTION IN EACH COMPONENT

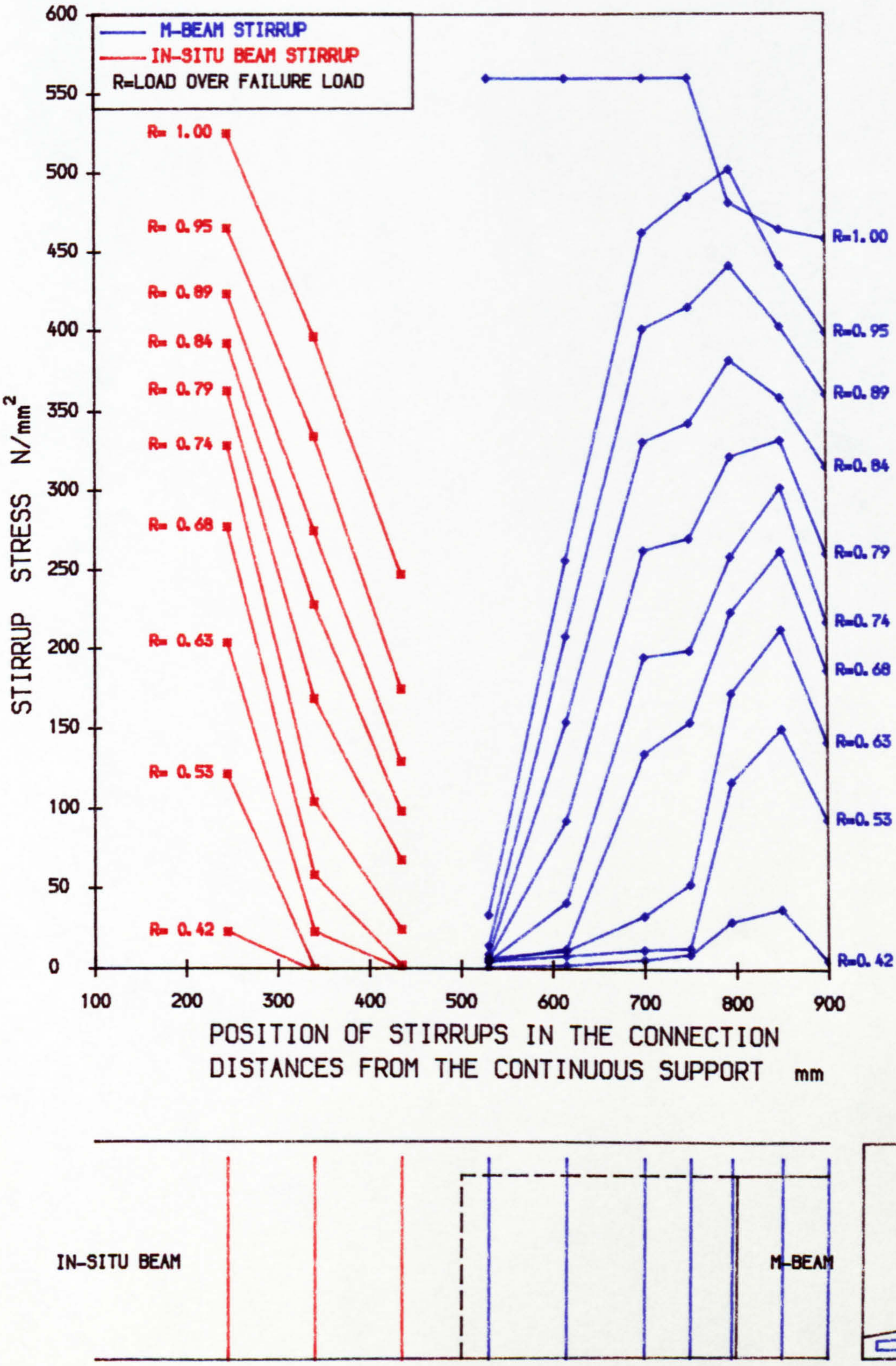

FIG. 5.6 STRESS IN THE SHEAR REINFORCEMENT OF THE CONNECTION BEAM E30AB-3

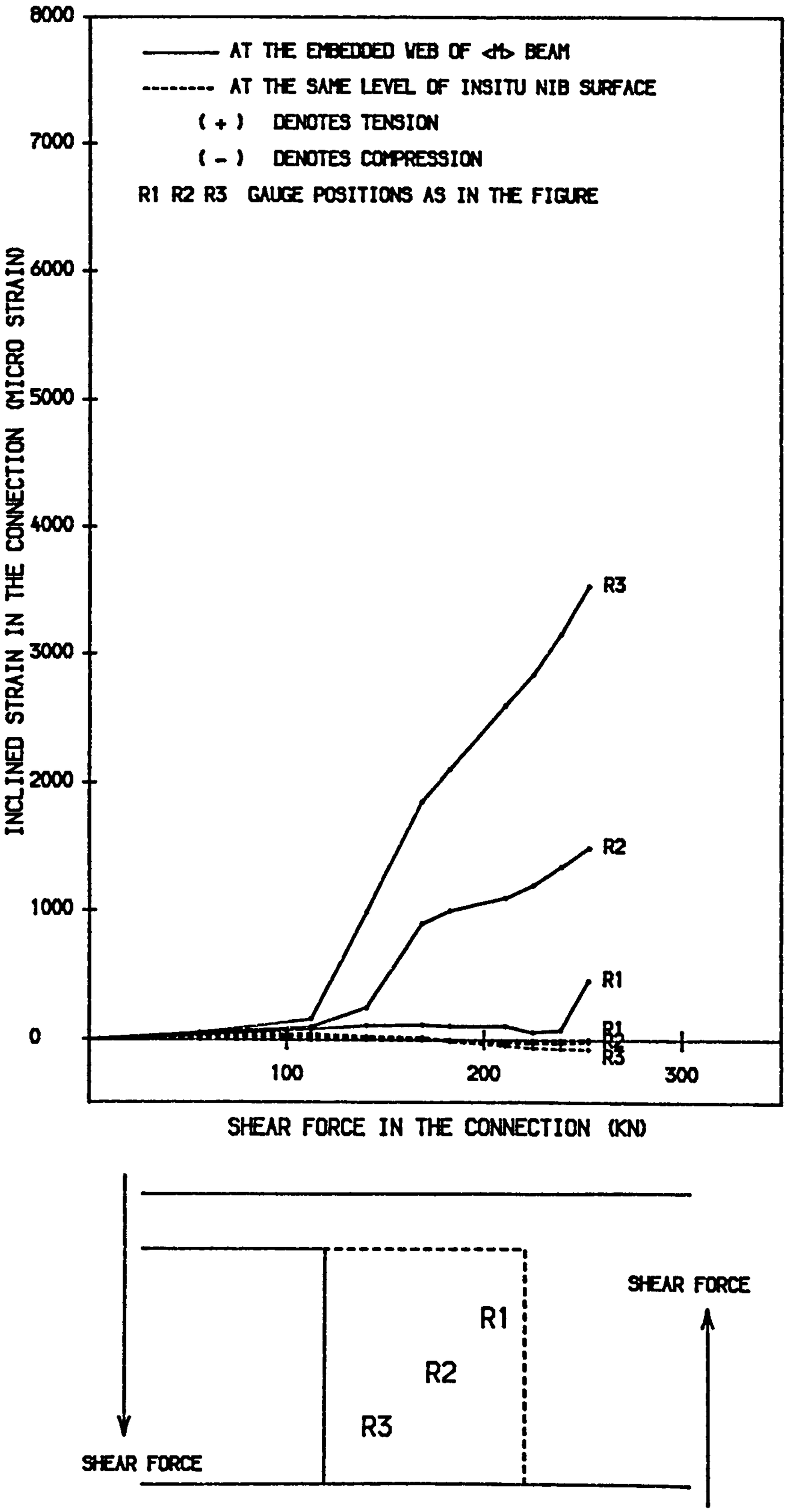

FIG. 5.7 COMPARISON OF INCLINED STRAIN IN 45 DEGREE DIRECTION IN EACH COMPONENT

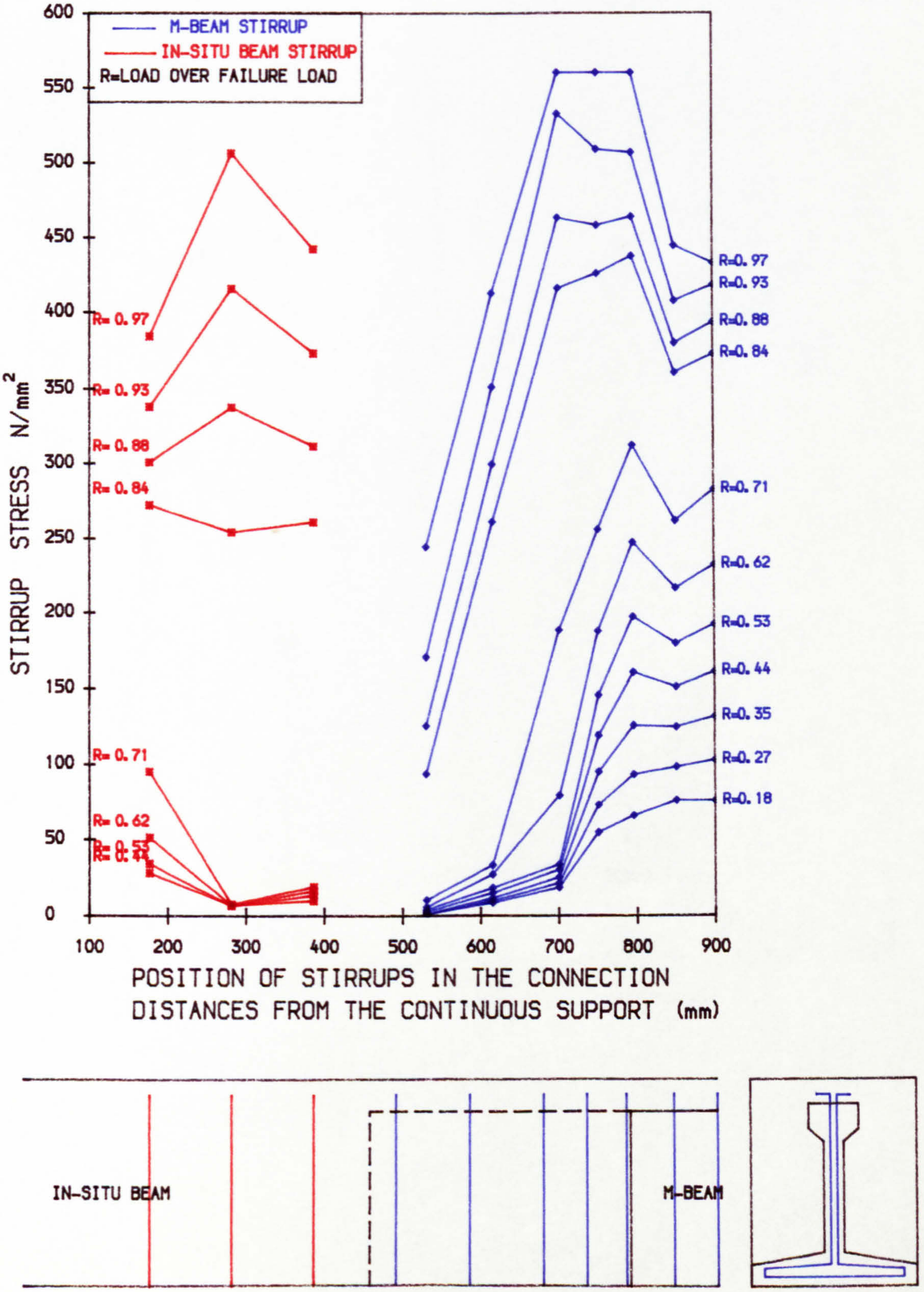

FIG. 5.8 STRESS IN THE SHEAR REINFORCEMENT OF THE CONNECTION IN BEAM E30BC-4

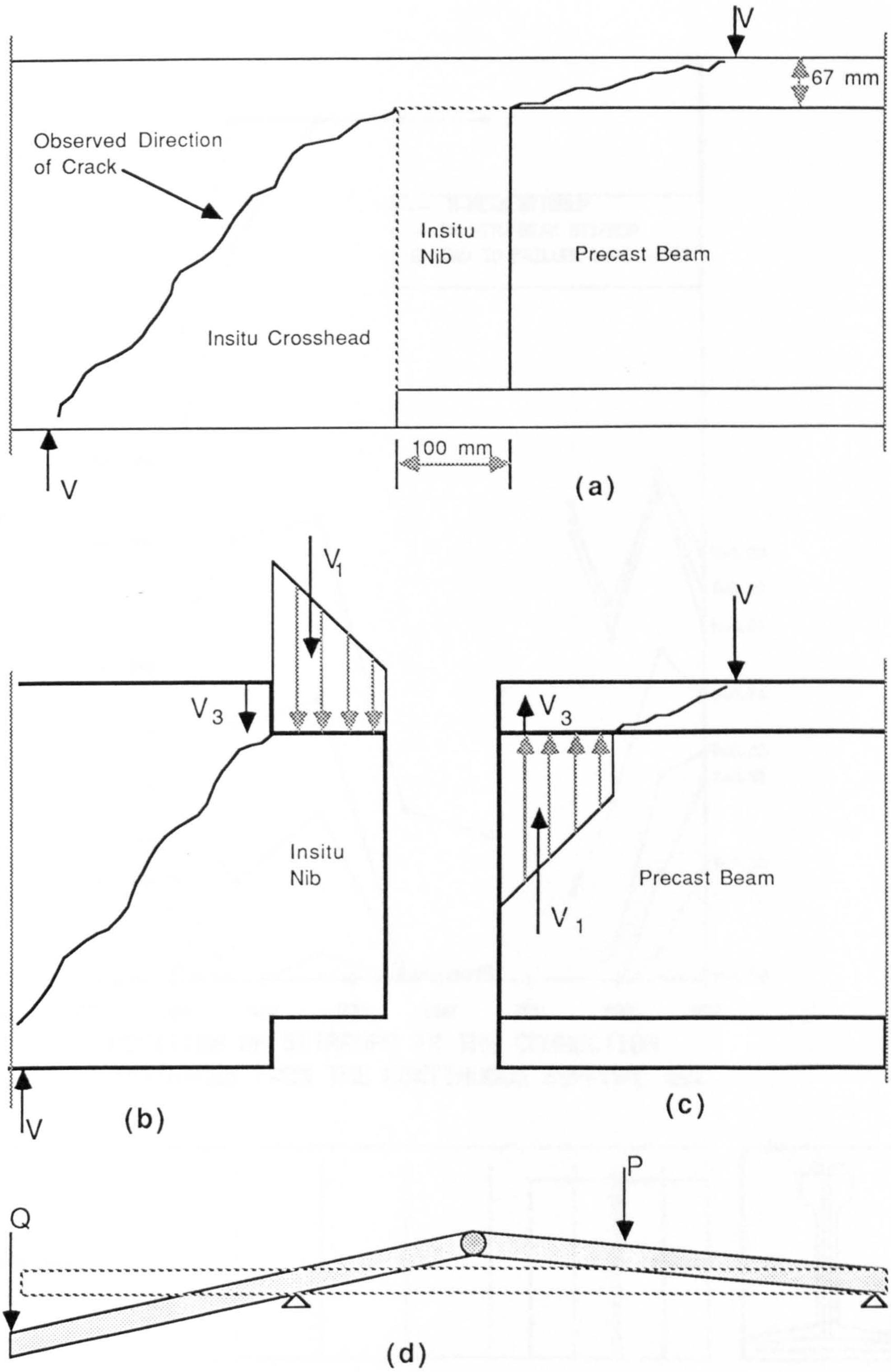

FIG. 5.9 a) 100mm Connection and Cracks at Failure
b,c) Freebody Diagram and Forces
d) Rotation at the Connection

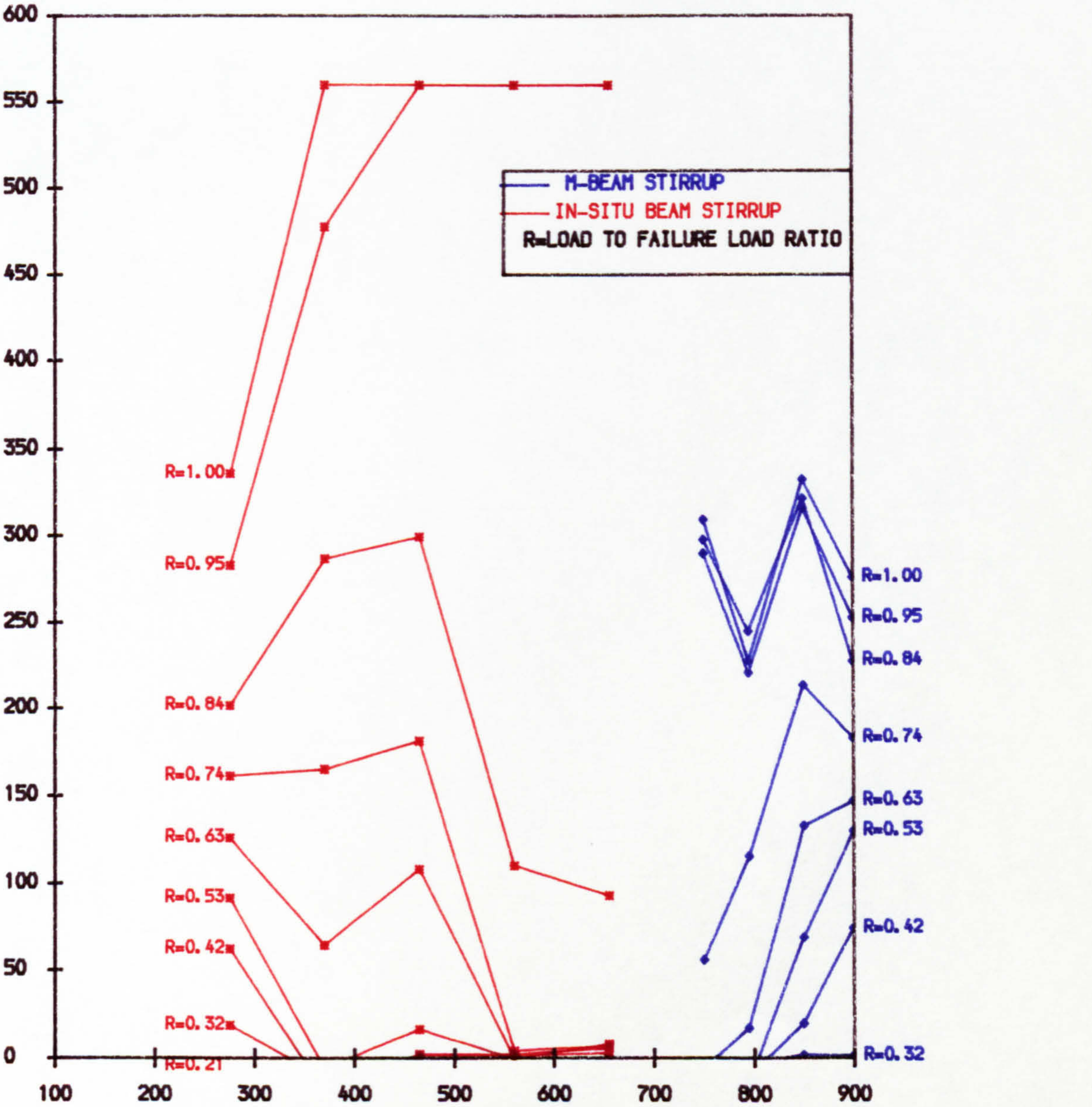

FIG. 5.10 STRESS IN THE SHEAR REINFORCEMENT OF THE CONNECTION IN BEAM E10CC-5

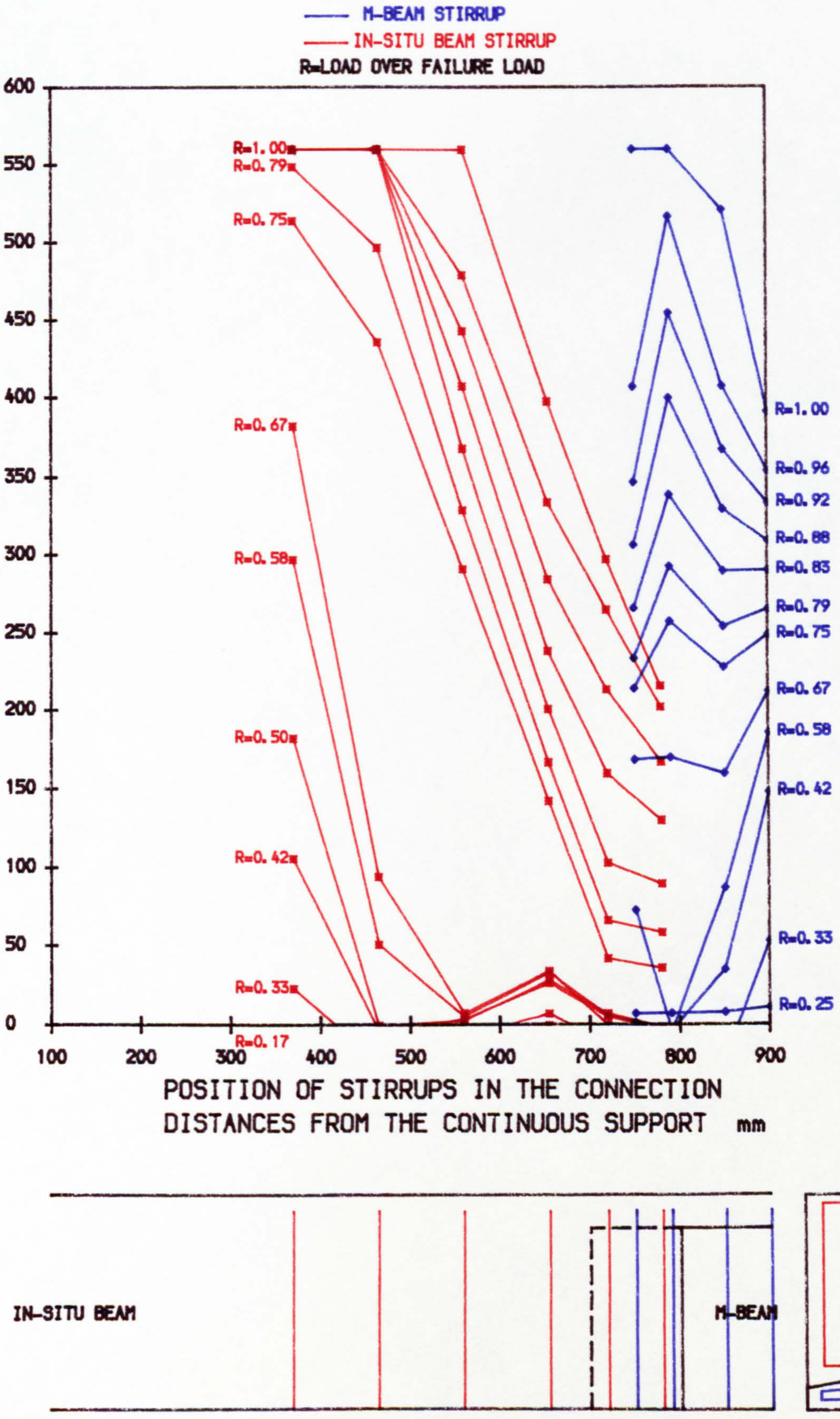

FIG. 5.11 STRESS IN THE SHEAR REINFORCEMENT OF THE CONNECTION IN BEAM E10CD-7

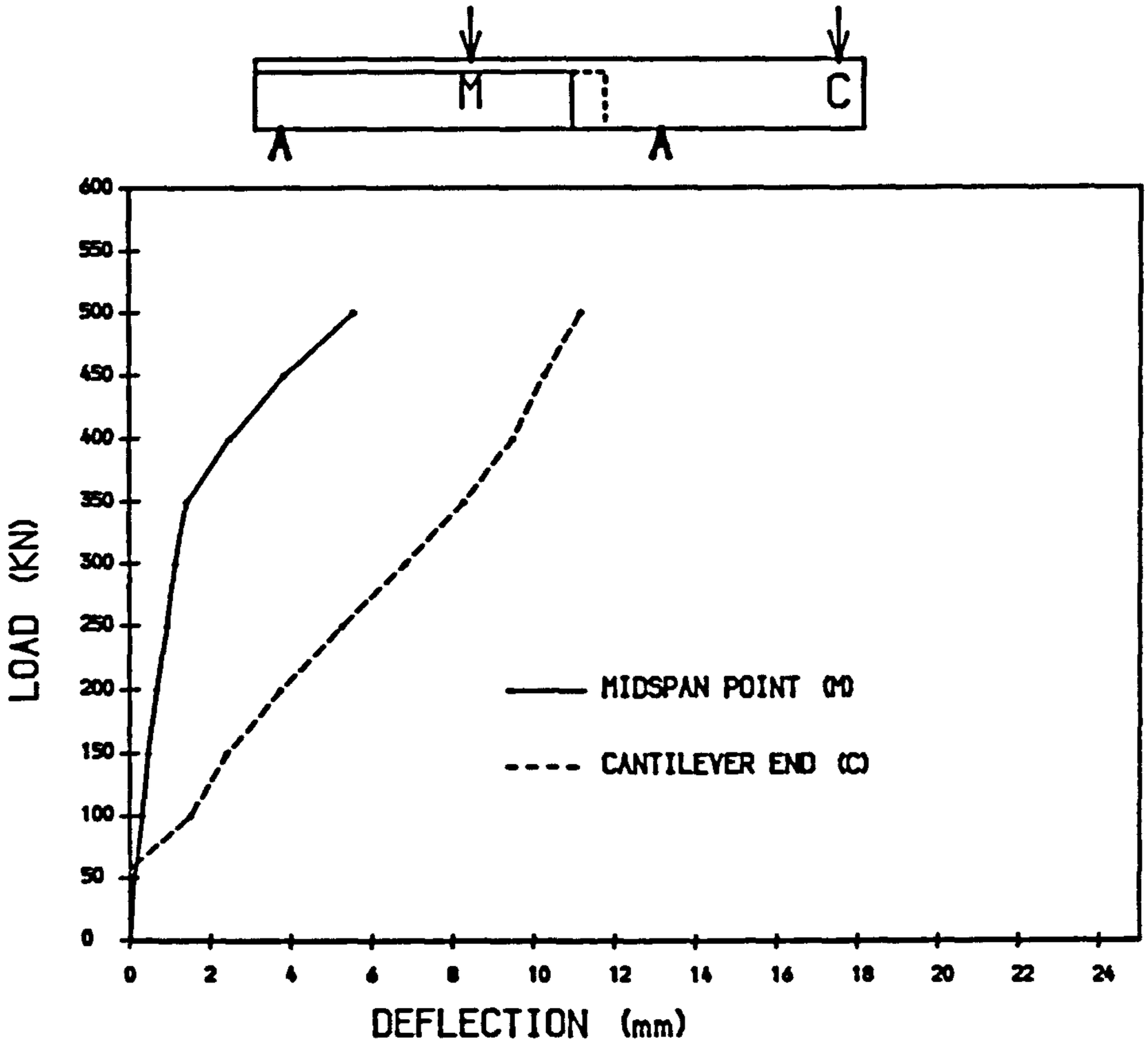

FIG. 5. 12 LOAD-DEFLECTION CURVE BEAM E30AA-1

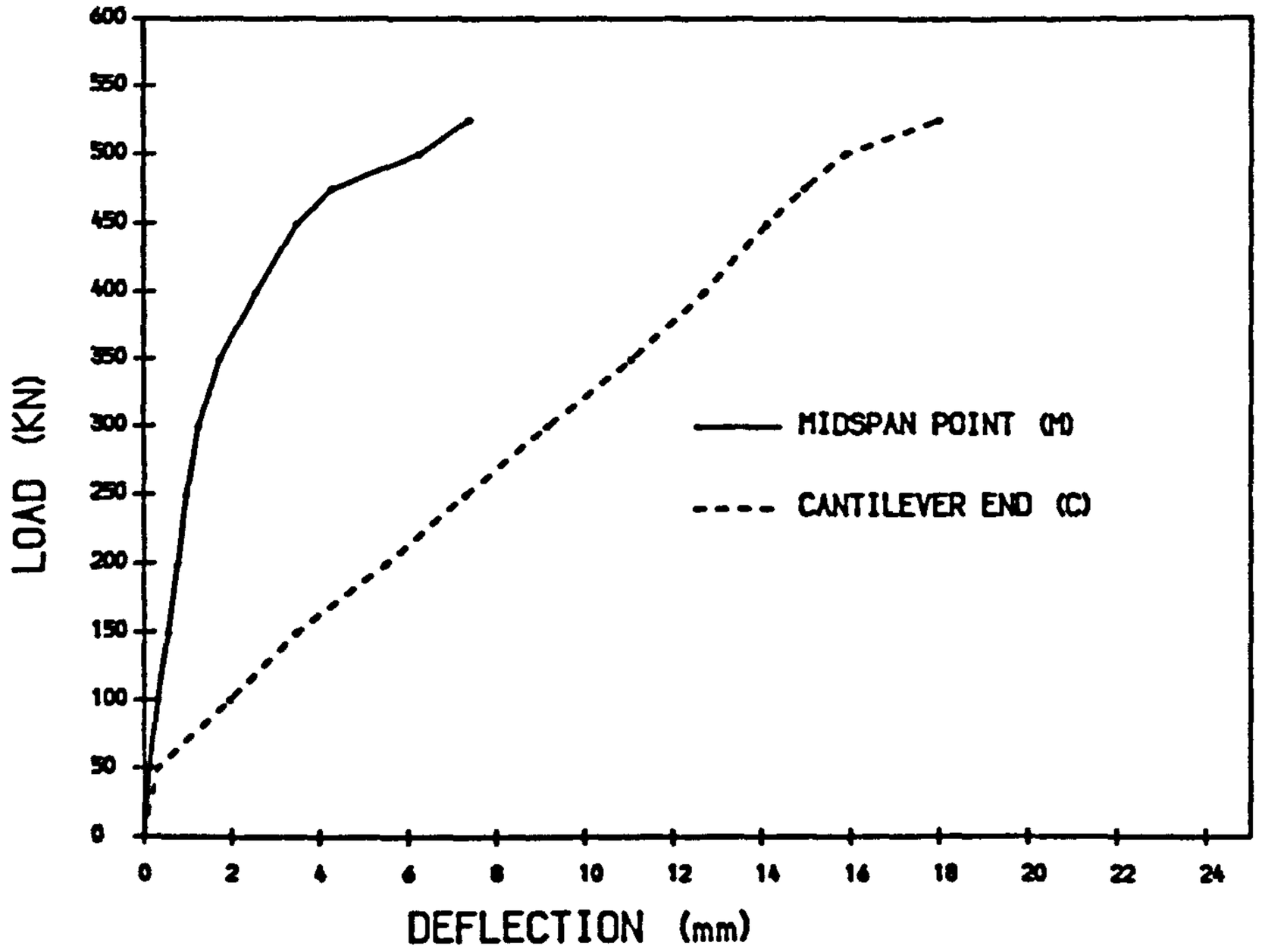

FIG. 5. 13 LOAD-DEFLECTION CURVE BEAM E30AA-2

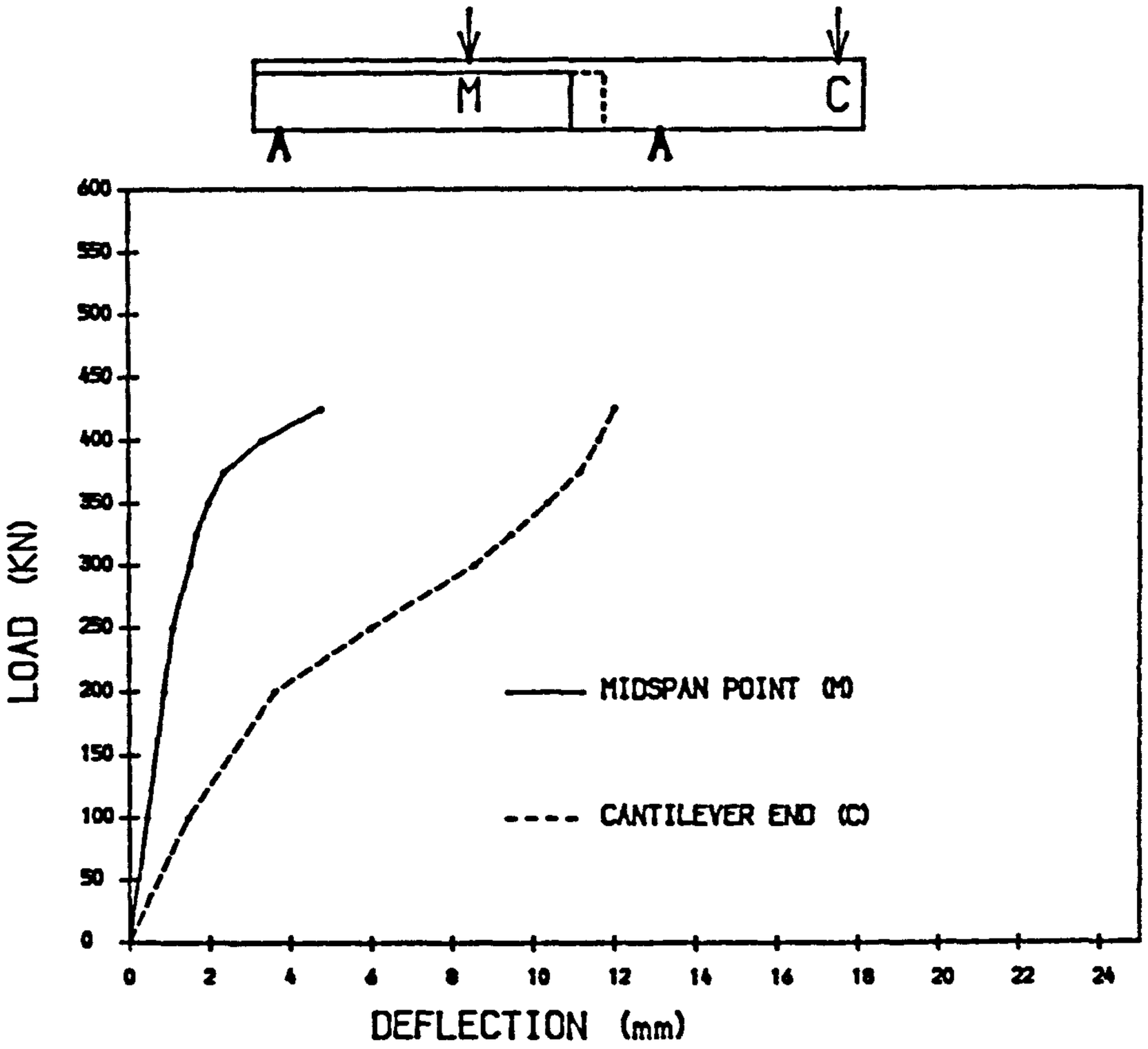

FIG. 5. 14 LOAD-DEFLECTION CURVE BEAM E30AB-3

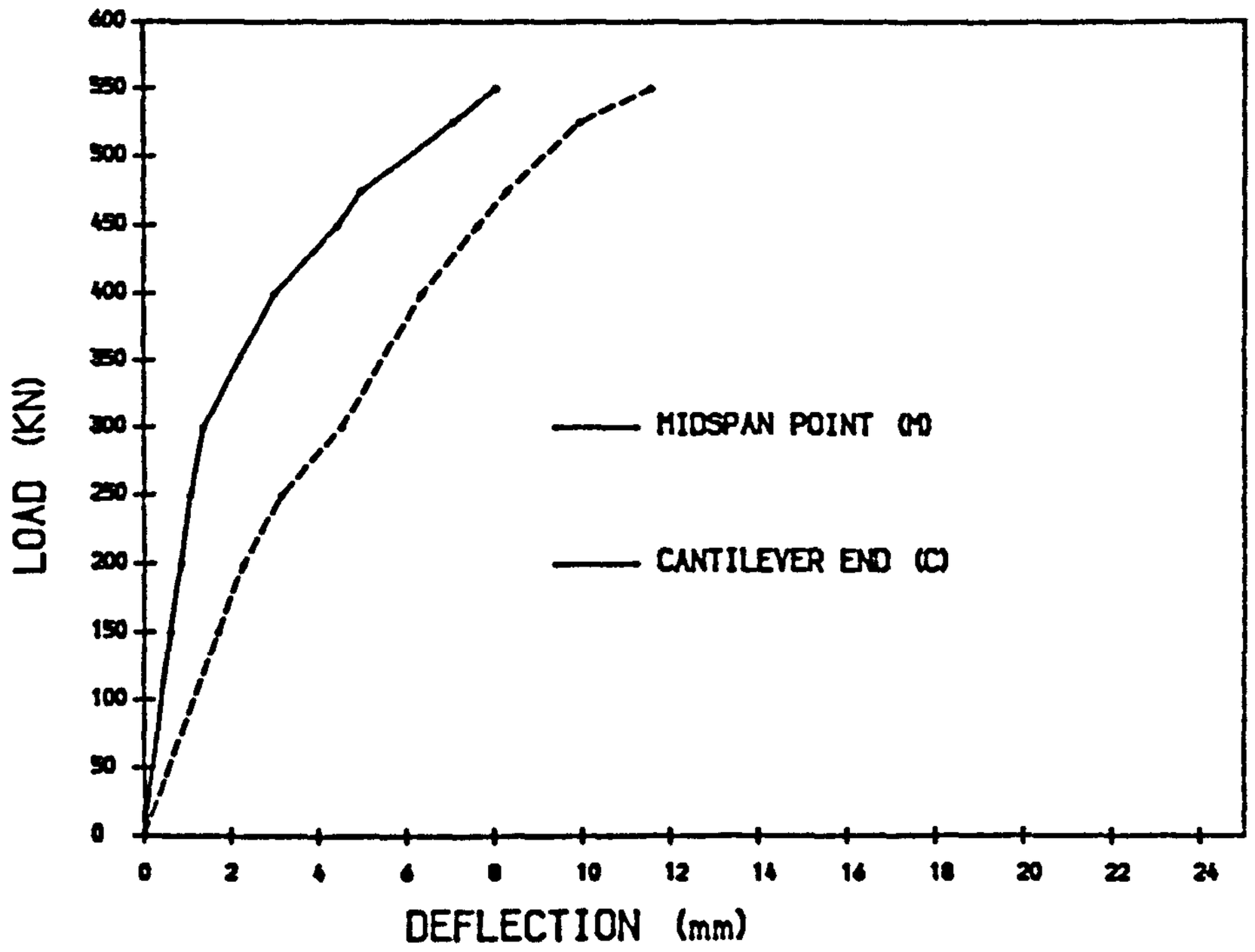

FIG. 5. 15 LOAD-DEFLECTION CURVE BEAM E30BC-4

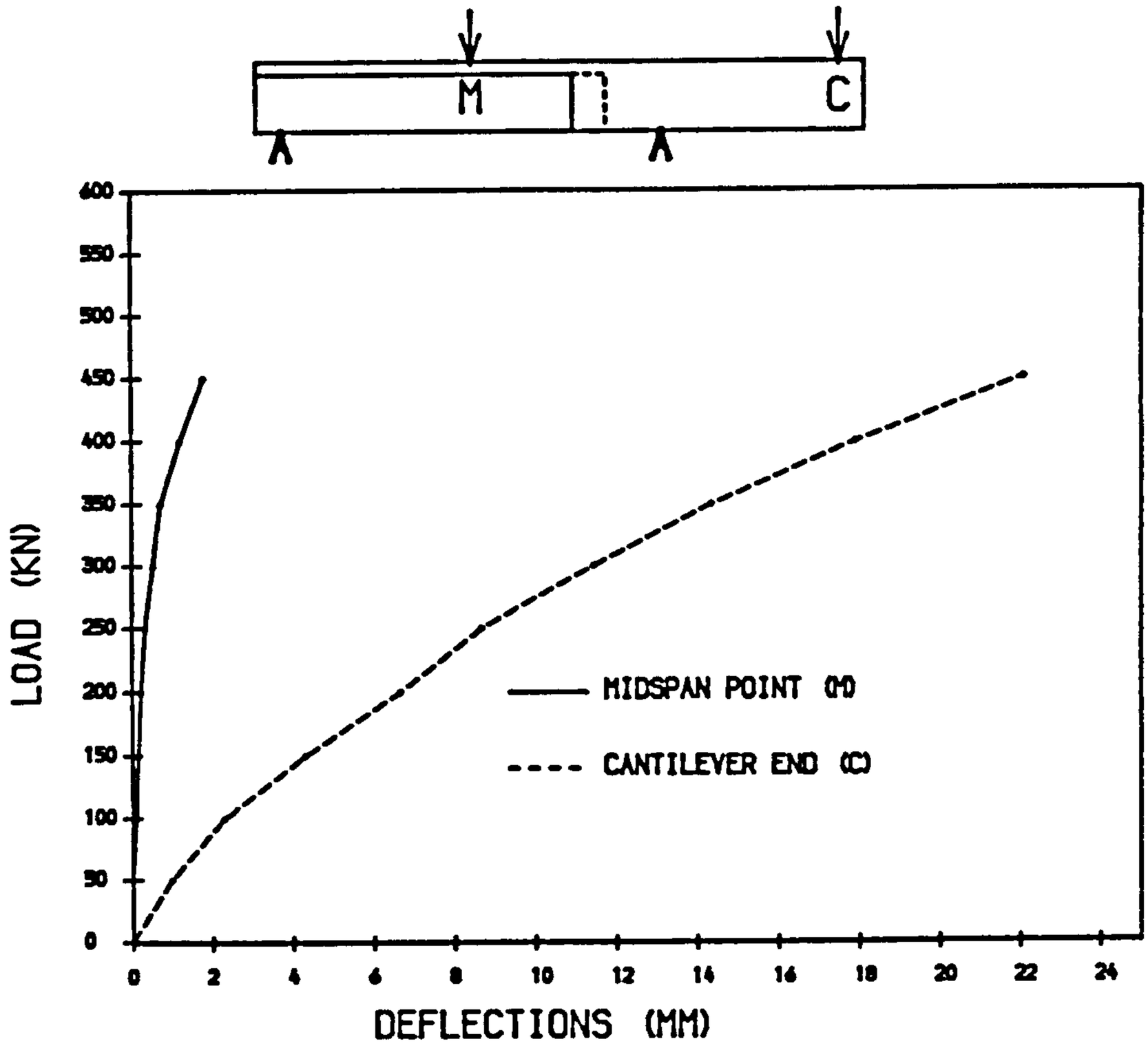

FIG. 5.16 LOAD-DEFLECTION CURVE BEAM E10CC-5

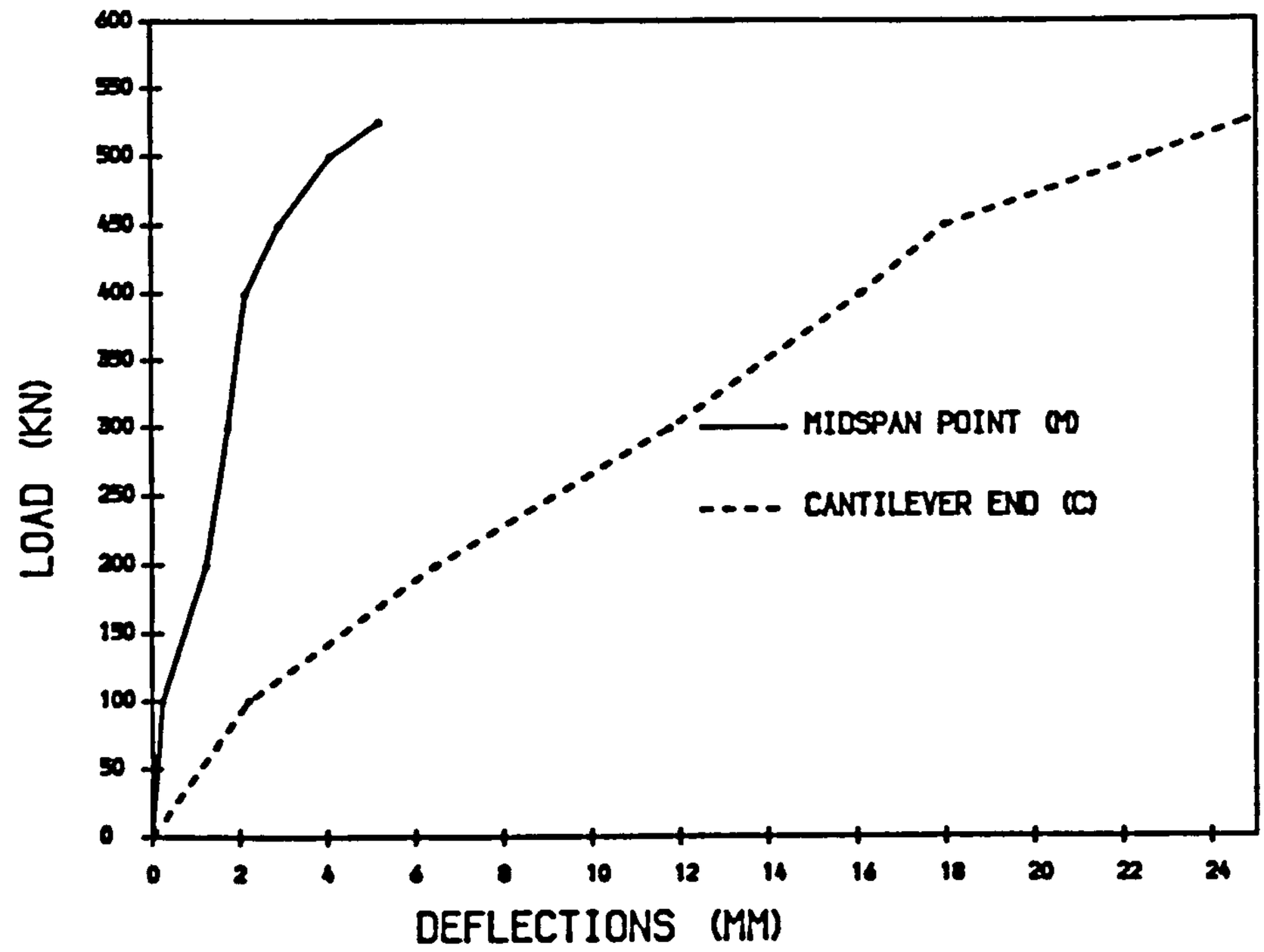

FIG. 5.17 LOAD-DEFLECTION CURVE BEAM E10CD-7

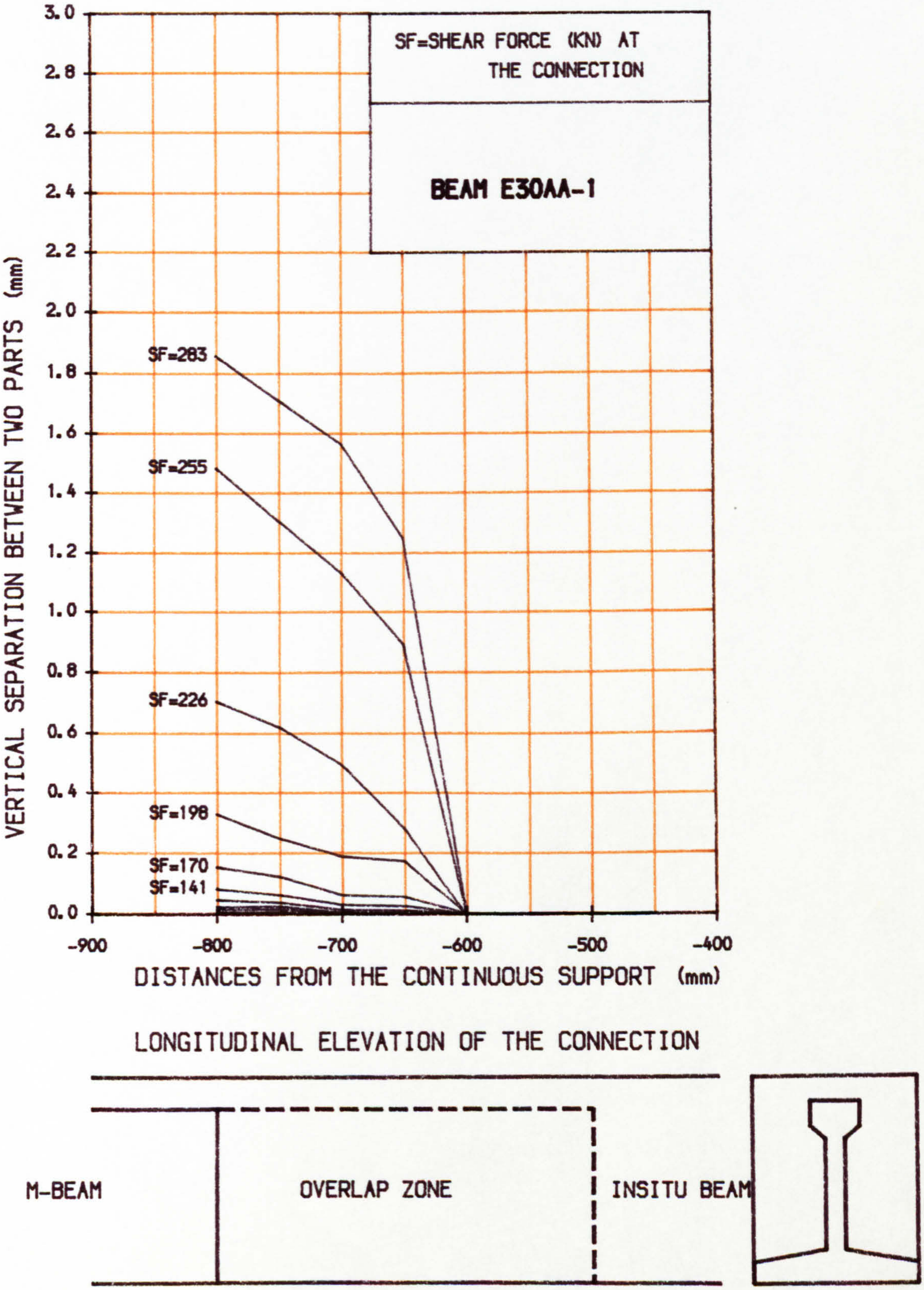

FIG. 5.18 VERTICAL SEPARATION BETWEEN PRECAST BEAM AND INSITU NIB

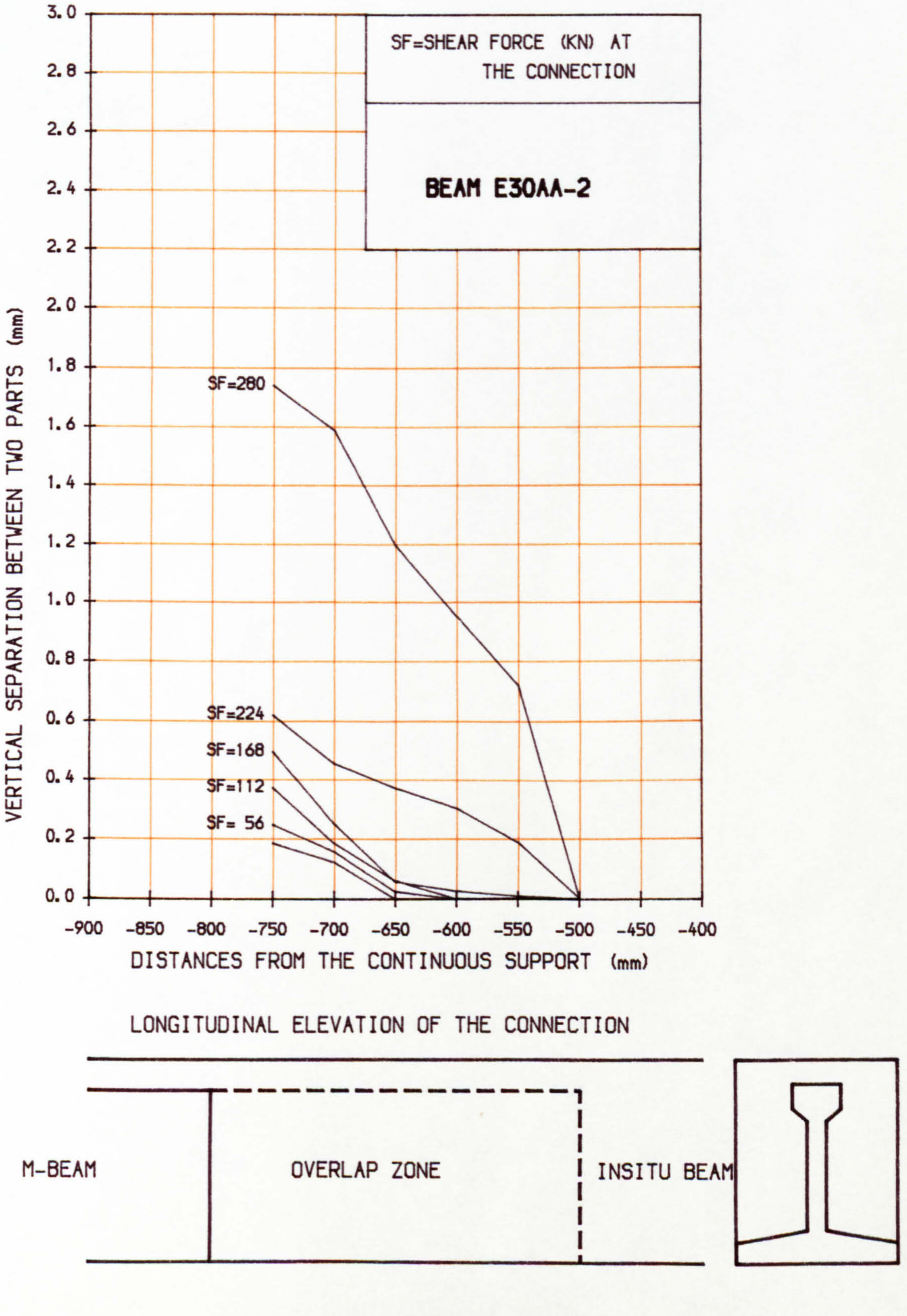

FIG. 5.19 VERTICAL SEPARATION BETWEEN PRECAST BEAM AND IN-SITU NIB

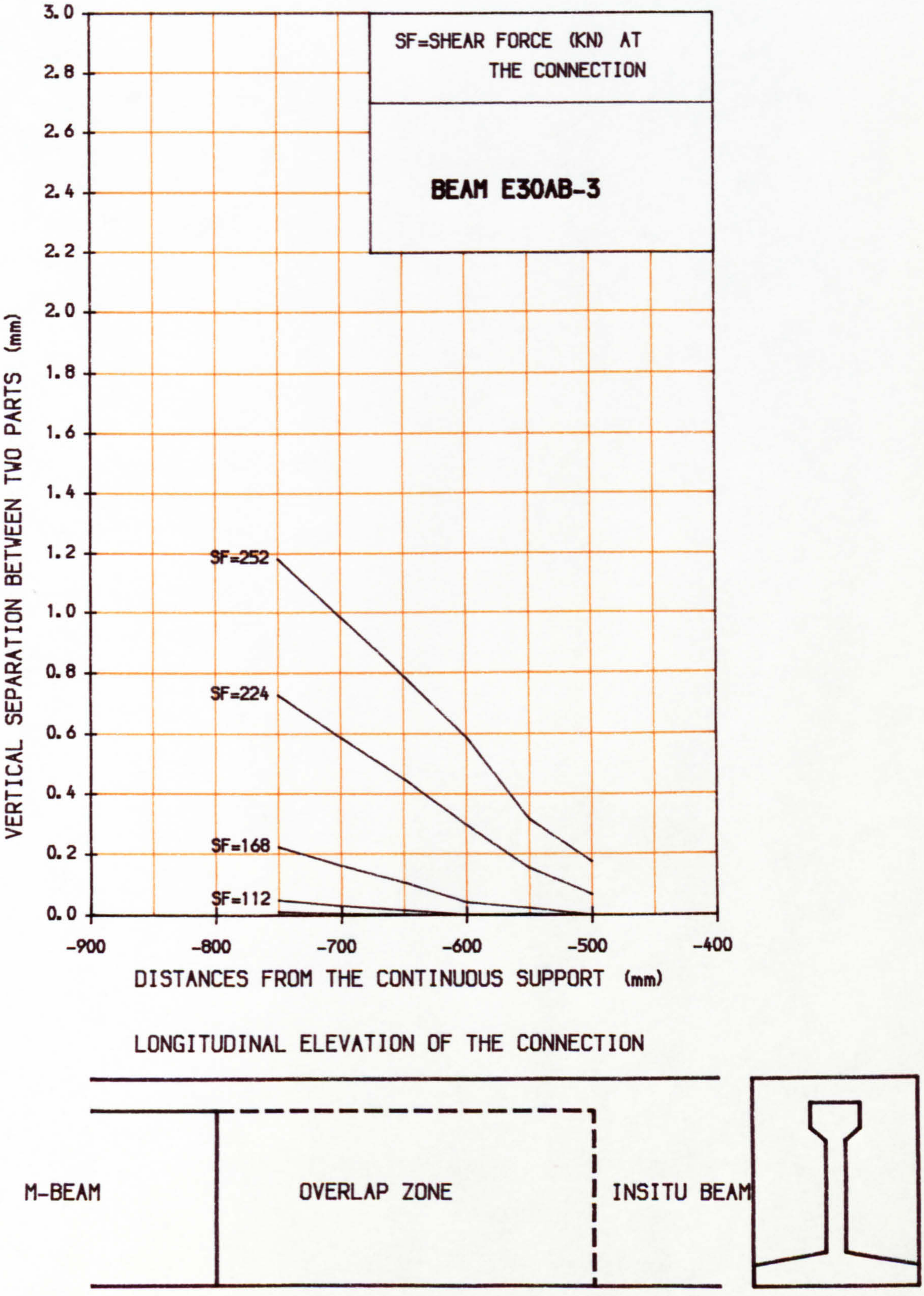

FIG. 5.20 VERTICAL SEPARATION BETWEEN PRECAST BEAM AND IN-SITU NIB

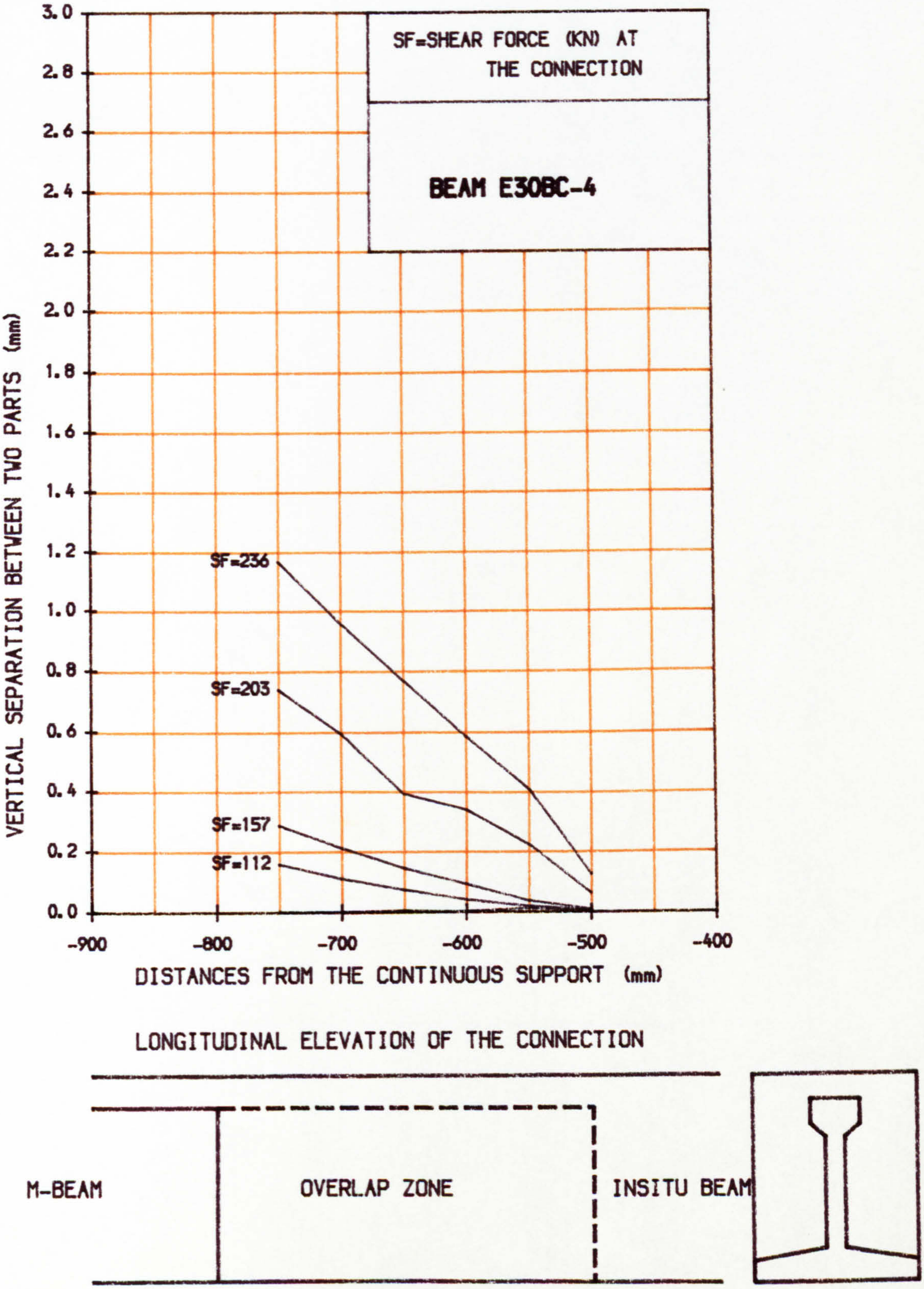

FIG. 5.21 VERTICAL SEPARATION BETWEEN PRECAST BEAM AND IN-SITU NIB

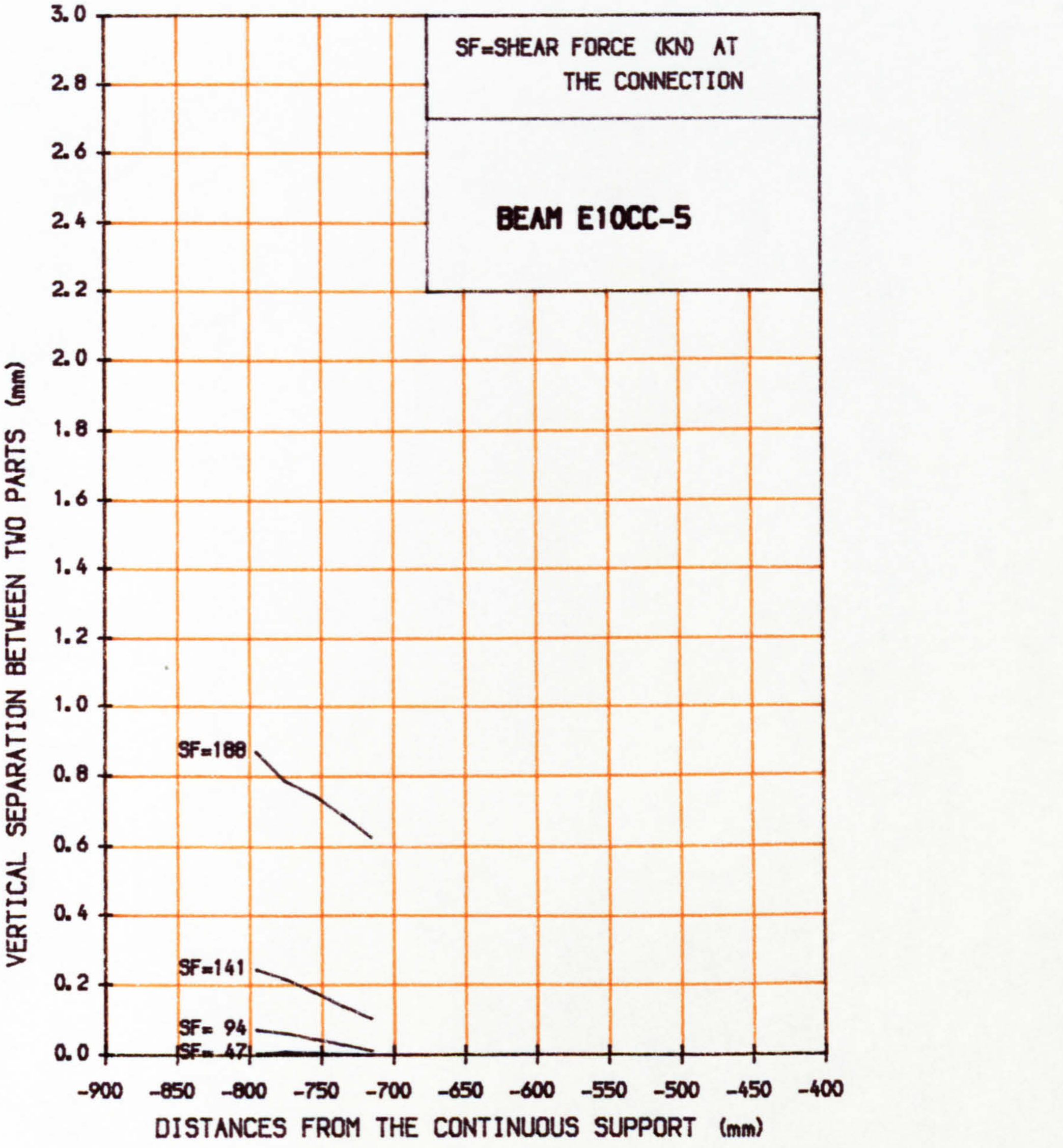

LONGITUDINAL ELEVATION OF THE CONNECTION

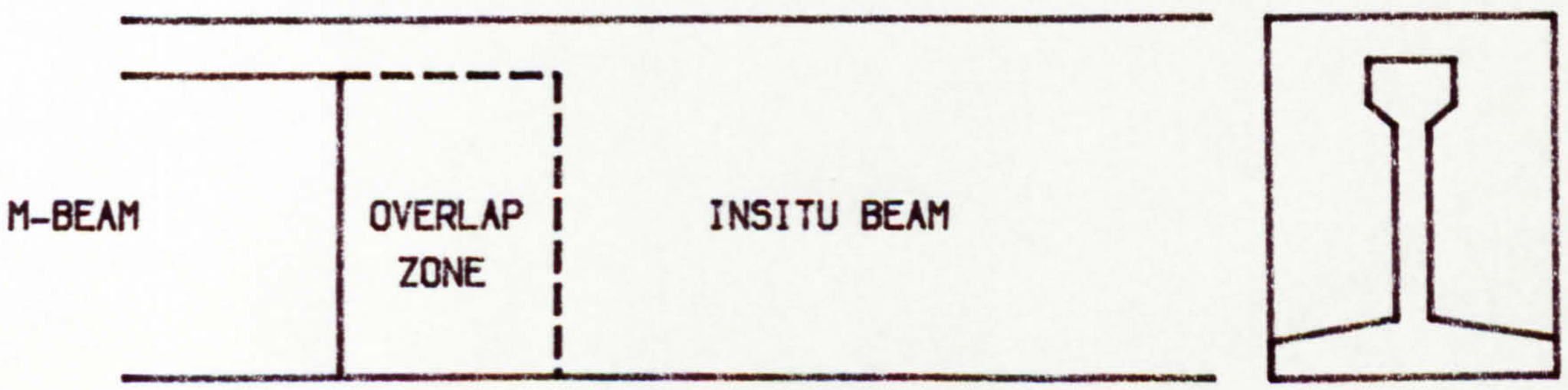

FIG. 5.22 VERTICAL SEPARATION BETWEEN PRECAST BEAM AND IN-SITU NIB

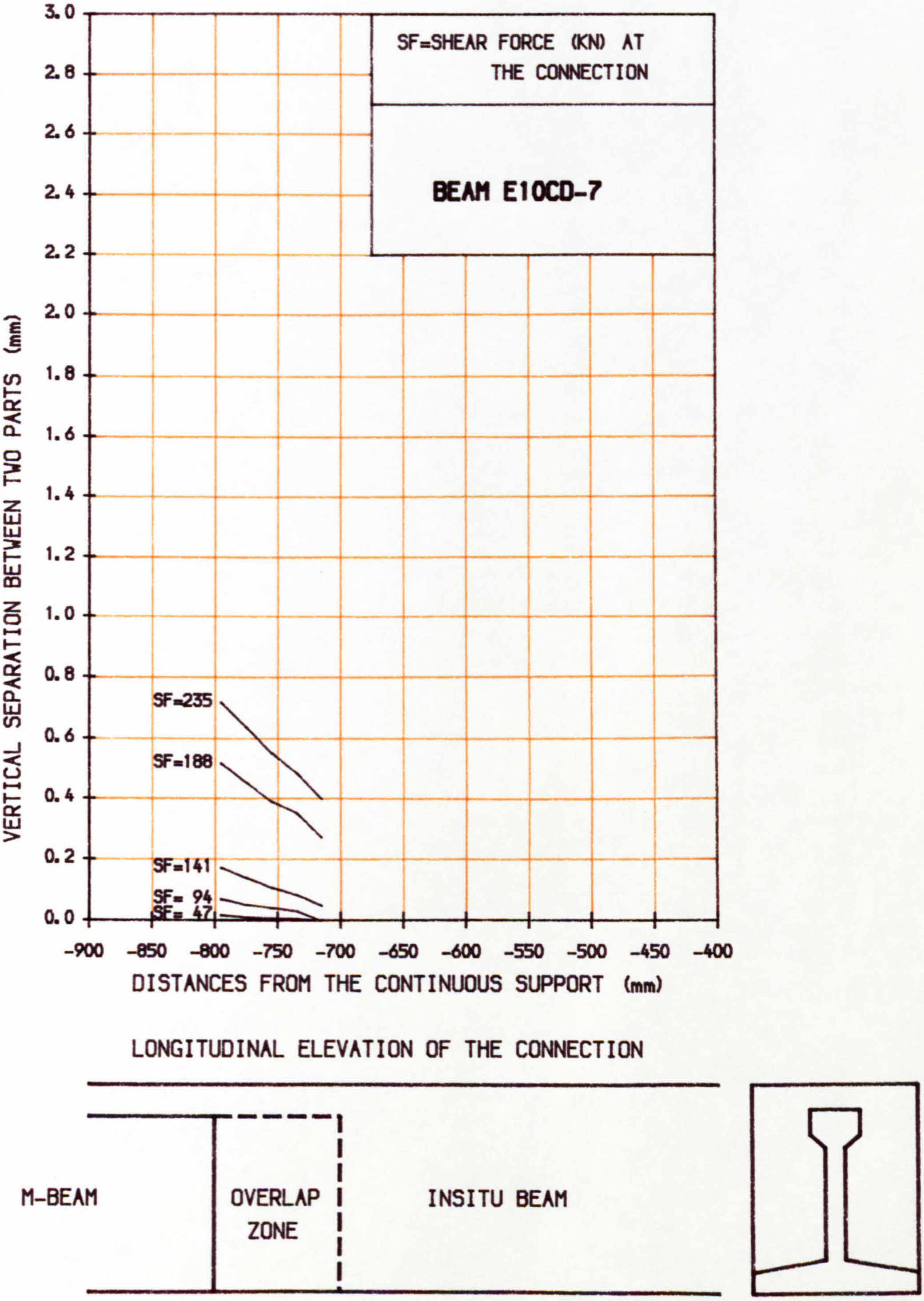

FIG. 5.23 VERTICAL SEPARATION BETWEEN PRECAST BEAM AND IN-SITU NIB

CHAPTER SIX

SHEAR TRANSFER MECHANISM IN PRECAST BEAMS WITHOUT TOP FLANGES

6.1 General

In previous chapter, the shear transfer between precast beams with small top flanges (M-beam) and in-situ concrete in continuous bridges has been investigated. The following investigation aims firstly to clarify the importance of the top flange effect in shear transfer and secondly to observe the efficiency of special modifications and detailing at the connection such as transverse prestressing or web shear connectors.

6.2 Description of the Connection

The same 1/3 scale model M-8 beams were used in this series but before casting the in-situ beam and nibs two pieces of polystyrene, as described in section 3.11g, were located underneath the top flanges of the precast beam along the whole length of the embedment zone and which was later removed prior to the testing. This feature enables the contact between in-situ nibs and the top flanges of precast beam to be removed and in fact simulates the connection between in-situ concrete and inverted 'T' beams without top flanges (see Fig. 6.1). This type of connection also represents an end block (see Figs. 2.4b and 3.12) which was suggested in the initial design of the first bridge designed using this new method of construction[3,4].

6.3 Change of Variables

The variables in this part of the investigation were special details designed to improve the shear transfer capacity of the connection. These were as

follows:

6.3.1 Control Reference

In addition to top flange elimination, no attempt was made in this test to increase the capacity of the connection in shear transfer, making it the control test.

6.3.2 Transverse Prestressing

The in-situ nibs were stressed transversely to apply a normal force to the web of the precast beam and thus increase vertical friction at the interface between the two components.

6.3.3 Web Shear Connectors

Horizontal bars were fixed in the web of the precast beam prior to casting the in-situ nibs. These were designed to act as dowels between the two parts and thus increase the shear strength of the connection.

6.3.4 Projecting Bars from the end of the Precast Beam

In previous tests all the bars and strands were cut off at the end of the precast beam. In this test all the bars and strands projected into the in-situ concrete for a length of 1.00 metre in order to observe their effect upon the shear transfer capacity of the connection .

6.4 Mechanism of Shear Transfer

The mechanism of shear transfer has been discussed for the beams with

effective top flanges in a previous chapter (see chapter five section 5.4). It was seen that when the top flanges of precast beam have contact with the In-situ nibs three different means of shear transfer exist at the connection. For the present condition this shear force has to be transferred by the following mechanisms:

6.4.1 Vertical Bond Between In-situ Nibs and Beam's Web

If the bond between precast and in-situ concrete can be relied upon, a part of the shear force can be transmitted by this means (the efficiency of the bond will be discussed in the next chapter). This part of the shear force is designated V_2 and is shown in Fig. 6.1c,d .

6.4.2 Top Slab over the Precast Beam

Since the top slab over the beam is cast monolithically with the in-situ beam and nibs it can increase the shear transfer capacity of the connection. The contribution of this part is designated V_3 (shown in Fig. 6.1c,d).

In the absence of other special details as previously described in 6.3.2 to 6.3.4 the shear strength of the connection should be:

$$V = V_2 + V_3 \qquad \text{.....(6.1)}$$

Comparing this with Eqn. 5.1 ($V = V_1 + V_2 + V_3$), term V_1 i.e the effect of mechanical interlock between two parts does not exist in Eqn. 6.1.

6.5 Loading Arrangement and General Details

Two point loads were applied through a span-cantilever arrangement

which is capable of producing a high shear force at the connection (see Fig. 3.10 for the bending moment and shear force diagrams). The embedment length remained at 300mm throughout this series. Shear reinforcement within the connection in the in-situ nibs was provided by four 6mm high yield open stirrups. It was shown in previous chapters that in most cases these stirrups did not carry any force but since new modifications were to be included in this series, it was thought that they could possibly change the situation, so these stirrups were provided in the nibs. Table 6.1 shows general details and the failure conditions for the tests in this series.

6.6 Evaluation of the Shear Transfer Capacity

The connection should be regarded as sound if either part of the connection (precast or in-situ beam) can develope its full shear strength at the ultimate stage. The serviceability of the connection is also important i.e crack width, separation between the two parts, relative rotation of parts at the connection and its effect on the overall deflection.

6.7 Experimental Results of the Control Reference Test

The reference test comprised a connection in which there was neither a top flange effect nor any other means of enhancing the shear transfer capacity. The beam failed at a surprisingly low load as a result of connection failure, when the shear force in the connection was equal to about 30% of the shear resistance of the precast beam itself. The high reduction in the shear transfer capacity of the connection in this test was clearly because no part of the shear force was allowed to be transmitted from the top flanges of the precast beam to the in-situ nibs (see plates 6.1 and 6.5).

As previously stated the connection detail in this test was intended to represent an end block (see Figs. 2.4b and 3.12) suggested[3] in the initial design of the first prototype bridge using this new type of construction. The original reason for requiring this end block was to reduce the shear stress across the end interface of the precast beam as it was assumed that the end surface of the precast beam transfers all the shear force, and that there was no relief of shear force along the embedded length of the connection.

It was shown from the experimental results of the previous chapter that there is actually a relief of shear force within the connection and the in-situ concrete nibs are subject to a non-uniform distributed load with higher intensity near the end of precast beam. The experimental results of this test confirms the importance of top flanges in shear transfer and the author would certainly recommend against using precast beam end block in the connection because of its adverse effect upon the shear strength of the connection caused by removal of the important top flange effect.

6.7.1 Stirrup Stress

Stirrup stresses for both precast beam and in-situ nibs have been plotted in Fig. 6.2. For the precast beam, for smaller stirrup spacing from the precast beam end lower stresses were observed showing the same trend as the connections with the top flange effect. This means that the shear force is changing along the precast beam within the connection. The only contact between the two parts are through the existing bond (between the web and in-situ nibs) and the top concrete. It was observed in this test that when the load was equal to about 94% of the failure load the bond between the web of the precast beam and the in-situ nibs failed, resulting in a substantial vertical separation, and subsequently the whole shear force shifted to the junction between the precast

beam and the top concrete slab which are joined by the projecting parts of the web stirrups.

This situation has been illustrated in Fig. 6.3. The precast beam is suspended by its stirrups (Fig. 6.3b,c) producing a high tensile stress in the stirrups (Fig. 6.2) in comparison with the case in which the same shear force is applied in a normal way I.e the load is applied through the beam rather than its stirrups.

6.7.2 Vertical Separation

The vertical separation between the in-situ nibs and the bottom flange of the precast beam was measured for all points along the embedment part and shown plotted in Fig. 6.4. Before failure of the bond occurred, observed figures for this displacement were much higher than those for connections with the top flange effect (discussed in the previous chapter), with an order of up to 10 times, and the subsequent slip between the two parts led to an overall separation of 20mm at the ultimate stage (see also plates 6.1 and 6.5).

6.8 Transverse Prestressing

In the prototype bridge deck transverse prestress may be employed to fulfil two functions. Firstly and primarily to resist transverse bending moments in the deck and secondly to resist long term shrinkage and thermal movements. In the design of the first bridge using this new method of construction[3,4] in this country, the provision of transverse prestressing was included specifically to increase the longitudinal shear transfer capacity of the connection.

For the connections in which the precast beam has a top flange it was

observed in chapter five that for all cases (except in beam E10CC5 with 100mm embedment length and no stirrups in the nibs) the connections were able to transfer the full ultimate shear resistance of the precast beam without transverse prestressing in the connection. Among these, in beam E30AB3, in addition to the elimination of nib stirrups and projecting bars the bond between in-situ nibs and the web of the precast beam was eliminated by applying a layer of bitumen on the web prior to casting the in-situ concrete. This was intended to simulate the destruction of bond in practice as a result of shrinkage and temperature movements. The connection was still able to transfer the full shear strength of the beam. Thus when the precast beam has top flanges even in the weakest conditions there is no necessity to improve the longitudinal shear resistance of the connection by transverse prestressing.

It is well known that all solid bodies in contact offer resistance to motion tangential to their contact surface and classical laws of friction indicate that the frictional force is :

a) Directly proportional to the load normal to the contact surface

b) Independent of the contact area and sliding velocity

c) Dependent upon the nature of material in use

The occurrence of interface resistance in concrete is essentially of two types:

i) The shear resistance in the presence of an externally applied axial compression, analogous to friction behaviour.

ii) The shear resistance without any significant compression as in composite construction. The surfaces may or may not be bonded together by casting one against the other and there may or may not be steel reinforcement crossing the joint plane.

In the case of shear associated with external compression across a joint, Jones[82] reports several tests in which two parts of a beam were post-tensioned together and the required load to shear the joint was determined for varying

amounts of prestress. Two different interface conditions were examined. In the first series smooth and dry surfaces were stressed together but in the second series a layer of 1/2" mortar was used initially to bond the units and then a prestressing force was applied. In the first part the proportionality constant (ratio of shear force to prestressing force) was observed to be between 0.45 and 0.62 for different types of surfaces. For the bonded joints the ratio was 0.56, 0.770 and 0.714 at the start of slip which subsequently dropped to 0.763, 0.665 and 0.645.

Gaston and Kriz[83] conducted a series of tests to determine the shear resistance of a joint consisting of two concrete members stressed together by bolts. To eliminate the dowel action of the bolts, oversize holes were provided. Some of the specimens were assembled without interface bond while in the others a 1" layer of mortar was used between the blocks. The interface area was also considered as a variable. It was observed that for a constant prestressing force slip increased slowly with increasing shear force until the maximum shear force was reached, when a sudden large slip occured. In the bonded specimens cracks formed at a 45° angle in the mortar close to the horizontal edges. The following equations were proposed for the shear resistance of the connection:

$v=0.78p+0.297 \quad N/mm^2$ (for unbonded connections) .....(6.2)

$v=0.7p+0.76 \quad N/mm^2$ (for bonded connections) .....(6.3)

where v is the shear stress resisted by the contact surface and p is the normal compressive stress due to prestressing.

Some further tests on this subject are reported by Rees[84] . 6" concrete cubes were bonded together with a mortar layer and then they were transversly post-tensioned. The following equation was suggested for the shear resistance of these types of connections:

$v=0.8p+1.1 \quad N/mm^2$ (for bonded connection).....(6.4)

where v and p are as in equations 6.2 and 6.3.

6.8.1 Experimental Results of the Test with Transverse Prestressing

In this test (WTFPCC8) the connection was transversly post-tensioned. All other details were similar to those of the control reference test (WTFCC6) i.e no top flange effect from the precast beam, and also the minimum number of projecting bars into the in-situ beam. Post-tensioning of the connection was achieved by four 9.8mm 7-wire strands through 160×160×15mm bearing plates (see plate 6.6) to distribute a total of 180 kN prestressing force over the web within the connection and produce an approximate prestress of about 2.65 N/mm^2.

6.8.1.1 Ultimate Strength and Failure Mode

The connection was able to transfer the full shear of the precast beam which eventually failed in a web crushing mode at a shear force which was about 10% more than the observed web crushing strength in the first series of tests. The possible reason for this increase will be discussed in the next section. It should be mentioned here that in the similar connection but without transverse prestressing (the control reference test WTFCC6) the connection failed at a shear force equal to 27% of the shear resistance in this test. This reveals the significant effect of transverse prestressing in shear transfer capacity of the connections without the top flange effect.

6.8.1.2 Stirrup Stress

Stresses have been plotted for all the stirrups within the connection

either in the precast beam or in the in-situ concrete (see Fig. 6.5). For the precast beam these stresses have been measured only for those stirrups in the connection itself but for the in-situ concrete the measurement has been continued beyond the connection and up to the support. It can be seen that in the precast beam the stresses are significantly lower than those observed in the first series (e.g see Figs. 5.2 , 5.4 or 5.6) with an order of 1 to 2. On the other hand substantial stresses were observed in the stirrups in the in-situ nibs (see Fig. 6.5). These had been found to be very small and for most of them almost zero in the first series of tests (compare Fig. 6.5 with Fig. 5.2). The reason for this considerable change in the behaviour of the connection can be explained as follows:

a) The in-situ nibs are transversly stressed onto the beam's web within the whole length of the connection resulting in a perfect composite action between them thus enabling monolithic behaviour.

b) The composite action will allow the two parts to share the transferring of the shear force. This is why high stresses were observed in the stirrups of the nibs. In the connections with the top flange effect (first series) the situation at the connection was like a beam resting on a support (top flanges resting on the in-situ nibs) in which a small length of the end of the precast beam and its adjacent nibs were very effective while the rest of the in-situ nib was not fully utilized.

c) The shear strength of the precast beam was observed to be slightly higher in comparison with the beams in the first series. The possible reasons are firstly the lower shear force carried by the precast beam within the connection as the stirrup stress diagram shows and secondly the provision of two 160×160×15mm steel bearing plates for the distribution of prestressing force may have functioned as external stirrups and increased the shear strength. It is notable from plates 6.2 and 6.6 that unlike previous tests in the

first and second series, in this test there was an inclined crack in the in-situ nib indicating that the shear force in the nib is significant. This high shear force has substantially increased the stirrup stress in the nibs (see Fig. 6.5) in comparison to previous tests.

6.8.1.3 Vertical Separation

The vertical separation between the in-situ nib and bottom flange of the precast beam were measured at different positions along the embedment length. These measurements are shown in Fig. 6.6. The magnitude of separation was substantially lower than those observed before e.g for a shear force of 280kN the maximum separation was three times lower than that of beam E30AA1. In addition to this, the vertical separation was zero within a length of about 165mm from the end of precast beam (see Fig. 6.6), which is more than half the embedment length, while in the first series for all cases (except beam E30AA1) the vertical separation was observed for the entire length of the connection.

The main cause of separation in this part is the destruction of bond between the web and in-situ nibs and subsequent slip at the interface. The transverse prestressing in this test has highly increased the interface friction and reduced the vertical separation.

6.9 Shear Transfer by Web Shear Connectors

Web shear connectors were used as an alternative to transverse prestressing. In this test four 10mm mild steel bars were threaded through previously made ducts in the precast beam web (see Fig. 3.14). The effect of the beam's top flanges was also eliminated in this test in order to determine the

effectiveness of the shear connectors. The transfer of shear force in this test will be by :

(i) Monolithic top slab (V_3 in Fig. 6.1).

(ii) Bond between web and in-situ nibs (V_2).

(iii) Additional effect resulting from the dowel action of the web connecting bars.

6.9.1 Ultimate Strength and Failure Mode

The web shear connectors were found to be fully effective and the connection was able to transfer the full shear strength of the precast beam which failed in a web crushing mode (see plates 6.3 and 6.7). The observed shear force at failure was 5.7% less than that observed for the connection with transverse prestressing. This could be attributed to the reason explained in section 6.8.1.2c.

6.9.2 Stirrup Stress

Experimental stresses have been plotted for all the stirrups in the connection (see Fig. 6.7). In the precast beam stresses were found to be much higher than those in the connection with transverse prestressing (compare with Fig. 6.5). On the other hand stirrup stresses in the in-situ nibs were lower as shown in Fig. 6.7, where the stirrup stresses in the nibs are almost zero up to about 80% of failure load but they increase suddenly on approach to failure.

Stress distribution in the stirrups is more or less similar to that observed in the first series indicating that in the connection with web shear connectors the web and in-situ nibs have not been behaving like a unique member as they did in the case of transverse prestressing. The sudden increase

in stress in the nib stirrups near failure may be attributed to bond failure between the in-situ nib and the web causing immediate transfer of bond force to web connectors.

6.9.3 Vertical Separation

The vertical separation was found to be much higher than before (see Fig. 6.8). For a shear force of 306kN the maximum separation was almost four times greater than that observed in the case of transverse prestressing (compare with Fig. 6.6). The reason for this change is again the loss of bond between two parts during the loading and subsequent slip at the interface. It should be mentioned here that in this test 10mm bars were threaded into the ducts on the web and the remaining voids was filled with concrete mortar. Vertical separation may be reduced by fixing these bars in the web prior to casting the precast beam. It is also possible to avoid reinforcing bars and use small sections of angle or channel welded to previously fixed steel plates on the web but more research work is required for these conditions.

6.10 Shear Transfer by Projecting Bars from the Precast Beam

In the previous tests of this series all reinforcing bars (except four 8mm bars at the bottom) were cut off at the end of the precast beam. In this test it was decided to leave all 13 bars projecting into the in-situ concrete beam while the top flange effect was eliminated in order to examine the contribution of projecting bars to shear transfer.

6.10.1 Ultimate Strength of the Connection

The shear force at failure was very close (about 93%) to the observed shear strength of precast beams in previous tests but neither the precast nor the in-situ beams themselves failed. Failure could thus be regarded as a connection failure though the connection was able to transfer 93% of the shear force. The failure was associated with a relatively large separation (see plates 6.4 and 6.8) between the components and splitting of the in-situ concrete along the projecting bars from the bottom flange of precast beam. It is also noticeable from plate 6.8 that the in-situ top flange near the loading point has sheared with a relatively wide diagonal crack. This implies that near failure the loss of bond between web and nibs has caused large separation and slip between the two parts and consequently an extra force has been transferred to the remaining parts of the connection (I.e in-situ top flange and dowel action of projecting bars). As a result, the in-situ top flange has sheared and the in-situ concrete cover to the bottom projecting bars has severely cracked.

6.10.2 Distribution of Stress In the Stirrups

Observed stirrup stresses have been plotted in Fig. 6.9 for both precast beam and in-situ nib. The trend is similar to that obtained in the first series i.e relatively high stresses in the precast beam stirrups which decrease toward its end and very low (mostly zero) stresses in the in-situ nib stirrups. This behaviour indicates that a large part of the nib does not contribute in shear transfer of the connection while the precast beam carries almost the full shear force to its end.

Since there is no top flange contact in the connection region the mechanism of shear transfer will be limited to:

(i) The bond between nibs and the web.

(ii) The in-situ top slab which is connecting the two parts continuously.

(iii) The dowel action of projecting bars from the end of precast beam into the in-situ concrete which has the most important contribution in this case.

It was mentioned earlier that in this test connection failed when the shear force was about 93% of the precast beam's shear strength. This is seen clearly from the stirrup stresses (see Fig. 6.9) when at the failure (R=1.0) most of the stirrups have attained their yield stresses.

6.10.3 Vertical Separation

Vertical separation was observed to be high in comparison with the tests in the first series and also in comparison with connections with transverse prestressing or web shear connectors in the second series. The reasons are firstly the absence of the top flange effect and secondly the lack of transverse restraint. Fig. 6.10 shows these separations for different positions of the connection. Vertical separations up to 7 times greater than those in the case of transverse prestressing and up to 1.5 times greater than that of the web shear connector case were observed. The ultimate separation was found to be about 10mm (see Plate 6.8).

6.11 Deflections

Deflections at the mid-span and cantilever end were measured and plotted for all the beams in this series. These are shown in Figs. 6.11 to 6.14. Most of the results discussed in section 5.12 of previous chapters were also observed here. For the first of this series (connection without any shear transfer

improving detail) in which the connection failed at a very low load, The deflections were found to be very high near the failure (see Fig. 6.11) though it was not possible to measure the exact deflection at the time of failure.

6.12 Comparison of Different Types of Connection

It was observed that in the connections without the top flange effect both transverse prestressing and web shear connectors can substantially increase the shear transfer capacity of the connection. This is because of the improved connection between the web and in-situ nibs which results in better composite action and a behaviour more or less similar to monolithic concrete. The improved composite action is reflected in the in-situ nib stirrup stress.

Fig. 6.15 shows the in-situ nib stirrup stresses for three different types of connections at the time of failure. In the case of transverse prestressing stresses are the highest while for the connection with web shear connectors these are about one third of the previous case. For other types of connections and also for all tests in the first series these stresses are almost zero, indicating that in the case of transverse prestressing excellent composite action exists and the in-situ nibs can efficiently share the shear force with the precast beam resulting in low vertical separation and rotation at the connection. In the case of web shear connectors although the connection was able to transfer the full shear strength the vertical separation is considerable (see Fig. 6.8). For the connection in which the projecting bars were used to transfer the shear force, the connection transferred some 93% of the shear strength of the beam and the failure was considered to be a connection failure. It should be mentioned that a connection with no shear improving details (WTFCC6) could transfer only 30% of the shear force (see section 6.7) which is mainly by the concrete and continuity bars in the top slab. The approximate percentage contribution of

precast beam's projecting bars is therefore 93%-30%=63% .

The projecting bars were thus regarded as forming a very helpful aid to shear transfer of the connections without top flange effect. The amount of projecting bars in beam WTFDCC9 was similar to that which might exist in practice (taking into account the model scale factor) but nevertheless more research work is required for different amounts and diameters of projecting bars. It would also be useful to investigate the combined effect of projecting bars and web shear connectors in shear transfer transfer capacity and their possible effect on reducing the vertical separation.

6.13 Design Recommendations

Where a continuous bridge deck is to be constructed using the new method and the longitudinal elements are inverted 'T' or similar sections without top flanges, the present investigation has shown important points which should be considered by the designers:

6.13.1 Choice of Connection Detail

It was observed in this part of the investigation that the absence of top flanges and the loss of bond between the precast beam and in-situ concrete either due to the initial smoothness of the surface or due to later shrinkage can significantly reduce the capacity for shear transfer, and thus one of the following details should be adopted in designing such connections:

a) "Transverse Prestressing". If the crosshead itself is to be prestressed transversly to take transverse bending moments it will also offer a most efficient assistance to transfer the longitudinal shear. The average transverse prestressing level used in the test was about 2.65 N/mm^2. In practice it is

likely that prestressing levels will be higher than this and hence the test result should cover most practical cases. The projecting bars from the precast beam may also be limited to the minimum required for taking the possible sagging moment produce by differential support settlement.

b) "Web Shear Connectors". Where transverse prestressing is not included in the design of the crosshead, web shear connectors can be used to transfer the longitudinal shear force. These connectors may be reinforcing bars threaded into previously formed ducts in the web before casting the in-situ concrete or alternatively be cast into the web of the beam. It is, however, essential to develope full dowel shear resistance to prevent the occurence of considerable slip and vertical separation.

When using web connectors projecting bars can be reduced to the required minimum for possible positive bending moment. The required area of the steel connectors may be obtained by using one of the shear friction theories which are discussed in the next chapter. The amount of shear force to be taken by the connectors may be assumed conservatively equal to the full design shear force of the beam. Alternatively as it was found that about 30% of the shear force is transferred by the top slab, the connectors may be designed for only 70% of the shear force.

c) "Projecting Bars". In absence of top flanges, the projecting bars from the precast beam into the in-situ concrete may be considered as a substitute for transverse prestressing or web connectors to assist transfer of the longitudinal shear force. It should be noted though that in the test this type of connection was able to transfer about 93% of precast beam's shear strength but since the precast beam was heavily reinforced for shear, the connection may be sufficient in beams with slightly lower shear force.

The projecting bars may consist totally of prestressing strands and non-prestressed bars (as in the test). In practice the best way is to leave

sufficient spaces between the beam stop-ends in the precast yard to obtain the required projecting lengths of strands rather than the costly job of bar couplers. Since there is no connection between nibs and the web, high vertical separation and rotation could be expected (as it was seen in that test) although the connection may transfer the full shear resistance of the beam. Clearly more experimental investigation is required to examine the effect of cross-sectional area , location and tensile strength of projecting bars upon the shear transfer capacity of the connection.

6.13.2 Shear Design of Precast and In-situ Nib

For the case of transverse prestressing and web shear connectors the shear force is transferred from the precast beam to the in-situ nibs gradually and there is some relief of shear force along the embedment length. It may be assumed that in the precast beam the shear force decreases linearly from its maximum (at the beginning of the connection) to zero (at the end of precast beam) and similarly in the nibs it increases from zero to maximum. The precast beam and in-situ nibs can be designed accordingly. If the shear force is going to be transferred by the projecting bars, since the force is transferred at the end, the precast beam should be designed to take the applied shear force for its entire length regardless of in-situ nibs. The in-situ nibs themselves are not subject to considerable shear force and may be reinforced with a nominal amount of stirrups.

Plate 6.1 Longitudinal Elevation of Beam WTFCC6 After Failure

Plate 6.2 Longitudinal Elevation of Beam WTFPCC8 After Failure

Plate 6.3 Longitudinal Elevation of Beam WTFSCC9 After Failure

Plate 6.4 Longitudinal Elevation of Beam WTFDCC10 After Failure

Plate 6.5 Elimination of Top Flanges
(The Connection Failure)

Plate 6.6 Provision of Transverse Prestressing (No Top Flange)
Condition in The Connection After Failure

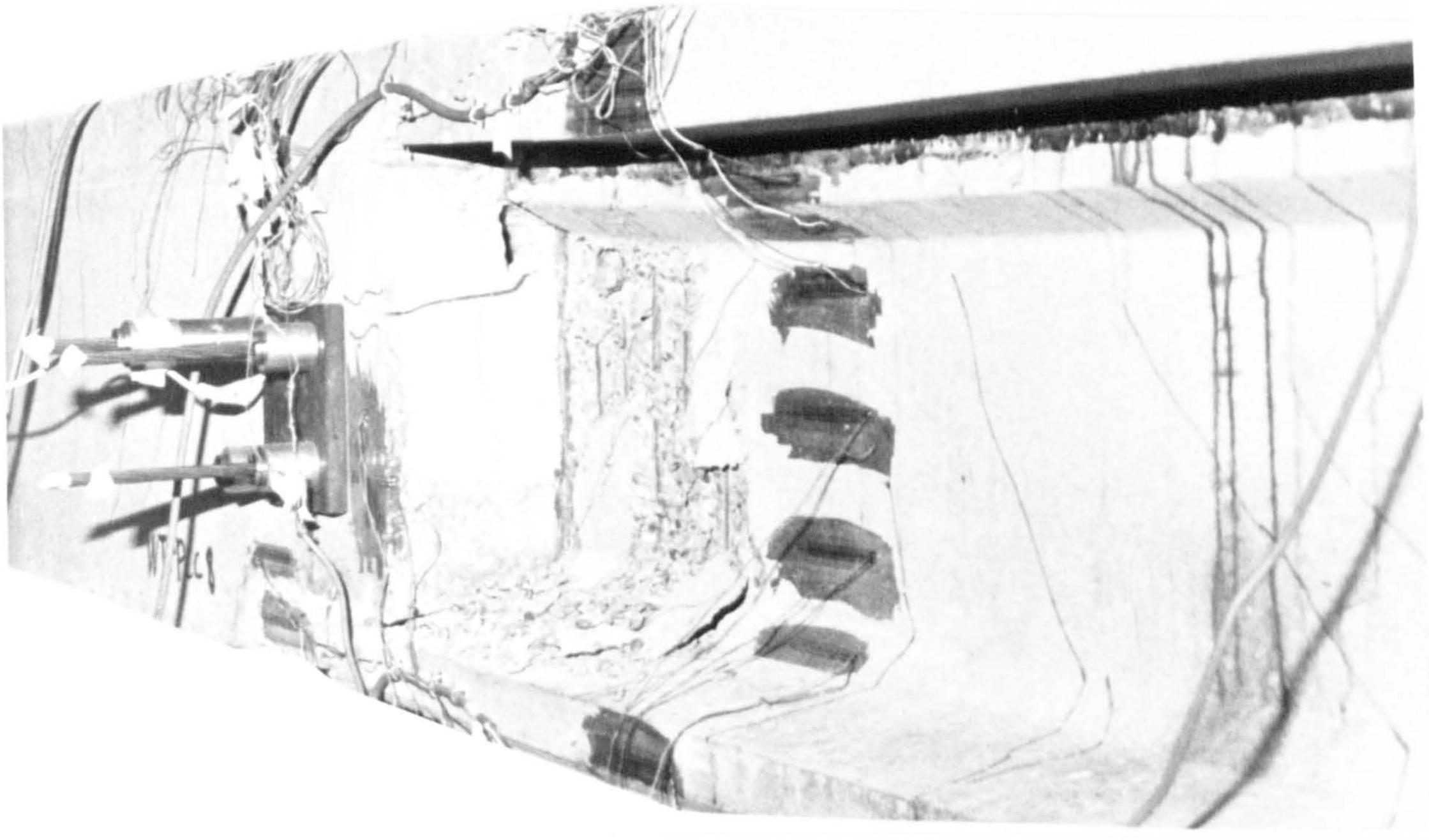

Plate 6.6a Provision of Transverse Prestressing (No Top Flange)
Condition in The Connection After Failure

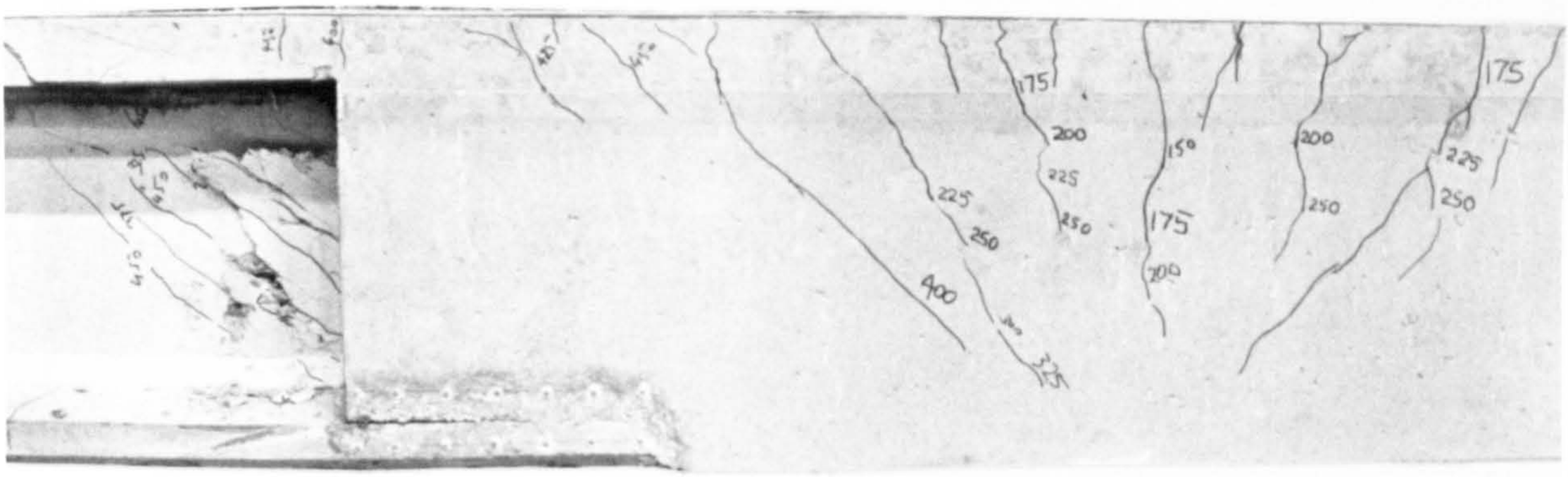

Plate 6.7 Conection with Web Shear Connectors (No Top Flange)
Condition in The Connection After Failure

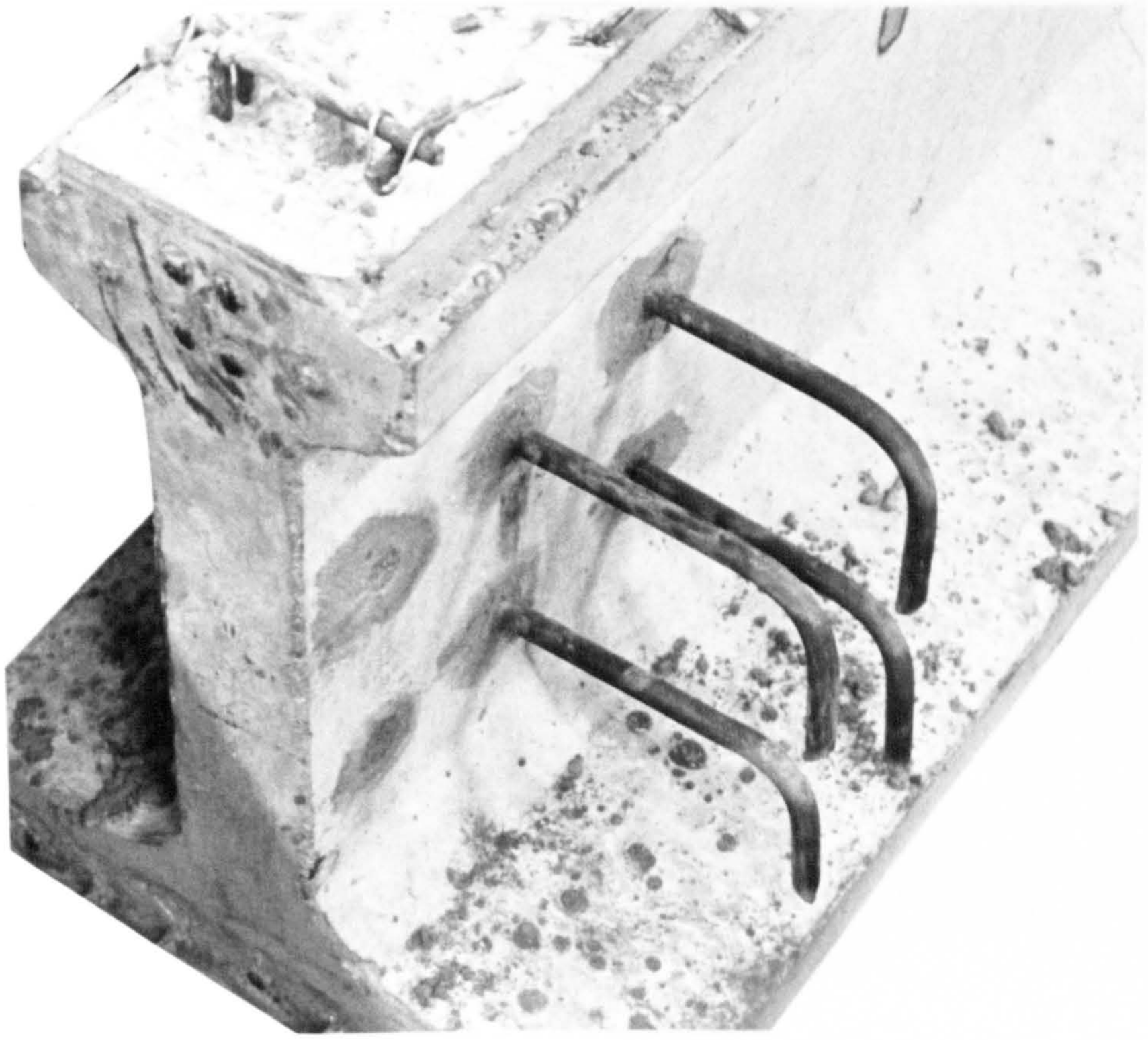

Plate 6.7a Shear Connectors in the Precast Beam Web

Plate 6.8 Projecting of All Bars into In-situ Part (No Top Flange)
Condition in The Connection After Failure

Table 6.1 Beam Details, Calculated and Experimental Results

(For the Connections without Top Flanges in the Beam)

	WTFCC6	WTFPCC8	WTFSCC9	WTFDCC10
Connection Length (mm)	300 mm	300mm	300mm	300mm
M-beam's Stirrups in the Connection	T6@85	T6@85	T6@85	T6@85
Nib's Stirrups in the Connection	T6@70	T6@70	T6@70	T6@70
Total Stirrup Ratio in the Conn.	0.45%	0.45%	0.45%	0.45%
Stirr. Ratio in the Insitu Beam Remote from the Conn.	0.2%	0.2%	0.2%	0.2%
No. of Projecting Bars	4 bars (bottom)	4 bars (bottom)	4 bars (bottom)	13 bar (all)
Special Feature in the Connection	None	Transv. Prestress	Web shear connectors	Projected bars
Cal. Shear Resist. of M-beam (kN)	315	315	315	315
Cal.Shear Resist. of Insitu Beam Remote from Conn.	265	265	265	265
Observed Shear Resist. (kN)	91	348	329	306
Type & Position of the Failure	Failure of the Connection	Web Crushing in the Precast Beam	Web Crushing in the Precast Beam	Very Large Vertical Separation Followed by Web Crushing

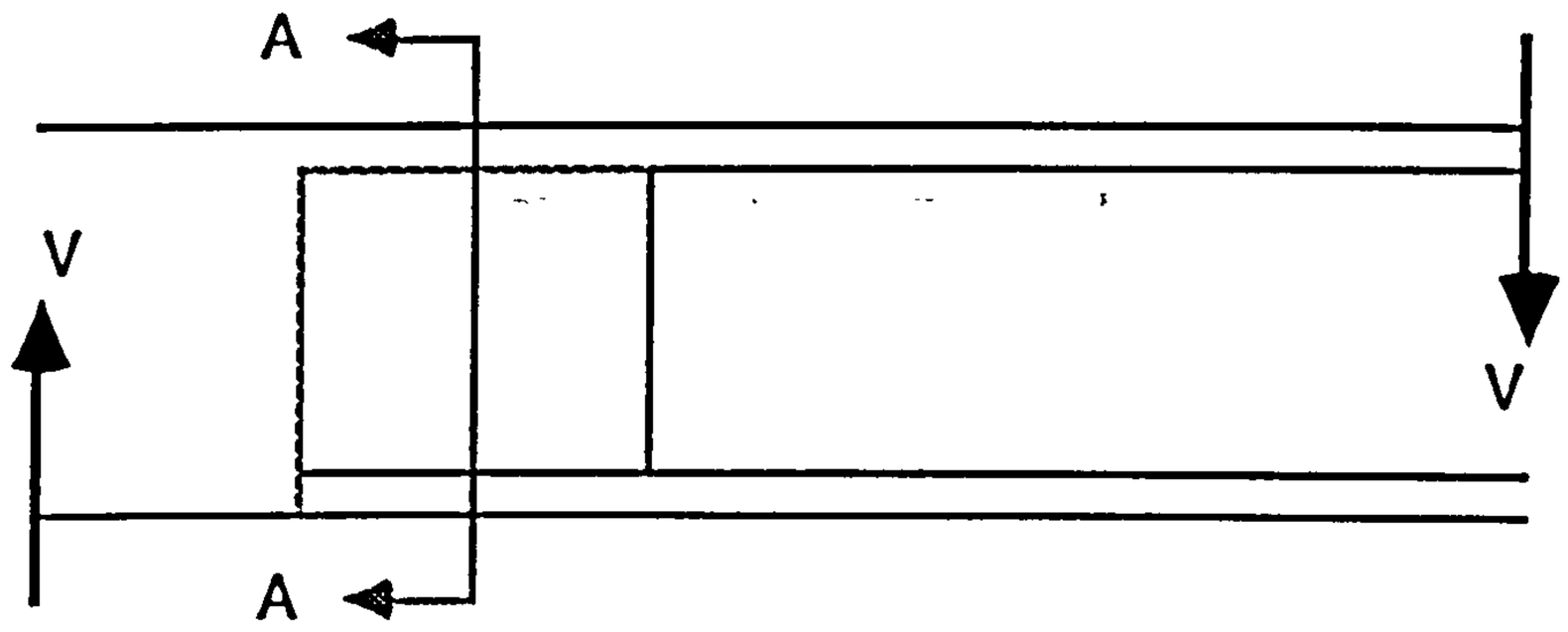

a) Shear forces acting in the connection

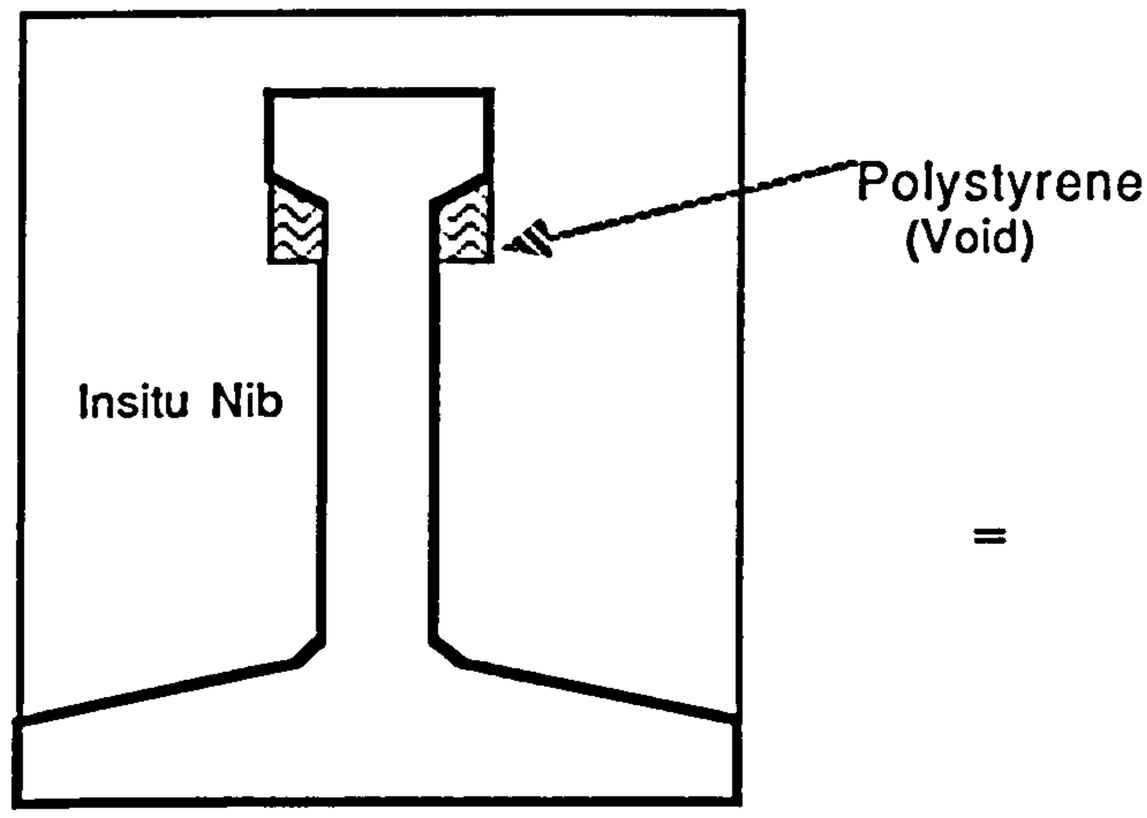

=

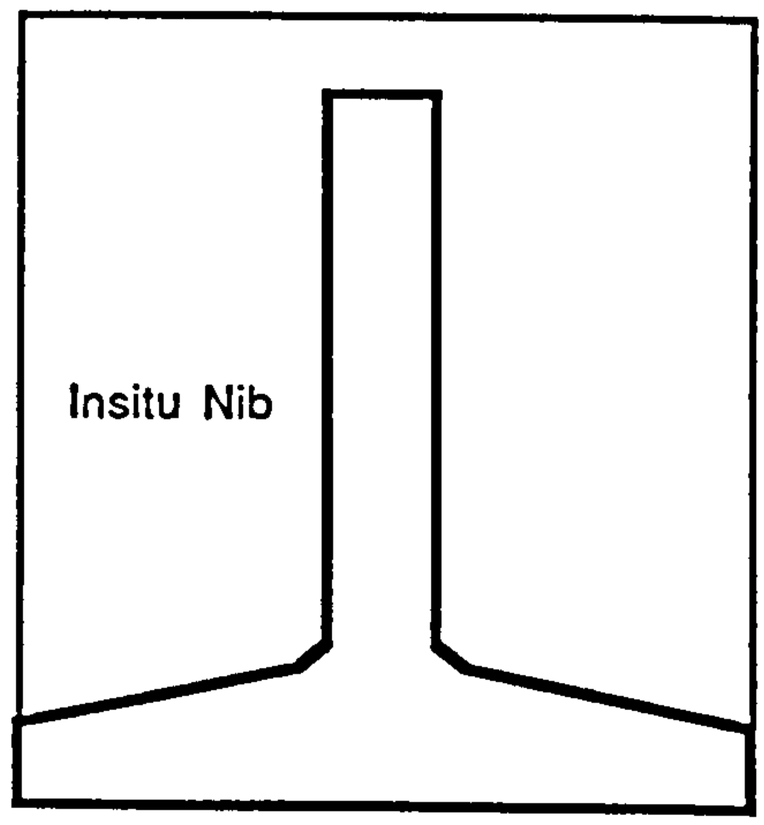

b) Section A : A

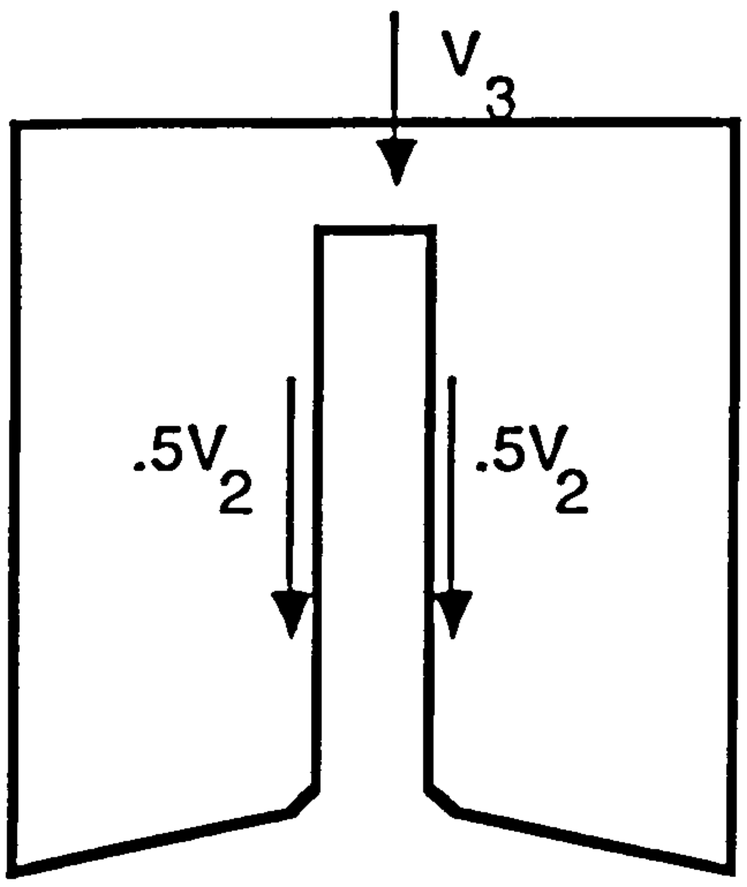

Elimination of top flanges

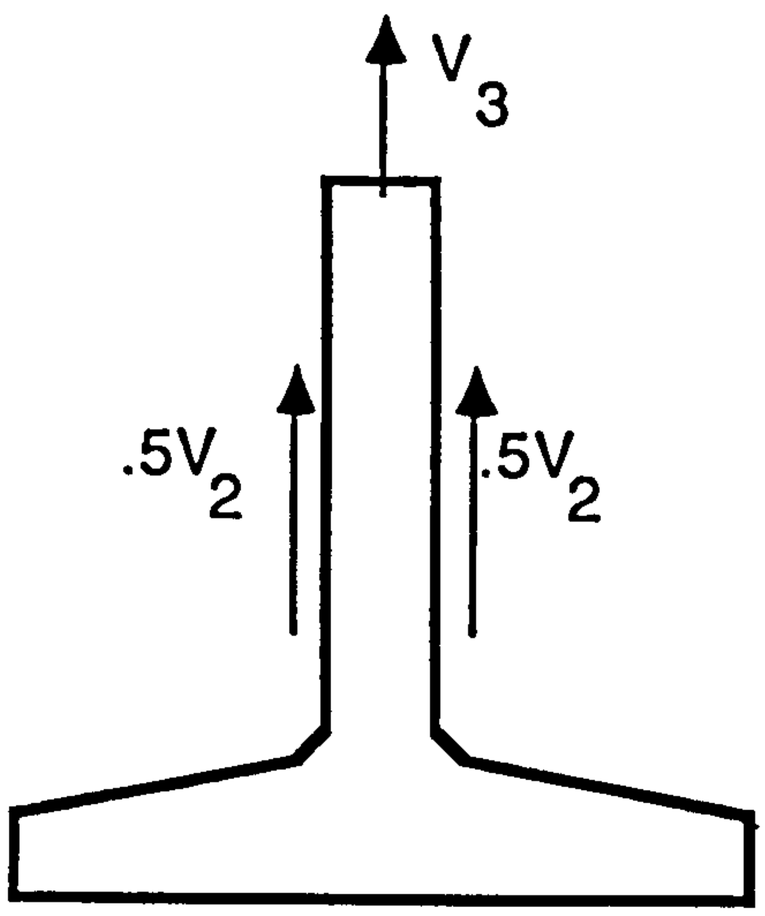

c) Insitu nibs

d) Precast beam without top flanges

FIG. 6.1 Freebody Diagram for The Connection
(Not to Scale)

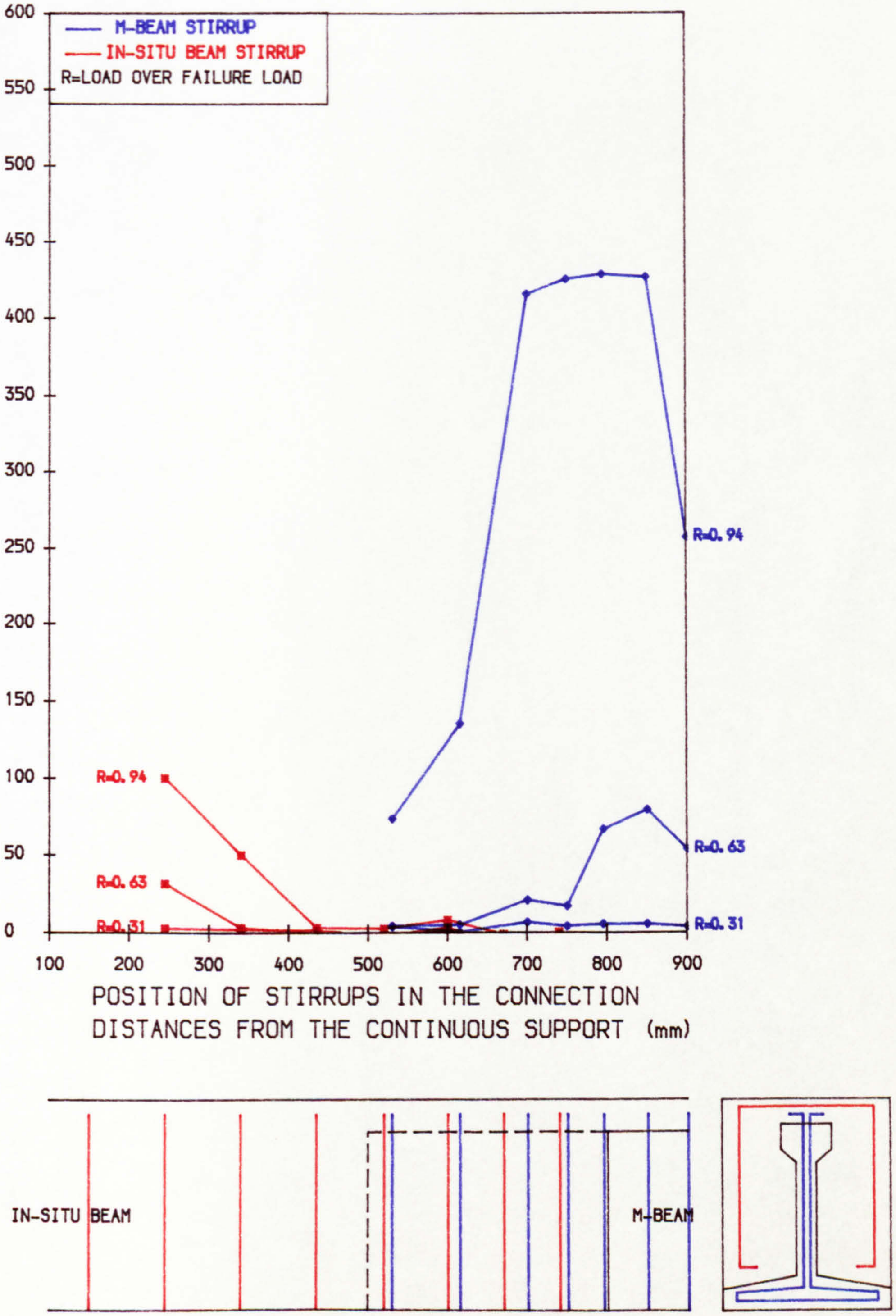

FIG. 6.2 STRESS IN THE SHEAR REINFORCEMENT OF THE CONNECTION IN BEAM WTFCC-6

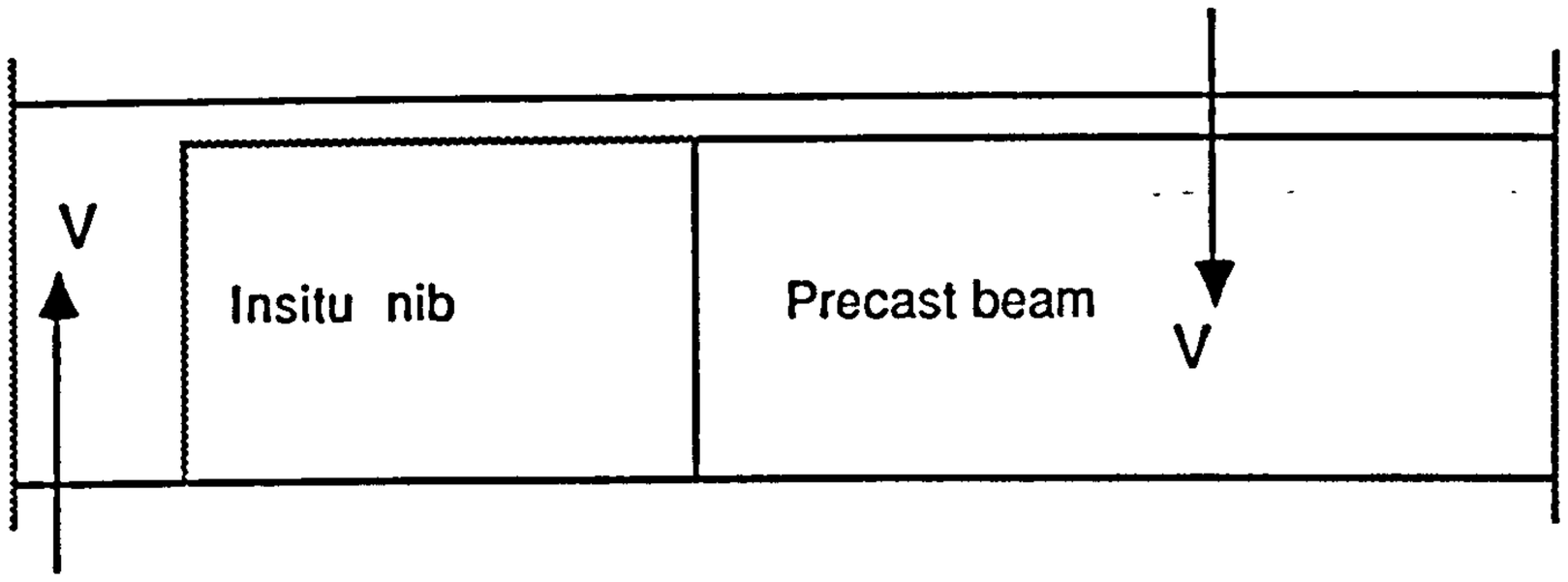

a) The Connection

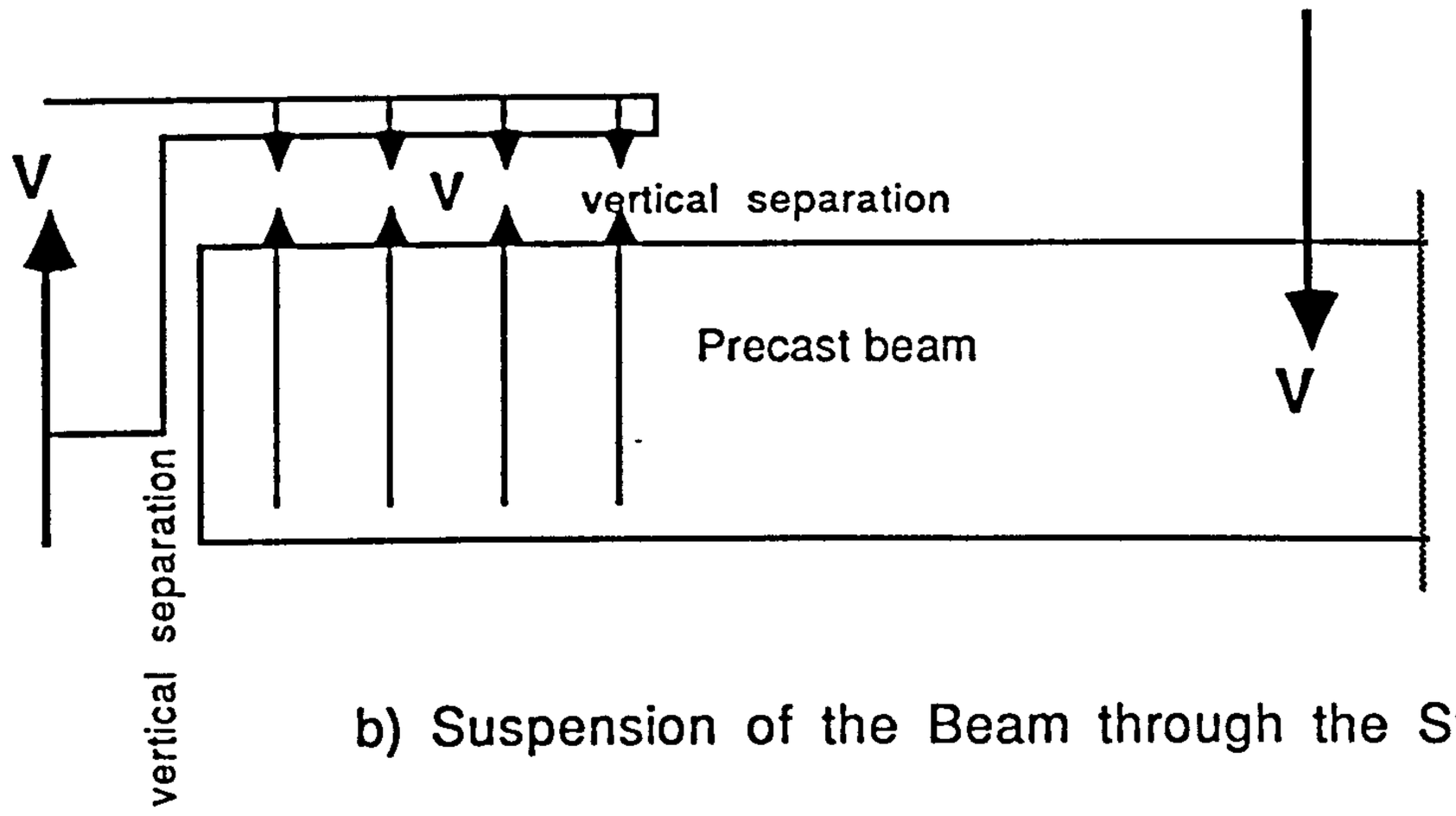

b) Suspension of the Beam through the Stirrups

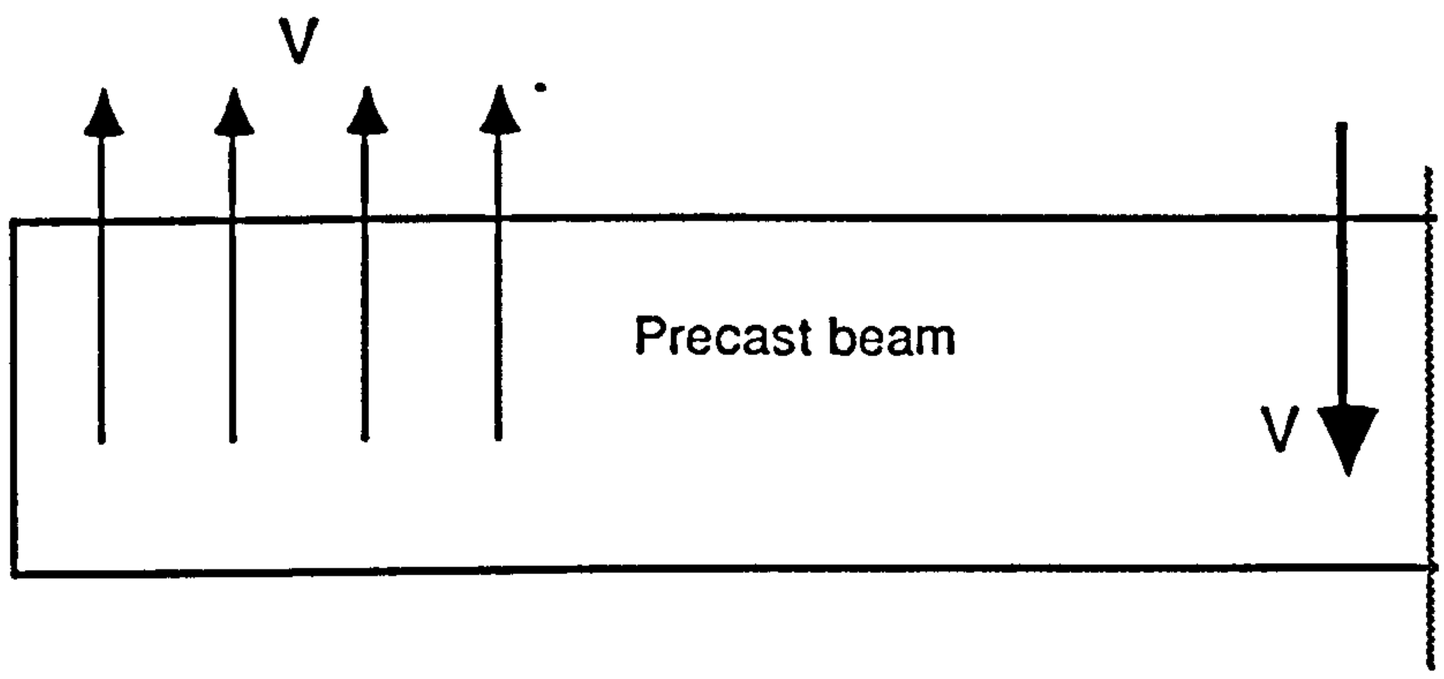

c) The Method of Shear Force Application to the Beam

FIG. 6.3. Behaviour of the Connection without Top Flanges

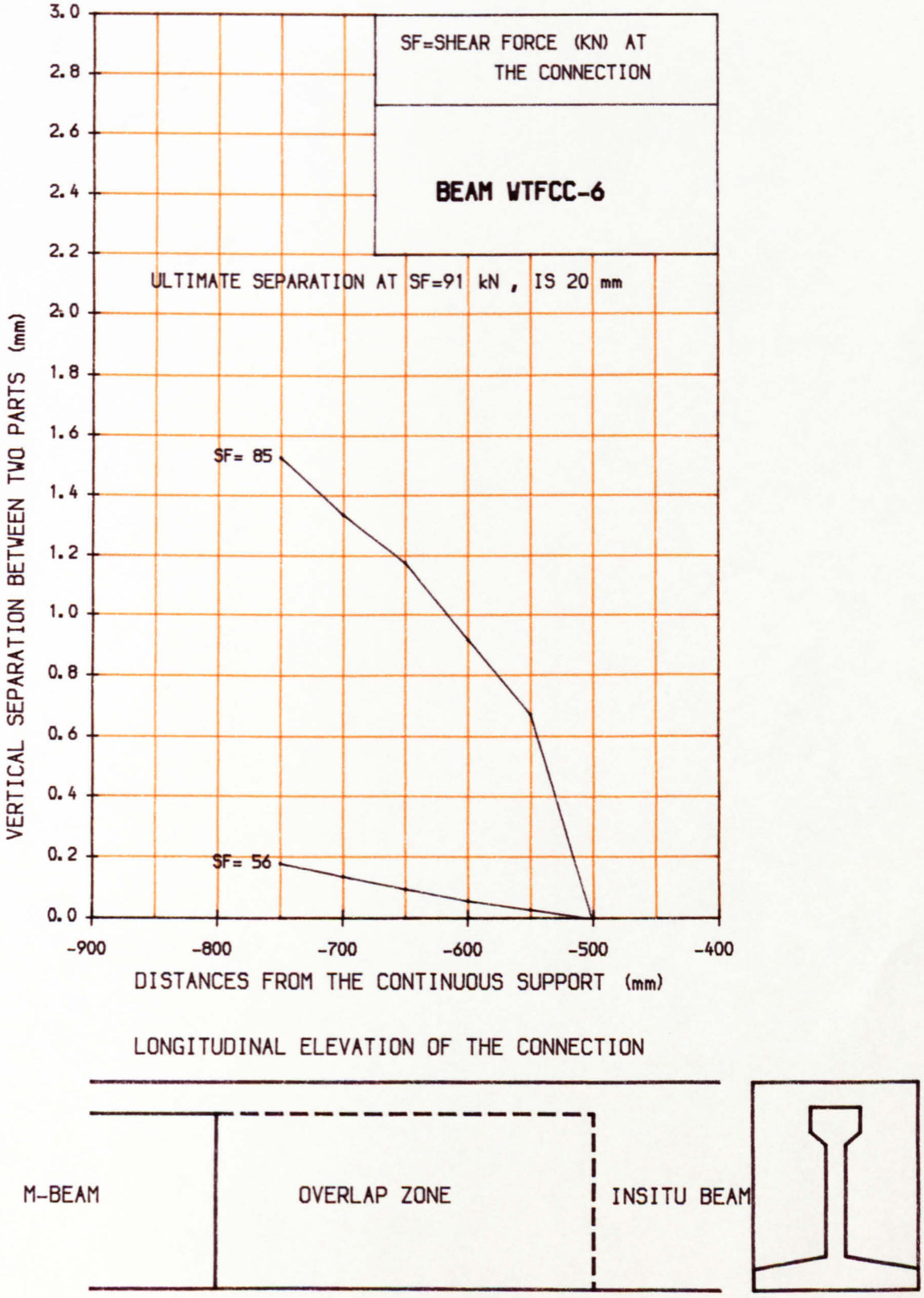

FIG. 6.4 VERTICAL SEPARATION BETWEEN PRECAST BEAM AND IN-SITU NIB

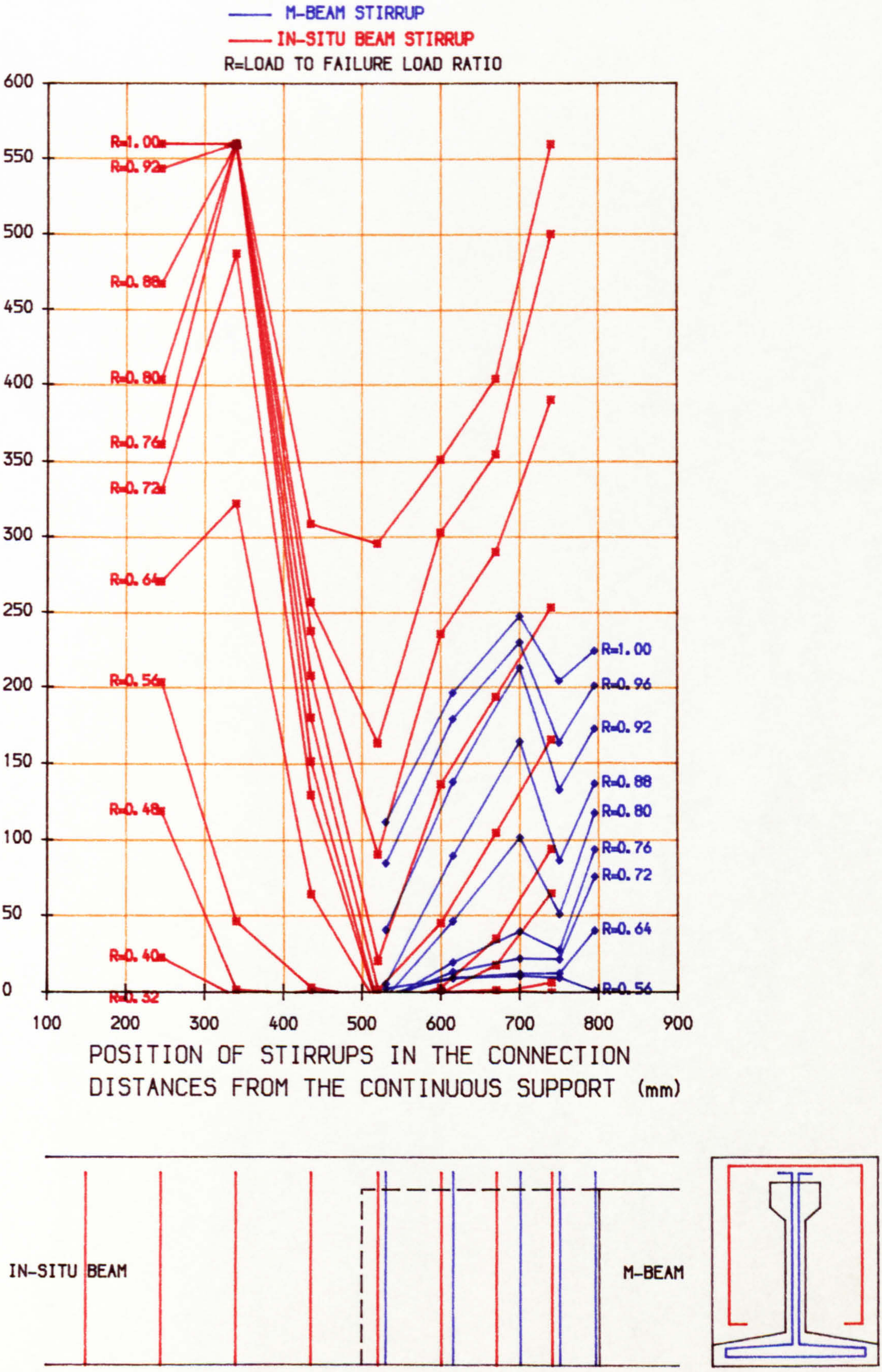

FIG. 6.5 STRESS IN THE SHEAR REINFORCEMENT OF THE CONNECTION IN BEAM WTFPCC-8

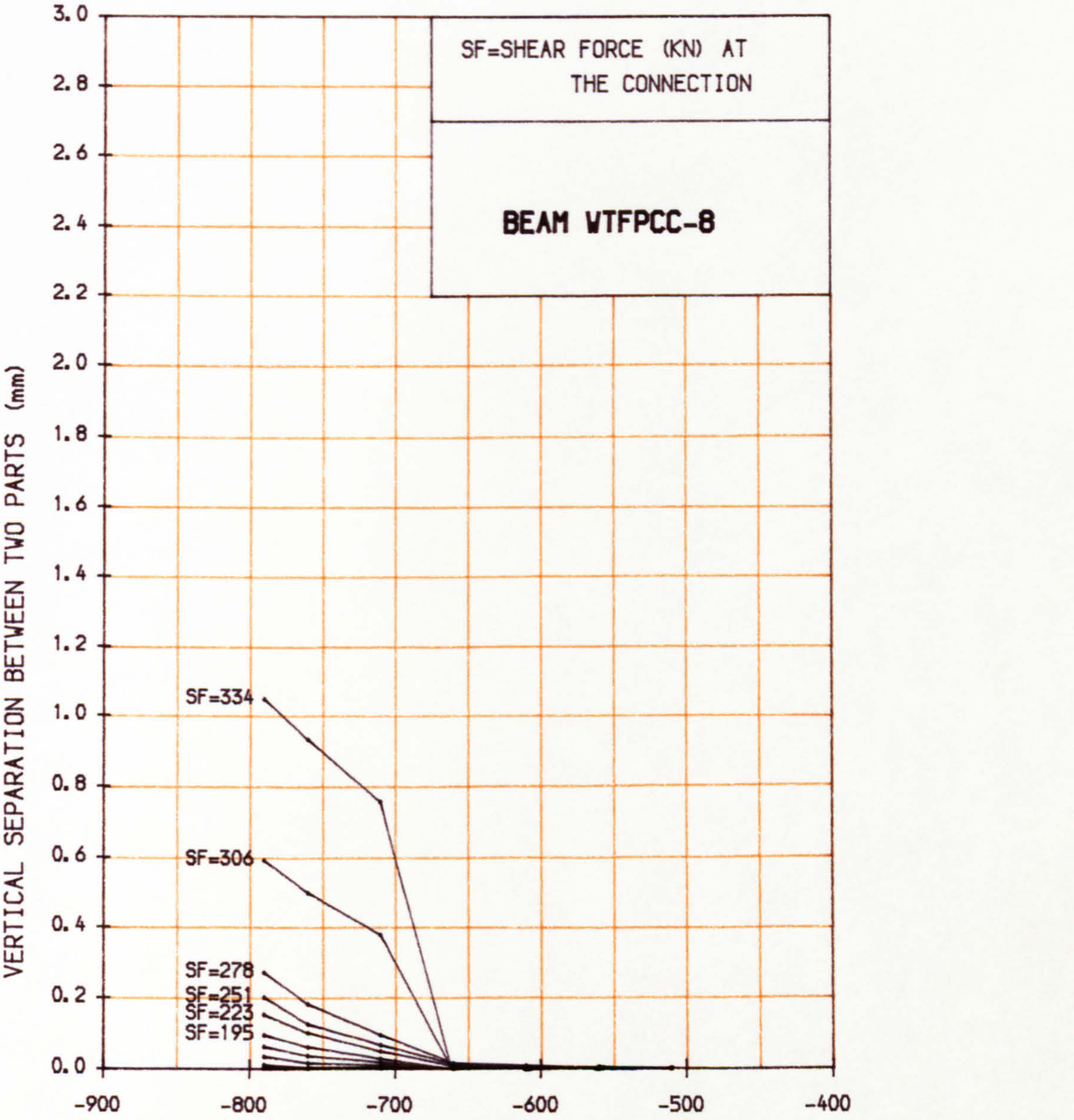

LONGITUDINAL ELEVATION OF THE CONNECTION

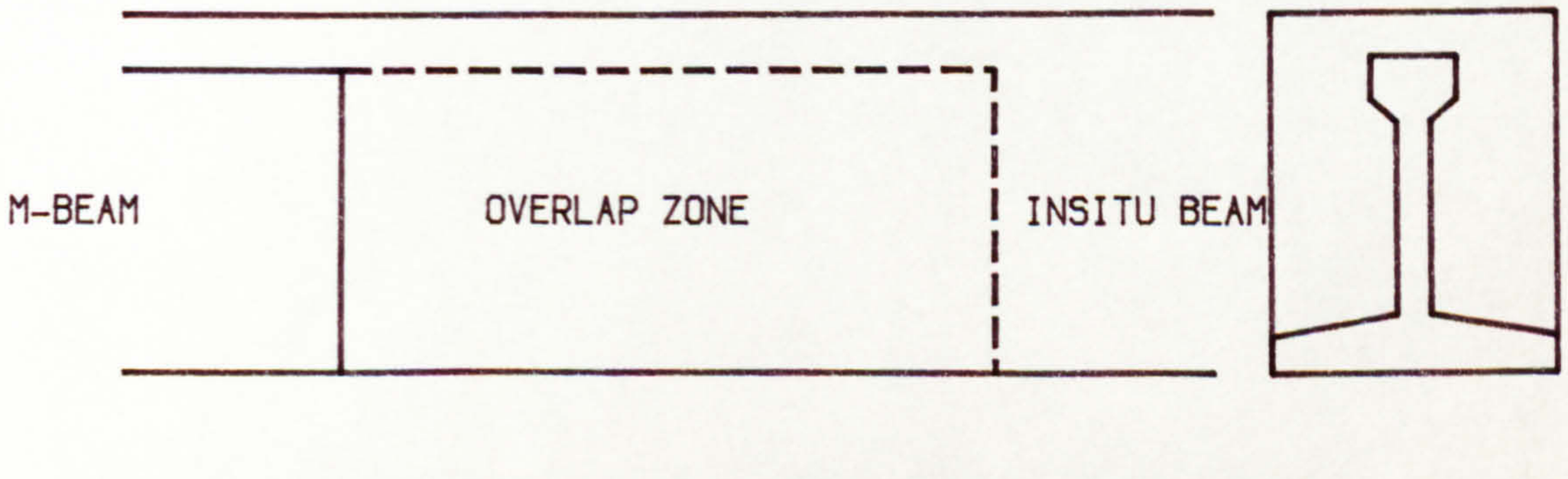

FIG. 6.6 VERTICAL SEPARATION BETWEEN PRECAST BEAM AND IN-SITU NIB

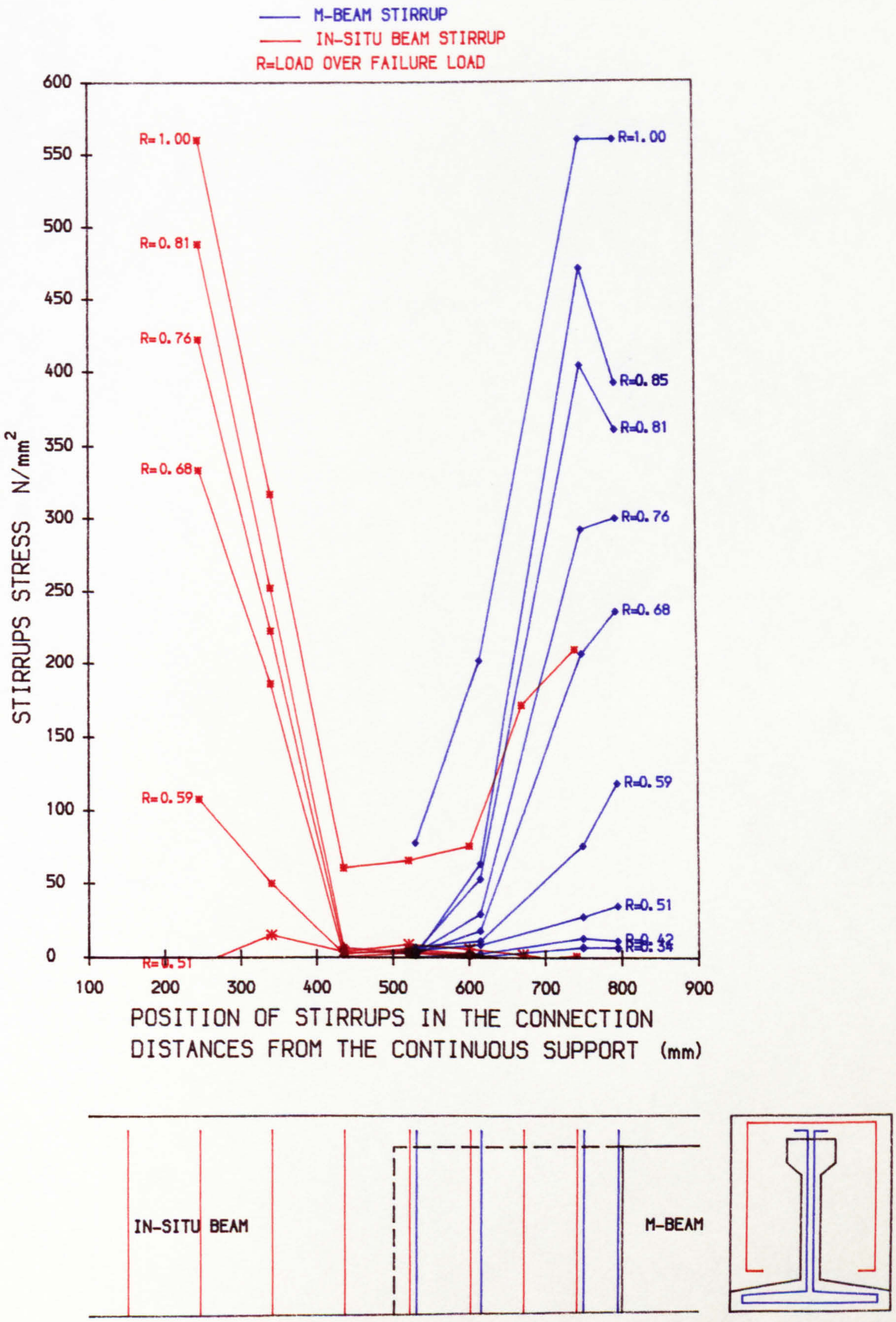

FIG. 6.7 STRESS IN THE SHEAR REINFORCEMENT OF THE CONNECTION IN BEAM WTFCC-9

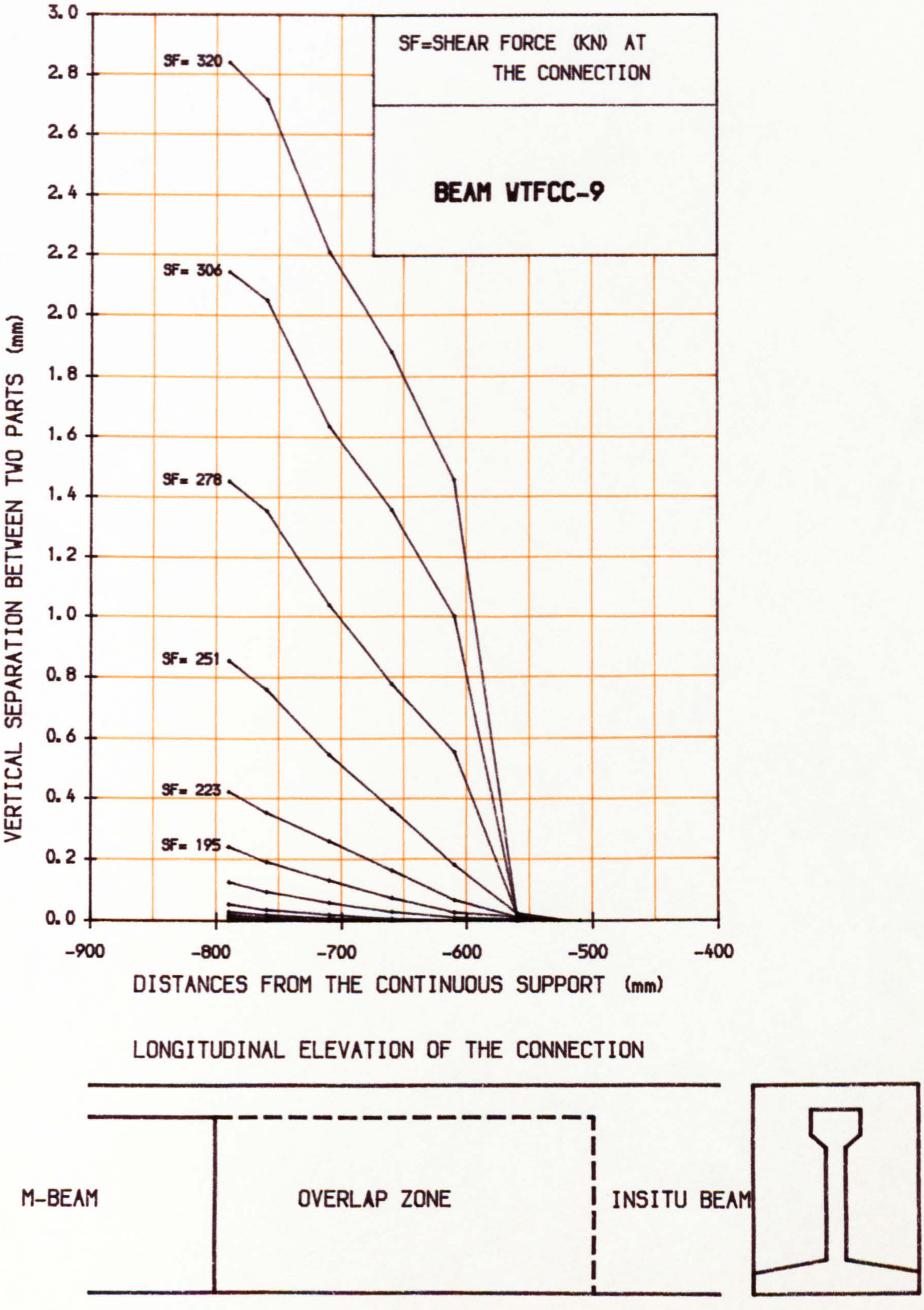

FIG. 6.8 VERTICAL SEPARATION BETWEEN PRECAST BEAM AND IN-SITU NIB

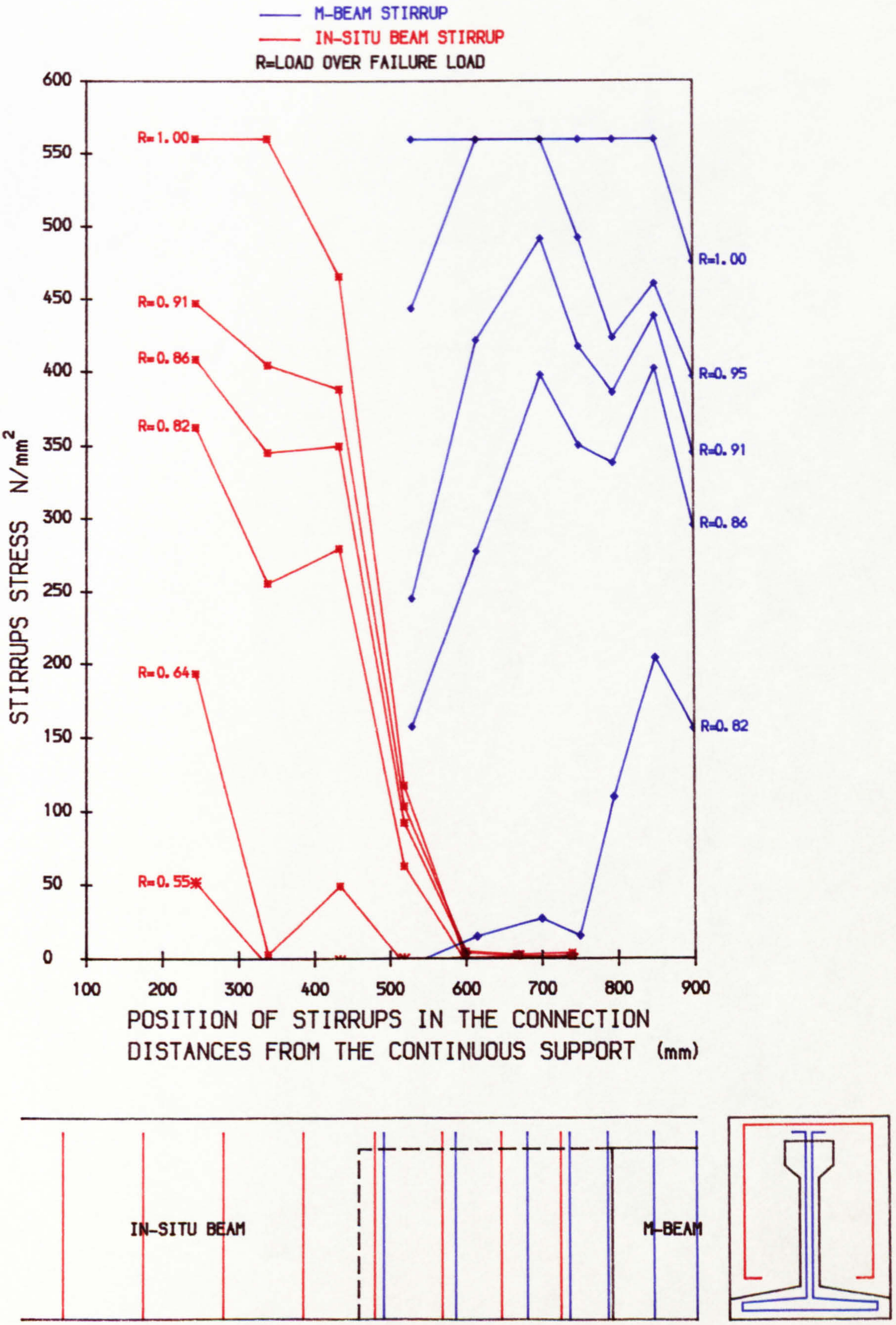

FIG. 6.9 STRESS IN THE SHEAR REINFORCEMENT OF THE CONNECTION IN BEAM WTFDCC-10

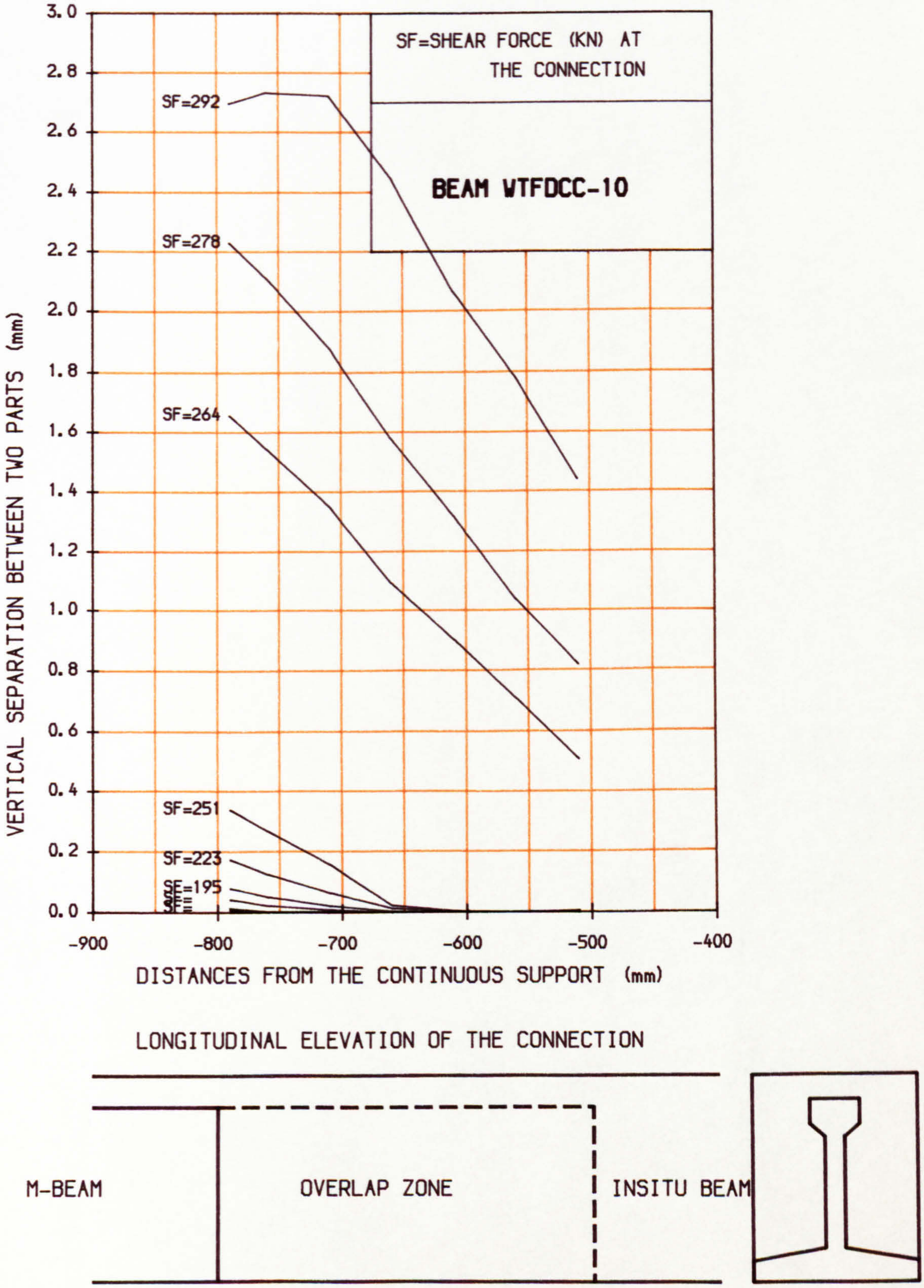

FIG. 6.10 VERTICAL SEPARATION BETWEEN PRECAST BEAM AND IN-SITU NIB

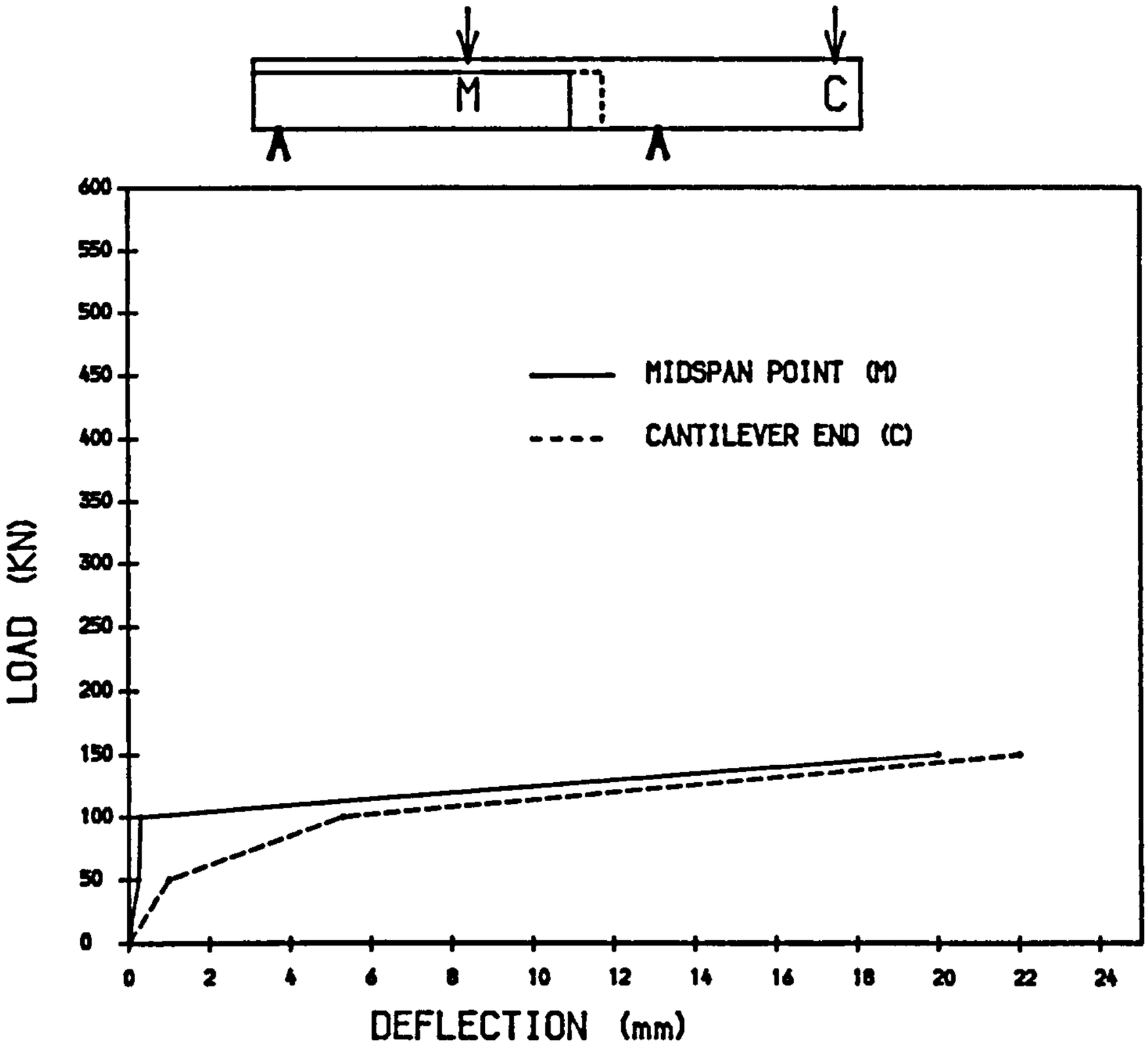

FIG. 6.11 LOAD-DEFLECTION CURVE BEAM WTFCC-6

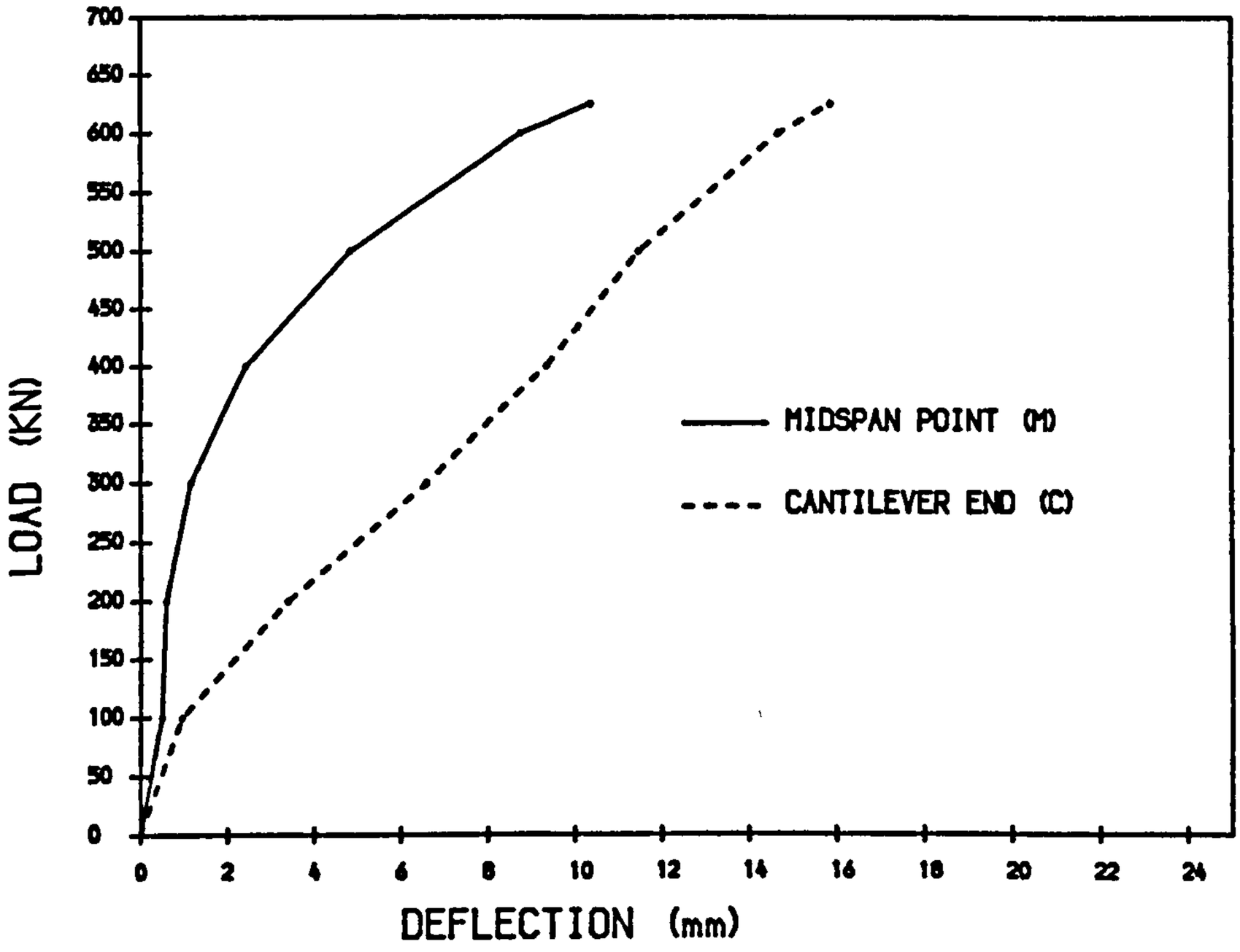

FIG. 6.12 LOAD-DEFLECTION CURVE. BEAM WTFPCC-8

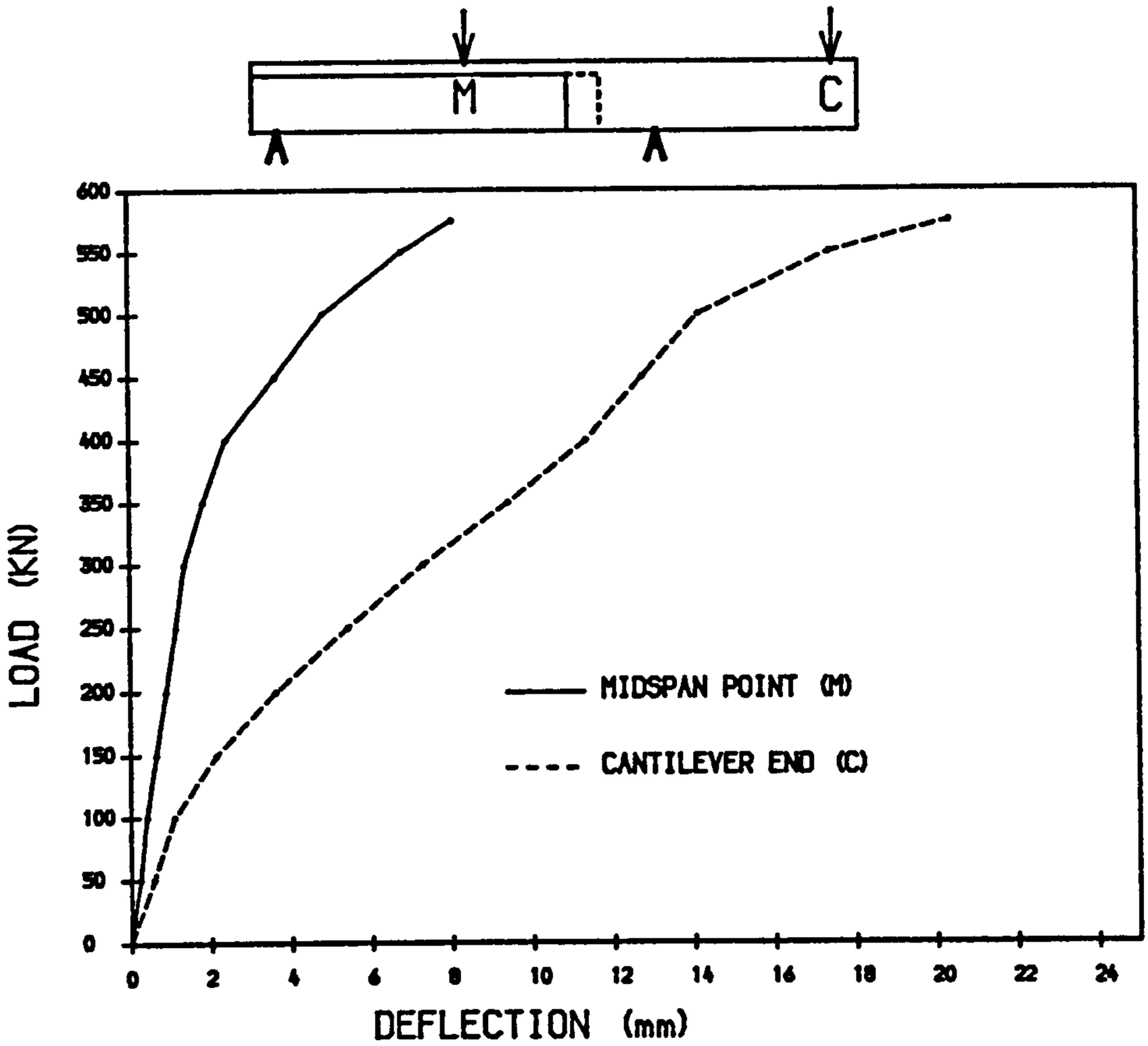

FIG. 6.13 LOAD-DEFLECTION CURVE BEAM WTFCC-9

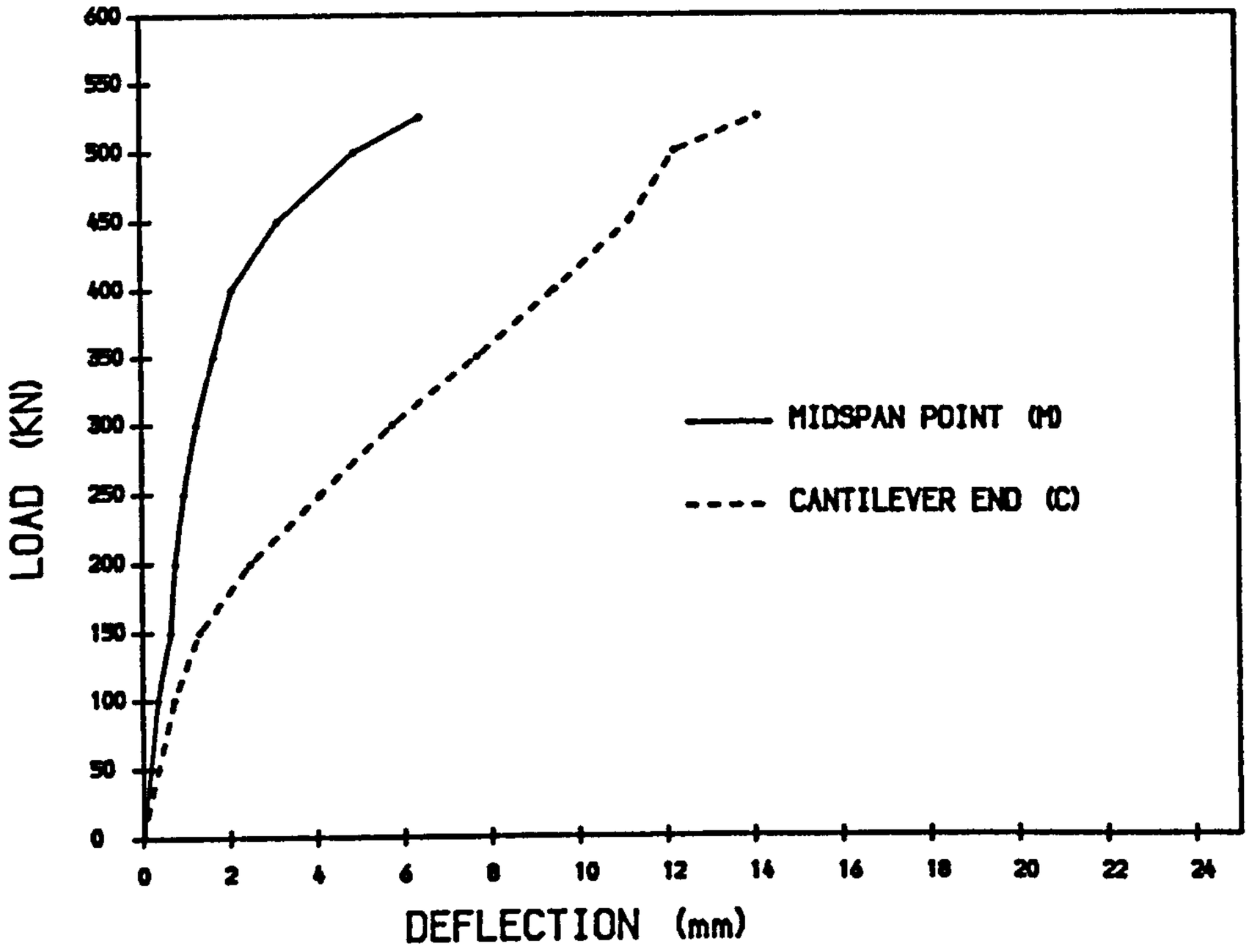

FIG. 6.14 LOAD-DEFLECTION CURVE BEAM WTFDCC-10

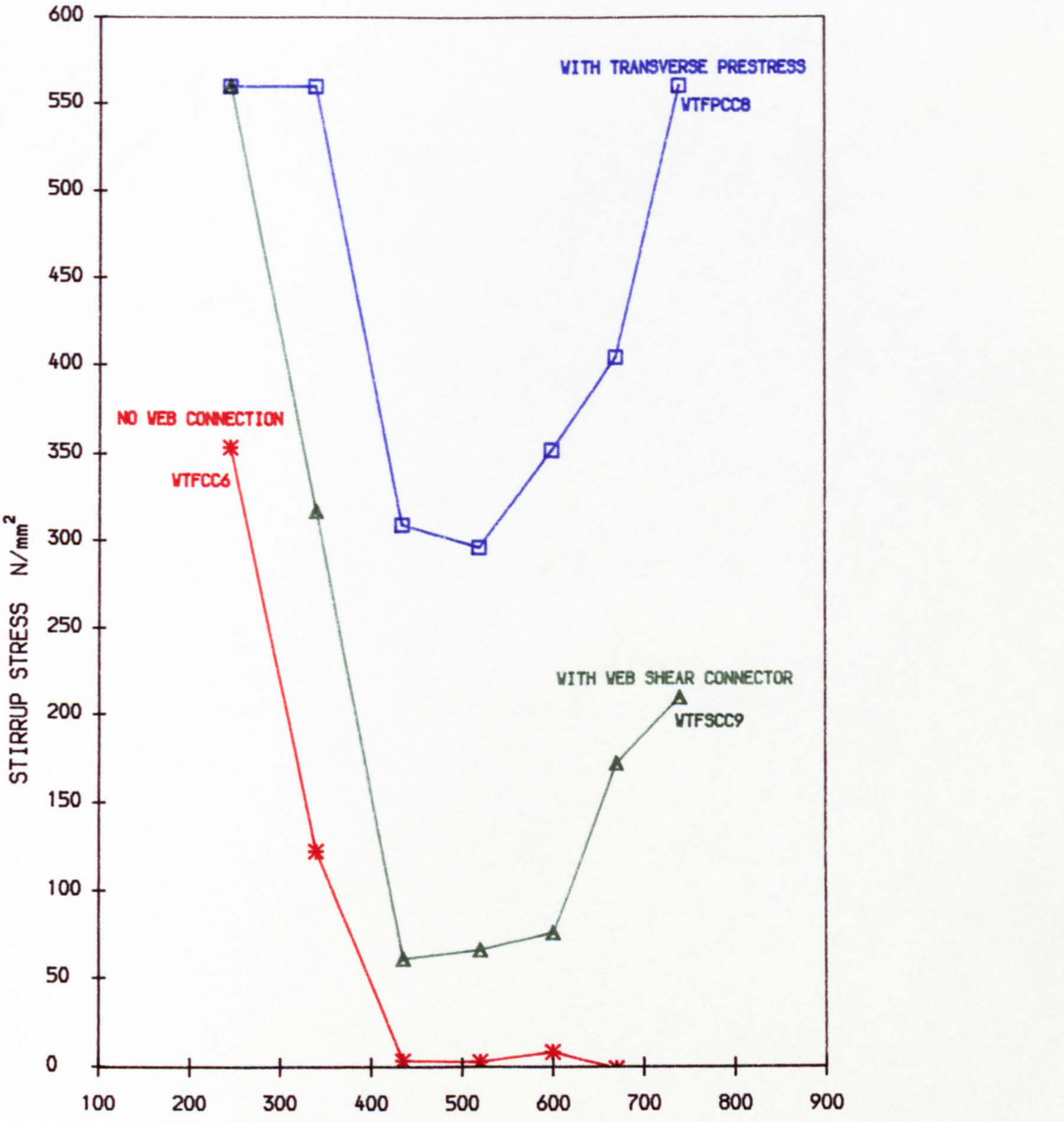

FIG. 6.15 COMPARISON OF INSITU CONCRETE STIRRUP STRESS FOR DIFFERENT TYPES OF CONNECTION AT FAILURE LOAD

CHAPTER SEVEN

COMPLEMENTARY DOWEL SHEAR TESTS

7.1 General

It has been seen in the previous chapter that when the precast section has no top flanges in the connection the web shear connectors can transfer longitudinal shear force by their dowel action. In this chapter the efficiency of these connectors with regard to bar size, steel strength, interface bond and concrete shrinkage (by using dry and wet curing conditions) will be examined with the use of small test specimens.

Each test specimen comprised a 100×100×100mm cube representing the precast beam web connected to a 300×300×100mm concrete representing the in-situ nib as described in chapter three section 3.13.1 and illustrated in Fig. 3.15. The different test conditions have also been summarised in table 3.2.

A joint in a precast concrete structure may be required to resist some or all of the forces which can occur at that point such as axial compression, axial tension, bending, shear and torsion. Since tension in reinforced concrete is taken by the reinforcement, discontinuity in the concrete at the joint does not affect its ultimate strength provided that the steel reinforcement is continuous. The transfer of axial compression is also independent of concrete discontinuity as long as uniform bedding of the contact surface is ensured. Hence the resistance to bending moment, being a combination of the above, presents no particular problem. The resistance to shear is usually provided by concrete (with support from the reinforcement) and this situation is affected by the concrete discontinuity along the shear plane.

In a monolithic reinforced concrete member the direct shear stress can be adequately resisted by the concrete, the problem being the principal tensile stress along an inclined plane. However, at a joint between the precast members where the plane of concrete discontinuity coincides with the shear

plane, the shear force must be transferred by alternative means. The most important parts of shear transfer in such a joint are as follows:

a) Adhesion (bond) created by the in-situ part of the joint.

b) Friction between the two faces in contact (provided by small surface asperities or by aggregate interlock).

c) Dowel action of the reinforcement bars, i.e resistance produced by these bars against the shear deformation (relative movement of the two parts).

7.2 Historical Background

In general two different cases have been considered by past researchers, firstly the dowel shear strength of the joint when other effects (bond and aggregate interlock) are eliminated and secondly the combined effect of bond, aggregate interlock and dowel action in the shear transfer capacity of the joint.

7.2.1 Dowel Shear Strength

The theoretical solution of the dowel mechanism was proposed by Timoshenko and Lessels[85] by considering its behaviour as a flexible beam on an elastic foundation. The stress distribution thus derived is shown in Fig. 7.1 indicating a high concentration of compressive stress in the concrete under the dowel. In applying this theory to determine the shear capacity of the dowel the problems are, firstly the choice of support reaction coefficient and, secondly the appropriate failure criterion. The early approach by Friberg[86] and Loe[87] was to consider the compressibility of the concrete immediately below the dowel for the first and the crushing strength of the concrete for the second. Marcus[88] made an extensive experimental study of dowel strength and arrived at a different type of expression which agreed with his range of parameters but was of limited general application.

In general two possible modes of failure have been suggested for the dowel mechanism:

a) Yielding of the dowel bar and crushing of the concrete under it.

b) Splitting of the concrete.

The main parameter upon which the failure mode of the dowel mechanism depends is the concrete cover to the bar. Tests have shown[90] that when the cover is greater than 6 to 7 times the bar diameter, the failure is governed by crushing of concrete and yielding of the bar. For smaller concrete cover, failure is produced by the concrete splitting, where splitting cracks open either at the bottom or at the side faces of the section.

For the prediction of the dowel strength in the first mode (simultaneous concrete crushing and bar yielding) several formulae have been proposed. Dulacska[91] and Mills[92] proposed the following idealized formula obtained from basic theory :

$$V_{dc}=kd_b^2\sqrt{f_{cu}\,f_y} \qquad \text{.....(7.1)}$$

where d_b is the diameter, f_{cu} and f_y are concrete and steel strength, k is a constant to be determined by testing and V_{dc} is the dowel strength. This equation can satisfactorily predict dowel strength when the dowel force is applied at the face of the concrete (zero eccentricity).

For the dowel strength in the case of concrete splitting, (low concrete cover), all the suggested formulae are empirical, and indicate that the dowel strength V_{ds} depends on a number of variables such as bar diameter, bottom and side concrete cover, concrete strength etc. . Krefeld and Thurston[93] suggested that for concrete beams:

$$V_{ds}=b\sqrt{f'_c}[1.3(1+180\rho/\sqrt{f'_c})c+d]/\sqrt{x_1/d} \qquad \text{(psi).....(7.2)}$$

or: $$V_{ds}=10.7b\sqrt{f'_c}[1.3(1+16.8\rho/\sqrt{f'_c})c+d]/\sqrt{x_1/d} \qquad \text{(SI).....(7.3)}$$

where: ρ=percentage of dowel reinforcement

c=concrete cover

x_1=distance of diagonal crack from beam support

d=distance from extreme compressed fibre to centroid of dowel

V_{ds}=dowel strength when the failure is by concrete splitting

Taylor[38] suggested the following empirical expression for the dowel strength of horizontal bars in reinforced concrete beams:

$$V_{ds}=9.1+0.0001[\Sigma(C_s+C_i)]^2 f_{ct} \quad \text{(in kN)} \quad \ldots\ldots\ldots\ldots\ldots\ldots(7.4)$$

where: f_{ct}=tensile strength of concrete (N/mm^2)

C_s=side cover to the dowel bar(s)

C_i=horizontal distance between adjacent bars

In a recent investigation Soroushian et al[94,95] carried out two series of push-off tests to investigate parameters affecting each mode of dowel failure. For the first mode of failure i.e yielding of the bar and crushing of the concrete (so called dowel action against concrete core) using mathematical equations for the behaviour of a beam on an elastic foundation together with experimental results, they derived practical relationships for dowel strength and load-deflection. They also came to the conclusion that the bar diameter is the main factor influencing the dowel behaviour in action against the concrete core. Other factors include steel and concrete strengths and bar inclination.

For the second mode of failure (concrete splitting), which they[94] refer to as dowel action against concrete cover, they concluded that the dowel behaviour in action against concrete cover is similar to action against the core before a crack separates the cover from the core. After this split cracking, behaviour depends on the bar size, contribution of concrete cover and stirrup locations in each part of specimen. An analytical expression for the prediction of dowel load

at split cracking was also suggested by this author.

7.2.2 Combined Behaviour of Dowel and Interface Shear

In general two types of tests have been undertaken in this category, first, the direct investigation of shear resistance by push-off tests on two blocks of concrete held in contact with different interface conditions (bonded, unbonded, rough, smooth and dowelled) to represent a connection or a joint in practice, and second, tests on actual composite beams from the point of view of horizontal shear transfer at the junction of a precast beam and in-situ concrete slab in composite construction. Hanson[9] reports several tests both of push-off and composite beam variety where he determined load-slip characteristics as well as ultimate strength for various types of bonded, unbonded and keyed interfaces. Saemann and Washa[96] further extended Hanson's work. In their investigation on interface action and the recommendation on allowable shear stresses, primary importance was placed on the nature of the concrete surface, and the shear transfer mechanism was attributed mainly to bond and surface interlock, the role of the steel transversing the shear plane being considered of a secondary nature.

In a somewhat different approach to the mechanism of interface shear, Birkeland and Birkeland[97] postulated a theory supported by Mast[98] where the shear resistance was claimed to be a direct function of the tensile strength of the steel bar crossing the shear plane. This theory (hypothesis) is called "shear friction". According to this theory the external shear force tends to produce slippage along the shear plane. Considering that the interface is rough, this slippage will separate the two parts in a direction normal to the interface, which in turn requires a balancing tensile force in the bar crossing the shear plane. Since the reinforcing bar is well anchored on both sides of the interface, this tension provides an external clamping force on the concrete resulting in

compression across the interface of equal magnitude. The interface resistance to shear force according to friction law is therefore:

$$V_u=\mu A_s f_y \qquad \text{.....(7.5)}$$

where μ is the coefficient of friction, depending on the nature of the surfaces and which should be obtained by tests. It has been also suggested by Mast[98] that because of inherent uncalculated loads arising from fabrication, erection,creep shrinkage, temperature changes and differential settlement, it is imperative that such a connection possesses ductility. This ductility must normally be obtained through the use of reinforcing steel, rather than through reliance on the brittle tensile or shearing strength of the concrete. In a later investigation Hofbeck, Ibrahim and Mattock[99] carried out a series of push-off tests on concrete specimens with and without pre-existing cracks along the shear plane. They concluded that the shear friction theory gives a conservative estimate of the shear transfer strength of initially uncracked concrete.

The American Building Code[81] ACI 318-83 introduces a shear friction design method in section 11.7 with the following equation:

$$V_u=A_{vf}f_y(\mu \mathrm{Sin}\alpha_f+\mathrm{Cos}\alpha_f) \qquad \text{.....(7.6)}$$

where A_{vf} , f_y and α_f are cross-section area, yield stress and the angle that the bar makes with the shear plane. For reinforcement normal to the shear plane (α_f =90°) the same equation (Eqn. 7.5) will be obtained. The coefficient of friction (μ) will change from 0.6 to 1.4 for different surfaces, the least being for concrete placed against hardened concrete not intentionally roughened.

The cross-sectional area of the contact surface is not considered in the shear-friction theory as in the classical friction law. This means that there is no bond between the two concretes and only the roughness of the surface is

considered by introducing different μ values. In practice however, there is some bond between the two concrete surfaces if one is cast against another, hence, the contact surface will have an increasing effect upon the shear transfer capacity of the joint. In fact the available data by Anderson[100], Hanson[9] and Hofbeck et al[99] show that:

$$v_u=v_s+\mu\rho f_y \qquad \text{.....(7.7)}$$

where v_s is the shear stress transferred by the bond and roughness between the two concretes and is found to have an appreciable value of ranging from 0.65 to 5.5 N/mm^2 according to circumstances.

Bennett and Banerjee[101] considered this bond effect and introduced the following equation for connections subjected to shear force:

$$V_u=(\alpha v_0 A_c+1.48A_s\sqrt{f_{cu}\, f_y}) \qquad \text{.....(7.8)}$$

where, for a smooth concrete interface:

α=ratio of contact area to total area

v_0=constant component of shear resistance

Since the second term in the right hand side of the above equation is dowel strength against concrete crushing (similar to Eqn. 7.1), and in their test specimens the top dowel bars are acting against concrete cover which has a lower strength, they suggested that only half of the area of the top bars should be considered to be effective.

The British Code BS8110[27] suggests in section 5.3.7d that if the shear force is to be transferred by the steel reinforcement crossing the interface of concrete surfaces, the ultimate shear force should be:

$$V_u=0.6F_b \tan\alpha_f \qquad \text{.....(7.9)}$$

where F_b is $0.87A_sf_y$ or the anchorage value of the reinforcement, whichever is the lesser and α_f is the angle of internal friction between the faces of the joint and $(\tan\alpha_f)$ varies between 0.7 and 1.7 (but is best determined by test). However, for a smooth interface $\tan\alpha_f = 0.7$. Removing the steel strength reduction factor (0.87) from F_b :

$$V_u = 0.6 \times 0.7 A_s f_y = 0.42 A_s f_y \quad \text{.....(7.10)}$$

Comparing with ACI equation (Eqn. 7.6) when applied to smooth surfaces, and with dowels normal to the interfaces, the ultimate shear will be $0.6A_sf_y$ i.e ACI prediction is 43% greater than BS8110 prediction.

7.3 Test Details and Change of Variables

The test specimens (see Fig. 3.15) are 'double shear' connections, i.e the total applied load is divided into two equal shear forces acting on the side interfaces. One dowel bar was used in each specimen passing through both interfaces and anchored into the surrounding block from each end. The following variables were examined:

a) Dowel bar size and strength (mild and high yield steel bars)

b) Curing, wet and dry conditions to observe the shrinkage effect

c) Bond between blocks (concrete cast against smooth concrete surface), unbonded interface using polythene sheet between the two concretes.

Concrete strengths for the central and surrounding blocks were identical to those used for the precast and in-situ concrete in the main test program.

7.4 Experimental Results

The ultimate failure load for each specimen together with appropriate notation showing different test details and conditions are shown in table 7.1.

7.4.1 Observed Mode of Failure

The specimen detail and testing arrangement indicate that the concrete cover to the bar does not control the failure because the top and bottom of the specimen are restrained between two thick steel plates for the application of external load as can be seen in Fig. 3.15. In the actual connection between the precast beam's web and the in-situ nibs using shear connectors there is also sufficient cover to the dowel bars to prevent the second mode of dowel failure (dowel action against concrete cover as explained in 7.2.1b). In fact all the test specimens exhibited the first mode of failure (dowel action against concrete core as explained in 7.2.1a).

In general a crack was observed along the bar in the weaker block which then followed the contact interface leading either to a corner or other side of the bar. Crack patterns after the failure have been shown for some of the specimens in Fig. 7.2.

7.4.2 Ultimate Shear Strength in Smooth-Bonded Connection

In the light of the discussion on dowel action and interface shear resistance, the following general expression may be derived for the quantitative assessment of joint strength.

$$V_u = V_s + V_d \quad \text{.....(7.11)}$$

V_s is the constant component of the shear resistance depending upon the surface roughness and the bond between two parts. V_d is the shear force carried by the dowel action and depends on a number of variables including A_s, f_y and f_{cu}. For the dowel area (A_s), most investigators agree that the dowel strength is proportional to it but there are different opinions in the way that f_y and f_{cu} have an effect. Some investigators including Dulacska[91], Mills[92], Bennett and Banerjee[101] suggest that the dowel strength is proportional to $\sqrt{f_{cu}f_y}$. Hofbeck et al[99] and also recommendations by the British[27] and American[81] Codes relate the dowel strength to f_y only.

The observed dowel strength by the author were found to have a linear correlation with steel strength (f_y) taking into account that a constant concrete strength was used throughout the investigation. Clearly more research work is required when the concrete strength is a variable. The experimental values of V_u have been plotted against A_sf_y in Fig. 7.3. The British and American code predictions for the same surface conditions (smooth & bonded) have been drawn on the same figure. The best line to fit the experimental results is:

$$V_u=46.0+0.52A_sf_y \quad \text{(kN)} \qquad \text{.....(7.12)}$$

where V_u and A_sf_y are in kN. The constant interface shear will thus be obtained by considering the total contact area, and thus providing an appropriate value of: $v_s=46000+28000=1.64 \ \ N/mm^2$

The BS8110 and ACI codes do not consider a constant shear strength for the interface and only introduce different factors (μ) due to conditions (bond and roughness) to be used in Eqn. 7.5. All the safety factors have been removed from the code prediction lines in Fig. 7.3. The observed safety factor depends on

the value of $A_s f_y$ and for $A_s f_y$=100 kN , the observed safety factor is 1.6 for ACI and 2.5 for BS8110 comparing with the code values of 1/0.9=1.11 and 1/0.87=1.15 respectively. For higher values of $A_s f_y$ the code predictions are closer to experimental values. Some tests were performed without using dowel bars so the constant interface shear strength was obtained. In practice however, the interface bond between precast and in-situ concrete can easily be affected by creep, shrinkage and temperature changes and that may be the reason for the conservative values suggested by the codes.

7.5 Shear Capacity of Smooth-Unbonded Connection

In this part of the investigation the bond between in-situ and precast concrete was eliminated by using polythene sheet at the interface to simulate the practical case in which the interface shear resistance (bond and interlock) has been destroyed as a result of shrinkage, creep, temperature change etc.

7.5.1 Ultimate Resistance and Failure Mode

In general, the observed shear resistance for these connections was lower than those observed for bonded connections, the difference being approximately equal to the failure load for the bonded connection without a dowel bar (see table 7.1). The observed values of failure load (V_u) were plotted against $A_s f_y$ shown in Fig. 7.4 together with ACI and BS8110 predictions (where all safety factors have been removed). All the specimens failed in the first type of dowel failure (action against core) explained in section 7.4.1.

It can be seen from Fig. 7.4 that the observed values are closer to the lines suggested by the codes (in comparison with bonded connections). The British Code is seen to give values with sufficient safety factor but the ACI

predictions are slightly unsafe especially for higher $A_s f_y$ values. The reason is that both code predictions (i.e $V_u=\mu A_s f_y$) are for μ values which consider some bond at the interface and there are no suggested μ values for a completely smooth-unbonded connection.

7.6 Shrinkage Effect

For each dowel bar size two curing conditions were considered. The first specimen was kept in the curing room with 100% humidity and the second specimen was left in dry conditions to allow shrinkage to occur. The observed shear transfer capacity for this condition was between 22% and 35% lower than those for specimens cured in wet conditions. It should be noted that in no case had the bond been completely destroyed as a result of shrinkage.

7.7 Application of the Results to Design of Web Shear Connectors

As discussed in a previous chapter (section 6.9), with the absence of top flanges in an inverted 'T' beam the shear transfer may be performed by the use of horizontal bars passing through the beam's web and anchored inside the surrounding in-situ nibs.

It was suggested in 6.13.1b that about 30% of the shear force is transferred by the monolithic top slab over the beam and therefore the web connection should be designed for 70% of the design shear force.

In practice the in-situ concrete nibs and crosshead are cast on site and may be subject to some shrinkage. In addition to that, the web surface is very smooth and even some dust and mould oil may exist on it. For these reasons it is recommended here that no account should be taken of the constant interface shear strength (discussed in 7.4.2) and only the effect of dowel bars should be

considered.

For the design of dowel bars in a smooth-unbonded connection, the most suitable method was observed (see section 7.5.1) to be the BS8110 method (see also Fig. 7.4). The following Eqn. therefore should be used to determine A_s.

$$V_u=0.6\times0.7\times0.87\ A_sf_y=0.36\ A_sf_y \quad \text{.....(7.13)}$$

Since the connection is a 'double shear' type , the required amount of dowel area (which passes through both interfaces) is half the value obtained for A_s from above equation i.e. :

$$A_s=0.5[V_u/0.36f_y]=1.39V_u/f_y \quad \text{..... (7.14)}$$

Table 7.1 Dowel Shear Test Results

No.	Details*	Failure Load(kN)	No.	Details*	Failure Load kN
1	R10BW	70.3	17	R16BW	102.5
2	R10BD	57.4	18	R16BD	77.8
3	R10UW	40.5	19	R16UW	56.0
4	R10UD	37.2	20	R16UD	58.8
5	T10BW	90.0	21	T16BW	143.5
6	T10BD	75.9	22	T16BD	111.2
7	T10UW	45.6	23	T16UW	97.0
8	T10UD	48.9	24	T16UD	88.0
9	R12BW	95.1	25	PBW	48.8
10	R12BD	75.1	26	PBD	36.1
11	R12UW	48.2	27	PUW	7.0
12	R12UD	45.0	28	PUD	5.0
13	T12BW	110.3			
14	T12BD	81.2			
15	T12UW	72.1			
16	T12UD	65.0			

* B : Bonded R : Mild Steel

U : Unbonded T : High Yield Steel

W : Wet Curing P : Plain Concrete (No Dowel Bar)

D : Dry Curing 10,12,16 : Bar Diameter (mm)

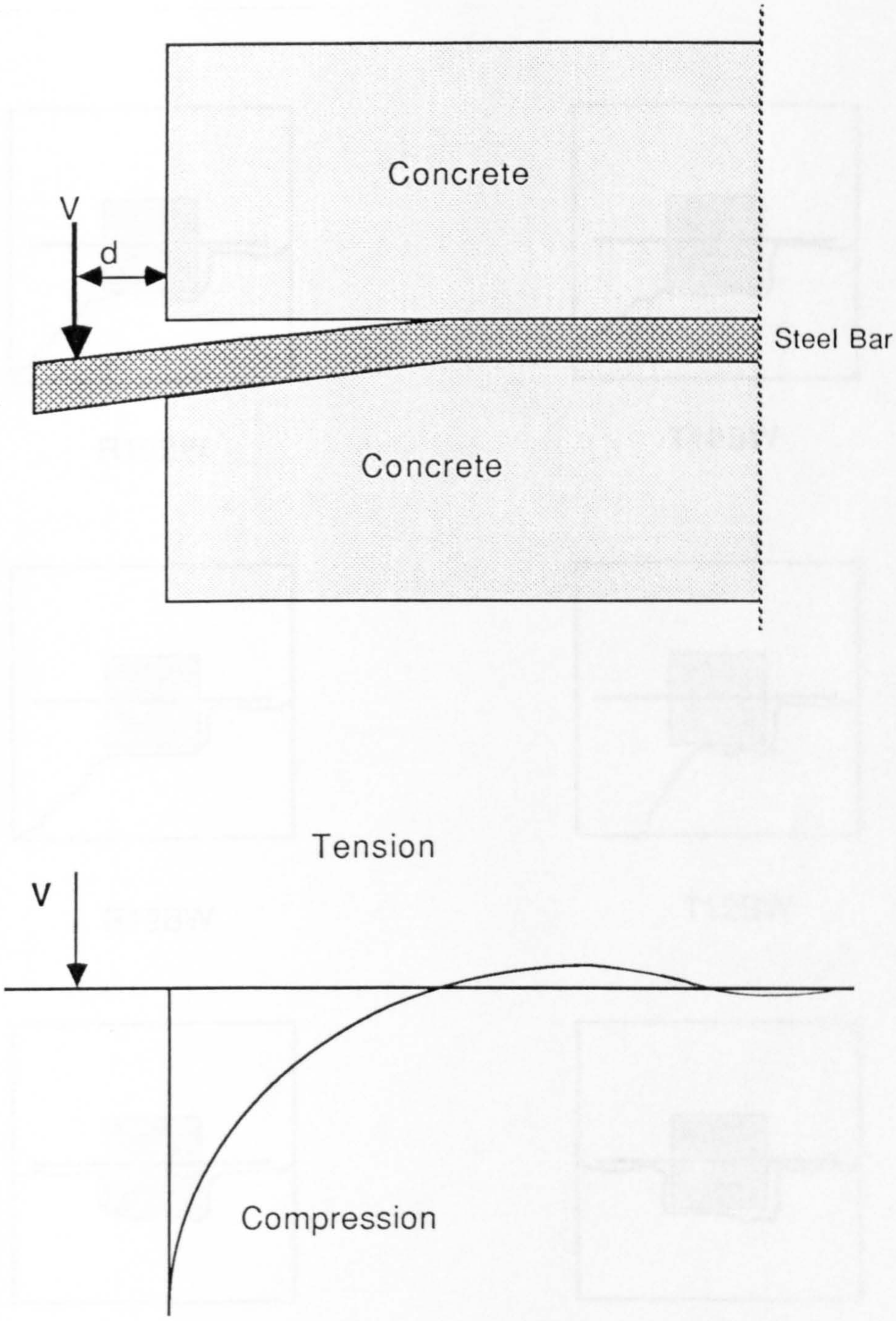

FIG. 7.1 Deformation and reaction under dowel[85]

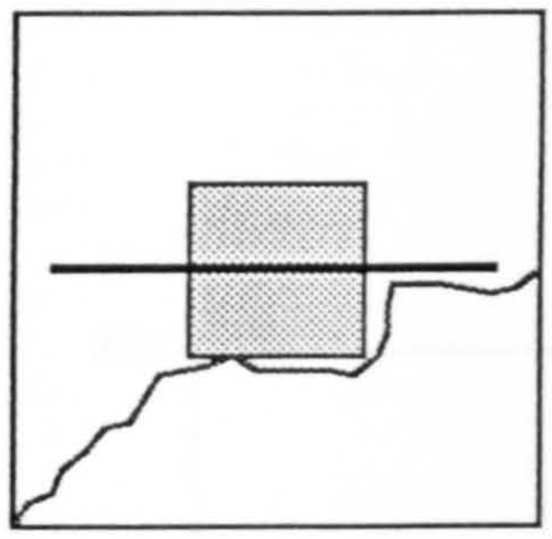

R10BW

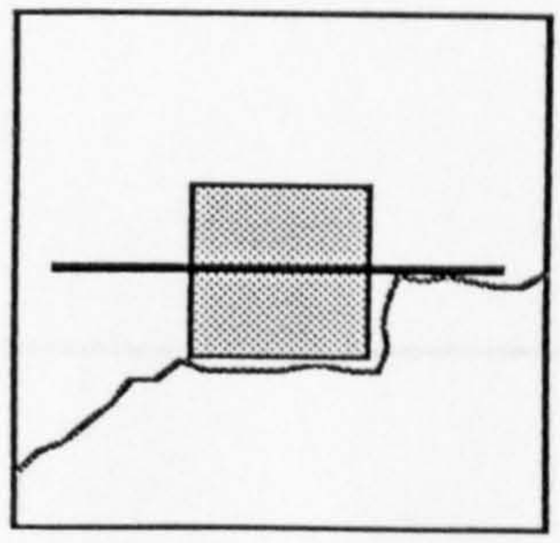

T10BW

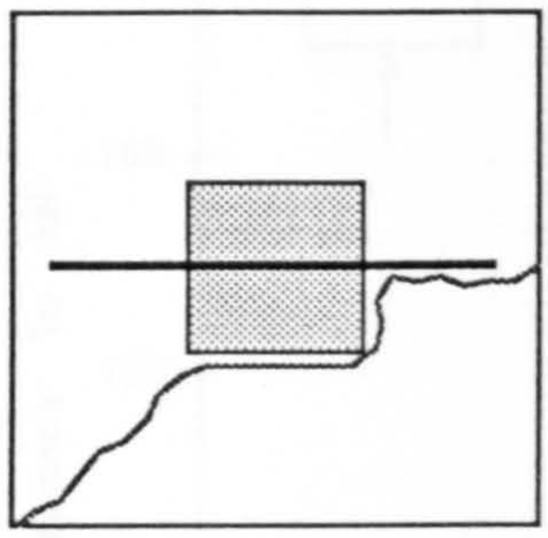

R12BW

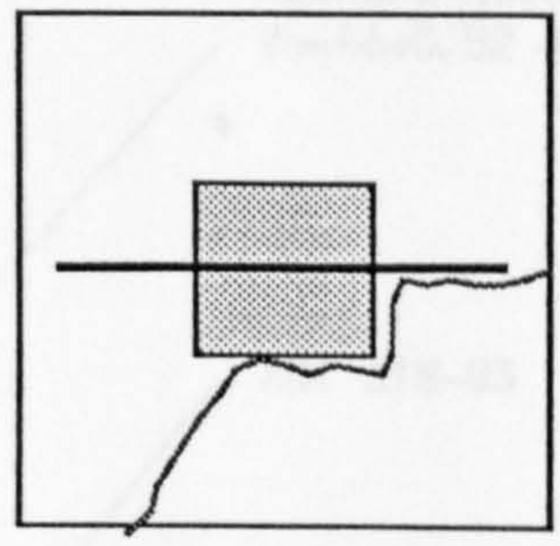

T12BW

R16BW

T16BW

FIG. 7.2 Crack Pattern in Some Specimens After Failure
(Shown on Plan Views)

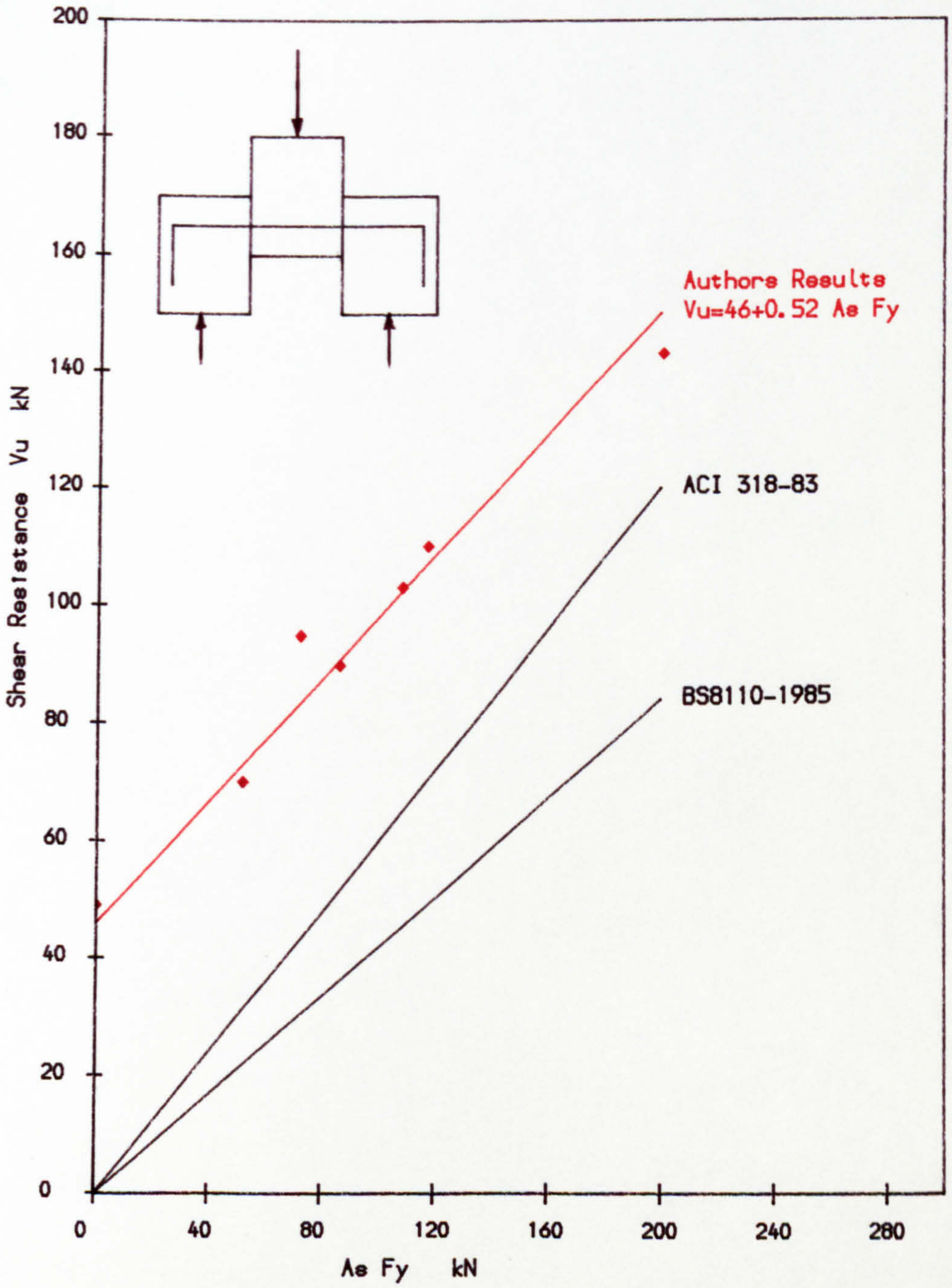

FIG. 7.3 DOWEL STRENGTH IN SMOOTH BONDED CONNECTION

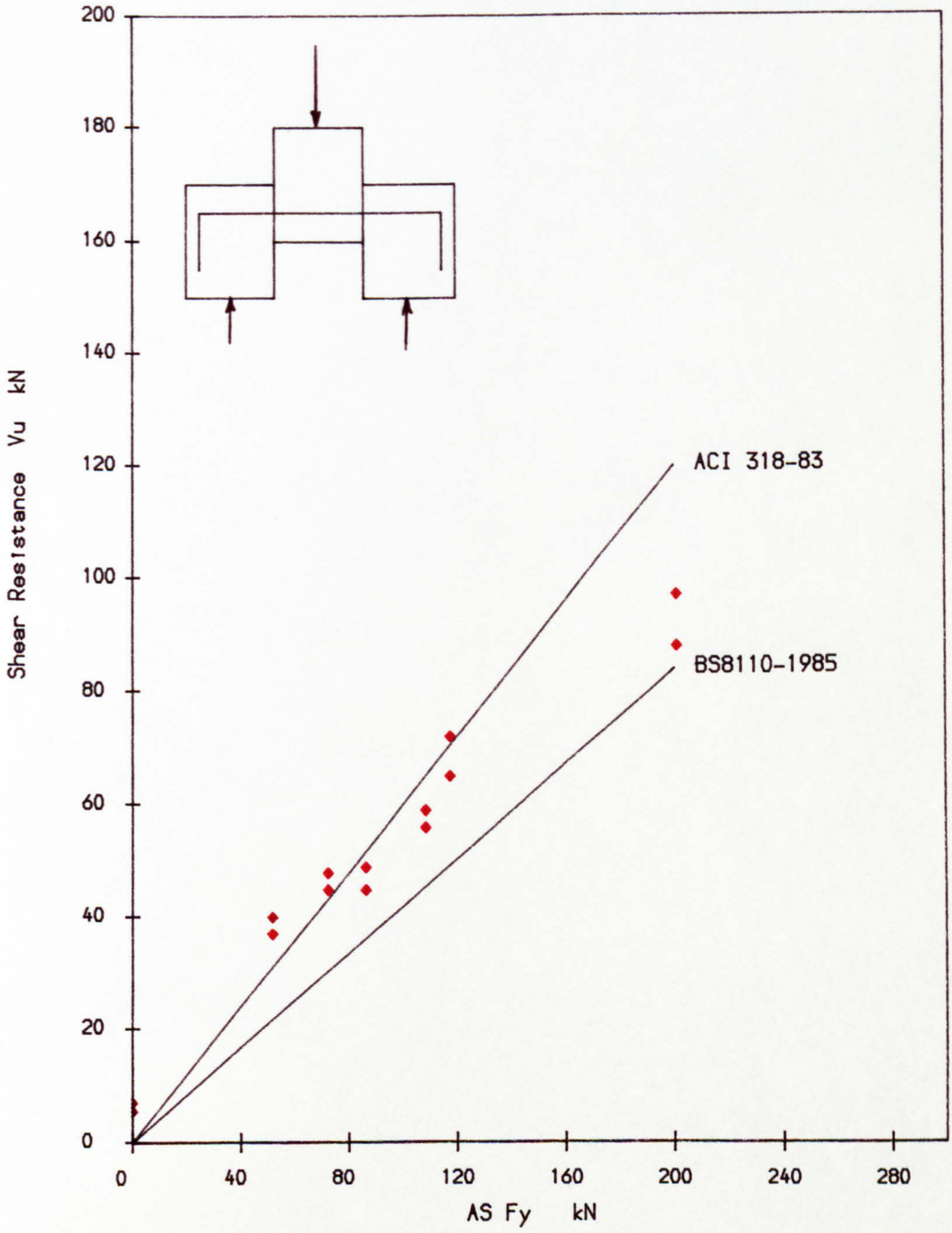

FIG. 7.4 DOWEL STRENGTH IN SMOOTH UNBONDED CONNECTION

CHAPTER EIGHT

CONCLUSIONS AND SUGGESTIONS FOR FURTHER RESEARCH

8.1.1 Shear In Composite Precast Prestressed Beams

Different aspects of composite beam behaviour when subjected to shear were observed and comparisons were made with current Codes of practice.

8.1.1.1 Web Shear Cracking Load

It was observed that all British Codes (BS8110, BS5400, CP110) have a sufficient margin of safety against web shear cracking and the observed mean was 1.21. The observed mean safety factors were 0.96, 1.05, 1.50 and 2.06 for American[81], Australian[70], European[72] and American Bridge (AASHTO)[73] Codes respectively, the most conservative one being the AASHTO Bridge Code.

8.1.1.2 Stirrup Stress

It was found in the composite beams with static loading that stirrups are unstressed up to the observed inclined cracking load but they experience an approximately linear increase afterwards and the modified truss analogy was found to be adequate. For the case in which the load was removed and the beam was loaded for the second time, the classical truss analogy gave a safer prediction of the stirrup stress.

8.1.1.3 Web Crushing

Considering protection against web crushing, it was found that British Codes are the most conservative ones (with an observed safety factor of up to

2.66) while American, European, and Australian Codes indicate more reasonable safety factors of 1.47, 1.60 and 1.69 respectively.

The web crushing strength is dependent upon the shear span to effective depth ratio (a/d) and the classical or modified truss analogies cannot precisely predict the stirrup stress for this situation. A mathematical model was produced to evaluate the stirrup stress with respect to both the shear span and the stirrup ratio (see section 4.5.4 for the proposed equation).

For the type of beams tested here, a limiting value was found for the a/d ratio in that for values smaller than this the required area of stirrups may be reduced (see section 4.5.4).

8.1.2 Enhanced Shear Strength near the Continuous Support

An increased shear resistance may be assumed for the beams near the support. Current Codes have different approaches but they do not distinguish between simple or continuous supports. In the present investigation this matter was examined for the continuous supports.

It was discovered that stirrup stress decreases linearly from a distance of 0.7d (d=effective depth) from the continuous support, and thus the enhancement should be allowed for at sections within this distance. Current Code predictions are considerably different. The CEB method appears to be unsafe while the simplified method of BS8110 and also Danish Code method seem to be the most conservative ones. The Australian Code approach showed a better prediction of the shear strength enhancement near the supports of a continuous beam.

8.1.3 Shear Transfer Between Precast Prestressed M-Beams and In-Situ Crosshead

A detailed investigation was made to find the most important mechanism of

shear transfer, factors affecting the shear transfer capacity, the need for strengthening by external means such as transverse prestressing and finally a practical and economical method for the design of connection.

8.1.3.1 Mechanisms of Shear Transfer in Beams with Top Flanges

The shear force is transferred from the M-beam to the in-situ nibs by:

a) The mechanical interlock (key) produced by the M-beam's top flanges and the in-situ nibs.

b) Monolithic concrete top slab joining the whole system together.

c) The bond between the web and in-situ nibs.

The most important mechanism proved to be the top flanges of the M-beam.

8.1.3.2 Distribution of Shear Force within the Embedment Length

From measurement of stirrup strain along the connection length in the precast beam, the variation of shear force, and hence the distribution of reaction forces between the two parts, were obtained. It was discovered that for an embedment length of 300mm (900mm in prototype) about 50% of the shear force is transferred within 50mm of the beam's end.

For the in-situ nibs the measured shear force distribution suggests that for a relatively large length the shear force is not high, and their relatively large thicknesses can carry the shear force without shear reinforcement. This fact was also verified by stirrup strain measurement in the nibs which was found to almost zero within that length. As a result embedment lengths of less than 300mm may be used in this type of connection.

8.1.3.3 Effect of Projecting Bars

For the beams with top flanges it was observed that the contribution of projecting bars to dowel action in shear transfer are not additive i.e the top flange mechanical interlock (key) is sufficient to transfer the design shear force. It is suggested that apart from those bars required for the possible positive moment near the supports as a result of differential settlement, there is no need for other bars to project from the beam. The provision of projecting bars or couplers is an expensive and time consuming practice and it may present both transportation and corrosion problems.

As a result of 8.1.3.2 and 8.1.3.3, it is recommended that for the beams with top flanges (such as M-beams) the nib stirrups can be eliminated (or kept to a nominal amount) and projecting bars may be reduced to the required amount to cope with possible positive moment.

8.1.3.4 Effect of Bending moment

The magnitude of bending moment was increased by changing the loading arrangement and it was observed that the shear transfer capacity of the connection was not changed significantly.

8.1.3.5 The Embedment Length Effect

The embedment length was reduced from 300mm to 100mm and the connection was able to transfer the full shear force when the in-situ nibs are provided with stirrups. It was seen however, that there was a considerable rotation at the connection in comparison with higher embedment lengths.

8.1.3.6 Transverse Prestressing

Since in the connections with top flange effect the weakest conditions, I.e unreinforced nibs and elimination of projecting bars, could not reduce the shear capacity of the connection (for the highest possible shear force) without transverse prestressing, it is therefore suggested that there is no need for this feature to provide longitudinal shear transfer strength.

8.1.4 Shear Transfer in Beams without Top Flanges

The effect of top flanges was eliminated deliberately in this stage of the research and it was seen that the connection suffered dramatic reduction in its shear transfer capacity. During this stage and in this condition other means of improving the shear transfer capacity were examined. They were as follows:

8.1.4.1 Transverse Prestressing

Transverse prestressing provided the most efficient mechanism of longitudinal shear transfer by increasing the interface friction in the absence of top flanges within the connection. In addition to that, relative rotation and vertical separation were greatly reduced by including this feature.

8.1.4.2 Web Shear Connectors

As a substitute for transverse prestressing, these connectors were observed to serve as a shear transfer mechanism by their dowel action. They could transfer the full shear force but the vertical separation at ultimate was considerable.

8.1.4.3 Projecting Bars

In connections without transverse prestressing or web shear connectors, the projecting bars from the end of beam were able to transfer the full shear force but very large relative rotation and vertical separation was observed, resulting from the lack of connection between the nibs and web and also the absence of top flanges which produce the most efficient mechanism.

8.1.5 Dowel Shear Tests

To obtain more information about the strength of web shear connectors (explained in chapter seven) a separate dowel shear specimen was designed and different interface conditions (bonded, unbonded, dowel bar size and strength). For the design of dowel bars connecting precast to in-situ elements where the surface is very smooth and the bond has been destroyed as a result of shrinkage, the experimental results from these specimens revealed that the BS8110 method provides an accurate and safe prediction of the failure load. For the case in which the interface shear (bond and interlock) exists, a mathematical model is proposed to predict the shear strength.

8.2 Suggestions for Further Research

8.2.1 Connections with Top Flange Effect

For this type of connection the following subjects may be investigated:

a) Effect of repeated loading on the shear transfer capacity of the connection.

b) Examination of the embedment lengths rather than those tested here e.g. 250mm, 200mm and 150mm with unreinforced nibs.

c) Shear transfer capacity when the connection is very close to the

support.

d) Effect of transverse prestressing for small embedment lengths.

e) The behaviour of the connection when it is in the region of large positive bending moment. This is useful to connect two beams at the mid-span or near it because of transportation restriction etc.

8.2.2 Connections Without Top Flange Effect

The following suggestions are made for this type of connection:

a) Effect of repeated loading

b) Examining different prestressing levels and finding the required minimum in the case of transverse prestressing.

c) Changing the number, size, strength and position of the dowel bars in the case of web shear connectors.

d) Changing the number and size of projecting bars and its effect upon the shear transfer capacity of the connection

d) Examining the associated effect of web shear connectors and projecting bars upon the shear strength of the connection.

REFERENCES

1. Anon.

"The Notham Bridge Southampton England" Copenhagen, Fifty years of Civil Engineering 1904-1954, Christiani and Nielsen, pp. 131-136, Feb. 1954.

2. Bouvy J.J.B.J.J.

"A special Method of Assembling Precast Beams into Continuous Structures by Prestressing on the Site". Amsterdam, Second Congress,Federation International de la Precontrainte, Session 2, paper No. 10, pp 414-419, 1955.

3. Sturrock, R.D

"Model Bridge Beams in Precast to In-situ Concrete Construction". Cement and Concrete Association Technical Report 488, Jan. 1974, London.

4. Pritchard, B.P

"The use of Continuous Precast Beam Decks for M11 Woodford Interchange Viaducts". The Structural Engineer, No. 10, Vol. 54, Oct. 1976.

5. Pritchard, B.P

"The Use of Continuous Precast Beam Decks for M11 Woodford Interchange Viaducts, DISCUSSION". The Structural Engineer, No. 5, Vol. 55, May 1977.

6. Leonhardt, F.

"Spannbeton fur die Praxis" (Precast Concrete for Practice). Berlin Wilhelm Ernstund sohn, 472 pages, 1955.

7. Kaar, P.H Kriz, L.B and Hognestad, E.

" Precast Prestressed Concrete Bridges, 1. Pilot Tests of Continuous Griders". Portland Cement Association(PCA) Development Department, Bulletin D34, 1960.

8. Mattock, A.H and Kaar,P.H

"Precast Prestressed Concrete Bridges, 4. Shear Tests of Continuous Girders". Journal of the PCA, Jan. 1961, D45.

9. Hanson,N.W

" Precast Prestressed Concrete Bridges, 2. Horizontal Shear Connectors". PCA Development Department, D35. 1960

10. Mattock, A.H and Kaar, P.H

"Prcast Prestressed Concrete Bridges, 3. Further Tests of Continuous Girders". PCA Bulletin D43, 1961.

11. Mattock, A.H

"Precast Prestressed Concrete Bridges, 5. Creep and Shrinkage Studies". PCA Bulletin D46, 1961.

12. Bennett, E.W

"Shear Strength of Prestressed Concrete Bridge Beams type 61. "Final Report for the West Riding County Council, University of Leeds, August 1971.

13. Bennett, E.W

"Full-Scale Tests on Two Types of Stirrups in Motorway Bridge beams". Report prepared for Leonard Fairclough Ltd., University of Leeds April 1972.

14. Mc Gregor, J.G

"Strength and Behaviour of Prestressed Concrete Beams with Web Reinforcement". Ph.D Thesis, University of Illinois August 1960.

15. Balasooriya, B.M

"The Diagonal Compression Mode of Shear Failure in Reinforced and Prestressed Concrete Beams". Ph.D Thesis, University of Leeds, August 1969.

16. Olsen, S.O, Sozen, M.A and Siess, C.P

"Investigation of Prestressed Reinforced Concrete for Highway Bridges, Part IV : Strength in Shear of Beams with Web Reinforcement". University of Illinois , Engineering Experimental Station, Bulletin No. 493, July 1967, p.36

17. Sethunarayanan, Rm.

" Ultimate Strength of Pretensioned I-Beams in Combined Bending and Shear". Magazine of Concrete Research, Vol. 12, No. 35, July 1960, pp 83-90.

18. Clarke, J.L and Taylor, H.P.J

"Web Crushing, A review of Research". C&CA Technical Report, TRA 509, 1975.

19. Ritter, W.

"The Hennebique Design Method (Die Bavweise Hennebique)". Schweizerische Bavzeitung (Zurich), Vol. 33, pp 59-61, Feb. 1899.

20. Morsch, E.

"Tests of Shear Stresses in Reinforced Concrete Beams (Versuche Uber Schubspannungen in Betone Sentragern)". Beton und Eisen (Berlin), Vol. 2, No. 4, pp 269-274, Oct. 1903.

21. Bresler, B and Mc Gregor, J.G

"Review of Concrete Beams Failing in Shear". Journal of The Structural Division , ASCE, Vol. 93, ST1, Feb. 1967, pp 343-372.

22. Hognestad, E

"What do We Know About Diagonal Tension and Web Reinforcement in Concrete? , A Historical Study". University of Illinois Bulletin Vol. 49, No. 50, March 1952, 47 pp.

23. Building Code Requirements for Reinforced Concrete (ACI 318-71)

". American Concrete Institute , Detroit, 1971, 78 pp.

24. ACI-ASCE Committee 326 .

"Shear and Diagonal tension". ACI Journal, Vol. 59, Jan. , Feb. , March 1962, pp 1-30, 277-334, 352-396.

25. Joint ASCE-ACI Task Committee 426,

"The Shear Strength of Reinforced Concrete Members". Journal of The Structural Division, ASCE, Vol. 99, ST6, June 1973, pp 1091-1187.

26. Shear Study Group,

"Report on The Shear Strength of Reinforced Concrete Beams". Institution of Structural Engineers Publication, January 1969.

27. BS8110 : 1985 Part 1

"Structural Use of Concrete" British Standard Institution.

28. Sozen, M.A , Zwoyer, E.M and Siess, C.P

"Investigation of Prestressed Concrete for Highway Bridges, Part I : Strength in Shear of Beams Without Web Reinforcement". Bulletin No. 452, University of Illinois, Engineering Experimental Station, April 1959.

29. Moe, J

"Discussion of Shear and Diagonal Tension by ACI-ASCE Committee 326". ACI Journal Vol. 44, No. 4, pt. 2, September 1962, pp 1334-1339.

30. Fenwick, R.C and Paulay, T.

"Mechanisms of Shear Resistance of Concrete Beams". Proceedings ASCE, Structural Division, Oct. 1968, pp 2325-2350.

31. Acharya, D.N and Kemp, K.O

"Significance of Dowel Forces on The Shear Failure of Reinforced Concrete Beams Without Web Reinforcement". ACI Journal, Vol. 62, No. 10, Oct. 1965, pp 1265-1279.

32. Taylor, H.P.J

"Shear Stress in Reinforced Concrete Beams Without Shear Reinforcement". Cement and Concrete Association, TRA 407, London, 1968.

33. Taylor, H.P.J

"Further Tests to Determine Shear Stresses in Reinforced Concrete Beams". Cement and Concrete Association, TRA 438, London, 1970

34. Taylor, H.P.J

"Investigation of the Forces Carried Across Cracks in Reinforced Concrete Beams by Interlock of the Aggregates". Cement and Concrete Association, TRA 447, London, 1970.

35. Paulay, T. and Loeber, P.J

"Shear Transfer by Aggregate Interlock". Shear in Reinforced Concrete, ACI Publication SP-42, Vol. 1, 1974, pp 1-15.

36. Taylor, H.P.J

"The Fundamental Behaviour of Reinforced Concrete Beams in Bending and Shear". Shear in Reinforced Concrete, ACI Publication SP-42, Vol. 1, 1974.

37. Jones, R.

"The Ultimate Strength of Reinforced Concrete Beams in Shear". Magazine of Concrete Research, Vol. 8, No. 23, August 1965, pp 69-84.

38. Taylor, H.P.J

"Investigation of the Dowel Shear Forces Carried by the Tensile Steel in Reinforced Concrete Beams". Cement and Concrete Association, TRA 431, London, 1969.

39. Krefeld, W.J. and Thurston, C.W

"Contribution of Longitudinal Steel to Shear Resistance of Reinforced Concrete Beams". Journal of the ACI ,Vol. 63, No. 3, March 1966.

40. Fenwick, R.C

"Shear Strength of Reinforced Concrete Beams". Ph.D Thesis presented to the University of Canterbury, Christchurch, New Zeland.

41. Lorensten, M.

"Shear and Bond in Prestressed Concrete Beams Without Shear Reinforcement". Stockholm, Forskningstitutet for Cement och Betong, 1964, pp 195, Handlingar Nr. 47.

42. Taub, J. and Neville, A.M

"Resistance to Shear of Reinforced Concrete Beams". ACI Journal, Vol. 51, 5 parts series, August-December1960, pp193-219, pp315-336, pp 433-463, pp 517-532, pp 715-730.

43. Kani, J.N.G

"The Riddle of Shear Failure and its Solution". ACI Journal, Vol. 61, April 1964, pp 441-467.

44. Kani, J.N.G

"A Rational Theory for the Function of web Reinforcement". ACI Journal, Vol. 66, No. 3, March 1969, pp 187-196.

45. Park, R. and Paulay, T

"Reinforced Concrete Structures" A Wiley-Interscience Publication, 1975.

46. Warner, R.F

"Design of Stirrup Reinforcement in Concrete Beams" International Association of Bridge and Structural Engineering (IABSE) , Publications, Vol. 23, 1963, pp 263-280.

47. Sethunarayanan, Rm.

"Ultimate Strength of Pretensioned I-Beams in Combined Bending and Shear". Magazine of Concrete Research, Vol. 12, No. 35, July 1960, pp 83-90.

48. Mathey, R.G and Watstein, D.

"Shear Strength of Beams Without Web Reinforcement Containing Deformed Bars of Different Strengths". ACI Journal, Vol. 60, No. 13, Feb. 1963, p 190.

49. Evans, R.H and Kong, F.K

"Shear Design and British Code CP114". The Structural Engineer, Vol. 45, No. 4, April 1967, p 156.

50. Regan, P.E and Placas, A.

"Limit State Design for Shear in Rectangular and T-Beams". Magazine of Concrete Research, Vol. 22, No. 73, December 1970, pp 197-208.

51. Bazart, P.E and Gambarova, P.G

"Rough Cracks In Reinforced Concrete". Journal of the Structural Division, ASCE, Vol. 106, No. 4, April 1980.

52. Sandro Del Poli, Pietro G Gambarova and Cengiz Karakoc

"Aggregate Interlock Role in R.C. Thin-Webbed Beams in Shear". Journal of The Structural Division, ASCE, Vol. 113, No. 1, Jan. 1987.

53. Regan, P.E

"Shear in Reinforced Concrete Beams". Magazine of Concrete Research, Vol. 21, No. 66, March 1969, pp 31-42.

54. Kani, G.N.J

"Basic Factors Concerning Shear Failure". ACI Journal, Vol. 63, No. 6, June 1966.

55. Kotsovos, M.D

"Mechanisms of Shear Failure". Magazine of Concrete Research, Vol. 35, No. 123, June 1983, pp 99-106.

56. Kotsovos, M.D , Bobrowski, J. and Eibl, J.

"Behaviour of Reinforced Concrete T-Beams in Shear". The Structural Engineer, Vol. 65B, No. 1, March 1987.

57. Ojha, S.K

"The Shear Strength of Rectangular Reinforced and Prestressed Concrete Beams". Magazine of concrete Research, Vol. 19, No. 60, Sept.1967, pp173-184.

58. Evans, R.H and Hosny, A.H

"The Shear Strength of Post-tensioned Prestressed Concrete Beams" Third Congres of FIP, Berlin 1958, Paper No. 11, Section 1, p 19.

59. Leonhardt, F. and Walther, R.

"The Stuttgart Shear Tests, 1961 : Contribution of the Treatment of The Problems of Shear in Reinforced Concrete Construction". London C&CA Library Translation No. 111, p 41.

60. Mlingwa, G.

"Vertical Prestressed Tendons as Shear Reinforcement in Prestressed Concrete Beams". Ph.D Thesis, Leeds University, 1978.

61. Clarke, J.L and Evans, D.J.

"Vertical Shear Strength of Composite Beams". Cement and Concrete Association, Technical Report No. 556, March 1983.

62. Tay, C.J

" Shear Strength of Full-sized Prestressed Concrete Composite Bridge Beams". Ph.D Thesis ,Leeds University, Dec. 1983.

63. Manton, B.H and Wilson, C.B

"M.O.T / C&CA Standard Bridge Beams" Cement and Concrete Association, March 1971.

64. CP110 : Part 1 : 1972

"The Structural Use of Cncrete" British Standard Institution, London.

65. BS1881 : Part 5 : 1970

"Methods of Testing Concrete" British Standard Institution, 1970

66. Balasooriya, B.M.A

"The Diagonal Compression Mode of Shear Failure in Reinforced and Prestressed Concrete Beams" Ph.D Thesis, Leeds University, August 1969.

67. Bennett, E.W and Balasooriya, B.M.A

"Shear Strength of Prestressed Beams With Thin Webs Failing In Inclined Compression" ACI Journal, Title No. 68-22, March 1971, pp 204-212.

68. BS5400 : Part 4 : 1984

"Code of Practice for Design of Concrete Bridges"

British Standard Institution, London, 1984.

69. Danish Standard

"Structural Use of Concrete, English Translation from: Dansk Standard DS411" Third Edition, March 1984, Translation Edition April 1986.

70. Standard Association of Australia

"SAA Prestressed COncrete Code" 1481, 1978.

71. ACI 318-77

"Building Code Requirements for Reinforced Concrete" American Concrete Institute, Detroit, Michigan, 1970.

72. CEB-FIP

" Model Code for Concrete Structures" Comite Euro- International du Beton, 1978.

73. AASHTO (American Association of State Highway and Transportation Officials)

"Standard Specification for Highway Bridges" Washington D.C. , 1977.

74. Olesen, S.O Sozen, M.A and Siess, C.P

"Investigation fo Prestressed Reinforced Concrete for Highway Bridges, Part IV, Strength in Beams with Web Reinforcement" Bulletin 493, Engineering

Experimental Station, University of Illinois, July 1967.

75. Arthur, P.D

"The Shear Strength of Pretensioned Concrete I-Beams with Unreinforced Webs" Ph.D Thesis ,The University of St. Andrews, Scotland June 1968.

76. Domone, P.L.

"Uniaxial Tensile Creep and Failure of Concrete" Magazine of Concrete Research, Vol. 26, No. 88, Sept. 1974.

77. Leonhardt, D.I.F

"Reducing the Shear Reinforcement in Reinforced Concrete Beams and Slabs" Magazine of Concrete Research, Vol. 17, No. 53, December 1965.

78. Ruhnau, J.

"Influence of Repeated Loading on Stirrup Stress of Reinforced Concrete Beams" Shear In Reinforced Concrete , Vol. 1, ACI Publication SP-42, 1974, pp 169-181.

79. Tay, C.J Bennett, E.W and Cusens, A.R

"Vertical Shear Strength of Composite Prestressed Beams : Part 2 : Fatigue Tests" Final Report to the Department of Transport by the University of Leeds , January 1985.

80. Cement and Concrete Association

"Handbook on the Unified Code for Structural Concrete, CP110 : 1972".

81. ACI 318-83

"Building Code Requirements for Reinforced Concrete" American Concrete Institute, Detroit , Michigan, 1983.

82. Jones. L.L

"Shear Tests on Joints Between Precast Post-tensioned Units" Magazine of Concrete Research, Vol.11, No. 31, March 1959 pp 25-30.

83. Gaston, K.R.A and Kriz, L.B.

"Connections in Precast Concrete Structures, Scarf Joints" Journal of Prestressed Concrete Institute, Vol. 9, No. 3, June 1964, pp 37-59.

84. Rees, M.

"Some Recent Developements in Structural Precast Concrete" Civil Engineering and Public Works Review, Vol. 57, No. 672, July 1962, pp 881-884.

85. Timoshenko, S. and Lessels, J.M

"Applied Elasticity" Westinghouse Technical Night School Press, East Pittsburg, 1925.

86. Friberg, B.F

"Design of Dowels in Transverse Joints of Concrete Pavements" ASCE, Vol. 105, 1940, pp 1076-1116.

87. **Loe, J.A**

"Dowel Bar Joints for Airfield Pavements" Proceedings of the Institution of Civil Engineers, Vol. 1, No. 3, Part 2, October 1952, pp 612-650.

88. **Marcus, H.**

"Load Carrying Capacity of Dowels at Transverse Pavement Joints" ACI Journal, Vol. 23, No. 2, October 1951,pp 169-184.

89. **Vintzeleou, E.N and Tassios, T.P**

"Mathematical Models for Dowel Action under Monolithic and Cyclic Conditions" Magazine of Concrete Research, Vol. 38, No. 134, March 1986, pp 13-22.

90. **Utescher, G. and Herrmann, M.**

"Versuche Zur Ermittlung der Tragfahigkeit in Betob Eingespannter Rundatahldollen aus Nichtrostendem Austenitischem Stahl" Deutscher Ausschuss fur Stahlbeton, Berlin, Wilhelm Ernst und Sohn, 1983, Heft 346, pp 49-104.

91. **Dulacska, H.**

"Dowel Action of Reinforcement Crossing Cracks in Concrete" ACI Journal, Vol. 69, No. 12, December 1972, pp 754-757.

92. **Mills, G.M**

"Partial Kinking Yield Criterion for Reinforced Concrete Slabs" Magazine of Concrete Research, Vol. 27, No. 90, March 1975, pp 13-22.

93. **Krefeld, W. and Thurston, C.W**

"Contribution of Longitudinal Steel to Shear Resistance of Reinforced Concrete Beams" ACI Journal, Vol. 63, No. 3, March 1966, pp 325-344.

94. **Soroushian, P. Obaseki, K. Rojas, M. and Jongsung,S.**

"Analysis of Dowel Bars Acting Against Concrete Core" ACI Structural Journal, July -August 1986, pp 642-649.

95. **Soroushian, P. Obaseki, K. Rojas, M. and Najm, H.S**

"Behaviour of Bars in Dowel Action Against Concrete Cover" ACI Structural Journal, March-April 1987, pp 170-176.

96. **Saeman, J.C and Washa, J.W**

"Horizontal Shear Connections Between Precast Beams and Cast-in -place Slabs" ACI journal, Vol. 61, No. 11, November 1964, pp 1383-1409.

97. **Birkland, P.W and Birkland, H.W**

"Connections in Precast Concrete Construction" ACI Journal, Vol. 63, No. 3, March 1966, pp 345- 368.

98. **Mast, R.F**

"Auxiliary Reinforcement in Concrete Connections" Journal of the Structural Division, Proceedings of the ASCE, Vol. 94, ST6, Paper 6002, June 1968, pp 1485-1504.

99. Hofbeck, J.A Ibrahim, I.A and Mattock, A.H

"Shear Transfer in Reinforced Concrete" Structural Research Report 68-1, University of Washington, College of Engineering, Feb. 1968.

100. Andeson, A.R

"Composite Design in Precast and and Cast-in-place Concrete" Progressive Architecture, Sept. 1960.

101. Bennett, E.W and Banerjee, B.E

"Strength of Beam-Column Connections with Dowel Reinforcement" The Structural Engineer, Vol. 51, No. 4, April 1976, pp 133-139.